Innate and cognate roles of B cells in T cell differentiation and memory

Vicky L. Morrison

Thesis submitted for the degree of Doctor of Philosophy

The University of Edinburgh

2010

Declaration

I declare that this thesis has been composed by myself, describes my own work, and has not been submitted in any other application for a higher degree.

Vicky L. Morrison
2010

Table of Contents

List of Figures and Tables

Chapter 4 – *S. typhimurium*-induced changes in the spleen include the accumulation of antigen-presenting macrophages and the loss of marginal zone B cells

Chapter 5 – The role of B cells in the generation of T cell memory and T follicular helper populations: use of the *Salmonella typhimurium* infection model

Chapter 6 – The role of B cells in the generation of T cell memory: use of MHC class II tetramers

Chapter 7 – Final discussion and summary

Chapter 8 – Appendices

Acknowledgements

First and foremost, I would like to thank my supervisor, David, for letting me loose in his lab, and providing excellent guidance over the past 3 years. A massive thank you also to the other members of the Gray lab. Especially to Sheila, for her fantastic mashing abilities and constant supply of gossip and pointless chat (as well as her limitless knowledge of immunological techniques), without which I would never have gotten this far! And to big Tom, for intellectual discussions, experimental tips, comments on my thesis chapters, and general chat (as well as for providing the data in figure 5.10C!).

A thank you also goes out to Cat, for the trips to the pub and the chance to off-load all my PhD stresses! Also, thanks to Sarah-Louise Kelly, my undergraduate honours student, for help with experiments, and cutting histology sections.

My husband, Grant, deserves a huge thank you, for lifts to/from KB at obscure hours of the day, listening to me practising talks (and being handy with the stopwatch!) and for generally putting up with me!! I am most grateful for the constant support I have received from him, and the rest of my family.

For reagents, I would like to thank Dr Marilyn Kehry at Biogen IDEC Inc. for the use of the anti-CD20 B cell depletion antibodies, the NIH Tetramer Core Facility for providing the tetramers, and Thomas Tedder at Duke University for the shipment of CD62L(E) bone marrow. Thanks also to others on the 2nd floor for saving the day if ever anything ran out, and for providing the odd antibody, here and there. Without these reagents several chapters of this PhD would not have been possible!

This work was funded by an MRC studentship, and the Wellcome Trust.

Abstract

B cells recognise antigens on micro-organisms through their B cell receptor (BCR) and via Toll-like receptors (TLRs), and thus respond in both innate and adaptive manners during the subsequent immune response. Innate recognition through TLRs has the potential to alter the behaviour of whole B cell populations. I show, here, that MyD88-dependent activation of B cells via TLR2 or TLR9 causes the rapid loss of expression of CD62L, by metalloproteinase-dependent shedding, resulting in the exclusion of these cells from lymph nodes and Peyer's patches, but not the spleen. Moreover, systemic infection with *Salmonella typhimurium* causes shedding of CD62L and the subsequent focussing of B cell migration to the spleen. I reveal that splenic B cells undergo further changes during *S. typhimurium* infection, including TLR-dependent differentiation of marginal zone B cells into IgM-secreting plasma cells. Together, these TLR-mediated alterations to B cells are likely to influence the development of immunity to pathogens carrying the appropriate ligands.

In addition to these innate responses of B cells, endocytosis of cognate antigen through their BCR allows antigen presentation. This, together with their ability to secrete cytokines, means they have the potential to drive T helper cell responses. I investigate the role of B cells in such $CD4^+$ T cell responses by following antigen-specific T cells *in vivo,* using both a peptide immunisation strategy and the *S. typhimurium* infection model. I use anti-CD20 B cell depletion antibodies to deplete B cells at various stages of the immune response, and analyse the effects on T follicular helper and memory cell populations. I show that both the generation and maintenance of T follicular helper cells is dependent on the presence of B cells. Furthermore, I demonstrate that B cells are necessary very early in immune responses, during the first 10 days, for efficient generation of memory T cells.

Abbreviations

Ab – Antibody

aCD20 – Anti-CD20 B cell depletion antibody

ADAM17 – A disintegrin and metalloproteinase domain-containing protein 17

Ag – Antigen

AID – Activation-induced cytidine deaminase

APC – Antigen presenting cell

Bcl-6 – B cell lymphoma-6 transcription factor

BCR – B cell receptor

BM – Bone marrow

BMDC – Bone marrow-derived dendritic cells

BrdU – Bromodeoxyuridine

BSA – Bovine serum albumin

CaM - Calmodulin

CFA – Complete Freud's adjuvant

CFU – Colony-forming units

dn – double negative

DNP – Dinitrophenyl

EAE – Experimental autoimmune encephalomyelitis

ELISA – Enzyme-linked immuno-sorbant assay

FCS – Foetal calf serum

FDC – Follicular dendritic cell

FRC – Fibroblastic reticular cell

FSC – Forward scatter

GC – Germinal centre

GlyCAM-1 – Glycosylation-dependent cell adhesion molecule-1

GM-CSF – Granulocyte macrophage colony-stimulating factor

H19env peptide – Immunodominant peptide from the envelope protein of the Murine Moloney Leukaemia virus

HEVs – High endothelial venules

hi – High

HKB – Heat-killed bacteria

ICOS (L) – Inducible co-stimulator (ligand)

IFNγ – Interferon-γ

Ig – Immunoglobulin

IL-12 – Interleukin-12

iLN – Inguinal lymph nodes

IMDM – Iscove's modified Dulbecco's medium

iNKT cell – Invariant natural killer T cell

iNOS – Inducible nitric oxide

int – Intermediate

Iono – Ionomycin

i.p. – Intraperitoneally

iso – Isotype control (-treated)

iTreg cell – Inducible regulatory T cell

i.v. – Intravenously

KLH – Keyhole limpet hemocyanin

KLRG1 – Killer-cell lectin-like receptor subfamily G, member 1

KO – Knockout

LB – Luria-Bertani

lo – Low

LN – Lymph node

LPS – Lipopolysaccharide

MAdCAM-1 – Mucosal addressin cell adhesion molecule-1

MFI – Mean fluorescence intensity

MHC – Major histocompatibility complex

mLN – Mesenteric lymph nodes

MPEC – Memory precursor effector cell

N/A – Not applicable

NS – Not significant

P. acnes – Propionibacterium acnes

PAMP – Pathogen-associated molecular pattern

PBS – Phosphate buffered saline

PD-1 – Programmed death-1

PI – Propidium Iodide

PKC – Protein kinase C

PMA – Phorbol myristate acetate

PNPP – p-Nitrophenyl phosphate

PP – Peyer's patches

RA – Rheumatoid Arthritis

RPMI – Roswell Park Memorial Institute medium

S. typhimurium – Salmonella enterica serovar Typhimurium

s.c. - Subcutaneously

SEA – Schistosomal egg antigen

SEM – Standard error of the mean

SLE – Systemic Lupus Erythematosus

SLEC – Short-lived effector cell

SSC – Side scatter

TACE – TNFα converting enzyme

TCR – T cell receptor

T_{FH} cell – T follicular helper cell

TGFβ - Transforming growth factor-β

Th cell – T helper cell

TIR – Toll-IL-1 receptor

TLR – Toll-like receptor

TNFα – Tumour necrosis factor-α

Treg cell – Regulatory T cells

WT – Wild type

CHAPTER 1: Introduction

Overview of immune responses

The immune system functions continuously to fight off invading pathogens, whilst regulating itself to prevent both autoimmunity and immunopathology. Due to the vast array of pathogenic organisms and the need to also recognise hazardous tumour cells, the immune system has evolved in mammals to be incredibly complex. Importantly, the distinction between self and non-self is an essential component of immune activation [1]. Cells specialised in immuno-surveillance monitor the body for pathogens, and transport fragments of any foreign material they encounter back to lymphoid organs. The subsequent activation of the innate and adaptive arms of the immune system is a complex process, involving multiple cell types and cellular interactions, within various tissues of the body. Ultimately, the clearance of the pathogenic micro-organism requires the immune cells to work together to perform their effector functions efficiently and rapidly, in order to prevent pathogen-mediated damage. The understanding of the mechanisms of immune cell activation, and the processes required for pathogen clearance and generation of protective immunity, is essential for the development of vaccines and therapeutic treatments.

While the innate arm of the immune system is activated rapidly and non-specifically in response to pathogen encounter, the adaptive cells (that is to say B and T lymphocytes) are slower to respond and require the recognition of cognate antigen. These two arms of immune defence are often thought of as distinct and separate, whereas, in reality, there is great overlap between the two, with cells from each phase having the ability to influence each other in an intricate network of interactions. Thus, while innate cells induce activation of adaptive cells, such adaptive cells in turn can feedback to enhance (or regulate) the functions of innate cells. Moreover, the rapid ‘innate’ responses of so-called adaptive immune cells should not be forgotten.

Spleen structure

Following the development of B and T cells in the bone marrow and thymus, respectively, mature lymphocytes migrate to the periphery, where they congregate in secondary lymphoid tissues. These organs are structured in a highly organised manner, which allows the innate and adaptive arms of the immune system to come together for efficient activation, in response to pathogen stimulation. One of the largest lymphoid structures within the body, and the major site of B cell localisation, is the spleen (figure 1.1A). Within the spleen, B and T cells are found predominantly in the white pulp, which surrounds the central arteriole, and is separated from the red pulp by the marginal zone [2]. The importance of the spleen in immune activation was demonstrated as early as 1976 by the observation that, following splenectomy in human patients, severe systemic bacterial infection (i.e. sepsis) occurred at high frequencies [3]. In addition to its vital role in immune activation, the spleen functions to filter the blood of dying erythrocytes and foreign particulate antigen.

- The red pulp

The spleen acts as a filter of the blood, removing dead and dying erythrocytes from the bloodstream, as well as foreign particles that have become systemic. The blood flows directly into the spleen through the splenic artery, which separates into vessels and subsequently arterioles. Specialised stress fibres in the red pulp region filter the blood, and any old erythrocytes with stiffening membranes bind to the cords and are subsequently phagocytosed by nearby macrophages [2]. Another important task of these red pulp macrophages is the recycling of iron from the erythrocytes they encounter. Iron from phagocytosed erythrocytes can either be released from the red pulp macrophages as a low molecular weight product, or stored within them as an insoluble complex [2]. Filtered blood then collects in the venous sinuses, and exits the spleen via the collecting vein.

- The white pulp

Lymphocytes are located within the white pulp and marginal zone regions of the spleen. In the white pulp, stromal cells form a network within the T cell zone, where T cells and dendritic cells are located. These stromal cells, called fibroblastic reticular cells [4], secrete chemokines, namely CCL19 and CCL21, which bind to their receptor, CCR7, and attract T cells and dendritic cells to the region [5,6]. CCL19 is also expressed by high endothelial venules (HEV) to encourage extravasation of $CCR7^+$ cells into the lymph nodes [5,7]. Meanwhile, follicular dendritic cells situated in the follicles secrete CXCL13, which attracts $CXCR5^+$ B cells to these sites (see figure 1.1C) [8]. The importance of the chemokine

receptors CCR7 and CXCR5 in organising lymphocytes within secondary lymphoid organs has been demonstrated, using $CXCR5^{-/-}$ $CCR7^{-/-}$ mice. These mice have severely disrupted organisation of the spleen, with poorly defined B and T cell zones, and they lack peripheral lymph nodes [6]. Within the host, lymphocytes regulate their expression of the chemokine receptors CCR7 and CXCR5 as a means of altering their homing patterns. For example, activated T cells downregulate CCR7, and concurrently upregulate CXCR5, to migrate to the follicular boundary, where they interact with B cells and provide 'help' for the induction of the germinal centre (GC) response [9,10]. Additionally, some $CXCR5^{+}$ T cells, known as T follicular helper cells (T_{FH} cells), permanently reside in the follicles and function in aiding B cell responses [11], as described in more detail below.

- The marginal zone

Surrounding the white pulp is the marginal zone (figure 1.1A), where some arterial branches terminate. Lymphocytes entering the spleen are thought to do so via the marginal zone, before migrating to the white pulp in response to the chemokine signals identified above. The resident cell populations within the marginal zone are the marginal zone B cells and two types of macrophage: the marginal zone macrophages, and the marginal zone metallophilic macrophages. The outer ring of marginal zone macrophages is located between the marginal zone and the red pulp regions, and is characterised by expression of the scavenger receptor, MACRO, and the C-type lectin, SIGNR1 [2]. The maintenance of the marginal zone macrophage population at its site in the marginal zone has been described to be dependent on chemokine signalling, namely through the chemokine ligands CCL19 and CCL21 [12]. Marginal zone metallophilic macrophages, on the other hand, are found at the inner region of the marginal zone, adjacent to the white pulp, and express the adhesion molecule SIGLEC1 [2]. These marginal zone metallophilic macrophages can be visualised using anti-MOMA-1 antibodies, which do not bind marginal zone macrophages [13]. The presence of the marginal zone B cells between these two populations of macrophages appears dependent on an interaction with the macrophages in this region [14], while the presence of such populations of macrophages have also been shown to require marginal zone B cells [15], highlighting a role for cellular interactions in marginal zone maintenance.

Marginal zone B cells, identified by their $IgM^{hi}IgD^{lo}CD21^{hi}CD23^{int\text{-}lo}$ phenotype (whereas follicular B cells are $IgM^{lo}IgD^{hi}CD21^{int\text{-}hi}CD23^{hi}$) [16], have been shown to be functionally distinct from follicular B cells [17]. The population of marginal zone B cells plays roles in both T cell-independent and T cell-dependent responses [18], although their rapid response

time in a T cell-independent process has led to their description as innate cells. These marginal zone B cells, in contrast to follicular B cells, are non-circulatory and apparently long-lived [19]. The specificities of marginal zone B cell receptors (BCRs) has been shown to be diverse, although the IgM they produce in response to T cell-independent antigen is of low affinity, as they have not undergone affinity maturation [16,20]. Due to the location of the marginal zone adjacent to the marginal sinuses, cells in this region are among the first to access systemic antigen, allowing for the rapid production of antibody by marginal zone B cells in response to systemic antigen [18]. Their positioning in this region with ready access to antigen may also offer a possible explanation for the theory that marginal zone B cells are better than follicular B cells at antigen presentation to T cells [21]. This matter of antigen uptake in the marginal zone is discussed more fully later.

- Architecture of other lymphoid tissues

Although the spleen is the major site of B cell localisation and vital for immune activation, other secondary lymphoid organs, including lymph nodes (see figure 1.1B) and Peyer's patches, are also involved in the efficient function of the immune system. Peyer's patches, situated in the intestinal wall, possess large proportions of B cells, which are involved in the production of IgA and the maintenance of mucosal immunity within the gut [22]. Cells within the Peyer's patches are also involved in tolerance to oral antigen, as Peyer's patch-null mice lack this ability to tolerate such antigens [22]. In the lymph nodes, B cell proportions are reduced compared to in the spleen, and only follicular, not marginal zone, B cells are present. Conversely, T cell proportions are increased in the lymph nodes. Specifically, naïve $CD4^+$ T cells are found in large numbers in these peripheral lymphoid organs, highlighting the importance of the lymph nodes for T cell priming [23]. Furthermore, many mutations have been described, which result in the lack of lymph nodes in mice, all of which are associated with impaired immune responses. Such mutations include aly (Alymphoplasia) [24] and lymphotoxin-α [25], although these mutations may also affect the development and/or function of immune cells. Together these other lymphoid tissues described here are also important in immune cell activation, and maintaining immunity at sites throughout the body.

Activation of $CD4^+$ helper T cells

The activation of the $CD4^+$ T 'helper' cell population occurs in the secondary lymphoid tissues, and requires multiple signals to be received by the T cell from an initiating antigen-presenting cell (APC). The professional APC that is highly efficient at inducing T cell activation is the dendritic cell, although other cells, including B cells and macrophages, can also present antigen to T cells. Conventional myeloid dendritic cells are found in an immature state in tissues throughout the body, such as Langerhan's cells in the skin, and are characterised by their large capacity for phagocytosis. They also express a series of innate receptors for pathogen recognition, such as Toll-like receptors (TLRs) and C-type lectin receptors, and are activated by signalling through such receptors, mediated by pathogen molecules (pathogen-associated molecular patterns, PAMPs) or host distress molecules (e.g. heat-shock proteins) [26,27]. Signalling of dendritic cells through these innate receptors induces their maturation and migration to lymphoid tissues, such as the draining lymph node [28], although dendritic cells can also be activated by other means including via signals from other innate cells [29]. Such activated or mature dendritic cells present antigen via MHC class II, together with high levels of co-stimulatory molecules [28], and are very efficient at inducing naïve T cell activation, hence the term professional APC. Once in the spleen or lymph node, mature dendritic cells migrate specifically to the T cell zone, due to their expression of the chemokine receptor CCR7 [27], where they interact with T cells.

Naïve T cells also congregate in the T cell zones of secondary lymphoid organs due to their $CCR7^+$ phenotype. Migration of activated dendritic cells directly to this site allows T cells to then 'meet' the dendritic cells and scan them for cognate antigen [30]. The subsequent activation of naïve T cells requires 3 defined signals from the initiating APC. The first signal is received through the T cell receptor (TCR) following binding to the relevant antigen/MHC class II complexes presented by dendritic cells, referred to as signal 1 [27]. Thereafter, co-stimulatory molecules, such as binding of CD28 on T cells to CD80 or CD86 on dendritic cells, deliver signal 2 to T cells [27]. Cytokine release by the APC constitutes signal 3, and directs the polarisation of the T cell response [27]. When T cells receive a signal through their TCR that is not accompanied by signals 2 or 3, the cell is likely to become anergic, which may lead to tolerance, in order to prevent immune reactions against self antigens that are presented in the absence of inflammatory signals [27,31].

T helper cell subset differentiation

Following receipt of the 3 signals identified above, T cells become activated, and differentiate into one of several subsets of effector cells, depending on the cytokine signals from the initiating APC and/or the surrounding environment. The resulting T helper cell subsets are characterised by the expression of particular transcription factors, and the secretion of specific cytokines. Each subset is tailored for specific types of infection and specialises in particular functions, such as driving production of specific antibody isotypes by B cells, subject to the requirements of the immune response at the time. A summary of the cytokine signals that drive T cell subset differentiation, their associated transcription factors, cytokines they produce, and immune responses in which they are involved, are presented in figure 1.2.

- Phenotype and functions of effector T helper cells

Briefly, Th1 cell differentiation is induced by IL-12 production by dendritic cells in an IFNγ-rich environment, and functions during intracellular bacterial and viral infections. This cell type typically expresses the transcription factor Tbet, and secretes large amounts IFNγ, as well as IL-2 [32]. IFNγ has diverse effects on immune cells, including the activation of macrophages, while IL-2 induces further T cell division. T cell help for B cells under Th1 conditions results in the secretion of IgG isotypes, specifically IgG2a/c, IgG2b and IgG3. Th2 cells, on the other hand, differentiate in response to IL-4 signalling, express the transcription factor GATA3, and secrete IL-4, IL-5 and IL-13 as their signature cytokines [32]. The original source of this IL-4 that drives Th2 cell differentiation is not thought to be dendritic cells, but may instead be basophils [33]. Th2 responses generate IgG1 and IgE production by B cells [34], and play roles in helminth infection, as well as allergic reactions. The cytokines produced by Th2 cells, namely IL-4, IL-5 and IL-13, have a range of effects on both immune and non-immune cells, including the activation of mast cells, eosinophils and basophils, generation of alternatively activated macrophages, contraction of smooth muscle and increased mucus production by goblet cells [35].

For many years the Th1 and Th2 cell subsets dominated the field until, recently, several more T cell subsets were discovered, namely Th17 cells and regulatory T cells (Treg cells). Th17 cells are characterised by their expression of Rorγt and secretion of IL-17 (A and F) and IL-22, and are thought to function in immune responses to extracellular bacteria and fungi, especially at the mucosal sites [32]. Their differentiation occurs in response to transforming growth factor-β (TGFβ) together with IL-6 production by APCs, while IL-23

may also be involved in their generation and/or maintenance [36]. Interestingly, TGFβ production alone or in conjunction with IL-2 gives rise to a further subset of T cells, the inducible regulatory T cells (iTreg cells) [37]. These cells, unlike the natural regulatory T cell population that develops in the thymus, are capable of differentiation in the periphery. Both natural and inducible Treg cells are thought to express the transcription factor FoxP3, while a proportion of them also appear IL-25^{+} (IL-2Rα^{+}) [37]. Regulatory T cells perform a critical function in regulating immune responses, a role demonstrated by the severe and lethal autoimmune disease that develops in FoxP3-null mice [38].

Meanwhile, controversy surrounds the latest T cell 'subset' of IL-9 producing Th9 cells, also involved in immunity to intestinal helminths. These cells are thought to develop either from Th2 cells following TGFβ signalling, or directly from early activated T cells when stimulated with IL-4 plus TGFβ [39]. Although the authors describe these Th9 cells as distinct from either Th1, Th2, or Th17 cells *in vitro* [39], whether or not this cell type really is a separate lineage of T helper cells remains a topic of debate [37]. For this reason, I have excluded Th9 cells from figure 1.2. Finally, a further subset of T helper cells is the T_{FH} cells, which differentiate in response to IL-21 and IL-6 [40], and are located in the B cell follicles. These cells, which express the transcription factor Bcl-6 (B cell lymphoma-6) [41,42] and are specialised at providing help for B cells, are discussed in greater detail later.

- The role of TGFβ in T cell regulation and differentiation

As mentioned above, one of the cytokines involved in determining the phenotype of the T cell response is TGFβ. TGFβ alone or with IL-2 leads to iTreg cell differentiation, while TGFβ plus IL-6 results in Th17 cell generation, or with IL-4 results in Th9 cells [37,39]. The TGFβ family consists of 3 related cytokines, TGFβ1, TGFβ2, and TGFβ3, which show high levels of homology [43]. Members of the TGFβ family of cytokines are widely distributed throughout the mammalian body, and are capable of influencing the functions of a large variety of cell types. TGFβ1, the main TGFβ family member expressed in the immune system, is synthesised in an inactive form [44]. Secreted TGFβ, in a complex with other proteins, requires a low pH, proteolysis and binding to cell surface proteins for activation [45]. Activated TGFβ then binds its receptor (TGFβR), which consists of the ALK5 subunit together with the TGFβRII subunit [44]. Treg cells secrete TGFβ, in conjunction with other cytokines (see figure 1.2), which can impact on cells in both the innate and adaptive immune system.

Multiple cell types within the immune system express the TGFβ receptor and thus can be regulated by this cytokine. These include macrophages, dendritic cells, natural killer cells, and B and T cells [45]. TGFβ1-mediated suppression of immune cells is a vital part in the control of inflammation, and without it death occurs around 4 weeks of age as a result of multifocal inflammation, leading to multiple organ failure [46]. Similarly, disruption of the TGFβ receptor signalling pathway ($TGF\beta R^{-/-}$) in an inducible system led to death following excessive inflammation [47]. These studies highlight the essential role of the TGFβ family members in the wholesale regulation of immune cells. However, the specific function of TGFβ-mediated regulation of the T cell compartment is not addressed in these reports.

More recently, a mouse strain has been generated, in which T cells express a mutant form of the TGFβ receptor, and thus cannot respond to TGFβ signals [43]. Specifically, these mice express a dominant-negative form of the TGFβ receptor type II under the control of the CD4 promoter (CD4-dnTGFβRII mice). This receptor, similar to its wild type counterpart, is capable of binding all 3 isoforms of TGFβ, however, due to the truncated nature of its intracellular domain, signal transduction within the cell is interrupted [48]. The lack of the CD8 silencer in this particular strain of mice allows the expression of the mutant form of the TGFβRII on all $CD4^+$ and $CD8^+$ T cells [43]. Studies in these mice have revealed the importance of TGFβ-mediated regulation of the T cell population, as these CD4-dnTGFβRII mice develop spontaneous autoimmune disease. Disease onset occurrs around 3-4 months of age, and is characterised by severe inflammatory bowel disease, infiltration of lymphocytes into multiple organs, and the presence of auto-reactive serum antibodies [43]. Therefore, similar to $TGF\beta 1^{-/-}$ and $TGF\beta R^{-/-}$ mice, in mice in which T cells alone cannot respond to TGFβ, excessive inflammation ultimately leads to death, albeit with delayed kinetics. Therefore, the inability of the T cell populations, alone, to respond to TGFβ signalling was enough to break self-tolerance and induce fatal autoimmunity, emphasizing the need for the TGFβ-producing Treg cell population and/or TGFβ-mediated suppression.

Interestingly, the generation of these CD4-dnTGFβRII mice has provided conflicting evidence as to the role of TGFβ in the development of Treg cells. While previous studies reveal TGFβ to be essential for the generation of Treg cells [49], others have shown in $TGF\beta 1^{-/-}$ mice that Treg cells develop normally in the absence of TGFβ [50]. Some data suggested that natural Treg cells could develop, but were poorly maintained in the periphery, in the absence of TGFβ [51]. Importantly, use of the transgenic CD4-dnTFGβRII mice revealed Treg cell numbers to be normal [52]. Thus, it seems likely that the development of

natural Treg cells in the thymus may be possible in the absence of TGFβ. However, the possibility remains that the maintenance of Treg cells in the periphery, and the generation of inducible Treg cells, may be more reliant on this cytokine [44]. Thus, although some Treg cells exist in the CD4-dnTGFβRII mice, the lack of TGFβ-mediated control of T cells resulted in the loss of tolerance to self-antigens, emphasizing the importance of TGFβ as a regulatory cytokine in the T cell compartment under steady-state conditions.

Furthermore, due to the reliance of Th17 cell (and possibly Th9 cell) differentiation on TGFβ, such responses are likely impaired in the CD4-dnTGFβRII mice. Indeed, such mice have been shown to lack Th17 cells, and do not develop Experimental Autoimmune Encephalomyelitis (EAE), a disease mediated by self-reactive Th17 cells [53]. Due to the novel nature of Th9 cells, they have not, as far as I am aware, been studied in these CD4-dnTGFβRII mice. Indeed, the use of these mice may be informative as to the need for TGFβ for IL-9 production, and provide information as to the distinctiveness of the Th9 cell lineage. The generation of these CD4-dnTGFβRII mice has, therefore, proven a useful tool in evaluating the specific roles of TGFβ signalling in T cells in immunity and regulation, and will continue to do so.

- T follicular helper cells (T_{FH} cells)

As stated above, a further subset of T cells is the T_{FH} cell population that, as their name suggests, resides within the follicles of secondary lymphoid organs and provides help for B cells. Specifically, T_{FH} cells function in aiding adaptive B cell responses, by driving the GC reaction, class switching of immunoglobulin, and plasma and memory cell differentiation [54], and indeed such responses of B cells are absolutely dependent on the presence of T helper cells [55,56]. The transcription factor Bcl-6 has been shown to be involved in the differentiation of T_{FH} cells, which occurs in response to IL-21 and IL-6 signalling [40,41,42], as outlined in figure 1.2. Without Bcl-6 expression in T cells, the development of T_{FH} cells is severely reduced [41], highlighting the importance of this transcription factor in their differentiation. Conversely, over-expression of Bcl-6 leads to the upregulation of the hallmark T_{FH} cell molecules, CXCR5 and PD-1, and thus an increase in the total number of cells with the T_{FH} cell phenotype [42].

Such T_{FH} cells are situated within the follicles due to their expression of the chemokine receptor CXCR5, while they do not express CCR7, and thus they migrate towards CXCL13 secreted by follicular dendritic cells [11]. T_{FH} cells can therefore be identified by flow

cytometry by this $CXCR5^+$ phenotype, as well as expression of either ICOS (inducible co-stimulator) or PD-1 (programmed death-1) [54]. By immunohistology of splenic tissue sections, $CD4^+$ T_{FH} cells can be seen clearly within the follicles, in close association with follicular B cells. Their expression of ICOS, a co-stimulatory molecule belonging to the CD28 family, is involved in the positive regulation of B cells during the GC reaction, as well as in the maintenance of the T_{FH} cell population [11]. Specifically, a B-T cell interaction in the follicular region, involving ICOSL and ICOS interaction, is required for the maintenance of cells with the T_{FH} cell phenotype [40], highlighting the vital role of B cells. In the absence of ICOSL expression by B cells, T_{FH} cell numbers are significantly reduced [40]. In addition to ICOS expression, T_{FH} cells can be identified by their high expression levels of the inhibitory molecule PD-1. PD-1 signalling appears to be involved in maintaining the function of T_{FH} cells, as in the absence of PD-1, although T_{FH} cell numbers were actually enhanced (for reasons unknown), their function in terms of cytokine production and help for B cells was diminished [57]. T_{FH} cells also express high levels of CD40 ligand, a co-stimulatory molecule for B cells, which together with ICOS and PD-1 are involved in the positive regulation of B cells during and after the GC reaction, and impact B cell differentiation into plasma and memory cells [11,57]. The details of the requirement for T_{FH} cells in the generation of B cell responses, including the roles of ICOS, PD-1 and CD40L, are discussed later, with reference to B cell activation and differentiation.

As discussed above, T helper cell subsets can be further characterised by their unique cytokine secretion profile. In the case of T_{FH} cells, the typical cytokine that they produce is IL-21. The optimal production of IL-21 by T_{FH} cells has been shown to be dependent on their expression of ICOS [58], suggesting that signalling through ICOS, perhaps via interaction with ICOSL expressed by B cells, is a positive feedback mechanism of IL-21 regulation. Not only is IL-21 required for the differentiation of T_{FH} cells [40], but this cytokine may also be involved in their maintenance. This conclusion is drawn from the observation that T_{FH} cells continue to express the IL-21 receptor, and thus IL-21 produced by T_{FH} cells may act in an autocrine manner to ensure the maintenance of this population [58]. However, more recent studies show that IL-21 is not required for the presence of T follicular helper cells in mice [59,60]. T_{FH} cell-derived IL-21 also impacts on the B cell GC reaction and their subsequent differentiation into effector and memory cells, a concept that is discussed fully later in relation to B cell effector and memory cell development.

- Plasticity of T helper cell subsets

Although the different lineages of T helper cell subsets, presented in figure 1.2, appear distinct, in reality the flexibility of effector cells to change phenotype from one to another remains a topic of dispute. The current thinking is that, while some effector subsets are mutually exclusive and inhibit each other's differentiation, others seem more flexible. The plasticity of effector $CD4^+$ T cells also appears dependent on their differentiation state: the further along the effector cell differentiation pathway, the less easy it is to alter effector phenotype. In other words, terminally differentiated effector T cells appear unable to alter their effector phenotype, whereas soon after activation effector cells may alter their subset according to signals received through cytokine receptors [61,62].

Looking specifically at cells of the Th1 and Th2 subsets, cells primed *in vitro* in either Th1- or Th2-inducing conditions may be able to switch from IFNγ to IL-4 production, or vice versa, at early stages of the culture. During the transition phase, $IFN\gamma^+$ $IL\text{-}4^+$ cells exist, before full differentiation under the new conditions [63]. These data comes to light, despite the observation that IFNγ and IL-4 are co-inhibitory [37], due to mutual inhibition of the master regulators, Tbet and GATA3, at the gene transcription level as a result of changes to gene accessibility due the histone arrangement [64,65,66]. However, cells that have endured more than 1 week of culture under Th1 or Th2 conditions lose the ability to switch effector phenotype and cytokine production, as they become terminally differentiated [63]. One mechanism of this stability is that Tbet or GATA3 expression by Th1 and Th2 cells, respectively, promotes a self-reinforcing feedback loop, which stabilises differentiation [66]. It should be noted, however, that Th1 and Th2 cells generated *in vivo* during infection may differ in their effector subset flexibility than those generated under strong polarising conditions *in vitro*, as has been suggested [32]. Moreover, Th17 cells appear much less rigid throughout the differentiation pathway, than Th1 and Th2 cells. Due to the requirement for TGFβ, Th17 cells share a close lineage with iTreg cell differentiation, and also appear able to switch to a Th1 phenotype and secrete IFNγ, thus have a close relationship with this subset [67]. In EAE, some activated autoimmune cells in the central nervous system secrete both IFNγ and IL-17, confirming the flexibility of the Th17 cell subset [68]. Furthermore, the most recently identified T helper cell subset, the Th9 cells, also show great plasticity, in that they share a common lineage with Th2 cells and may secrete IL-4 [39]. This raises the issue as to whether these cells should truly be considered as a separate effector cell subset. Therefore, in many cases, categorising a T cell response according to the most prevalent cytokine is inaccurate, and does not reflect the heterogeneity of the T effector cells involved.

- The plasticity of T follicular helper cells

The flexibility of the T_{FH} cell population is also a subject of controversy. Chtanova and colleagues describe the T_{FH} cell lineage as entirely separate from the Th1 and Th2 subsets, due to their specific expression of the transcription factor, Bcl-6, and other genes in a highly distinctive profile [69]. Further research also shows T_{FH} cells to be separate from the Th17 cell lineage [40]. One of the studies that identified Bcl-6 as the transcription factor expressed by T_{FH} cells showed that over-expression of this transcription factor resulted in the inhibition of other T helper effector cell lineages [41]. This repression of the Th1 and Th17 lineages was found to be due to Bcl-6 binding to the promoters of the Th1 and Th17 master regulator transcription factors, Tbet and Rorγt, and repressing the production of the cytokines, IFNγ and IL-17 [42]. Together, these data suggest that T_{FH} cells are a distinct subset, unrelated to Th1 and Th17 cells.

Furthermore, the transcription factors Bcl-6 and Blimp-1 are mutually exclusive in lymphocyte populations [70]. As Blimp-1 has been implicated in effector T helper cell development [71,72], this transcription factor may be a specific marker for effector Th cells, as is the case in both the B cell and $CD8^+$ T cell compartments [71]. Conversely, as stated above, Bcl-6 is essential for T_{FH} cell differentiation [40,41,42]. Therefore, again, these data on expression of the transcription factors Bcl-6 and Blimp-1 point to the T_{FH} cell lineage as separate from other effector T helper cell subsets. Indeed, Blimp-1^+ effector T helper cells appear unable to provide B cell help, and thus cannot perform T_{FH} cell functions [72].

However, a more recent review discusses the potential for T_{FH} cells isolated during an immune response to resemble Th1, Th2 or Th17 effector cells [63]. Indeed, during helminth infection, $GATA3^+$ Bcl-6^+ cells have been isolated, which the authors called T_{FH} cells due to their expression of CXCR5 and location in the follicles, highlighting the possibility either that effector Th2 cells can gain the T_{FH} cell phenotype during infection, or vice versa [73,74]. These data is further supported by the observation that newly activated T helper cells upregulate CXCR5 and migrate into the follicles [75]. Therefore, the possibility remains that antigen-activated T helper cells found in follicles soon after immunisation/infection may differ in phenotype and function from true T_{FH} cells that initiate B cell selection and differentiation post-GC, as has been suggested in a recent review [71]. Thus, again, labelling T cells as 'follicular helpers' or 'T_{FH} cells' due to their expression of CXCR5 may mask different types of T_{FH} cells, and one should keep in mind the potential diversity in this subset when discussing T_{FH} cells identified in this way.

Immunological memory

One of the defining characteristics of adaptive immune cells is their ability to generate memory. This memory is the basis of immunity to disease and the reason that vaccines are effective in protecting the host from infection. Such protective immunity is long-lived, although putting a numerical figure on the longevity of memory cells in humans is a difficult task. However, the concept of immunological memory has long been accepted, and more recently the cellular basis has been determined. While protective immunity by B cells consists of both memory cells and long-lived plasma cells, which maintain levels of serum antibodies, T cell memory consists only of memory cells, while long-lived effector cells are absent. Thus, the longevity of immune memory is as a result of the development of specialised memory cells, with a lifespan of ~4-6 weeks [76], and the maintenance of these memory cell clones (perhaps for the life of the host?) by means of homeostatic turnover. Here, the development and characteristics of memory cells in the T cell population are discussed.

During the initial phase of the T cell response, antigen-specific T cells rapidly expand in response to antigenic stimulation. It is well documented that the clonal expansion of $CD8^+$ T cells is greater than that of $CD4^+$ T cells. In other words, at the peak of the primary immune response, antigen-specific cytotoxic T cells account for a much larger proportion of the $CD8^+$ T cell repertoire than effector T helper cells do of the $CD4^+$ T cell repertoire [77]. In both cases, most of the antigen-specific T cells that are generated differentiate into short-lived effector cells, and function in pathogen clearance. In the case of $CD4^+$ T cells, the effector cells will be of a specific subset phenotype, as described in figure 1.2, depending on the infectious agent and cytokine environment. Most of these T cells found at the peak of the primary response that recognise antigen will undergo the cell death process during the contraction phase, the onset of which correlates with the disappearance of antigen due to pathogen clearance [77].

However, a proportion of activated antigen-specific T cells survive the contraction phase, and go on to form memory cells, although the identity of the survival signal(s) involved remains ill-defined. The resulting memory cells differ from their naïve counterparts in terms of functional ability to respond to pathogens. Specifically, memory cells mount an accelerated and enhanced response when antigen is encountered for a second time [76]. Although the concept of immune memory has long been accepted, and the adaptive cell

types with a memory feature have been identified, dissecting the pathways and processes that lead to memory development, as well the phenotype of antigen-specific memory cells, has been a slow procedure.

- $CD4^+$ T cell memory characteristics

The memory population of T helper lymphocytes generated after immune activation differs from naïve T cells in several characteristics. Firstly, the frequency of antigen-specific memory cells retained after antigen exposure is greater than the frequency of naïve cells specific for that particular antigen [76]. Secondly, in addition to this quantitative difference in memory $CD4^+$ T cells, they also differ qualitatively from naïve T cells. In this respect, not only are memory cells longer lived than naïve cells, but they also differ in terms of their response to antigen.

Specifically, memory T helper cells respond stronger and faster to antigen, and thus are likely to be more efficient at antigen clearance [78]. Some evidence suggests that memory T cells can respond to lower doses of antigen, and do not rely so heavily on co-stimulation from the initiating APC, thus explaining the faster response time [78,79]. Recent analysis of T cell-APC interactions using *in vivo* imaging suggests memory T cells are also more efficient at surveying antigen on APCs than naïve T cells, a trait that also promotes a faster response time [80]. Furthermore, memory T cells differ in their cytokine-producing ability, compared to naïve cells. For example, memory cells are thought to produce significantly larger amounts of IL-2 in response to antigenic stimulation compared to naïve cells, increasing their potential for rapid division [79]. The explanation for this ability to rapidly secrete cytokines is due to the altered, more open, chromatin structure within memory cells [77]. Additionally, some studies report that memory $CD4^+$ T cells secrete a broader range of cytokines, compared to naïve or primary effector cells, such that pathogen clearance will be efficient even under different inflammatory conditions, or when the pathogen enters via a different route [78]. This flexibility in memory cell cytokine secretion, and the lack of distinction between Th1/Th2/Th17 cell subset phenotypes in the memory phase, remains an important area of investigation.

- The models of T helper cell memory differentiation

The pathway leading to T helper cell memory generation, and the exact signals required for memory cell differentiation, remain elusive. A diagram of the possible differentiation pathways of $CD4^+$ T cell subsets is shown in figure 1.3 (adapted from [77]). Several theories

exist as to the developmental relationship between effector and memory T helper cells: is it a linear pathway where effector cells further differentiate into memory cells (figure 1.3A)? Or are these two pathways separate in a diverging model [81] (figure 1.3B)? If the latter is the case, then this leaves us with questions regarding the initial choice between effector and memory cell differentiation: how does a newly activated T cell decide whether to become an effector cell or a memory cell?

The discovery of central and effector memory cells in the $CD4^+$ T cell population, which differ in their expression of surface markers and localisation within the host (discussed further below), complicates matters further [82] (figure 1.3C). In humans, central memory T cells have a $CCR7^+$ $CD62L^+$ phenotype and therefore can enter the lymph nodes and home to the T cell zones, whereas effector memory T cells are $CCR7^-$ and heterogeneous for CD62L expression, but express other adhesion molecules and chemokine receptors that allow migration to inflamed tissues, but such cells are not attracted to the T cell zones of secondary lymphoid organs [83]. For a more detailed analysis and discussion of these effector and central memory cells, see below. So-called 'effector' memory cells appear to have a more limited lifespan, and reduced proliferative capacity, when compared to 'central' memory cells [84]. This particular model (figure 1.3C) suggests that 'early' and 'late' effector cells vary in their memory-generating capacity. However, the distinction between 'early' and 'late' effector cells, as well as between effector and effector memory cells, in terms of surface markers and function is less clear. Clearly, further research in this field is necessary to gain answers to these questions.

- The difficulties in studying $CD4^+$ T cell memory

However, due to the low numbers of antigen-specific $CD4^+$ T cells found during immune responses, it is difficult to study T helper cell memory generation *in vivo*. In the past, transgenic T cell transfers have been used by as a tool for analysing antigen-specific $CD4^+$ T cell responses following immunisation [85]. However, this system has several drawbacks, namely the vastly large and non-physiological numbers of responding T cells of the same clone. Furthermore, the generation of a stable memory population in this system proved difficult ([85] and my unpublished data). Indeed, work by Hataye *et al* showed that clonal abundance controls cell survival, and it is necessary to transfer low numbers of transgenic T cells (~1000) for a stable memory population to be generated after immunisation [86]. Using this method of transferring low numbers of T cells, and detecting donor cells using an enrichment protocol, it was shown that, although T helper cell memory was long-lived, it

was not entirely stable, but declined steadily over time [86]. These data contrast to that from analysis of $CD8^+$ T cell memory, in which the number of memory cells of a particular specificity is thought to be relatively consistent over long periods of time, due to homeostatic turnover [77].

Despite overcoming some of the problems of the transgenic T cell transfer model, this system of transferring low numbers of antigen-specific T cells is not ideal for studying memory generation, as it relies on measuring transferred rather than endogenous T cell responses, and thus does not truly reflect *in vivo* responses to antigen. Recent advances in experimental methods, and the advent of MHC class II tetramers (see below), have resulted in the development of better techniques for the study of endogenous $CD4^+$ T cell memory generation *in vivo*, in polyclonal systems. Thus, the processes and differentiation pathways involved in T helper cell memory generation may be unravelled in the near future. Indeed, this thesis uses such techniques to investigate the specific requirement for B cells in T helper cell memory generation. In the meantime, lessons may be learnt from the understanding of $CD8^+$ T cell memory development.

- Studies of $CD8^+$ T cell memory generation

The larger numbers of antigen-specific $CD8^+$ T cells during a primary immune response, and the success of MHC class I tetramers, make cytotoxic T cell differentiation pathways easier to study *in vivo*, without the need for transgenic T cell transfers. Kaech and colleagues have gone some way to dissecting the differentiation of effector and memory cells in $CD8^+$ T cells [87,88,89]. Joshi *et al*, for example, distinguished between terminally differentiated short-lived effector cells (SLECs) and memory precursor effector cells (MPECs) using the cell surface markers as follows: SLECs were identified as IL-$7R^{lo}$ $KLRG1^{hi}$, whereas MPECs, which had greater potential for memory generation, were defined as IL-$7R^{hi}$ $KLRG1^{lo}$ [87]. Additionally, the authors state that the relative levels of Tbet expression (which is also the Th1 master regulator in $CD4^+$ T cells) regulate the generation of SLECs and MPECs in the $CD8^+$ T cell population. Specifically, high expression of Tbet leads to SLEC differentiation, whereas low levels of Tbet promotes MPEC development [87]. It would be interesting to determine if the expression levels of Tbet reflect the affinity of the TCR for antigen. The authors, therefore, suggest a relatively divergent model of differentiation, with the cell fate decision being made early in the response [88]. Although both MPECs and SLECs have an effector cell phase, terminally differentiated SLECs appear unable to further differentiate into memory cells.

Meanwhile Rutishauser and colleagues revealed a role for the transcription factor Blimp-1 in determining the effector/memory fate of $CD8^+$ T cells. Blimp-1 was found to promote effector cell differentiation, and acted as a marker for effector cell identification, while the absence of this transcription factor led to an increased prevalence of memory precursor cells [89]. Conversely, the transcription factor Bcl-6 has been implicated in the generation of memory cytotoxic T cells [90]. These data, therefore, also point to a relatively divergent model of effector and memory cell differentiation, with cells becoming either Blimp-1-expressing effectors or Bcl-6-expressing memory cells. These ground-breaking studies have provided great insight into the differentiation model of $CD8^+$ T cells. These data also allow us to speculate on the potential parallels in $CD4^+$ T cell memory generation.

- Implications for $CD4^+$ T cell memory generation

The differentiation pathways of cytotoxic and helper T cells may (or may not) be similar. Certainly, some parallels between $CD4^+$ and $CD8^+$ T cell effector and memory phenotype have already been discovered. For example, IL-7Rα expression, reported above to be a $CD8^+$ MPEC marker [87], has also been seen in memory cells of the $CD4^+$ T cell population [91], and reflects the dependence on IL-7 signalling for homeostatic turnover of memory cells (see below). Furthermore, Blimp-1 expression by effector cells is similar in $CD8^+$ and $CD4^+$ T cells [92], as well as in the B cell population [93]. Together, these data support the notion that the pathways of effector and memory cell differentiation may be similar in the cytotoxic and helper T cell compartments (as well as in B cells), and perhaps controlled by the transcription factors Bcl-6 and Blimp-1. The identification of SLECs and MPECs in the $CD4^+$ T cell population would be required to further support this theory.

The potential role of Tbet expression in regulating cell fate between effector and memory differentiation is an interesting mechanism, which also requires future investigation in $CD4^+$ T cells. In addition to the roles of transcription factors, other observations have been made in relation to the effector/memory cell fate decision in T cells. Firstly, the strength of the signal received through the TCR is thought to determine whether the cell differentiates into an effector or memory cell [94,95]. Factors that contribute to signal strength include antigen concentration, expression levels of MHC and co-stimulatory molecules on the APC, and the duration of the APC-T cell interaction. For example, a sustained APC-T cell interaction may induce effector cell differentiation, while a transient but sufficient signal may result in memory generation [84]. Ahmed and co-workers suggest that antigen levels are important in

determining memory generation, with low levels driving the differentiation of cells into 'central' memory cells, resulting in the accumulation of memory cells of this type [77]. This may be a mechanism to ensure T cell clones of the highest affinity enter the memory pool. Secondly, the size of the memory pool generated is directly proportional to the amount of expansion during the primary response, a process driven by OX40 signalling [96], suggesting that this co-stimulatory molecule plays a role in the cell fate decision. Also, a direct role of B cells is essential for T helper memory cell differentiation, a requirement that is discussed in much greater detail below, with respect to B cell antigen presentation.

- Identification of memory T helper cells using cell surface markers

The use of cell surface markers to determine T helper cell activation status and subset phenotype has proved challenging. Unfortunately, there do not appear to be any definitive markers for memory T helper cells. However, some combinations of markers have been outlined for naïve, activated, or memory T cell distinction. These markers are predominantly adhesion molecules and chemokine receptors, and thus memory cells are identified by their altered migration patterns *in vivo*. Naïve T cells, for example, have been described as $CD62L^{hi}$ $CD44^{lo}$, while activated and memory T cells have a $CD62L^{lo}$ $CD44^{hi}$ phenotype [97] (figure 1.4A). While CD62L mediates cell rolling on the endothelium and is involved in lymphocyte entry into the lymph nodes (see below), CD44 binds to Hyaluronan and mediates cell binding to the extracellular matrix and other cells [98].

With the discovery of central and effector memory populations within the $CD4^+$ T cell compartment, these cells too were separated according to their expression of adhesion molecules and chemokine receptors. Specifically, central memory cells are $CCR7^+$ $CD62L^{hi}$, whereas effector memory cells have a $CCR7^-$ phenotype and were seen to be heterogeneous for CD62L expression [82], thus reflecting their altered migration to the T cell zones within secondary lymphoid organs (figure 1.4A). These effector and memory T helper cell distinctions are discussed further in the next paragraph. Meanwhile, the cytotoxic T cell memory population has its own identifying markers. As mentioned above, the most recent studies reveal MPECs to have an $IL\text{-}7R^{hi}$ $KLRG1^{lo}$ phenotype, whereas SLECs are $IL\text{-}7R^{lo}$ $KLRG1^{hi}$ [87], although it remains to be seen whether or not these markers hold true in T helper cell memory populations. Expression of IL-7Rα seems an obvious choice for memory cell identification, due to the role of IL-7 in the maintenance of memory cells (see below). However, the function of KLRG1 (killer-cell lectin-like receptor subfamily G1), shown to provide an inhibitory signal in natural killer cells, on T cells (specifically effector

cells) remains unknown [99]. Identifying these cell surface markers in the $CD4^+$ T cell compartment would therefore go some way to determining if SLECs and MPECs exist in the T helper cell population, and may provide a useful method of distinguishing effector and memory cell populations.

Recently, Ly6C, originally described as a marker for activated T cells, has been identified as a possible marker for the identification of memory $CD4^+$ T cells [97]. In $CD8^+$ T cells, Ly6C has been implicated to function in homing [100], and has been reported to be expressed exclusively by memory cells [101]. In $CD4^+$ T cells, on the other hand, Ly6C may function in regulating cytokine production by Th1 and Th2 effector cells by initiating an inhibitory signal [102]. Whether this cell surface marker really is a novel method of identifying memory $CD4^+$ T cells is investigated further in this thesis (see chapter 6).

- Memory T helper cell migration patterns

As mentioned, the identification of naïve and activated, as well as central memory and effector memory, $CD4^+$ T cells is often performed on the basis of expression of particular cell surface molecules. Many of these molecules are adhesion molecules and chemokine receptors, and their differential expression on T cell subsets reflects their altered migration patterns *in vivo*. Specifically, naïve T cells are identified by their $CD62L^+$ $CCR7^+$ phenotype (figure 1.4A). The expression of the selectin CD62L and the chemokine receptor CCR7 result in naïve T cell migration across the high endothelial venules into the lymph nodes, and their subsequent accumulation in the T cell zone by attraction to the chemokines CCL19 and CCL21 [103]. Activated effector T cells, on the other hand, display a very different migration pattern. Effector T cells tend not to express CCR7 or CD62L, and therefore do not migrate to lymph nodes, but instead express adhesion molecules such as LFA-1, VLA-4 and PSGL-1, together with chemokine receptors, including CXCR3, which allow the migration of effector T cells to sites of inflammation (figure 1.4A) [103,104]. Effector memory T cells appear to resemble effector T cells in terms of adhesion molecule and chemokine receptor expression, and similarly migrate preferentially to inflamed tissues rather than lymph nodes [83] (figure 1.4A). Conversely, central memory T cells retain the ability to migrate to both inflamed tissues and lymph nodes, by expressing molecules required for both lymph node homing (CCR7 and CD62L) and tissue homing (CXCR3 and other adhesion molecules), as outlined in figure 1.4A [83].

As mentioned, chemokine receptors such as CXCR3 enable effector and memory T cell populations to migrate to sites of inflammation within the body. In addition to these inflammatory chemokine receptors, some sub-populations of memory cells express tissue-specific adhesion molecules and chemokine receptors [104]. The best example of this tissue-specific homing of memory T cells is to the gut. As can be seen in figure 1.4B, lymphocyte migration to the gut requires expression of the integrin α4β7 and/or the selectin CD62L, which bind to MAdCAM-1, and the chemokine receptor CCR9, which recognises the gut-associated chemokine CCL25 [103]. Expression of these molecules by a memory T cell would ensure migration to the gut. Alternatively, skin-specific chemokine receptors include CCR10 and CCR4, which bind CCL27 and CCL17, respectively, in the skin tissue [104]. A more detailed description of the adhesion molecules and chemokine receptors required for T cell entry into specific tissues, such as the gut and skin, is given in figure 1.4B.

Thus, the precise identification of memory T helper cells is a confusing process, with different research groups using varying combinations of cell surface markers. Really, the only failsafe method of pinpointing memory cells directly *ex vivo* in a polyclonal system (i.e. without using cell transfers) is to look for antigen-specific T cells that survive after antigen clearance.

- Maintenance of memory T helper cells

The signals required for memory cell differentiation might be distinct from those required for memory cell survival and long-term maintenance, although dissecting the requirements for memory cell generation versus maintenance is a difficult task. It appears that, although memory cells are long-lived (~4-6 weeks or more [76]), they require signals to survive and maintain their numbers over long periods of time, by homeostatic turnover. The specific requirements for T helper memory cell survival have been investigated *in vivo*.

One signal that has dominated this area of research is the role of antigen, and presentation by APCs, in the maintenance of memory T helper cells. The requirement for antigen has proved difficult to study *in vivo,* as it is necessary to ensure complete antigen clearance in order to investigate the longevity of memory cells. In many instances, antigen persists for long periods of time, such as in persistent viral infections, or can form antigen depots, such as on follicular dendritic cells. Therefore, many studies made use of cell transfers from primed mice into either mice incapable of antigen presentation (MHC-deficient) or into mice with a different MHC haplotype that donor cells do not recognise. Some studies concluded

that, in the complete absence of antigen presentation, T helper cell memory was short-lived [105], suggesting antigen presentation is essential in memory maintenance [106]. However, a more recent report suggested T helper cell memory to survive independently of MHC class II [107]. Furthermore, the transfer of memory T helper cells into MHC class II-deficient hosts resulted in the loss of function of memory T cells over time [108,109], suggesting TCR signalling is involved in the long-term maintenance of memory cells, or their function, in this system. Despite these discrepancies in results, presumably due to the vastly different systems used, the current thinking is that, although antigen may not be essential in situations where competition is absent (such as in experiments using immuno-deficient mice, which possess unlimited niches for memory cells to inhabit), the presence of antigen is likely to increase the likelihood of memory cell survival [110]. Thus, if we think of a limited number of memory cell niches within the host, competition exists between cells for survival. In such a setting, cells that receive antigenic stimulation through the TCR are, therefore, likely to be favoured over those that do not receive such signals [110]. However, whether or not there is an absolute requirement for antigen presence remains a controversial topic.

In addition to TCR signalling, cytokine signals also appear essential for the maintenance of memory T helper cells. Namely, IL-7 promotes the survival and homeostatic turnover of the memory helper and cytotoxic T cell populations [111], hence the use of IL-7Rα expression as a means of identifying memory T cells. The role of IL-15, which is also necessary in maintaining $CD8^+$ T cell memory [112], in T helper cell memory maintenance remains disputed, but appears less essential [113]. This opinion is supported by the observation that memory $CD4^+$ T cells express lower levels of the IL-15 receptor than memory $CD8^+$ T cells, indicating that T helper cell memory maintenance is less dependent on IL-15 [114]. Thus, signals through both the TCR and IL-7R appear to be vital in the maintenance of T helper memory cells *in vivo* [115].

Furthermore, some studies also highlight the potential involvement of B cells in the maintenance of T helper cell memory [106,116], as well as in their generation (see below). The maintenance of memory $CD4^+$ T cells appears to be dependent on B cells, although their antigen presentation seems to not be essential [116]. Therefore, B cells may be providing a signal other than the MHC class II/TCR interaction for the survival of memory T cells. Thus, many questions remain unanswered in reference to both the development and maintenance of $CD4^+$ T cell memory, and specifically the need for B cells continues to be an area of active research.

Overview of B cell functions

The B cell population consists of several different subsets, which differ in their phenotype and function. As mentioned above, marginal zone and follicular B cells are found within the spleen. A further subset of B cells, the B1 cells, are located primarily in the peritoneal cavity, although small numbers of these cells are also detectable in the spleen. These B1 cells, identified by their $B220^{int}$ $CD5^{int}$ phenotype, are one of the main producers of cross-reactive 'natural' antibody, involved in the early stages of immune defence [117]. In the past, the focus of B cell function has been on the GC reaction, and the subsequent generation of plasma cells and memory. Thus, the diversity of B cell functions is often overlooked.

B cells have both innate and adaptive roles in immune defence, and are therefore at the interface of these two arms of the immune system. Traditionally, B cells are thought of as members of the adaptive immune response, due to their roles as antigen presenters, their major function as producers of high affinity class-switched antibody, and their ability to generate memory cells. However, B cells also respond rapidly to pathogen ligands through innate receptors, such as TLRs, resulting in the production of cytokines and cross-reactive antibody, and thus also function in the early innate immune response to pathogens.

- Toll-like receptor (TLR) structure and signalling

Toll was first identified in Drosophila, and found to have a role in host defence against fungal infection [118,119]. Since then, a mammalian homologue of Toll was discovered [120]. The family of mammalian proteins relating to Drosophila Toll were found to share conserved regions, and was thereafter named the Toll-like receptors (TLRs). Similar to that in Drosophila, this family of proteins was also found to function in the immune system, and induce inflammation [121]. TLRs are a family of type 1 transmembrane proteins, found in both mice and humans, which are characterised by the presence of a leucine-rich repeat extracellular domain and a highly conserved Toll-IL-1 receptor (TIR) cytoplasmic domain [121]. These receptors are found on the cell surface and in the endosomal compartment, and recognise structurally conserved molecules of pathogens, called PAMPs. Such pathogen ligands include LPS, foreign DNA and RNA, and flagellin, while host 'danger' factors, such as heat shock proteins, can also act as ligands [121]. Signalling through these TLRs results in activation of distinct yet overlapping signalling pathways, involving adaptor proteins such as MyD88 and TRIF. An overview of TLR location, ligands, and signalling pathways is presented in figure 1.5 (adapted from [122]).

Ultimately, TLR signalling leads to the activation of transcription factors, including members of the NFκB family, and transcription of target genes (see figure 1.5B). The target genes of NFκB are predominantly inflammatory molecules, and include cytokines (IL-1, IL-6, IL-12, TNFα), adhesion molecules (ICAM, VCAM), inducible enzymes (inducible nitrous oxide, iNOS), MHC class II, and anti-microbial peptides (e.g. β-defensins), to name but a few [123]. The cytokines IL-1, IL-6 and TNFα initiate an inflammatory response and activate innate cells, while induction of iNOS and anti-microbial peptides are involved in direct pathogen killing. In addition to this innate response that mediates pathogen killing, NFκB targets help to prime the adaptive immune response. For example, the up-regulation of MHC class II molecules by cells such as dendritic cells and macrophages, which possess TLRs, allows antigen presentation to T cells and, in conjunction with IL-12, initiates Th1 cell differentiation and subsequent IFNγ production [123]. Thus the recognition of microbial compounds through TLRs is a vital mechanism in the efficient induction of immune responses. However, it is not only innate cells that express these pattern recognition receptors, but B cells, too, express TLRs, and thus can respond to pathogen molecules directly.

- Stimulation of B cell TLRs

Murine B cells are known to express TLRs 1-9 at the mRNA level [124], although expression levels are thought to vary between subsets. When stimulated through these TLRs *in vitro*, B cells are induced to proliferate and differentiate into antibody-secreting plasma cells in a T cell-independent manner. Notably, plasma cell differentiation is most pronounced in marginal zone and B1 subsets of B cells, while TLR stimulation only marginally promotes plasma cell differentiation in follicular B cells [125]. IgM is the most dominant antibody isotype secreted by B cells in response to TLR stimulation, although both IgG and IgA can also be detected [125]. Likewise, *in vivo* responses to T-dependent antigens also require TLR signalling in B cells for optimal antibody production [126,127]. Specifically, these studies found that B cell MyD88 signalling is required for IgM and IgG2a/c responses. In addition to antibody production, TLR stimulation of B cells also induces upregulation of cell-surface MHC class II and co-stimulatory molecules [124], enhancing antigen-presenting capacity, and secretion of cytokines such as IL-6, IL-10 and IFNγ [124], allowing the regulation of helper and regulatory T cell responses [128]. Therefore, the rapid innate response of B cells to pathogens via TLR stimulation has a direct impact, not only on the developing adaptive B cell response, but also on the magnitude and phenotype of the helper T cell response.

Although TLR-induced activation of B cells is important for early plasma cell differentiation and for enhancing their antigen presenting capacity, this mechanism has been implicated in autoimmunity, as a means of breaking B cell tolerance by bypassing the requirement for T cells. For example, TLR9 stimulation by CpG DNA has been implicated in Systemic Lupus Erythematosus (SLE) and Rheumatoid Arthritis (RA), diseases which are characterised by DNA-specific autoantibodies [129]. Class switched IgG2a and IgG2b autoantibodies in SLE are dependent on B cell signalling through TLR9 and MyD88 [130]. This TLR is therefore a potential therapeutic target to reduce disease severity. Contradictory data, however, suggests B cell TLR9 stimulation as a means of IL-10 production, which functions in regulating autoimmunity [131,132]. Thus, individual TLRs have the potential to drive activation or regulation, and the involvement of TLR stimulation of B cells in the induction or exacerbation of autoimmune disease is a topic of interest, and a potential therapeutic target.

- B cells as antigen-presenting cells

Although TLR stimulation of B cells can induce plasma cell differentiation and cytokine production in a T cell-independent process, an interaction with T helper cells is required for several aspects of B cell function, namely GC formation, somatic hypermutation, class switching, and memory generation. The initiation of this cognate interaction between B and T cells requires antigen presentation by B cells via MHC class II, the binding of antigen-specific T cells, and the formation of an immunological synapse between the two cells.

B cells recognise cognate antigen through their BCR, and subsequently internalise this antigen by BCR-mediated endocytosis. This process is particularly efficient when antigen concentrations are low [133], as the BCR binds specific antigen with high affinity and can therefore concentrate very low levels of antigen for efficient presentation [134]. Particles are then broken down internally, and peptides presented via MHC class II. The expression of HLA-DO, which modulates the function of HLA-DM, means that antigen internalised through the BCR is favoured for presentation via MHC class II molecules [135]. Furthermore, cross-linking of the BCR as a result of antigen binding stimulates the up-regulation of surface CD86, a key co-stimulatory molecule [136]. The presentation of antigen by B cells, together with the expression of co-stimulatory molecules, allows a direct interaction between B cells and T cells. Both cell types benefit from the resulting dialogue, with B cells receiving T cell ‘help’, and T cells receiving co-stimulatory and cytokine signals

required for effector cell differentiation. Therefore, not only do T cells influence the developing B cell response, but B cells also impact on the T cell response.

- B cell influence on T helper cell differentiation

The role of B cells as APCs in influencing T helper cell responses was considered minimal, when compared to that by dendritic cells. While dendritic cells are efficient 'professional' APCs, B cells were thought to make only a minor contribution to T cell activation. However, the antigen-presenting capacity of B cells has been studied both *in vitro* and *in vivo* to determine the extent of their contribution to T helper cell responses.

Initially, *in vitro* experiments showed that different B cell subsets might have varying capacities to present antigen. Specifically, marginal zone, rather than follicular, B cells were found to be the main antigen presenters [21]. Whether or not this is true *in vivo* is difficult to determine. If marginal zone B cells are better APCs *in vivo,* this may reflect their positioning in the marginal zone, where they have ready access to systemic antigen [2]. Such *in vitro* studies expanded to *in vivo* models, with the generation of B cell-deficient mice by means of depletion antibodies. Long-term B cell depletion was achieved by treatment with anti-μ-chain antibodies from the birth of the mice. Data from these mice suggested B cells were an important APC in the lymph nodes [137,138]. Alternatively, some authors used lymphocyte transfers into immuno-deficient mice to determine the role of B cells as APCs. Data from this system suggested a role for B cells as APCs in the activation of memory rather than naïve T cells [139].

However, both these model systems have their drawbacks. Specifically, analysing cell function *in vitro* may not reflect their true *in vivo* function due to the simplicity of the culture, while the treatment of mice with depletion antibodies from birth results in unnaturally high levels of circulating antibody of a particular specificity as well as large amounts of cell death, which may impact on other immune cells. Thus, it was only with the advent of B cell-deficient mice by genetic mutation that the function of B cells in driving T helper cell responses *in vivo* could be more fully dissected. B cell-deficient μMT mice were generated by disrupting one of the membrane exons of the μ-chain constant region [140]. Thereafter, another B cell-deficient strain, the JHD mice, were developed by deletion of the J_H segments in the heavy chain [141]. Using these systems, B cells have since been shown to play an important role in the induction of T cell responses, although the exact part they play in T cell priming remains controversial. While some data reports impaired T cell

priming and proliferation following immunisation [142,143,144], others state that B cells are dispensable for the primary response [145,146]. Constant *et al* reveal a role for B cells in the priming of T cells to protein, not peptide, antigen *in vivo* [147,148]. Further data suggests that antigen presentation by B cells results in a bias towards the induction of Th2 responses [149,150]. The latest report indicates a role for B cells in the development of early Th1 and Th17 responses, a process that is dependent on TLR-induced cytokine secretion by B cells rather than direct antigen presentation [151].

The studies investigating T cell memory responses in B cell-deficient mice are more conclusive. T cell memory generation appears to be significantly impaired in the absence of B cells, a phenomenon shown in both viral [152,153] and bacterial [154,155] infection systems, as well as following protein antigen immunisation [156,157]. Chan and colleagues developed a mouse in which B cells are present but cannot secrete antibody, and therefore contain no circulating immunoglobulin [158]. These mice allowed the distinction between antibody production and antigen presentation by B cells, and their relative roles in T cell memory development. The authors found T cell memory to be normal in these mice, suggesting that B cell antigen presentation is essential for T cell memory generation, whilst antibody production is dispensable [158]. $CD4^+$ T cell memory is also severely impaired in bone marrow chimeras in which the B cell compartment is deficient in MHC class II [142], again indicating that B cell antigen presentation via MHC class II is required for the generation of T cell memory. Furthermore, B cells might be required for the maintenance of the T helper cell memory population once it is generated, a mechanism that is independent of B cell antigen presentation (see above) [116].

- T cell-independent antibody production

The B cell population as a whole has the ability to respond to pathogen stimulation in either a T cell-dependent or -independent manner, and subsequently differentiate into antibody-secreting plasma cells. In part, the dependence on T cells is determined by the subset of the B cell, and the nature of the stimulus. Looking at B cell subset production of antibody, B1 cells in the peritoneal cavity and splenic marginal zone B cells are primed for the rapid production of IgM in a T cell-independent manner, in response to innate signals such as through TLRs. The prompt differentiation of marginal zone B cells into plasma cells in a T cell-independent manner usually occurs in the red pulp regions of the spleen, and is termed an extrafollicular plasma cell response, although such extrafollicular plasma cell responses can also occur in a T cell-dependent manner [159]. The signal strength of antigen

recognition is thought to regulate the choice between extrafollicular and GC responses [160]. The resulting IgM generated in a T cell-independent process is of low affinity, as the cells have not undergone somatic hypermutation. The plasma cells that develop in the absence of T cell help are short-lived [161], and do not form long-lived plasma cells that re-locate to the bone marrow. This early IgM response likely impacts directly on both pathogen clearance and the developing adaptive immune response.

- T cell-dependent GC formation and plasma/memory cell differentiation

In addition to this early production of low affinity IgM by marginal zone and B1 cells, the secretion of high affinity class-switched antibody, mainly by follicular B cells, is a vital component of the adaptive arm of the immune response. The differentiation of high affinity class-switched plasma cells, together with memory cells, is as a result of the GC reaction, and is essential for long-lived immunity to pathogens. Such plasma cell and memory development are dependent on signals received from T helper cells [55,162].

Activated follicular B cells require a cognate interaction with $CD4^+$ T cells, usually near the B-T cell boundary, to drive the GC reaction. For this interaction to occur, antigen-activated B and T cells must regulate their chemokine receptor expression and alter their localisation. Activated T cells upregulate CXCR5 expression, and thus migrate towards the follicle [75], while B cells stimulated via the BCR upregulate CCR7 and migrate towards the T cell zone [163]. Some B cells that receive the necessary signals from the B-T cell interaction form a GC. Both the development and maintenance of GCs is dependent on B cell expression of Bcl-6 [164], a transcription factor that T_{FH} cells also depend on. During the rapid B cell proliferation within the GC, the BCR undergoes affinity maturation, as a result of mutations in the variable regions of the immunoglobulin genes [55]. Rapidly dividing centroblasts in the dark zone undergo somatic hypermutation and class switch recombination, which is dependent on the enzyme activation-induced cytidine deaminase (AID), before re-expressing the BCR on the surface, as centrocytes in the light zone [55,165]. Thereafter, B cells are selected for by follicular dendritic cells in the light zone region, which possess antigen in the form of immune complexes on their surface. This mechanism maintains B cell tolerance to self-antigens. Any cells that do not receive survival signals, in the form of antigenic stimulation through the BCR coupled with co-stimulatory signals from T_{FH} cells, die by apoptosis in this region [55,166]. The transcription factor Blimp-1 then regulates B cell differentiation into plasma cells, which is accompanied by the downregulation of Bcl-6, although the exact signals that determine differentiation into plasma cells or memory cells is

unknown [93,166]. Thus the transcription factors Bcl-6 and Blimp-1 appear to regulate B cell differentiation into effector and memory cells [72]. The plasma cells generated following the GC reaction may be short-lived, and be dispatched to the inflammatory site, or long-lived cells that migrate to the bone marrow [167]. Whether such long-lived plasma cells have an inherently long lifespan, and/or whether they require replenishment from the memory B cell pool, remains unknown.

As outlined above, T_{FH} cells are vital in the efficient generation of B cell responses. This was demonstrated by the observation that, in mice that lack Bcl-6 expression in T cells (and thus lack T_{FH} cells), GCs and antibody production were significantly impaired [41]. Recent papers have shown specific T_{FH} cell surface molecules to bind B cells and initiate their selection and survival post-GC. For example, PD-1, expressed by T_{FH} cells, binds its ligands PD-L1 and PD-L2, which are expressed at high levels on GC B cells, and initiates plasma cell differentiation. In the absence of PD-1 or its ligands, there is a significant reduction in long-lived plasma cell numbers [57]. Furthermore, ICOS and CD40L on T_{FH} cells bind ICOSL and CD40, respectively, on B cells to positively regulate their survival following B cell proliferation in the GC [11].

T_{FH} cell-derived IL-21 also acts directly on B cells, playing a role in driving the GC reaction, for the induction of proliferation, affinity maturation and plasma cell differentiation [60,168]. Specifically, although B cell development and maturation occur independently of IL-21 signalling, IL-21 acts as a co-stimulator in conjunction with BCR stimulation to increase B cell proliferation [169]. Furthermore, IL-21 has important roles in class switch recombination, plasma cell differentiation and antibody production, functions illustrated by the severe defect in IgG production in IL-21R$^{-/-}$ mice, in both naïve and immunised animals [170]. While GCs developed in these IL-21R$^{-/-}$ mice, memory B cell generation was enhanced, whereas long-lived plasma cell numbers were significantly reduced [168]. Similarly, in the absence of IL-21 production by T cells, GCs do not persist, and memory generation is accelerated, although such memory cells are of poor quality as they have not undergone efficient affinity maturation [60]. This study also implies that B cell memory generation is independent of T_{FH} cell-derived IL-21, while plasma cell development shows a dependence on IL-21. Thus, IL-21 signalling in B cells appears to be one of the mechanisms involved in determining the cell fate decision between memory and effector cell generation. Together, these data emphasize the requirement of T_{FH} cells for optimal B cell responses.

Lymphocyte migration and CD62L

Some immune cells continually migrate throughout the body, circulating between lymphoid organs, non-lymphoid tissues, and sites of inflammation [2]. In the case of lymphocytes, they migrate between such sites via the bloodstream and/or lymphatics, pausing a while in secondary lymphoid organs before moving on. This circulation of lymphocytes is important for immune surveillance, while the pausing of cells in the spleen and lymph nodes allows for cellular interactions, necessary for priming. While lymphocyte access to the spleen is uninhibited due to the direct flow of blood into this organ, the main route of lymphocyte entry into the lymph nodes from the bloodstream is across specialised structures called high endothelial venules (HEVs). One of the key molecules necessary for the transmigration process is CD62L (L-selectin).

CD62L is an adhesion molecule belonging to the C-type lectin family, and is composed of a calcium-dependent lectin domain, an epidermal growth factor-like domain, and 2-9 short consensus repeat units [171]. A schematic showing the structure of CD62L is shown in figure 1.6A. Calmodulin constitutively binds the cytoplasmic tail of CD62L, maintaining its expression at the cell surface [172]. CD62L binds carbohydrate ligands such as those induced on inflamed endothelium and those constitutively expressed at HEVs [171]. More specifically, CD62L ligands include sulphated carbohydrates of glycosylation-dependent cell adhesion molecule-1 (GlyCAM-1) at lymph node HEVs [173], mucosal addressin cell adhesion molecule-1 (MAdCAM-1) at Peyer's patch HEVs, and CD34 at HEVs and inflamed endothelium [174]. Binding of lymphocyte CD62L to its ligand(s) on endothelium occurs early in the lymphocyte-endothelium interaction, and initiates tethering and rolling of cells [175,176]. Thereafter, firm adhesion occurs, which is mediated by lymphocyte integrins, such as LFA-1, binding to ICAM-1 on the endothelial layer, allowing the subsequent transmigration from the bloodstream into tissues or lymph nodes.

CD62L is essential for lymphocyte entry into the lymph nodes across the HEVs, as blocking antibodies against CD62L have been shown to inhibit lymphcyte binding to HEVs both *in vitro* and *in vivo* [177]. Meanwhile $CD62L^{-/-}$ mice display a 70-90% reduction in lymph node size and cellularity, with the remaining lymphocytes thought to enter via the lymphatics [178]. Interestingly, these $CD62L^{-/-}$ mice display increased lymphocyte numbers in the spleen, indicating that CD62L is not required for entry into this lymphoid organ. Unsurprisingly, $CD62L^{-/-}$ mice have delayed or impaired immune responses, likely due to the

inability of lymphocytes to enter the lymph nodes, for efficient activation, and the inhibition of leukocyte entry into sites of inflammation to carry out their effector function [179,180].

- CD62L expression and shedding

Naïve lymphocytes, including B cells, are $CD62L^+$ and express varying levels of this molecule depending on the organ from which they are isolated. Upon stimulation with cognate antigen or by phorbol esters such as PMA, CD62L undergoes an activation-induced conformational change, and is shed from the cell surface [181]. A diagram representing the shedding process is shown in figure 1.6B. Upon cell stimulation, serine residues on the cytoplasmic tail of CD62L are phosphorylated by members of the protein kinase C (PKC) family [182]. This phosphorylation results in the dissociation of Calmodulin, which in turn allows a conformational change in CD62L [183]. This altered structure reveals the cleavage site in the extracellular domain, allowing binding by the protease, and shedding from the cell surface. The enzyme responsible for shedding of surface CD62L is a zinc-containing membrane-associated metalloprotease, a disintegrin and metalloproteinase (ADAM) 17 (also known as TACE, TNFα converting enzyme), which is also responsible for the cleavage of TNFα [184]. This enzyme is thought to have relaxed sequence specificity, recognising instead the shape of the target molecule, while the distance of the cleavage site from the membrane appears particularly important [171].

Cleavage of CD62L from the cell surface by lymphocytes occurs rapidly, with 90% of lymph node cells shedding CD62L in response to PMA within 1 hour [185]. While shedding of CD62L is a short-term mechanism of expression regulation, full activation of lymphocytes also results in control of CD62L expression at the gene transcription level. In addition to shedding induced by cognate antigen and PMA, lymphocytes are thought to shed CD62L following cross-linking by binding of CD62L to its ligands. This would therefore imply that, following binding to HEVs, CD62L is shed during extravasation. However, there are conflicting reports as to whether or not this is the case [181,186,187].

CD62L cleavage occurs immediately extracellular to the transmembrane region [187] (see figure 1.6B), leaving behind a 6kDa transmembrane fragment while the extracellular domain is released and can be readily detected in the bloodstream [188]. The released segment remains functionally active, binding HEVs and activated endothelium and acting as a ‘buffer’ to moderate cell binding, and thus regulating leukocyte entry into inflamed sites [188]. It should be noted that, in addition to activation-induced shedding, CD62L also

undergoes cleavage during constitutive turnover, which is thought to be mediated by another, as yet unidentified, protease [189].

CD62L expression levels can be used as a method of determining lymphocyte subsets. For example, as mentioned above, activated lymphocytes stimulated via the BCR or TCR are $CD62L^-$. Additionally, in the B cell population, immature transitional (T1) B cells, which migrate from the bone marrow to the spleen to complete the maturation process, are $CD62L^-$ [190]. This ensures they do not enter the lymph nodes or sites of inflammation, and is therefore a mechanism to prevent these cells from encountering antigen, which would result in their deletion, and therefore restrict the B cell repertoire [191,192]. CD62L has also been used as a means of identifying central and effector memory T cells, as was discussed above [82]. Generally speaking, T cells are consistently found to express greater levels of CD62L than B cells, which may explain why T cells preferentially migrate to the lymph nodes while B cells are found in greater numbers in the spleen [193].

- Role of CD62L in immune responses

CD62L expression is important in the development of immune responses, as CD62L-deficient mice have reduced leukocyte migration to inflamed sites and impaired delayed-type hypersensitivity responses [194], due to the inability of leukocytes to exit the blood and traffic to infected regions. Primary T cell proliferation and cytokine production is also impaired in $CD62L^{-/-}$ mice [195], probably due to the lack of functional lymph nodes, which are involved in T cell priming. Furthermore, the metalloprotease-mediated shedding of CD62L following lymphocyte activation is crucial, as mice expressing a mutant form of this molecule, that cannot be cleaved from the surface of T cells, exhibited impaired responses to viral infection and delayed viral clearance [181,196]. These data highlight that, not only is expression of CD62L necessary for efficient immune responses, but also its regulation by shedding is a vital process. However, all of the work to date on CD62L has focussed on T cell populations, and little is known about B cell regulation of CD62L expression in altering migration patterns *in vivo*, and the consequences of impaired modulation.

Systems utilised for investigating lymphocyte responses *in vivo*

Clearly, when studying immune cells such as B cells to further investigate their roles in immune responses, it is essential to use *in vivo* systems as much as possible. In this PhD, I investigate the innate and cognate functions of B cells, and their role in the induction of T cell differentiation and memory generation. Therefore, I made use of *in vivo* models to study these topics. Specifically, for studying the early innate responses of B cells, I used a murine infection model of *Salmonella.* Furthermore, I wanted to follow $CD4^+$ T cell responses *in vivo*, in order to determine the impact of B cells. As mentioned above, analysing T helper cell differentiation pathways using mouse models is notoriously difficult in comparison to $CD8^+$ T cells, due to the small numbers of antigen-specific cells generated. Here, I made use of two systems for the detection of antigen-specific T helper cells *ex vivo*. These two systems, the *Salmonella* infection model and the use of MHC class II tetramers, are introduced below.

- Salmonella typhimurium infection model

In order to study TLR-dependent B cell responses and follow antigen-specific effector and memory T cells *in vivo,* the murine infection model of typhoid fever, *Salmonella enterica* serovar Typhimurium (*S. typhimurium*), is used. This intracellular Gram-negative bacterium enters the human host via the oral route, as a result of the intake of contaminated food or water. In the gut, a proportion of bacteria survives the low pH of the stomach and enters the small intestine. There, they use a type III secretion system to invade the epithelial cells and M-cells of the Peyer's patches [197]. Bacterial-induction of macrophage apoptosis allows the evasion of destruction in the Peyer's patches [197]. Thereafter, the bacteria are thought to gain entry, first, into the mesenteric lymph nodes, and subsequently enter the bloodstream, spleen and liver [198]. Once in these sites, the bacteria reside and multiply within macrophages. The human disease, typhoid fever, continues to have a significant global burden on human health. The potential for vaccine development as a means to prevent infection, instigated the development of the murine model of this infection.

A non-virulent strain of *S. typhimurium* was generated, called aromatic-dependent ($aroA^-$) or SL3261, which requires aromatic derivatives not present in mammalian tissues [199]. Use of this strain as a live attenuated vaccine in mice was shown to confer protection from future infection by a virulent strain [199]. It is this particular strain of *S. typhimurium*, SL3261, that I use to investigate B cell responses and T cell differentiation in this PhD. Although the natural route of infection is via oral uptake, I use intravenous administration, here. However,

as this bacterium naturally becomes rapidly systemic, I do not foresee the route of entry to be disadvantageous. The immune response generated in response to the aroA$^-$ strain has been well characterised in the mouse model. Systemic infection results in the development of strong Th1 and antibody responses [200,201]. Early in infection, the macrophage response is required to control the initial phase of bacterial growth [202], while specific Th1-associated cytokines (IFNγ, TNFα, IL-12) are also crucial [203,204,205]. The peak of bacterial numbers in the spleen and liver is around day 7 of infection, and thereafter bacteria are reduced to very low levels by 4-6 weeks post-infection. However, a few viable bacteria remain as far out as 12 weeks post-infection, suggesting chronic low-level infection of *S. typhimurium* is a possibility [206].

The necessity of TLR signalling for the generation of immune responses to *Salmonella* is well characterised using *in vivo* infection models. C3HeJ mice, for example, which lack TLR4 expression and so cannot respond to LPS, are highly susceptible to *Salmonella* infection [207]. TLR4 is thought to be important early in infection for cytokine production and killing of bacteria during the exponential growth phase, whereas TLR2 (which recognises bacterial glycolipids and lipopeptides) plays a role later [208,209]. The lack of the MyD88 adaptor protein during the primary immune response to an attenuated strain of *S. typhimurium* results in significantly increased bacterial load during the initial few weeks of infection, but these mice are able to subsequently clear infection, albeit with delayed kinetics [151,210]. These mice that have an impairment in MyD88 signalling show reduced IL-12 production and therefore diminished Th1 responses to infection [211]. Some data also suggests that MyD88$^{-/-}$ mice may, in fact, mount a skewed Th2 response [210]. This skewing towards a Th2 environment may be an outcome of the reduced Th1 response, and ultimately reflect the lack of dendritic cell-derived IL-12. Together, the data from MyD88$^{-/-}$ mice emphasize the requirement for TLR signalling in both the early innate response by macrophages, and on the development of the adaptive response, in this infection model.

- The involvement of B cells in S. typhimurium infection

The specific role of B cells in the *S. typhimurium* infection model has also been studied [154,155,212]. B cells appear dispensable for the primary immune response to attenuated strains of *Salmonella,* with bacterial load at the peak of infection, and the primary T cell cytokine response, equivalent in B cell-deficient and wild type mice [155]. However, protective immunity is absolutely dependent on the presence of B cells, with B cell-deficient mice showing hugely impaired IL-2 and IFNγ production by T cells after bacterial clearance,

and increased mortality during challenge [154], suggesting an absence of T cell memory [154,155,212]. Transfer of immune serum did not restore protection in B cell-deficient animals, suggesting one important role of B cells in this model is the presentation of antigen to T cells for the generation of memory, a function not influenced by the presence of antibody [154]. To transfer protection from immunised to naïve mice, both immune serum and T cells are required [213], indicating that protective immunity may be dependent on memory formation in both the B and T cell compartments.

Recent work from our laboratory has addressed the specific role of B cell TLR stimulation in *Salmonella* infection [126]. Using mixed bone marrow chimeras, in which the B cell compartment alone is deficient in MyD88 ($MyD88^{B-/-}$), reveals that primary T cell IFNγ production during *S. typhimurium* infection is reduced, suggesting B cells play an important role as APCs in driving the early Th1 response [126]. Thus the early role of B cells in influencing T cell priming appears dependent on TLR stimulation of B cells. Looking at antibody production, IgG2a/c is reduced in $MyD88^{B-/-}$ chimeric mice during *S. typhimurium* infection [126] and this correlates with the impairment of T cell production of IFNγ. The authors imply that the reduction in the early Th1 response is causing impaired help for B cells, and therefore, lower class-switched antibody responses [126]. Here, I want to expand on this data, and further investigate the early TLR-induced responses of B cells in this *S. typhimurium* infection model. I also use this infection model for studying the generation of $CD4^+$ T cell memory, and the involvement of B cells in this process.

- The use of MHC class II tetramers

Another method of following *in vivo*-generated endogenous antigen-specific $CD4^+$ T cell responses over time is the use of MHC class II tetramers. MHC class II tetramers are composed of the MHC class II α and β chains with the peptide of interest covalently bound. This complex is labelled with biotin, and four of these molecules are then bound by Streptavidin PE. For a diagram of MHC class II tetramer structure, see chapter 6 (figure 6.1A, page 177). The peptide used in all experiments shown here is the H19env peptide, which is the immuno-dominant peptide from the envelope protein of the Moloney murine leukaemia virus. The tetramers containing this peptide, originally developed by Schumacher's laboratory [214], have been used in conjunction with MHC class I tetramers to follow $CD4^+$ and $CD8^+$ T cell responses, respectively, in mice infected with the Moloney murine leukaemia virus [214]. The kinetics of antigen-specific $CD4^+$ T cell expansion and decline following immunisation of mice with the H19env peptide have also been established

using these MHC class II tetramers [215]. Immunisation of peptide in Complete Freud's Adjuvant (CFA) s.c. leads to a peak in primary T cell numbers on ~day 9. Thereafter, antigen-specific T cell numbers decline, and a stable of pool of memory cells is generated. Importantly, these memory cells were detectable >150 days post-immunisation, indicating that this is a suitable system for investigating T cell memory populations.

By using MHC class II tetramers, T helper cells can be directly visualised *ex vivo* by flow cytometry, allowing antigen-specific cells to be phenotyped, for example by expression of cell surface markers. However, detecting cytokine production to determine their cell subset phenotype is more difficult, and is only possible in the *Salmonella* model. Therefore, by using both the *S. typhimurium* infection model and the peptide immunisation system, it is hoped that the role of B cells in T cell memory generation can be fully investigated.

- The use of anti-CD20-mediated B cell depletion

Since the generation of B cell-deficient mice by means of gene disruption, the role of B cells in the generation of immune responses has been examined in various models and systems. However, the use of such B cell-deficient mice is not without its problems. Firstly, B cell-deficient μMT mice appear to have abnormal T helper cell compartment, in that $CD4^+$ T cells isolated from B cell-deficient mice are strongly inhibitory towards B cells [216], and T cells primed in the absence of B cells are unable to provide B cell help [217]. Secondly, spleen and lymph node architecture are likely disrupted in B cell-deficient mice, as the normal development of these organs is dependent on B cells. For example, follicular dendritic cells provide the network in the follicles and GCs, and are dependent on B cells for their differentiation [218]. Components of the marginal zone, too, are dependent on B cells for their generation and maintenance [15]. Thus, lymphoid tissue structure will no doubt be severely disrupted when developed in the absence of B cells, and so any impairment in immune responses in B cell-deficient mice may be attributed to defects in other cell compartments rather than the lack of B cells. To overcome some of these identified issues, here, I make use of a B cell depletion system in order to investigate the role of B cells in the induction of T helper cell responses.

The depletion of B cells *in vivo* using an antibody that targets the B cell-specific surface protein, CD20, has been approved for use in humans in the form of the drug Rituximab [219]. CD20 expression is restricted to B cells, with expression initiated around the time of immunoglobulin rearrangement in the pre-B cell population in the bone marrow, and

maintained throughout maturation to naïve B cell status. Memory B cells, too, express this molecule, but expression is lost upon differentiation into plasmablasts and plasma cells [220]. CD20 functions as a calcium channel, and is thought to regulate cell cycle progression by altering calcium (Ca^{2+}) flux [221]. The fact that CD20 is expressed only by B cells, is not shed from the cell surface, and is not internalised upon antibody binding makes it a perfect target for depletion antibodies [219]. Monoclonal depletion antibodies against CD20 have been developed for use in humans and mice, with several clones and design variations available. Interestingly, there is no cross-reactivity between the human and mouse forms [222], so in this PhD the anti-human form of CD20 is used as a control in all experiments, and mice treated with this isotype control antibody reflect the non-depleted group. Following injection of either mice or humans with anti-CD20 depletion antibodies intravenously, B cells are depleted by various mechanisms, including antibody-dependent cellular cytotoxicity, complement activation, and induction of apoptosis [222,223,224]. The phagocytic network appears vital in the depletion process [225,226].

- Anti-CD20 (Rituximab) clinical trials in humans

A chimeric IgG1 antibody, consisting of mouse anti-human CD20 variable regions fused to human immunoglobulin constant regions, is available for use in humans, in the form of the drug Rituximab. This drug was first approved for the treatment of B cell lymphoma, such as B cell non-Hodgkin lymphoma, in 1997, as >90% of B cell lymphoma were found to express CD20 [219]. Following approval for use in humans, McLaughlin *et al* conducted an influential phase III clinical trial in B cell lymphoma patients, using a 4-dose treatment programme [227]. The overall response rate, as defined by >50% reduction in disease for at least 28 days, was 50% of the 166 patients. Of these, 6% were complete responders, who remained disease-free for >28 days following treatment. By 13 months after treatment, 53 of the 76 responders had not yet relapsed. Of the 50% of patients classed as non-responders, the majority (56 of 75) had a reduction in disease. Notably, there were no reports of serious infections following treatment, however, there was no untreated control group for comparison. Furthermore, some adverse side effects were reported following the first treatment, and there was one case of an immune response against the chimeric antibody [227]. This initial study therefore showed anti-CD20 B cell depletion therapy to be a promising treatment of lymphoma. Since then, further clinical trials have taken place using Rituximab as treatment for autoimmune diseases (reviewed in [228,229,230]), including SLE [231,232], RA [233], and Multiple Sclerosis [234], among others. The results from these trials are highly variable, and most lacked sufficient patient numbers to make results

significantly valid. Interestingly, some success has been reported in SLE and RA where disease symptoms improved but autoantibody levels were not affected [229], suggesting that B cells may be having a pathogenic effect that is independent of antibody production, such as contributing to the anti-self T cell response via antigen presentation.

Most clinical trials have focussed on the efficacy of Rituximab treatment, and there is little research on the global effects of depleting B cells on the host immune system or on mounting immune responses. As B cells are an important cell type in both innate and adaptive immune responses, and are essential for the generation and/or maintenance of several other cell types, one might expect the depletion of these cells to have knock-on effects on the immune system as a whole. One depletion study in humans reports T cell numbers and *ex vivo* proliferation responses to be normal [235], while another revealed no differences in absolute numbers of $CD3^+$, $CD4^+$, or $CD8^+$ cells [227]. It is perhaps not surprising that no differences were seen in whole T cell populations, but T cell subsets such as memory cells and T_{FH} cells, which are thought to require signals from B cells for their generation and/or maintenance, were not specifically analysed.

It seems likely that the depletion of B cells will result in an immuno-compromised host. Indeed, a case study of 4 Rituximab-treated peritransplantation patients, out of a group of 62, revealed unusual serious viral infections, whereas there were no cases of viral infections in the non-Rituximab treated control group [236]. These 4 patients with viral infections all had impaired T cell responses, as measured by T cell number recovery. Another study, comparing humoral responses to recall antigens before and after Rituximab treatment, reported significantly lower responses post-treatment [237]. The authors conclude that this loss of existing humoral immunity following treatment was because of reduced numbers of plasma cells, as a result of the inability of such cells to be replenished from the memory B cell pool due to their depletion. Furthermore, antibody responses to neo-antigens were, rather unsurprisingly, significantly decreased in Rituximab-treated patients, suggesting that vaccines given during the period of depletion will be ineffective [238].

Together, these studies in humans provide only very minimal information on the global effects of B cell depletion on the immune system. Further data is required on the effects of B cell depletion on other cell types, such as $CD4^+$ T cell subsets. A recent review summarising the data in this field reports B cell depletion to result in a reduction in T cell activation, due to abolishment of antigen presentation by B cells, and a possible increase in

numbers and function of Treg cells, although the mechanism for this remains unclear [239]. Dissecting the knock-on effects of B cell depletion on other immune cells in humans is a difficult task, and studies in mice may provide further insight.

- Anti-CD20-mediated B cell depletion in mice

Although anti-CD20 has been extensively tested in humans, relatively few studies have been conducted in mice. The studies that haven been performed in mice have done so in one of two systems. Firstly, a transgenic mouse strain in which the B cell population expresses the human form of CD20 has been generated [240,241]. In these 'humanised' mice, B cell depletion is achieved using a form the human drug (clone 2h7) mirroring the clinical trial treatment strategy, and therefore closely resembles depletion in humans. Secondly, an anti-mouse CD20 IgG2a monoclonal antibody (clone 18B12), developed by immunising $CD20^{-/-}$ mice with CD20-transfected cell lines, is available for B cell depletion in mice [240]. The ability to deplete B cells in mice has provided insight into the likely kinetics of B cell depletion and repopulation, the study of which is impossible in humans.

Studies using B cell depletion systems in mice have investigated the efficacy of B cell depletion in regular and autoimmune-prone mice [240,242], measuring variables such as B cell numbers in different lymphoid tissues. In the mouse model of SLE, B cell depletion resulted in the amelioration of disease, and reduced levels of autoantibodies [240]. However, the authors observed greater resistance to B cell depletion in autoimmune prone strains of mice compared to wild type mice [240]. This would suggest that, in humans, B cell depletion might be less efficient in patients with established autoimmune disease. In another study using the mouse model of spontaneous autoimmune thyroiditis, depletion of B cells either before or after disease onset improved symptoms [242]. Again, the authors reported some resistance to depletion in certain subsets of B cells in these autoimmune mice, with anti-CD20 treatment depleting only 50-80% of splenic B cells [242]. It would be interesting to determine the mechanism(s) of resistance of these cells, as this too may be relevant to depletion in humans. A further study, in the mouse model EAE, revealed B cell depletion to reduce the numbers of antigen-specific Th1 and Th17 cells in the central nervous system, pointing to a role of B cells in the priming of these T helper cells in this model of Multiple Sclerosis [243]. However, a conflicting study showed B cell depletion in EAE to exacerbate disease, due to the role of so-called regulatory B cells [244].

Further studies in mice have determined the mechanism of action of anti-CD20 depletion, that is to say how are B cells depleted [225,241,245]. These reports indicate B cell depletion to occur by several mechanisms, including complement activation, Fc receptor-mediated phagocytosis and induction of apoptosis. However, as far as I am aware, no studies have investigated the impact of B cell depletion on other cell types within the immune system in non-autoimmune animals. Thus, the potential impact of anti-CD20-mediated B cell depletion on the immune system as a whole requires in-depth analysis, and may have significant implications on the ability of the host to fight infection and maintain protective immunity.

Therefore, the clone of anti-mouse-CD20 for use in wild type mice (clone 18B12) is used here to further investigate the effects of depleting B cells on the T helper cell populations, specifically T_{FH} cells and memory cells. This method has several advantages over the use of B cell-deficient mice, such that it allows the control of the presence or absence of B cells during specific times of the immune response. Thus, I use this anti-CD20-mediated B cell depletion system to identify the timing of the involvement of B cells in T helper cell responses in the *in vivo* models outlined above, namely *Salmonella* infection and peptide immunisation.

Aims of this PhD

Generally speaking, the aim of this PhD is to further investigate the roles of B cells in both the innate and adaptive arms of the immune response. Specifically, the first chapters focus on the so-called innate responses of B cells, following TLR stimulation. I look at the changes to migration and the differentiation into plasma cells, and highlight the importance of these early B cell responses during infection. Thereafter, I more fully investigate the role of B cells as APCs in the generation of T helper cell responses; using both the *S. typhimurium* infection model and a peptide immunisation system. I ask questions as to the timing of the involvement of B cells, and discuss the possible model of memory generation and the specific function that B cells may be providing.

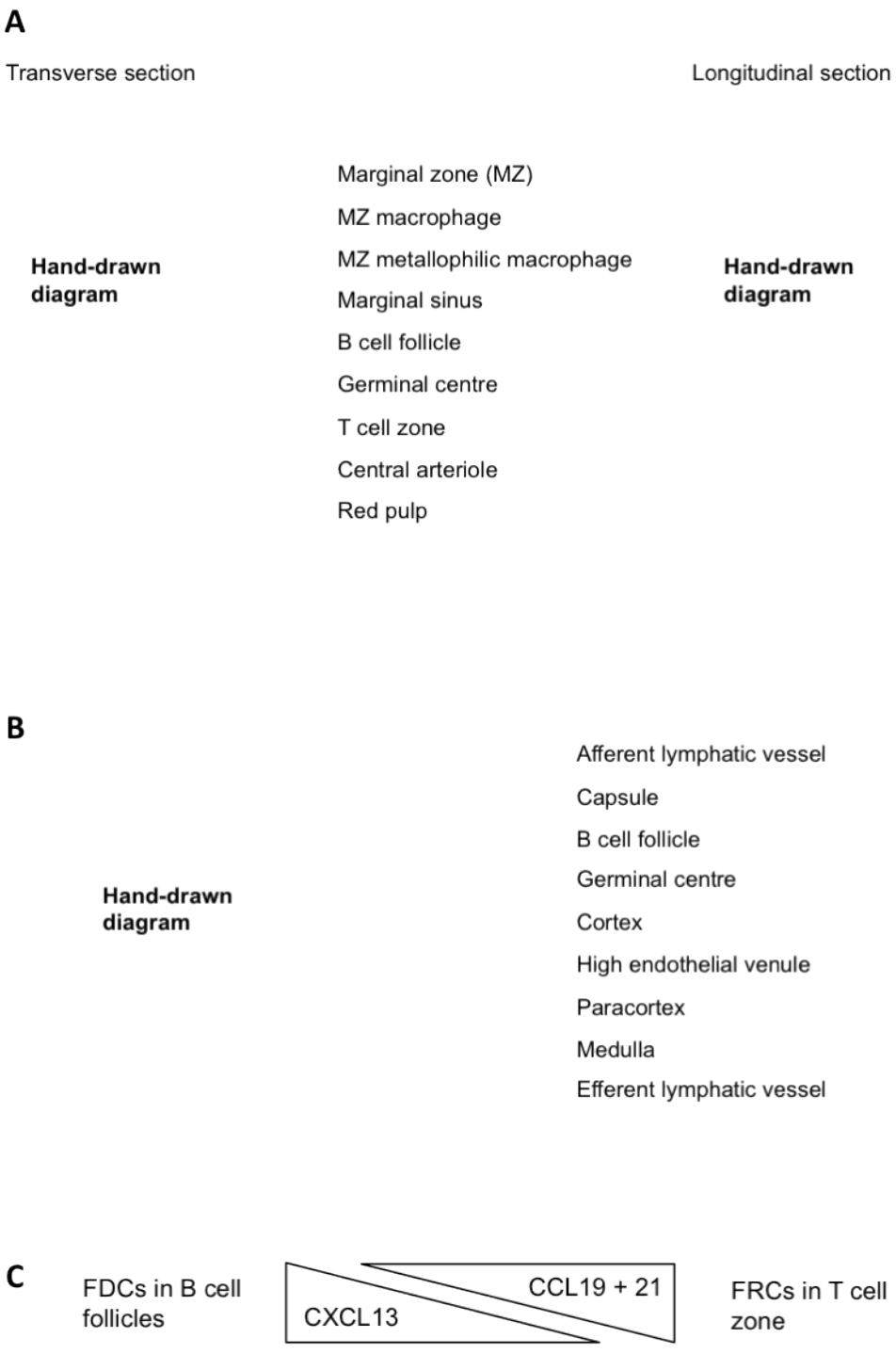

Figure 1.1: Structure of secondary lymphoid organs. Presented are schematics of the structure of the spleen (A) and lymph nodes (B) of mice. The chemokine gradients present in the spleen and lymph nodes are outlined in (C). MZ = marginal zone, FDC = follicular dendritic cell, FRC = fibroblastic reticular cell.

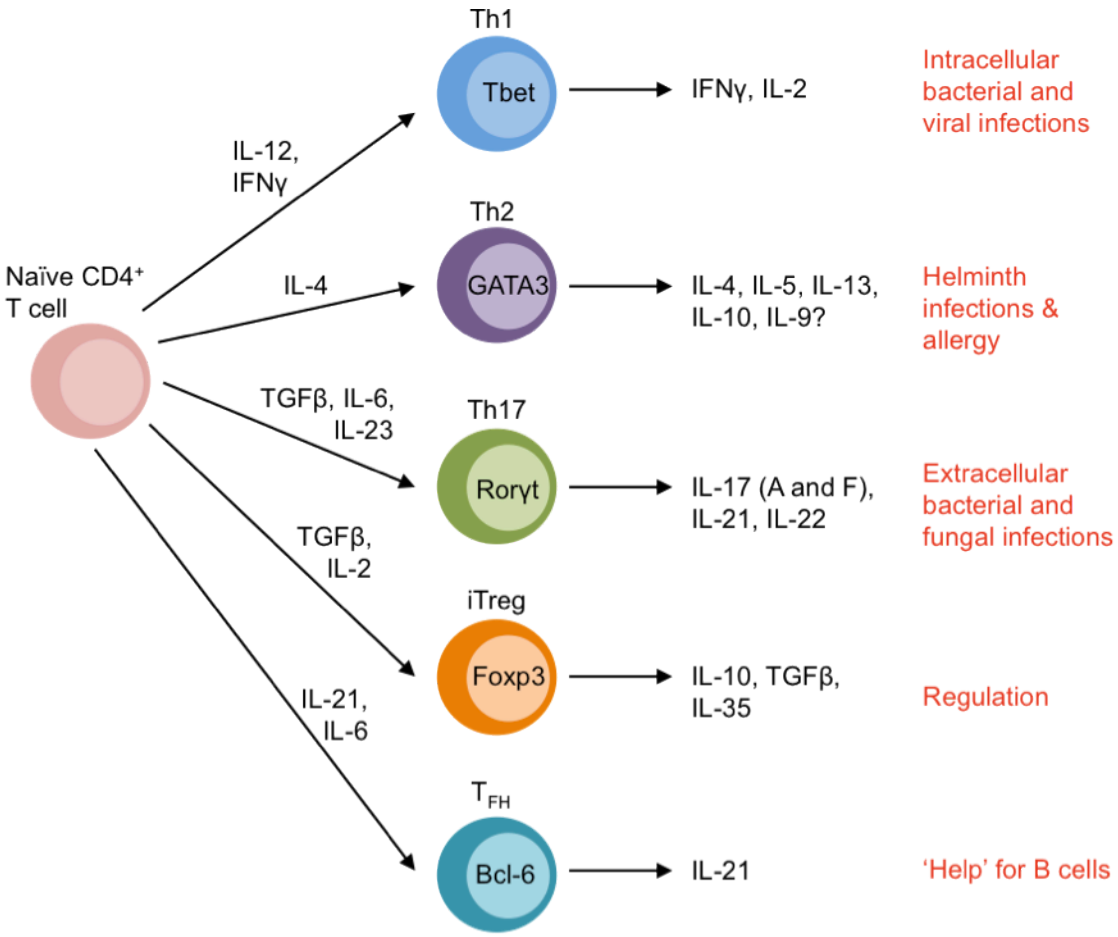

Figure 1.2: T helper cell subsets. Naïve T helper cells have the potential to differentiate into the subsets shown here, depending on the cytokine signals received from the initiating APC and/or the surrounding environment. The subsets can be distinguished by their transcription factor expression and panel of cytokines secreted, as indicated here. The specific roles each subset plays, in terms of infection/function, are also described in the figure.

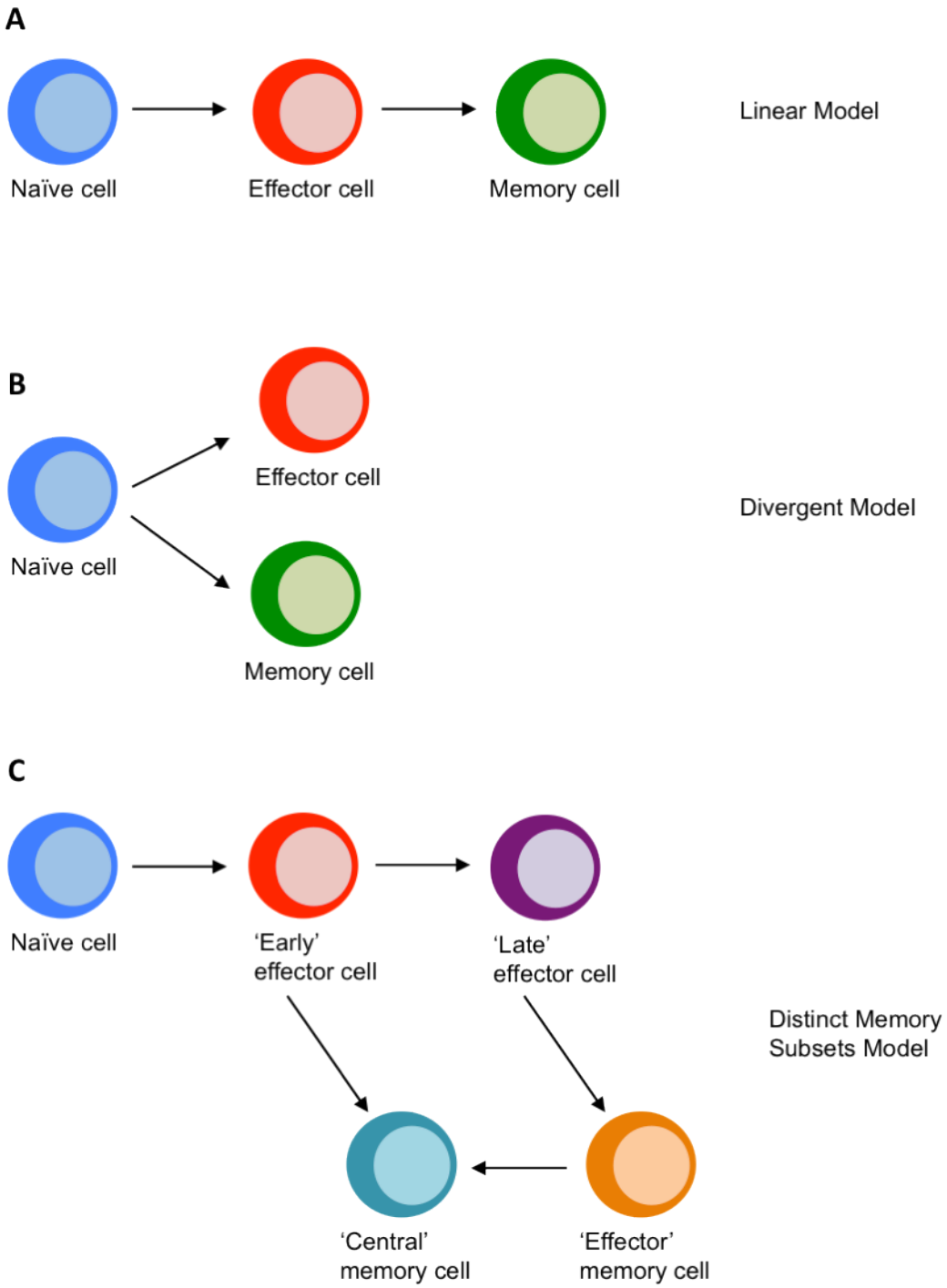

Figure 1.3: T helper cell memory differentiation models. The differentiation pathway of naïve $CD4^+$ T cells into effector and memory populations remains unknown. Here, the possible models are presented (A-C).

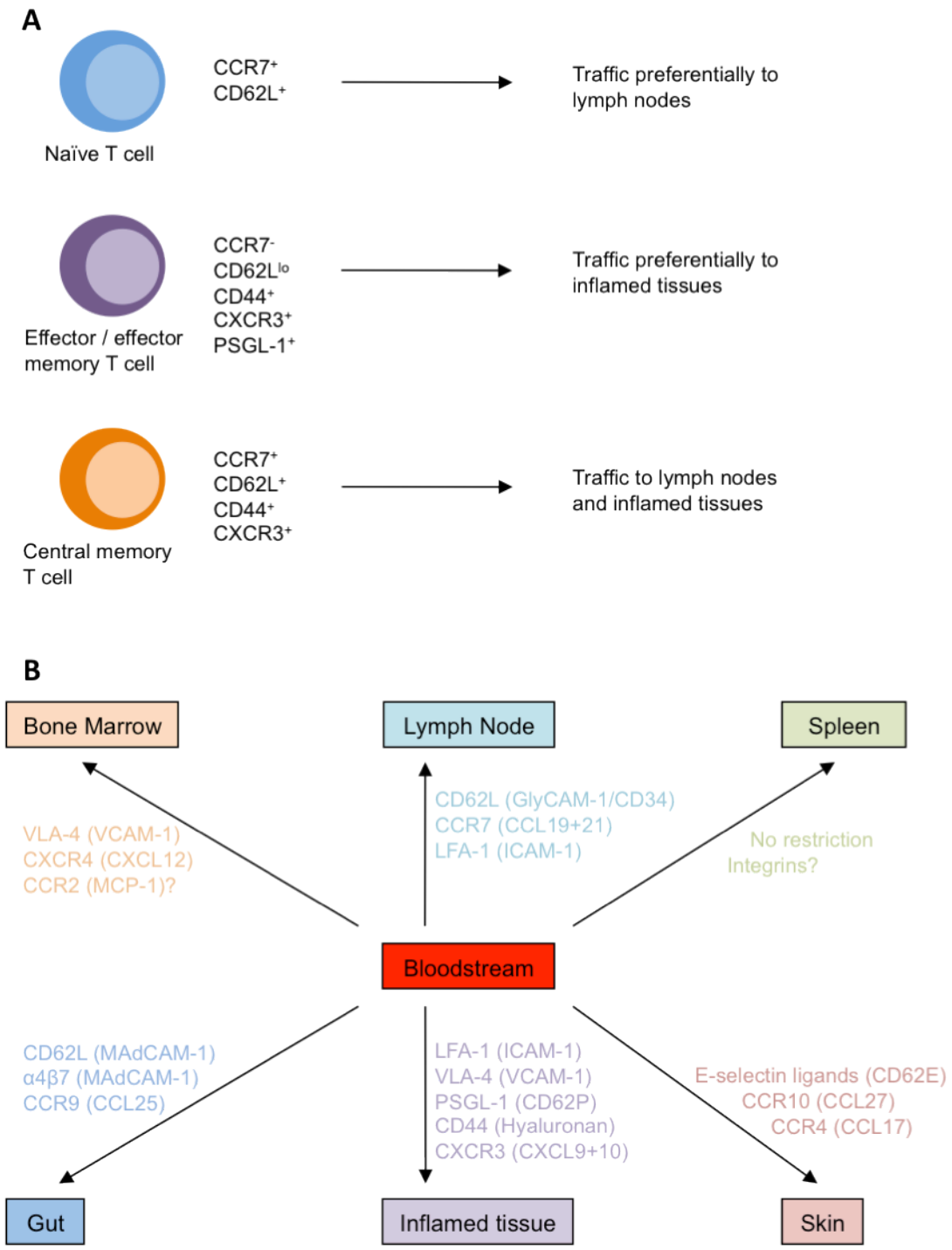

Figure 1.4: Migration of T cell subsets to specific sites within the body. (A) Detailed description of surface adhesion molecules and chemokine receptors expressed by naïve, effector and memory T cells. (B) Presented is a schematic detailing the molecules required to be expressed by T cells for entry into specific sites within the body. The ligands of such molecules are given in brackets.

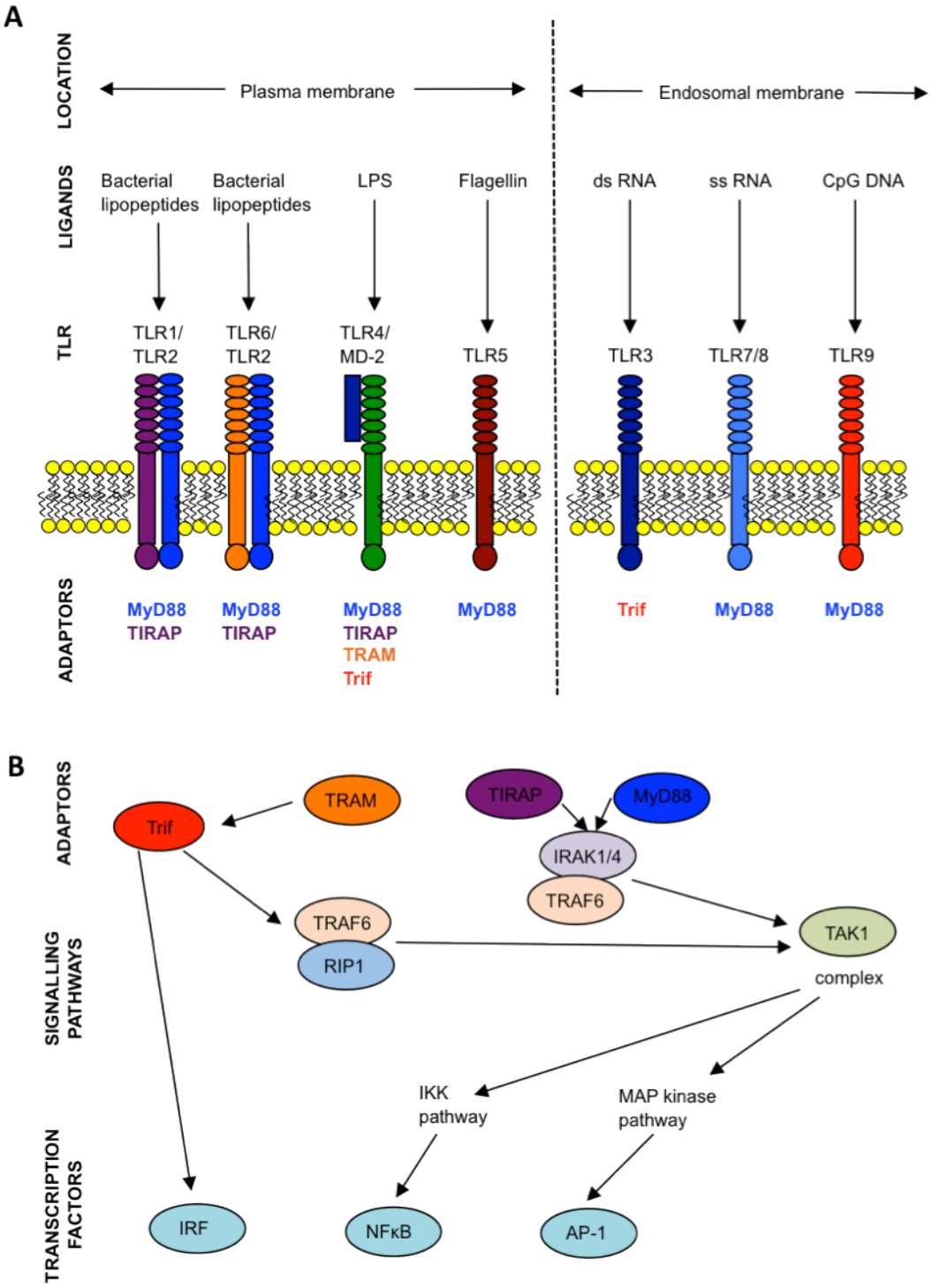

Figure 1.5: Toll-like receptor signalling. Presented is an overview of TLR signalling. (A) TLR location, ligands and adaptor proteins. (B) A summary of the TLR intracellular signalling pathways leading to transcription factor activation within the nucleus.

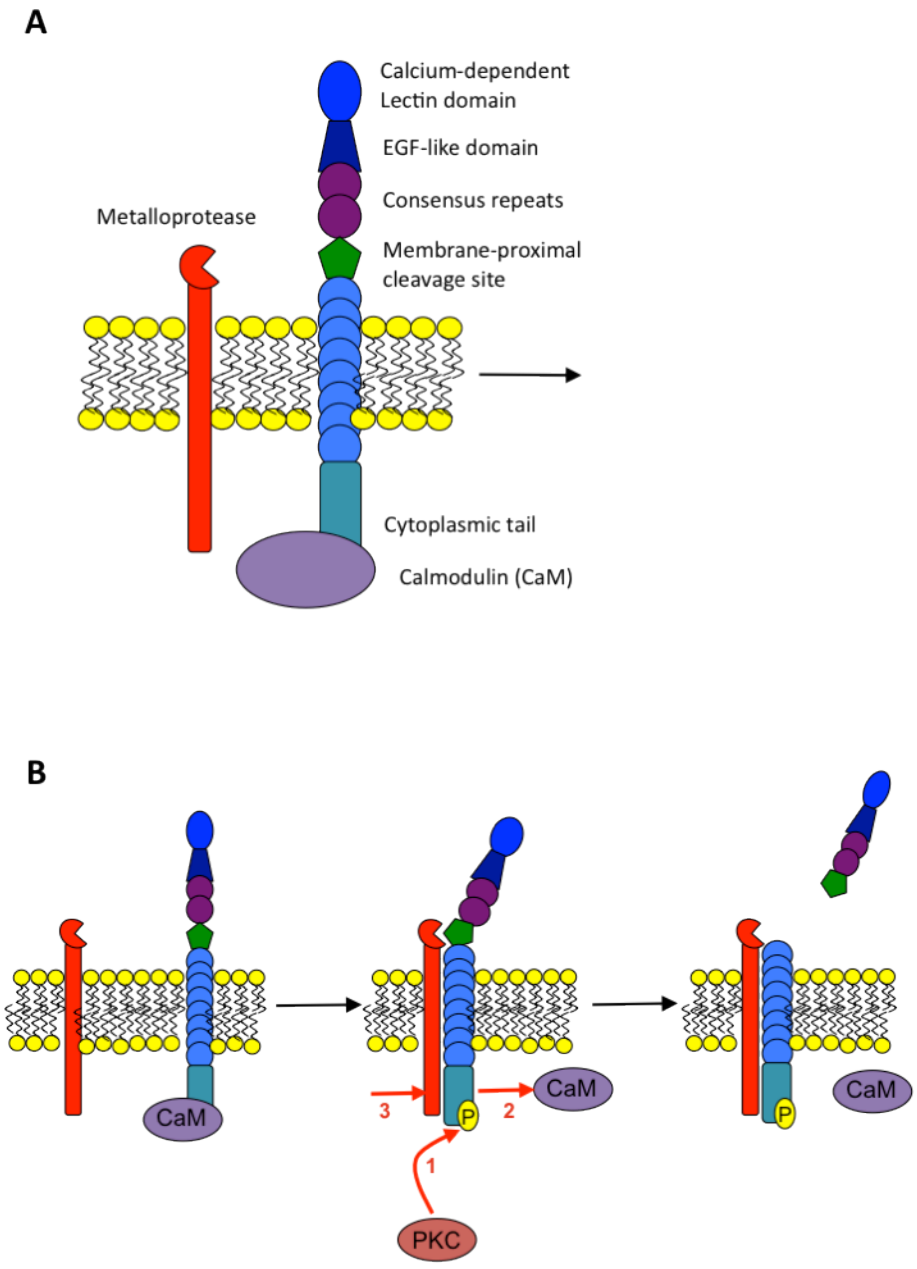

Figure 1.6: CD62L structure and mechanism of shedding. (A) Presented is a schematic of the structure of CD62L, with the component parts labelled. (B) A schematic representation of the mechanism by which CD62L is activated and cleaved from the cell surface. In the middle panel, the numbers 1-3 represent the sequence of events. CaM = Calmodulin, PKC = protein kinase C, P (in yellow) = phosphorylation at a serine residue on the cytoplasmic tail.

CHAPTER 2: Materials and Methods

Mice

C57BL/6, MyD88$^{-/-}$ [246], TRIF$^{-/-}$ [247], TLR2$^{-/-}$ [248], TLR9$^{-/-}$ [249], Ly5.1^{+}, CD4-dnTGFβRII [43], μMT [140], and CD1d$^{-/-}$ [250] mice were bred and maintained at the School of Biological Sciences Animal Facility, University of Edinburgh, UK. Bone marrow from CD62L(E) mice [181] was a kind gift from Professor Thomas F. Tedder (Duke University, NC, USA). Details of the mouse strains and housing conditions can be found in table 2.1. In all experiments, mice aged 6-10 weeks were used, and all genetically modified mice were backcrossed 6-10 generations to C57BL/6. For experiments using CD4-dnTGFβRII mice, only heterozygous mice were used. Experiments were covered by a Project Licence granted by the UK Home Office under the Animals (Scientific Procedures) Act of 1986. Locally, the University of Edinburgh Ethical Review Committee approved this licence.

Generation of CD62L(E) bone marrow chimeras

Mixed bone marrow chimeras were generated as previously described [75]. Briefly, B cell-deficient μMT recipient mice were sub-lethally irradiated with 8Gy of gamma irradiation from a sealed source. The following day, they were reconstituted with $2x10^6$ CD90-depleted mixed inoculum bone marrow cells. These inocula consisted of 50% μMT bone marrow and 50% either wild type or CD62L(E) bone marrow. Therefore, in the CD62L(E) chimeras, all B cells arose from the CD62L(E) cells, while all other hematopoietic cells arose from both the CD62L(E) and μMT cells. Chimeras were left for 8-10 weeks to reconstitute before use in experiments.

Anti-CD20 B cell depletion

To deplete B cells, C57BL/6 mice were treated with a single dose of 250μg of anti-mouse CD20 [240] (clone 18B12, IgG2a isotype, Dr Marilyn Kehry, Biogen IDEC Inc., San Diego, CA) diluted in PBS. As a control, some mice were treated with anti-human CD20 (clone 2B8, Dr Marilyn Kehry, Biogen IDEC Inc.), which has no cross-reactivity with mouse CD20, so these mice are non-depleted controls. The timing of anti-CD20 treatment is shown in each individual experiment.

Immunisations

CpG DNA: For CpG DNA immunisations, mice were immunised intravenously with 20µg of CpG DNA (InVivogen, Autogen Bioclear UK Ltd., Wiltshire, UK) diluted in PBS, or mock immunised with PBS alone. Mice were bled pre-immunisation and at various times after immunisation, with blood samples prepared, as described below, for lymphocyte extraction.

H19env peptide: For studies using MHC class II tetramers, mice were immunised with the immuno-dominant peptide from the envelope protein of the Moloney murine leukaemia virus (H19env peptide), N-EPLTSLTPRCNTAWNRLKL-COOH (Cambridge Research Biochemicals, Billingham, Cleveland, UK). Usually, for the primary immunisation, the peptide was emulsified in Complete Freud's Adjuvant (CFA, Sigma, UK) using a sonicator. Subsequently, 200µg of peptide antigen was administered subcutaneously into the hind legs in a total volume of 200µL (100µL each back leg). For boosting, $2x10^6$ peptide-pulsed dendritic cells were prepared as detailed below, and injected intravenously in a volume of 200µL. In some experiments, for the boost immunisation 200µg of peptide was administered together with 10µg LPS (from *E. coli*, Sigma, UK) intraperitoneally and subcutaneously (100µl i.p. and 50µl in each back leg s.c.).

DNP-KLH: For immunisation with DNP-KLH/Alum, keyhole limpet hemocyanin (KLH) was coupled to dinitrophenyl (DNP, Sigma) as previously described [251]. 200µg of DNP-KLH precipitated in Alum was administered intraperitoneally for the primary injection in a total volume of 200µL, and both intraperitoneally and subcutaneously for the boost immunisation (100µl i.p. and 50µl in each back leg).

In vivo B cell labelling

For the *in vivo* labelling of B cells, mice were injected intravenously with 1µg anti-CD19 PE and/or 1µg anti-CD21 FITC (both from BD Biosciences, San Jose, CA) in a total volume of 200µL as previously described [252]. Tissues were removed 20 minutes post-injection, and processed on ice to minimise further binding.

Bone marrow-derived dendritic cell generation, activation and peptide pulsing

Bone marrow-derived dendritic cells (BMDC) were generated by a modified version of the procedure developed by Inaba *et al* [253]. Briefly, femurs and tibia were extracted from mice and flushed with medium. Bone marrow was broken down by passage through a 21-gauge needle (BD Biosciences). $2x10^6$ cells were cultured in 10mL medium, further supplemented with 20ng/mL granulocyte macrophage colony-stimulating factor (GM-CSF, Peprotech EC Ltd., London, UK). Plates were incubated at 37°C in humidified 5% CO_2 atmosphere. On day 3, 10mL of fresh medium containing GM-CSF was added to the plates. On days 6 and 8, 10mL medium was removed from the plates, and 10mL fresh medium containing GM-CSF was added. On day 10, dendritic cells were harvested, and cultured at $2x10^6$ cells/mL with 0.1μg/mL LPS (InVivogen, Autogen Bioclear Ltd.) overnight (~16 hours). The following day, cells were harvested, washed, and cultured at $2x10^6$ cells/mL with H19env peptide at 50μg/mL for 90 minutes. BMDC were further washed with medium to remove peptide before transfer. As mentioned above, $2x10^6$ cells were injected i.v. in a total volume of 200μL.

Salmonella enterica serovar Typhimurium infection

The aroA$^-$ attenuated strain of *S. typhimurium* (SL3261) was used for all infections [199]. Bacteria were grown as stationary-phase overnight (16 hour) cultures in Luria-Bertani (LB) broth (Difco Laboratories, Surrey, UK). Animals were injected intravenously with ~$1x10^6$ viable bacteria, diluted in PBS. Infectious dose was determined by plating bacteria onto LB agar plates and culturing overnight at 37ºC, then counting the number of colony-forming units (CFU). This was then multiplied up to determine the number of viable bacteria given per mouse. Similarly, splenic bacterial load during infection was determined by taking part of the spleen of known weight, making a cell suspension in PBS, and plating it out onto LB agar plates. The total number of bacteria, per spleen, was calculated by multiplying the number of CFU by dilution factor, dividing by the weight of the spleen section cultured, and finally multiplying by total spleen weight.

Media

For the generation of BMDC, Roswell Park Memorial Institute (RPMI) medium was used. This was supplemented with 10% foetal calf serum (FCS, Sigma), Penicillin/Streptomycin at 100μg/mL and L-Glutamine at 2mM (Gibco, UK). Medium was further supplemented with GM-CSF at 20ng/mL.

For lymphocyte extraction and B cell cultures, Iscove's modified Dulbecco's media (IMDM) was used, supplemented with 5% FCS and Penicillin/Streptomycin as detailed above (complete IMDM). For T cell cultures, complete IMDM was additionally supplemented with 50μM 2-Mercapto-ethanol (BDH Laboratory Supplies, Poole, UK).

For tetramer staining, IMDM was supplemented with Penicillin/Streptomycin, as detailed above, and 10% FCS.

Cell isolation

Single cell suspensions were prepared from spleen, lymph nodes, and Peyer's patches by manual disruption in complete IMDM. Peritoneal washes were performed, by injecting medium into the intact peritoneal cavity, to isolate peritoneal cells. Bones were flushed with medium as described above, to isolate bone marrow, and then broken down using a 21-gauge needle. Where appropriate, samples were depleted of erythrocytes using red blood cell lysis buffer (Sigma).

B/T cell purification

Cells within single cell suspensions were labelled with anti-CD19 or anti-CD4 microbeads (Miltenyi Biotech, Bisley, UK) using 10μL beads plus 90μL medium per 10^7 cells. After incubating for 30 minutes on ice, cells were washed and sorted over a single LS column, for the case of $CD4^+$ T cells, or two consecutive LS columns, for the case of $CD19^+$ B cells, according to the manufacturer's instructions (Miltenyi Biotech). B cell purity was in excess of 98% (data not shown).

Lymphocyte isolation from the blood

For lymphocyte extraction, blood samples were collected in heparin (LEO Laboratories Ltd., Bucks, UK). PBS was added to dilute samples before loading onto lympholyte (Cedarlane Labs Ltd, Hornby, Canada) at an approximate ratio of 1:1. Samples were spun at 1000xg for 20 minutes at room temperature. The lymphocyte layer was isolated, and washed extensively with PBS before staining or transfer, to remove all traces of lympholyte.

In vitro TLR stimulation cultures

For *in vitro* TLR stimulation cultures, splenocytes or purified B cells were cultured at $4x10^6$ cells/mL in complete IMDM in 6 or 24 well plates. Endotoxin-free TLR ligands (InVivogen) were utilised at the following concentrations: the TLR2 ligands zymosan,

peptidoglycan and PAM_3 CSK4 were used at 10, 10 and 0.2 μg/mL, respectively; the TLR3 ligand polyI:C was utilised at 25 μg/mL; LPS (TLR4) from *E. coli* was used at 1 μg/mL; flagellin (TLR5) from *S. typhimurium* was used at 0.1 μg/mL; the TLR7 ligand loxoribine was used at 100 μM; the TLR9 ligand unmethylated CpG DNA (ODN 1826 5'-TCC ATG ACG TTC CTG ACG TT-3') was used at 5 μg/mL. PMA and ionomycin (Sigma) were used at 10 ng/mL and 1 μg/mL, respectively. Schistosomal egg antigen (SEA) and heat-killed *Propionibacterium acnes* were kind gifts from Dr Andrew McDonald (University of Edinburgh, UK), and were used at various concentrations as described in the figures. Where appropriate, the metalloprotease inhibitor Ro 31-9790 (Roche Research Products, Welwyn Garden City, UK) was used at 50 μg/mL. Most TLR stimulation cultures were for 4 hours, or as otherwise stated in the figures. For the recovery of CD62L expression, cells were harvested after 4 hours, washed, and plated out again at $4x10^6$ cells/mL in fresh medium.

Preparation of *S. typhimurium* antigens and *in vitro* cultures

Bacterial antigens from *Salmonella enterica* serovar Typhimurium were prepared as previously described [254]. Briefly, overnight stationary phase cultures of the SL3261 attenuated strain were heat-inactivated at 85ºC for 10 minutes. Around $2.5x10^6$ CFU bacteria that had undergone heat-inactivation were used for *in vitro* cultures with B cells to look at CD62L expression. For B cell restimulation cultures, 10-fold dilutions of heat-killed bacteria starting at 1/5 were performed in triplicate and cultured together with sorted B cells at $2x10^6$ cells/mL for 5 days. Supernatants were collected and analysed for cytokines by ELISA as detailed below. For B cell culture with live bacteria to analyse CD62L expression, around $2.5x10^6$ CFU bacteria were used. To prepare the crude sonicate, overnight-cultured bacteria (SL3261 strain) were sonicated, and debris removed by centrifugation. To make the C5 antigen, overnight culture of the C5 virulent strain of *S. typhimurium* was EDTA-treated, sonicated, and centrifuged to remove cellular debris. The supernatant was then alkali-treated with NaOH at 37°C for 3 hours, and subsequently neutralised with HCl. Both the crude sonicate and C5 antigen were used at 20 μg/mL when analysing B cell CD62L expression.

For T cell restimulation cultures, purified T cells at $1x10^6$ cells/mL were cultured together with gamma-irradiated (30Gy) splenocytes (also at $1x10^6$ cells/mL) to act as antigen presenting cells, and the C5 antigen added at 20, 10, 5, and 1 μg/mL. Supernatants were collected at day 1 of culture for IL-2 detection, and day 3 of culture for IL-10, IL-17 and IFNγ detection. For T cell cultures, medium containing 2-Mercaptoethanol was utilised.

In vivo proliferation assay using BrdU

In the Salmonella *infection model*: Mice were injected with 2 mg bromodeoxyuridine (BrdU) intraperitoneally on days 2, 4 and 8 of *S. typhimurium* infection. The following day (days 3, 5, and 9), spleens were removed and single cell suspensions prepared.

In the peptide immunisation tetramer system: Mice were injected with 2 mg BrdU i.p. for 3 consecutive days before harvest. Spleens were removed 6 weeks after immunisation, at the memory time-point, and on day 5 post-boost.

BrdU staining: Proliferation, as determined by BrdU incorporation, was measured using a FITC-BrdU Flow Kit (BD Biosciences) as described in the manufacturer's instructions. Briefly, cells were surface stained with anti-CD19 PE and anti-CD4 APC, washed, then resuspended in fixation / permeabilization buffer overnight. The following day, cells were washed and DNase treated for 1 hour at 37ºC, then stained with anti-BrdU FITC for 30 minutes at room temperature in the dark. Each sample had an isotype control counter-part. Cells were further washed before analysis.

Cell transfers

For cultured TLR-stimulated cell transfers: Purified B cells from Ly5.1^{+} donor mice were cultured with CpG DNA for 4 hours, as described above, or left unstimulated. After harvesting, cells were washed extensively in PBS, and 5x10^{6} cells injected intravenously into recipient C57BL/6 mice. The CD62L^{lo} phenotype of CpG-stimulated cells was confirmed by flow cytometry.

For CD62L^{hi} cell transfer: CD62L^{hi} lymphocytes were isolated from the blood as follows. Blood was collected into heparin from donor Ly5.2^{+} mice by cardiac puncture. Lymphocytes were extracted on lympholyte, as described above. 5x10^{6} unsorted lymphocytes were injected intravenously into recipient Ly5.1^{+} uninfected or day 6 *Salmonella*-infected mice. Prior to transfer, the CD62L^{hi} phenotype of donor cells was confirmed by flow cytometry.

Flow cytometry

Before staining, cells were washed in FACS buffer (PBS with 0.05% Sodium azide and 3% FCS). The following antibodies were used for flow cytometry (all BD Biosciences unless otherwise stated): anti-CD19 PE, anti-CD4 APC, anti-B220 PerCP, anti-CD21 FITC (clone 7G6), anti-CD21 PE-Cy7 (clone 7E9), anti-CD23 PE, anti-CD5 biotin (ebioscience, San Diego, CA), anti-Ly5.1 biotin, anti-CD62L FITC (Abcam, Cambridge, UK), rat IgG2a FITC isotype control (Abcam), anti-CD80 biotin, anti-CD86 biotin, anti-MHC class II FITC (clone M5114, in-house), anti-GL7 FITC, anti-IgD biotin (clone 1126C, in-house), anti-CD40 FITC (in-house), anti-CD20 PE, anti-CD138 APC, anti-CD44 FITC (in-house), anti-CD44 APC, anti-CD25 APC, anti-Ly6C FITC, anti-CD28 biotin, anti-CD40L FITC (clone MR1, in-house), anti-KLRG1 PE-Cy7 (ebioscience), anti-IL-7Rα FITC (ebioscience), Streptavidin-PerCP, Streptavidin-APC. For more details of the antibodies used for flow cytometry, see table 2.2. Cells were stained for 20 minutes on ice and then washed 3 times in FACS buffer. Where appropriate, cells were further stained with Streptavidin for 20 minutes on ice, and washed again. Samples were analysed on a FACSCalibur or LSR II flow cytometer (BD Biosciences) using CellQuest or FACS-Diva software, respectively, and data analysed using FlowJo software (Tree Star Inc, San Carlos, CA).

MHC class II tetramer staining

Two-three million cells isolated from the spleen, draining lymph nodes or bone marrow were added to 96 well round bottom plates. In some cases, these had been sorted over a single column for $CD4^+$ T cells, as described above, to enrich this population. Cells were washed in IMDM containing 10% FCS. PE-labelled MHC class II tetramers, containing the H19env peptide or tetramers containing an irrelevant peptide as a negative control (both from the NIH Tetramer Core Facility, Atlanta, GA), were diluted 1/100. 25µL of diluted tetramer or isotype control was added to each well, and incubated at 37°C for 3 ½ - 4 hours, agitating regularly to prevent cell clumping. The following antibodies were then added without washing, and incubated at room temperature for 10-15 minutes: anti-CD19 PerCP (BD Bioscience), anti-CD4 APC e-fluor 780 (ebioscience), and anti-F4-80 APC or PE-Cy7 (both ebioscience), together with T cell activation marker antibodies listed above and in table 2.2. Cells were then washed 3 times in FACS buffer, and resuspended in 100µL for acquisition. Before acquisition, 100µL of Propidium Iodide (PI, Sigma), diluted 1 in 200 in FACS buffer, was added to each sample. Samples were analysed on a LSR II flow cytometer (BD Biosciences) using BD FACS-Diva software, and data analysed using FlowJo software (Tree Star Inc.).

T follicular helper cell staining

Five million splenocytes were taken, washed twice in PBS, and stained with Live/Dead fixable aqua fluorescent stain (Invitrogen, Carlsbad, CA, diluted 1 in 500 dilution in cold PBS, 20μL per sample) for 20 minutes on ice. After washing in FACS buffer, cells were stained with the following antibodies, in the presence of Fc receptor blocking antibody (clone 2.4G2, in-house): anti-CXCR5 biotin (BD Bioscience), anti-ICOS PE (ebioscience), anti-PD-1 PE-Cy7 (Biolegend, San Diego, CA), anti-CD4 APC e-fluor 780 (ebioscience), and anti-CD44 FITC (in-house). See table 2.2 for more details of the antibodies used for T follicular helper cell staining. Cells were stained for 1 hour on ice, and then washed in FACS buffer. Cells were then stained with Streptavidin-APC (BD Biosciences) for a further 30 minutes, on ice. After washing, cells were either resuspended in FACS buffer for acquisition or fixation / permeabilization buffer for intracellular transcription factor staining (see below).

Intracellular cytokine, transcription factor, and Ki67 staining

For intracellular cytokine staining, splenocytes were stimulated with PMA/ionomycin (Sigma) at 10ng/mL and 1μg/mL, respectively, for 4 hours, in the presence of Golgi Stop (BD Biosciences). For transcription factor and Ki67 staining, cells were taken directly *ex vivo*. In all cases, cells were washed and surface stained, as described above, with anti-CD4 PerCP (BD Biosciences) and either anti-CD44 PE (BD Biosciences) or anti-CD44 FITC (Abcam). Cells were then washed and fixed in fixation / permeabilization solution (ebioscience) overnight. The following day, intracellular staining was performed in permeabilization buffer (ebioscience, diluted 1 in 10 in distilled water) for 30 minutes, on ice, using the following antibodies (all ebioscience, unless otherwise stated), together with Fc receptor blocking antibody (clone 2.4G2, in-house): anti-IFNγ FITC (Biolegend, San Diego, CA), anti-IL-17 PE, anti-FoxP3 APC, anti-Tbet PerCP-Cy5.5, anti-Rorγt-PE, anti-Ki67 PE (BD Bioscience), rat IgG PE isotype control, rat IgG FITC isotype control (Biolegend), rat IgG APC isotype control, rat IgG PerCP-Cy5.5 isotype control. For further details of the antibodies used, see table 2.2. After intracellular staining, cells were washed in permeabilization buffer, then resuspended in FACS buffer, as above, for acquisition.

Cytokine ELISA

Culture supernatants were assayed to determine the concentrations of IL-2, IL-6, IL-10, IL-17A, and IFNγ. The standard capture ELISA technique was performed, using commercially available paired antibody sets. Briefly, Nunc Maxisorp plates (Fisher Scientific, Loughborough, UK) were coated overnight at 4°C with the relevant capture antibody at 5μg/mL in PBS. After washing, plates were blocked for 2 hours at room temperature with 1% bovine serum albumin (BSA, Sigma) in PBS. Plates were washed and supernatants, together with standards, added and incubated for a further 2 hours. Where appropriate, supernatants and standards were diluted in BSA. Following washing, the relevant biotinylated detection antibodies were added for 1 hour. Streptavidin-alkaline phosphatase (Sigma) was then added and incubated for 45 minutes. Finally, the substrate p-Nitrophenyl phosphate (PNPP, Southern Biotechnology Associates, Birmingham, AL) in Diethanolamine substrate buffer (1 tablet per 5mL) was added and the colour allowed to develop. The plates were read at 405nm using Labsystems Multiskan plus, and data analysed using GraphPad Prism software. The unknown cytokine concentrations were determined by extrapolation from the standard curve. The limits of detection are as follows: IL-2 = 0.3ng/mL, IL-6 = 0.3ng/mL, IL-10 = 0.1ng/mL, IL-17A = 0.1ng/mL, IFNγ = 0.8ng/mL. All antibodies were from BD Biosciences. Throughout this thesis, IL-17 refers specifically to IL-17A.

Antibody ELISA

Serum was separated from whole blood after centrifugation at 10,000 g in a micro-centrifuge for 5 minutes, and stored at -20°C until quantification by ELISA. To quantify the levels of antigen-specific antibody in the serum, Nunc Maxisorp plates (Fisher Scientific) were coated with the relevant antigen at 10μg/mL (for *S. typhimurium* SL3261 crude sonicate and DNP) or 20μg/mL (for H19env peptide) and incubated at 4°C overnight. Plates were then blocked with 1% BSA for 2 hours at room temperature before being washed. Serum was then added, serial two-fold dilutions performed across the plate, and incubated for a further 2 hours at room temperature. Dilutions were performed in BSA. After washing, alkaline phosphate-labelled detection antibodies, specific for the different antibody isotypes (Southern Biotechnology Associates), were added and the plates incubated for another 1 hour at room temperature. Following a final wash, plates were developed and read as described above for the cytokine ELISA.

Immunohistology

Spleens were placed in cryomoulds (BDH Laboratory Supplies, Poole, UK) in OCT-embedding medium (BDH Laboratory Supplies) and stored at -80°C until required. Tissue sections of 5µm in thickness were cut, dried and fixed in acetone, before being stored at -20°C until use. Sections were blocked in 1% BSA for 20 minutes, and then stained with the following antibodies (all BD Bioscience unless otherwise stated): anti-IgM Texas Red (Southern Biotechnology Associates), anti-Ly5.1 FITC (Abcam), purified anti-IgD, anti-MOMA-1 biotin (Abcam), anti-F4-80 FITC, anti-MHC class II biotin (clone M5114, in-house), anti-CD11b PE, Streptavidin Alexa fluor 350 (Invitrogen), Streptavidin-FITC (Southern Biotechnology Associates), anti-rat IgG Alexa fluor 350. Between staining with primary and secondary antibodies, and after secondary antibody staining, slides were washed 3 times for 5 minutes each by immersion in PBS. After staining, cover slips were mounted using Mowiol (Hoechst, Frankfurt, Germany). Slides were viewed on an Olympus BX50 microscope under reflected light fluorescence, and images captured using OpenLab software (Improvision, Walthman, MA). A summary of the antibodies used for histology can be found in table 2.3.

Statistics

Student's *t*-test and two-way ANOVA tests were used to calculate significance values where appropriate. Such statistical analysis was performed using Prism GraphPad (GraphPad Software Inc., San Diego, CA).

Data from repeat peptide immunisation experiments was pooled, where indicated, using MINITAB software (Minitab Inc., Pittsburgh, PA), and analysed using a general linear model ANOVA, and Tukey's multiple comparison test, adjusting the means with 'experiment' as a factor (table 6.6 only).

Throughout, p-values are given in the figures, and illustrated as follows: p=0.01 to 0.05 *, p= 0.001 to 0.01 **, p<0.001 ***, NS = not significant (p>0.05).

Mouse strain	Housing	Screening	Reference
C57BL/6	Normal cages on water	None	N/A
MyD88$^{-/-}$	Filter cages on water	PCR for Neomycin	[246]
TRIF$^{-/-}$	Filter cages on water	PCR for Neomycin	[247]
TLR2$^{-/-}$	Filter cages on water	PCR for Neomycin	[248]
TLR9$^{-/-}$	Filter cages on water	PCR for Neomycin	[249]
Ly5.1^{+}	Normal cages on water	Stain for Ly5.1	N/A
μMT	Filter cages on water	Stain for CD19	[140]
CD4-dnTGFβRII	Filter cages on water	PCR for dominant negative TGFβRII and CD4 promoter	[43]
CD1d$^{-/-}$	Filter cages on water	PCR for Neomycin, stain for CD21 by CD23	[250]
CD62L(E) chimeras	Filter cages on Borgal	Stain for CD19 & CD62L	[75,181]

Table 2.1: Mouse strains utilised. The table contains details of the mouse strains used in this PhD, together with the housing conditions, screening procedures, and relevant reference(s). N/A = not applicable.

Staining protocol	Antibody	Source	Dilution
B cell subsets	Anti-CD21 FITC (clone 7G6)	BD Bioscience	1 in 100
	Anti-CD21 Pe-Cy7 (clone 7E9)	BD Bioscience	1 in 200
	Anti-CD23 PE	BD Bioscience	1 in 200
	Anti-CD5 biotin	ebioscience	1 in 200
B cell activation	Anti-CD62L FITC	Abcam	1 in 100
	Anti-CD80 biotin	BD Bioscience	1 in 200
	Anti-CD86 biotin	BD Bioscience	1 in 200
	Anti-MHC class II FITC	In-house (clone M5114)	1 in 100
	Anti-GL7 FITC	BD Bioscience	1 in 100
	Anti-IgD biotin	In-house (clone 1126C)	1 in 100
	Anti-CD40 FITC	In-house	1 in 100
	Anti-CD20 PE	BD Bioscience	1 in 200
	CD138 APC	BD Bioscience	1 in 200
T cell activation	Anti-CD62L FITC	Abcam	1 in 100
	Anti-CD44 FITC / APC	In-house/BD Bioscience	1 in 100/200
	Anti-CD25 APC	BD Bioscience	1 in 200
	Anti-Ly6C FITC	BD Bioscience	1 in 100
	Anti-CD28 biotin	BD Bioscience	1 in 200
	Anti-CD40L FITC	In-house (clone MR1)	1 in 100
	Anti-KLRG1 PE-Cy7	ebioscience	1 in 200
	Anti-IL-7Ra FITC	ebioscience	1 in 100
Tetramer staining	Tetramer-PE	NIH	1 in 100
	Control tetramer-PE	NIH	1 in 100
	Anti-CD4 APC e-fluor 750	ebioscience	1 in 200
	Anti-CD19 PerCP	BD Bioscience	1 in 200
	Anti-F4-80 APC / PE-Cy7	ebioscience	1 in 200
T follicular helper cell staining	Anti-CXCR5 biotin	BD Bioscience	1 in 200
	Anti-ICOS PE	ebioscience	1 in 200
	Anti-PD-1 PE-Cy7	Biolegend	1 in 200
	Anti-CD44 FITC	In-house	1 in 100
	Live/Dead stain AmCyan	Invitrogen	1 in 500
Intracellular staining	Anti-IFNg FITC	Biolegend	1 in 100
	Anti-IL-17 PE	ebioscience	1 in 100
	Anti-FoxP3 APC	ebioscience	1 in 100
	Anti-Tbet PerCP Cy5.5	ebioscience	1 in 100
	Anti-Rorγt PE	ebioscience	1 in 100
	Anti-Ki67 PE	BD Bioscience	1 in 50
	Anti-BrdU FITC	BD Bioscience	1 in 100
	Rat IgG FITC isotype control	Biolegend	1 in 100
	Rat IgG PE isotype control	ebioscience	1 in 100/50
	Rat IgG APC isotype control	BD Bioscience	1 in 100
	Rat IgG PerCP Cy5.5 isotype control	ebioscience	1 in 100

Table 2.2: Summary of antibodies used for flow cytometry. The table contains details of the antibodies used in each of the flow cytometry staining protocols, including fluorochrome, source and dilution used. Optimal dilution was calculated by titration.

To visualise	Antibody	Source	Dilution	Secondary antibody
Marginal zone	Anti-IgM Texas Red	Southern Biotech	1 in 100	N/A
	Anti-IgD purified	BD Bioscience	1 in 100	Anti-rat Alexa 350
	Anti-CD19 PE	BD Bioscience	1μg i.v.	N/A
	Anti-CD21 FITC	BD Bioscience	1μg i.v.	N/A
MZ metallophilic macrophages	Anti-MOMA-1 biotin	Abcam	1 in 50	Streptavidin FITC
Macrophages	Anti-F4-80 FITC	BD Bioscience	1 in 100	N/A
	Anti-CD11b PE	BD Bioscience	1 in 100	N/A
Antigen-presenting cells	Anti-MHC class II biotin	In-house (clone M5114)	1 in 100	Streptavidin Alexa 350
Transferred cells	Anti-Ly5.1 FITC	Abcam	1 in 50	N/A

Table 2.3: Antibodies used for immunohistology. Details of the antibodies used in immunohistology, including fluorochrome, source, dilution and secondary antibodies, are displayed in the table. MZ = marginal zone, N/A = not applicable.

CHAPTER 3: TLR-mediated loss of CD62L focuses B cell traffic to the spleen during *S. typhimurium* infection

Introduction

B cells as antigen presenters and antibody producers are a major component of the adaptive immune response, however, they also have the ability to respond to pathogens in an innate fashion. They do this by recognising structurally conserved pathogen ligands through TLRs expressed at the cell surface and in the endosomal compartment. Murine B cells express an array of these TLRs [124], although there is differential expression in certain subsets. As mentioned in the introduction, stimulation through these receptors induces B cell proliferation and differentiation into antibody-secreting plasma cells [125,126,127]. Additionally, stimulation of B cell TLRs results in enhanced antigen presenting capacity, by inducing upregulation of MHC class II and co-stimulatory molecules, and cytokine secretion [124]. Thus TLR-stimulated B cells show signs of activation and have the potential to programme early $CD4^+$ T cell responses, as has been reported [151].

This study began with the observation that certain TLR ligands alter B cell expression of CD62L *in vitro*. This adhesion molecule binds carbohydrate ligands expressed at HEVs and sites of inflammation, initiating lymphocyte tethering and rolling, and allowing subsequent migration of cells into tissues [175,176]. CD62L has been shown to be essential for the entry of lymphocytes into the lymph nodes across the HEVs, and therefore $CD62L^{-/-}$ cells are unable to enter the lymph nodes by this means [178]. CD62L is not required, however, for lymphocyte entry into the spleen [178]. As mentioned in the main introduction, immune responses are impaired in these $CD62L^{-/-}$ mice [179,180], highlighting the importance of this adhesion molecule.

An interesting characteristic of CD62L is its ability to be rapidly shed from the cell surface by a metalloprotease, ADAM17 (also known as TACE) [184]. Surface expression of CD62L is therefore highly regulated, with cells controlling expression both at the cell surface by shedding, and internally by transcription regulation. Naïve B and T cells (which are $CD62L^+$) have previously been shown to shed CD62L rapidly, in response to cognate

antigen and PMA stimulation [185]. However, the effects of TLR ligands on B cell expression of CD62L have not previously been reported.

To study TLR-dependent B cell responses in a more natural environment, the *S. typhimurium* infection model is used. The roles of TLRs [207,208,210] and of B cells [154,155,212] in this model have been studied separately, however less attention has been paid to the specific effects of B cell TLR stimulation. Data from our own laboratory, which does address this, made use of mixed bone marrow chimeras in which the B cell compartment lacked the MyD88 adaptor protein ($MyD88^{B-/-}$). Although the focus was on antibody production, primary T cell IFNγ production was found to be impaired in the absence of B cell MyD88 signalling [126], suggesting that B cell TLR stimulation is important in initiating antigen presentation by B cells, which in turn drives the early Th1 response in this model. A more recent paper from our laboratory confirms the role of MyD88 signalling in B cells in driving the early Th1 response in this infection [151]. This dependence on B cells for optimal Th1 cell priming was due mainly to cytokine production, and did not rely on direct antigen presentation by B cells [151].

In this chapter, I characterise the changes in CD62L expression that results from activation of B cells by a variety of TLR ligands. As CD62L is necessary for the migration of lymphocytes from the bloodstream to the lymph nodes across the HEVs, I hypothesised that TLR-stimulated B cells would display altered migration patterns *in vivo*. I go on to analyse B cell expression of CD62L during *S. typhimurium* infection, how this impacts upon their migration, and discuss the likely effects this will have on the developing T helper cell response.

Results

B cells isolated from the blood express higher levels of CD62L than those found in the spleen and lymph nodes

B cells were isolated from the blood, spleen and lymph nodes of wild type mice and analysed for their expression of CD62L. B cells in the blood were found to express the highest levels of CD62L, while B cells in the lymph nodes express intermediate levels, and those in the spleen express low levels (figures 3.1A & B). The splenic population of B cells displays a bimodal pattern of CD62L expression (figure 3.1A, left). The B cell subsets within the spleen were therefore identified, and CD62L expression levels between them compared. Follicular B cells were found to express higher levels of CD62L than marginal zone B cells (which is consistent with previously published data [255]), while B2 cells express greater amounts of CD62L than B1 cells (figure 3.1C). Thus B cells from different organs, and different B cell subsets, express varying levels of CD62L.

Loss of CD62L expression on B cells in response to some TLR ligands

B cells are known to lose expression of CD62L following the ligation of their BCR [256]. I wished to know whether activation via innate receptors, such as TLRs, altered expression of this molecule. To examine the effect of TLR stimulation of B cells on their expression of CD62L, purified B cells were cultured with a variety of TLR ligands *in vitro*. I found that B cells lose expression of CD62L in response to specific TLR ligands, namely PAM_3 CSK4 (a TLR2 ligand), CpG DNA (TLR9 ligand), and partially lose CD62L in response to poly I:C (a TLR3 ligand). However, stimulation with zymosan, peptidoglycan (both TLR2 ligands), LPS, flagellin or loxoribine (ligands for TLRs 4, 5, and 7, respectively) did not induce loss of this molecule (figure 3.2A). The partial loss in response to Poly I:C was found to be dose-dependent (figure 3.2B), and therefore I would suggest that complete loss is likely to occur in response to a higher concentration of this stimulus.

Using cells from $MyD88^{-/-}$, $TRIF^{-/-}$, $TLR2^{-/-}$, and $TLR9^{-/-}$ mice, it was confirmed that the loss of CD62L on B cells in response to PAM_3 CSK4 is MyD88- and TLR2-dependent, its loss in response to poly I:C is TRIF-dependent, and in response to CpG DNA is MyD88- and TLR9-dependent (figure 3.2C). All knockout B cells lost CD62L expression when stimulated with PMA/ionomycin (figure 3.2C) or by cross-linking their BCR (data not shown).

Loss of CD62L expression by B cells stimulated with CpG DNA is rapid and due to shedding from the cell surface

An analysis of CD62L expression over time after CpG stimulation revealed that B cells lost surface expression of CD62L within 2 hours of culture (figure 3.3A). This expression was not restored within the 12 hours analysed. B cells lost CD62L expression within 4 hours, even in response to very low concentrations of CpG DNA (figure 3.3B). To establish whether B cells lose CD62L expression *in vivo* in response to CpG DNA, mice were injected with 20 μg CpG DNA. As can be seen in figure 3.3C, the percentage of B cells in the blood that express high levels of CD62L was significantly reduced at 2, 4, and 8 hours after injection. B cell populations in the blood returned to normal by 24 hours post-injection. Expression of CD62L on B cells, as determined by MFI, was significantly reduced at 2 hours post-immunisation (figure 3.3D).

As splenic B cell subsets differed in their expression levels of CD62L (figure 3.1C), I wanted to investigate if all B cell subsets lose CD62L expression following CpG DNA stimulation. The data presented in figure 3.3E reveal that both follicular and marginal zone B cells (the two main B cell populations in the spleen) lost expression of CD62L following CpG stimulation.

It seems likely that the mechanism by which B cells rapidly down-regulate CD62L is by shedding from the surface, as characterised previously with respect to activation by PMA [181]. To demonstrate that this was the case, the metalloprotease inhibitor Ro 31-9790 was used, which has previously been shown to inhibit CD62L shedding [257]. Ro 31-9790 also inhibits shedding of TNFα [258] and is therefore thought to target ADAM17 (TACE). When this inhibitor was included in the B cell culture with CpG DNA, the loss of CD62L from the cell surface at the 4-hour time-point was completely abolished (figure 3.3F). This confirms that the loss of surface CD62L by B cells in response to CpG DNA was due to shedding by the surface metalloprotease ADAM17 (TACE), and not any other mechanism.

CpG-stimulated B cells are excluded from lymph nodes and Peyer's patches

It is well known that CD62L is essential for leukocyte entry into the lymph nodes across the high endothelial venules [177]. I predicted, therefore, that CpG-stimulated B cells that have a $CD62L^{lo}$ phenotype would show altered migration patterns *in vivo*. To investigate this, I transferred CpG-stimulated or unstimulated B cells, after 4 hours of culture (figure 3.4A), into congenic Ly5-distinct hosts, and looked the following day at their localisation. The CpG-stimulated $CD62L^{lo}$ donor cells were excluded from the lymph nodes and from Peyers' patches, but trafficked normally to the spleen (figure 3.4C). Although equivalent numbers of

unstimulated and CpG-stimulated B cells were found in the spleen, these B cells differed in their localisation within the white pulp. Unstimulated B cells were dispersed throughout the white pulp, whereas CpG-stimulated B cells localised specifically to the B/T cell border (figure 3.4D). As CXCR5 expression is known to determine localisation within the white pulp, CXCR5 levels were analysed on these stimulated B cells (figure 3.4B). However, no differences in CXCR5 expression were identified, which suggests that a mechanism(s) other than CD62L shedding is involved in B cell localisation within the follicle. These data conclude that TLR stimulation of B cells can impact on their migration patterns *in vivo* via changes in surface expression levels of CD62L.

B cells recover surface expression of CD62L around 2-3 days after stimulation, and subsequently gain entry into lymph nodes and Peyer's patches

Having established the kinetics of CD62L shedding from the surface of B cells in response to TLR stimulation, I next analysed the recovery of expression both *in vitro* and *in vivo*. Following culture with CpG DNA, B cells were washed extensively and either plated out again with fresh media *in vitro*, or adoptively transferred into Ly5-distinct recipient mice. Figure 3.5A shows that B cells recovered CD62L expression after 3 days in culture, and *in vivo* the re-expression happened after 2 days (figure 3.5B, top). The adoptive transfer showed that donor CpG-activated B cells were present in the lymph nodes and Peyer's patches by day 5 (figure 3.5B, middle & bottom), in numbers equivalent to unstimulated B cells. The lag of 3 days between CD62L re-expression in the spleen on day 2, and B cell migration to lymph nodes and Peyer's patches on day 5 is likely due to the normal homing patterns of B cells, in that they pause in secondary lymphoid tissues before re-entering the circulation.

B cells stimulated with CpG DNA in the presence of the inhibitor later shed CD62L, and are excluded from lymph nodes and Peyer's patches

In order to prove without any doubt that it was the effect of CpG DNA on B cell expression of CD62L, and not any other effect of TLR stimulation, which was responsible for the exclusion of these cells from the lymph nodes, I stimulated B cells with CpG DNA in the presence of the inhibitor and transferred them *in vivo*. The theory was that B cells stimulated with CpG DNA in the presence of the inhibitor would retain expression of CD62L, and retain the ability to migrate to the lymph nodes.

The data presented in figure 3.6A show that B cells stimulated with CpG DNA alone shed CD62L, while in the presence of the inhibitor remain $CD62L^{hi}$, as seen above. After washing, cells were either left *in vitro* for a further 4 hours, or transferred *in vivo* for 4 hours. In both cases, these cells subsequently shed CD62L (figure 3.6B and figures 3.6C & D, respectively). *In vivo,* these cells were excluded from the lymph nodes and Peyer's patches, in a similar manner to cells stimulated with CpG DNA alone (figure 3.6E). Thus, this experimental design is not suitable for confirming that it is the shedding of CD62L, and not any other effect of CpG DNA on B cells, that is causing the altered migration patterns *in vivo*.

B cells shed CD62L when stimulated with antigens from *Salmonella*

Although interesting that B cells shed CD62L in response to purified TLR ligands, I wished to investigate if B cells shed CD62L when encountering TLR ligands in the form of pathogenic bacteria. To do this, B cells were stimulated with antigens from the Gram-negative bacteria *Salmonella enterica* serovar Typhimurium (hereafter referred to as *S. typhimurium*). The data presented in figure 3.7A reveal that B cells shed CD62L when stimulated with heat-killed bacteria, a crude sonicate of bacteria or a semi-purified C5 antigen. However, no shedding occurred in response to live bacteria *in vitro*.

To determine if a specific TLR and adaptor molecule is responsible for shedding induced by these bacterial antigens, knockout cells were used. The data in figure 3.7B show that TLR2 and the adaptor molecule MyD88, rather than TLR9 or TRIF, are utilized to induce shedding in response to these bacterial antigen preparations.

B cells also shed CD62L in response to the Gram-positive bacteria *P. acnes* but not when stimulated with Schistosomal egg antigen

I wished to determine whether or not B cells shed CD62L in response to other antigens that potentially contain TLR ligands. Therefore, B cells were stimulated with various concentrations of a heat-killed preparation of the Gram-positive bacteria, *P. acnes* (figure 3.8B), or with Schistosomal egg antigen (SEA, figure 3.8C), and compared these results to stimulation with *S. typhimurium* antigens (figure 3.8A). B cells were found to shed CD62L in a dose-dependent manner when stimulated with heat-killed *P. acnes*. Although shedding does not reach minimum levels as indicated by CpG DNA, this was presumably due to the use of sub-optimal concentrations. However, no shedding was apparent in response to physiological concentrations of SEA (figure 3.8C).

Altered localisation of B cells during *S. typhimurium* infection

The data shown so far would predict that TLR-induced changes in CD62L expression will result in altered migration of B cells during systemic infection with *S. typhimurium*. To test this hypothesis, wild type mice were infected with *S. typhimurium*, and B cell localisation measured during infection. The data presented in figures 3.9A & B show that *S. typhimurium* infection caused profound alterations in the localisation of B cells. In the lymph nodes and Peyer's patches there was a rapid decrease in both the percentages (figure 3.9A) and absolute numbers (figure 3.9B, lymph nodes only) of B cells during the first week of infection. This was most apparent in the Peyer's patches, where the proportion of B cells dropped from around 80% in uninfected mice, to 20% by day 8 of infection. In the spleen, the percentage of B cells remains unchanged at day 4, and was reduced at day 8 (figure 3.9A), largely due to an influx of other cells (eg. macrophages). However, looking at absolute numbers (figure 3.9B), there was actually a 2- to 3-fold increase in splenic B cell numbers at day 4 when compared to uninfected mice, and numbers remained elevated at day 8 of infection.

The increase in B cell numbers in the spleen at this early stage of infection does not seem to be due to B cell proliferation, as BrdU incorporation by B cells was little above background, and minimal in comparison to T cell division (figure 3.9C and D). Together these data support the notion that B cells shed CD62L in response to bacteria, and consequently are excluded from lymph nodes, so enter the spleen in greater numbers, as entry to the spleen is independent of CD62L [259].

TLR-deficient mice show a reduced accumulation of B cells in the spleen during *S. typhimurium* infection

In order to determine if the accumulation of B cells in the spleen during *S. typhimurium* infection is dependent on TLR signalling through the MyD88 adaptor protein, B cell localisation was examined during the infection of MyD88-deficient mice. The data presented in figure 3.10A reveal that there was a reduced loss of B cells from the Peyer's patches at day 7 of infection. Meanwhile, there was also reduced accumulation of B cells in the spleen at day 7 when compared to wild type mice (figure 3.10B). Together, these data suggest that the altered localisation of B cells during *S. typhimurium* infection is predominantly MyD88-dependent, and therefore mediated by TLR signalling.

CD62L^{hi} B cells shed and migrate to the spleen, not lymph nodes, when transferred into *Salmonella*-infected mice

The data shown so far suggests that B cells shed CD62L during *S. typhimurium* infection in a TLR-dependent manner, and that this is the cause of the altered migration patterns. To address this more directly, CD62L^{hi} B cells were isolated from the blood of Ly5.2^{+} donor mice, and transferred into either *S. typhimurium*-infected or uninfected Ly5.1^{+} recipient mice. Ly5.2^{+} donor B cells were identified (see figure 3.11A for example staining) and CD62L expression analysed, after 18 hours. The results displayed in figure 3.11B demonstrate that in uninfected mice, donor Ly5.2^{+} B cells migrated to both the lymph nodes and the spleen, whereas in infected mice the Ly5.2^{+} B cells were found in much greater numbers in the spleen, and significantly reduced numbers in the lymph nodes. Donor cells identified in the spleens of uninfected mice had maintained their CD62L^{hi} phenotype, whereas in the spleens of infected mice, donor B cells had shed and were predominantly CD62L^{lo} (figure 3.11C). These data confirm that B cells shed CD62L early during *S. typhimurium* infection and that this is the cause of their enhanced entry into the spleen and relative exclusion from the lymph nodes and Peyer's patches.

When B cells are unable to shed CD62L, primary T cell responses are impaired during *S. typhimurium* infection

In order to give insight into the effect of B cell shedding of CD62L on the developing immune response, cells from a strain of mice that express a mutant form of CD62L, which cannot be shed from the surface (CD62L(E) mice), were used. These mice were generated by replacing the membrane-proximal region of the CD62L gene (containing the site of metalloproteinase binding) with that of E-selectin (CD62E), which is not cleaved from the cell surface, and thus does not contain a metalloproteinase binding site [181]. Therefore the extracellular CD62L domain in the CD62L(E) mice resembles normal CD62L in all ways, except that it cannot be cleaved from the cell surface. Using bone marrow from these mice, I generated mixed bone marrow chimeras, in which the B cell compartment expresses the mutant CD62L(E), while other cells predominantly express normal CD62L (hereafter referred to as CD62L(E) chimeras). Therefore, in these mice, B cells alone are unable to shed CD62L from their surface.

It was firstly confirmed that B cells from these CD62L(E) chimeras did not shed CD62L when stimulated with CpG DNA *in vitro* (figure 3.12A). The chimeric mice were then infected with *S. typhimurium*, and the very early immune response analysed on day 4. The

bacterial load in the CD62L(E) chimeras was equivalent to the wild type chimeras at this time-point (figure 3.12B). However, the T cell cytokine response, in terms of IL-10, IL-17 and IFNγ, was impaired in the CD62L(E) chimeras (figure 3.12C), suggesting that early T cell activation is impaired when B cells are unable to shed CD62L. Unfortunately, due to the lack of availability of these mice, I was unable to extend this study any further. It would have been interesting to see if the T cell response recovered to normal levels, and if bacterial clearance was delayed in these mice.

TLR2 and TLR9 are involved in early cytokine responses, as well as antibody responses, during *S. typhimurium* infection, but are not required for bacterial clearance

In order to further characterise the general roles of TLR2 and TLR9 in *Salmonella* infection, the primary, memory and antibody responses were analysed in $TLR2^{-/-}$ and $TLR9^{-/-}$ *Salmonella*-infected mice.

At the primary time-point, splenic bacterial load in both the $TLR2^{-/-}$ and $TLR9^{-/-}$ mice was equivalent to that of wild type mice (figure 3.13A). Looking at T cell activation, in terms of expression of the activation markers CD62L, CD44 and CD25, there were no obvious signs of reduced activation in either the $TLR2^{-/-}$ or $TLR9^{-/-}$ animals (figure 3.13B). However, T cell cytokine production, namely IL-10 and IFNγ, appeared reduced in the $TLR2^{-/-}$ mice (figure 3.13C). T cell cytokine responses in $TLR9^{-/-}$ appeared normal (figure 3.13C). Looking at B cell activation in these mice, there were no significant differences between groups in the expression of the activation markers CD62L, CD80 and CD86 on day 7 of infection (figure 3.13D). B cell IL-6 production appeared reduced in the $TLR2^{-/-}$ mice, while IFNγ and IL-10 production appeared normal (figure 3.13E). However, cytokine production by B cells from the $TLR9^{-/-}$ mice was, if anything, enhanced (figure 3.13E).

Infected $TLR2^{-/-}$ and $TLR9^{-/-}$ mice were also analysed 8 weeks post-infection, when bacterial clearance and T cell memory were analysed. As can be seen in figure 3.14A, bacteria had almost been cleared in both strains of knockout mice, as well as in wild type mice. Bacterial loads were minimal in comparison to those on day 7 of infection (compare figure 3.14A to figure 3.13A), suggesting bacteria were being cleared. Bacterial loads in the $TLR9^{-/-}$ mice appeared significantly higher than the wild type mice, however, as this is at the limit of detection for this assay, no strong conclusions can be made. T cell cytokine production, in terms of IL-2, IL-10 and IFNγ production, was equivalent in all 3 groups (figure 3.14B),

indicating that T cell memory generation was normal in the absence of TLR2 or TLR9. T cell IL-17 production appeared higher in the wild type group than either of the knockout strains, but due to variability this was not a significant difference, and T cell IL-17 production in both the TLR2$^{-/-}$ and TLR9$^{-/-}$ mice is likely to be normal.

B cell cytokine production in response to heat killed bacteria at this memory time-point follows similar kinetics to that at the primary response. IL-6 production in the TLR2$^{-/-}$ mice appeared reduced, while IL-10 and IFNγ production was largely normal (figure 3.14C). Again, cytokine production, mainly IL-6 and IFNγ, by B cells from the TLR9 $^{-/-}$ mice appeared slightly enhanced (figure 3.14C). This may be simply because there were perhaps greater numbers of bacteria present in the spleen of these mice (figure 3.14A), and therefore there was more antigen present.

B cell antibody production has also been shown to be dependent on TLR activation, more specifically; certain subclasses of immunoglobulin, namely IgG1, IgG2b and IgG2c, are thought to be MyD88-dependent [126]. Here, it can be seen that IgG1 and IgG2c production was significantly impaired in both the TLR2$^{-/-}$ and TLR9$^{-/-}$ mice, but IgG2b responses were normal (figure 3.15).

Together, these data suggest that TLR2 and TLR9 are involved in the early T and B cell cytokine production, and for antibody responses, in the *Salmonella* infection model. However, neither TLR2 nor TLR9 were essential for bacterial clearance, or for T cell memory generation.

Discussion

The data presented here indicate that stimulation of B cells through TLRs 2, 3, and 9 induces shedding of CD62L, which impacts on their migration patterns and results in their exclusion from lymph nodes and Peyer's patches. During *Salmonella typhimurium* infection, this process causes B cells to accumulate in the spleen during the first week. Additionally, using TLR-deficient mice, TLR2 and TLR9 were found to be involved in early B and T cell cytokine responses, as well as antibody responses, during *S. typhimurium* infection.

Regulation of B cell expression of CD62L

The differential expression of CD62L by B cells isolated from different organs (figure 3.1B) would suggest that surface expression of this molecule is rapidly and regularly altered. Circulating B cells were found to express very high levels of CD62L, presumably to allow them to bind to HEVs and migrate into lymph nodes. As cross-linking of CD62L by its ligand induces shedding [186,187], one might predict that CD62L shedding would therefore occur during extravasation, as has been suggested [260,261]. Indeed this would fit with the data presented here, that B cells within lymph nodes were found to express lower levels of CD62L than B cells found in the blood. However, this is a controversial topic and others provide evidence that CD62L is not shed upon extravasation [181]. As CD62L is not required for entry into the spleen, this may be the default site of migration for $CD62L^{lo}$ B cells. Within the spleen, marginal zone B cells were found to express lower levels of CD62L than follicular B cells (figure 3.1C). This may be because follicular B cells continuously circulate around the body between secondary lymphoid tissues, while marginal zone B cells are predominantly non-circulating and remain in the spleen [262]. However, both follicular and marginal zone B cells within the spleen were found to shed CD62L when stimulated with CpG DNA (figure 3.3E) indicating that this phenomenon is not restricted to any specific subset of B cells.

B cell shedding of CD62L in response to specific TLR ligands

Stimulation of B cells with certain TLR ligands (PAM_3CSK4, Poly I:C and CpG DNA) induced shedding of CD62L by B cells *in vitro,* while other TLR ligands did not have such an effect (figure 3.2A). Interestingly, PAM_3CSK4, which binds TLR2/1 hetero-dimers, induced shedding, while other TLR2 ligands, zymosan and peptidoglycan, which bind TLR2/6 hetero-dimers, had no such effect. Differences with the zymosan signal could be explained by its dependence on dectin-1 [263] which is not expressed by B cells [264].

However, the reason is more likely to be due to differential expression of TLR1 and TLR6 by B cells. There is evidence to suggest that, although B cells express TLR6 at the mRNA levels [124,125], they display a greater proliferative response to TLR2/1 stimulation than to TLR2/6 [125], which would support the notion of increased expression of TLR1 compared to TLR6. Therefore, although these two forms of TLR2 signal via the same pathway and so produce the same effects [265], differential expression would account for the differences seen between these stimuli.

Shedding of CD62L by B cells in response to TLR stimulation has not previously been reported. However, other groups have indicated that human neutrophils rapidly lose expression of CD62L following stimulation with TLRs *in vitro* [266,267], and this method has been utilised to detect defects in the TLR signalling pathway [266]. However, these two articles do not agree on which TLRs induce shedding. On the one hand, Von Bernuth *et al*. suggested that shedding of CD62L by human neutrophils was stimulated by ligands for all the TLRs expressed by granulocytes (TLRs 2/1, 2/6, 4, 5, 7, 8) [266]. In contrast, Hayashi *et al.* only saw neutrophil shedding of CD62L in response to TLRs 2/1, 2/6, 4, and 7/8 but not TLRs 3, 5 or 9 [267]. The differences seen between these results in relation to TLR5-induced shedding may be due to different mechanisms of extracting neutrophils, or the varying concentrations and sources of flagellin used. These results also contrast to my own data on mouse B cell shedding of CD62L (figure 3.2A), in that I do not see shedding induced by TLRs 4, 5, or 7. Importantly, in addition to the shedding induced by defined TLR ligands, I also saw shedding of CD62L by B cells in response to *Salmonella* antigens (figure 3.7A). This shedding appears to be largely MyD88-dependent, but not mediated entirely by either TLR2 or TLR9 (figure 3.7B). However, no shedding was observed in response to live bacteria *in vitro* following 4 hours of culture. This is likely due to the short incubation time of this culture, where there will be little bacterial death (B cells alone are unlikely to induce bacterial killing) and, therefore, only small amounts of accessible TLR ligand.

Furthermore, the interaction between the TLR signalling pathway and the shedding of CD62L remains ill-defined. The mechanism of CD62L shedding is thought to be controlled by Calmodulin binding to the cytoplasmic domain. The release of Calmodulin, initiated by the phosphorylation of serine residues on the cytoplasmic domain of CD62L, allows a conformational change in CD62L which exposes the cleavage site [172,183]. As this phosphorylation of the intracellular tail of CD62L is mediated by members of the protein kinase C family, and some members of this family may be activated during TLR signalling

[268], this is perhaps the mechanism of interaction of these two signalling pathways. However, whether the specific PKCs required for CD62L phosphorylation are activated in the TLR signalling pathways remains to be determined. Clearly, additional study of the signalling pathway, which leads from the intracellular TLR signal to the phosphorylation of CD62L, is required.

The roles of TLR2 and TLR9 in *S. typhimurium* infection

The TLRs that induce shedding of CD62L by B cells in response to bacteria (TLRs 2, 3, and 9) are not the most abundant or obvious TLR ligands to have an effect during *Salmonella* infection. Although the immune roles of LPS (TLR4) and flagellin (TLR5) in the *Salmonella* infection model have been investigated [269,270], the TLRs highlighted here have received less attention. Interestingly, it has been noted that infection with *S. typhimurium* results in an increase in expression of TLRs 2 and 9 in the infected liver (unfortunately, the spleen was not investigated), suggesting they have the potential to play a role [271]. Here, the roles of these receptors were more fully analysed, using TLR2- and TLR9-deficient mice.

TLR2 was found to be involved in early B and T cell cytokine responses (figures 3.13C & E), however it remains unclear whether this is due to the lack of TLR2 on B and T cells themselves (B cells certainly express TLR2 [124], and human T cells have also been shown to express TLR2 [272]), or due to an impairment in the function of other cell types, such as dendritic cells. The authors who originally made the $TLR2^{-/-}$ mice suggested that, as the major target ligand is peptidoglycan, TLR2 was more likely involved in the recognition of Gram-positive bacteria [248]. Therefore, by extrapolation from this, TLR2 would seem unlikely to play a major role in the Gram-negative bacterial infection of *S. typhimurium*, where the peptidoglycan is not exposed to as great an extent. Another study agrees with this theory, showing that TLR2-deficient macrophages produce similar amounts of cytokine to wild type macrophages when stimulated with heat-killed *S. typhimurium* [273]. This is in contrast to a study by Weiss and colleagues, which states that TLR2 is involved later in the immune response for efficient macrophage function [208].

Some limited data on the role of TLR9 in *Salmonella* infection has previously been published. Incubation of hepatocytes with CpG DNA, for example, was seen to significantly inhibit the intracellular growth of *S. typhimurium in vitro*, suggesting that stimulation via TLR9 can enhance bacterial killing [274]. Rumio *et al.* also demonstrated that pre-treatment with CpG-DNA for 72 hours *in vivo* increases survival when mice are then infected with

virulent *S. typhimurium* [275], again suggesting a role for this TLR in inducing bacterial killing. The authors propose that this increased survival is due to the responses of Paneth cells, although they did not investigate this directly. This effect may, instead, be partly due to the TLR9-induced changes in B cell localisation and activation. The data presented here in figures 3.13-3.14 indicate that both primary and memory B and T cell cytokine responses are largely normal in the absence of this receptor. At day 7, B cell cytokine responses actually appeared greater in the TLR9$^{-/-}$ mice when compared to wild type mice. As TLR9 is documented to have stimulatory, not inhibitory, effects on B cells [124,125], this result seems perplexing. The only explanation may be that the TLR9$^{-/-}$ mice have slightly higher bacterial loads and therefore, with more antigen present, B cells are making larger cytokine responses. Although TLR9$^{-/-}$ mice appear to have higher bacterial loads at week 8 post-infection (figure 3.14A), and indeed this does reach statistical significance, in reality these bacterial loads are at the limit of detection, and therefore I cannot conclude that bacterial clearance is in any way impaired in these mice.

How B cells would be activated by bacterial DNA during infection remains to be clarified, as it seems that unless it is released as 'soluble' material following bacterial cell death, the bacterial particles would require receptor (BCR)-mediated uptake [276,277] and so only *Salmonella*-specific B cells might be activated via TLR9. However, the data presented in figure 3.6 suggest that this is not the case, as B cells cultured with CpG DNA plus the inhibitor later shed CD62L after extensive washing to remove the stimulus. Therefore, it appears that the CpG DNA was taken up by the whole B cell population. Furthermore, stimulation of TLRs 2 and 3 is unlikely to be B cell specificity-dependent, as these receptors are located on the cell surface, and have the potential to stimulate a polyclonal population of B cells.

Both TLR2 and TLR9 were found to be required for a full spectrum of antibody subclass production, as the deficient mice had reduced levels of IgG1 and IgG2c (figure 3.15). This is consistent with previous findings where TLR2$^{-/-}$ mice showed reduced IgG production in response to *Salmonella typhi* porin immunisation, although the authors did not look at specific IgG subclasses [278]. Previous data from other members of our laboratory also support my findings: TLR signalling, in the form of MyD88, has been shown to be essential for efficient antibody responses, specifically IgG2c and IgM responses to T-dependent antigens [126]. There are discrepancies between this data and my own data, in terms of reduced IgG1 seen in figure 3.15 that was not seen previously, and conversely reduced IgM

which was observed previously in the MyD88$^{B-/-}$ chimeras but is not seen here. These differences are likely due to the mice (MyD88$^{B-/-}$ chimeras versus TLR knockouts) and antigens (protein immunisation versus *S. typhimurium* infection) used. Here, using specific TLR knockout mice it was possible to identify the roles of individual TLRs on antibody production, as opposed to the more profound impairment in TLR signalling seen in MyD88-deficient mice. However, I am unable to determine whether these receptors are required on the B cells themselves or on other cell types. To determine this, a B cell chimera system for each of the TLR2$^{-/-}$ and TLR9$^{-/-}$ would need to be used.

Despite the apparent impairments in primary T cell and antibody responses, bacterial load at the peak of infection on day 7 was equivalent in the wild type, TLR2$^{-/-}$ and TLR9$^{-/-}$ groups (figure 3.13A). This lack of effect on bacterial numbers is likely a timing issue, that at the time-point analysed there was no significant difference but perhaps the kinetics of bacterial growth and decline might differ between groups. Similarly, both TLR2- and TLR9-deficient mice were able to clear bacteria and generate normal T cell memory (figure 3.14), indicating that TLR2 and TLR9 are ultimately dispensable for the recovery from this infection. This is not surprising, as previously reported data indicate that MyD88-deficient mice, which have a more profound impairment in TLR signalling, are able to clear this infection but suffer from a significantly higher bacterial load during the early stages of infection [151,210].

Interestingly, the amount of cytokine produced by B cells at week 8 of infection is comparable to at day 7 (figures 3.13E & 3.14C). While T cell cytokine responses were greatly enhanced at week 8 when compared to day 7 (figures 3.13C & 3.14B), indicative of T cell memory, the same does not hold true for B cell cytokine production. This would suggest that B cell cytokine production does not show memory (although this is not to say that B cells themselves do not have a memory phenotype). Indeed this absence of B cell cytokine memory has been observed before in our laboratory (T.A. Barr, S. Brown & D. Gray, unpublished data).

The kinetics of TLR-induced shedding of CD62L by B cells

The TLR-induced shedding of CD62L by B cells had a profound impact on their migration *in vivo*. These TLR-stimulated B cells were completely excluded from the lymph nodes and Peyer's patches, and trafficked only to the spleen (figure 3.4). Interestingly, B cells stimulated with CpG DNA in the presence of the inhibitor Ro 31-9790 later shed CD62L both *in vitro* and *in vivo,* and were therefore excluded from the lymph nodes and Peyer's

patches (figure 3.6). These data demonstrate that CpG DNA must enter the cell, presumably in vesicles, and continue stimulating the cell even after both the CpG DNA and the inhibitor have been washed off. Therefore, the inhibitor cannot be used to confirm, without any doubt, that it is the effect of CpG DNA on B cell CD62L, and not any other effect of TLR9 stimulation, that is responsible for the exclusion of these cells from the lymph nodes. In order to show conclusively that the key molecule is CD62L, the shed-resistant (CD62L(E)) B cells would have to be used. In this situation, I would expect that B cells which cannot shed CD62L from their surface would continue to migrate to the lymph nodes and Peyer's patches after stimulation with CpG DNA. Unfortunately, due to the availability of these mice, it was not possible to perform this experiment.

The data here suggests that, following a single stimulation with TLR ligands, B cell CD62L returns to normal levels in 2-3 days, and these cells are then able to traffic normally to the lymph nodes and Peyer's patches (figure 3.5). Others have shown that, in T cells, activation by anti-CD3 induces a similar short-term reduction in surface CD62L, with normal levels achieved 2-3 days later [172,279]. This is followed, 7 days later, by full activation of T cells and down-regulation of surface CD62L as a result of transcriptional regulation [279]. In the *Salmonella* infection model, the reduction of B cell numbers in the lymph nodes and Peyer's patches is only apparent for the first 8 days of infection, and thereafter B cells numbers in these organs begin to return to normal (figure 3.9). In the spleen, B cell numbers are elevated on days 4 and 8, but not from day 12 onwards. This would suggest that the focussing of B cells to the spleen by TLR-induced changes in CD62L expression, as seen in *Salmonella* infection, is a short-term phenomenon.

The implications of B cell accumulation in the spleen

The data presented indicate that, during *Salmonella* infection, TLR stimulation of B cells induces a short-term reduction in levels of surface CD62L, which in turn results in increased B cell trafficking to the spleen (Figure 3.9). This may be a mechanism to non-specifically attract a polyclonal population of B cells to the spleen. This is likely to have two effects. First, it will enhance the BCR-dependent activation/selection of antigen-specific B cells in the spleen, both by exposing greater numbers of B cells to bacterial antigens and also by TLR-mediated augmentation of expression of MHC class II and co-stimulatory molecules [142,144,149]. Second, the subsequent polyclonal activation by these and other TLR ligands, will drive B cell cytokine production [124]. This cytokine release by B cells has a significant effect on the programming of the early, primary $CD4^+$ T cells response [151]. The fact that

TLR-stimulated B cells localise to the B/T cell border within the white pulp of the spleen (figure 3.4D) would support the notion that these B cells may be interacting with T cells, and have the potential to drive early T cell responses. Indeed the data presented in figure 3.12 suggest that this is the case: The CD62L(E) chimeras, in which the B cell compartment is unable to shed CD62L, show impaired T cell priming in *S. typhimurium* infection. Although these data provide evidence to support the theory of B cells influencing early T cell responses, it should be noted that a proportion of the T cells in these chimeras also have an impairment in their ability to shed CD62L, which may impact upon their activation status, and subsequent cytokine production.

In addition to driving T cell responses, the non-specific accumulation of B cells in the spleen may enhance the secretion of natural antibody directly to the site where the bacteria have amassed. Therefore, TLR-induced IgM in the spleen could bind to the bacteria and contribute to the initiation of the primary response, as has been reported [280,281], and ultimately enhance bacterial killing. However, splenic bacterial load on day 4 of infection in the CD62L(E) chimeras was equivalent to that in wild type mice (figure 3.12B), suggesting that the accumulation of B cells to the spleens of wild type mice is not impacting on bacterial numbers. This lack of impact on numbers of bacteria colonising the spleen may simply be a timing issue, in that although no difference was seen on day 4, perhaps differences in bacterial numbers may be apparent at an earlier or later time-point. A detailed analysis of bacterial load over time, in the CD62L(E) chimeras, would be required.

Whether the TLR/CD62L-mediated changes to B cell migration enhance the initiation of the adaptive immune response to *Salmonella* or whether TLR-activated B cells also play roles in the regulation of the inflammatory response [282,283,284] or changes to lymphoid tissue structure during infection [285,286], the global change in migration behaviour upon TLR ligation will likely have significant consequences for the immunopathology of this infection.

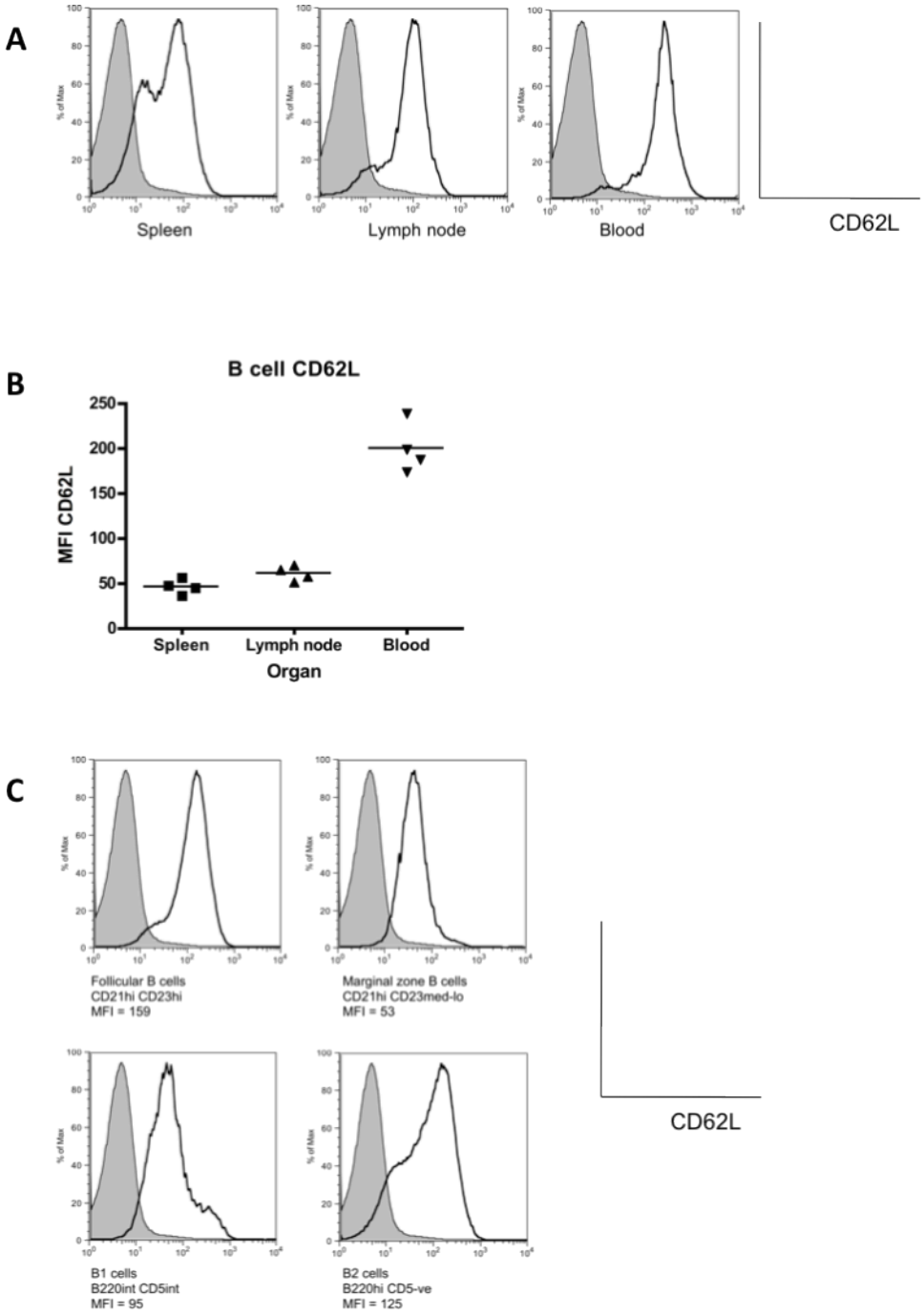

Figure 3.1: B cells from different organs and different B cell subsets express varying levels of CD62L. (A) and (B) Lymphocytes were isolated from spleens, lymph nodes and blood of naïve C57BL/6 mice and stained for B cell expression of CD62L, by gating on $CD19^+$ cells. (C) Cells from the spleen were stained for B cell subset expression of CD62L. In (A) and (C) shaded line represents the isotype control and bold line represents B cell CD62L expression. Data are representative of cells from three C57BL/6 mice.

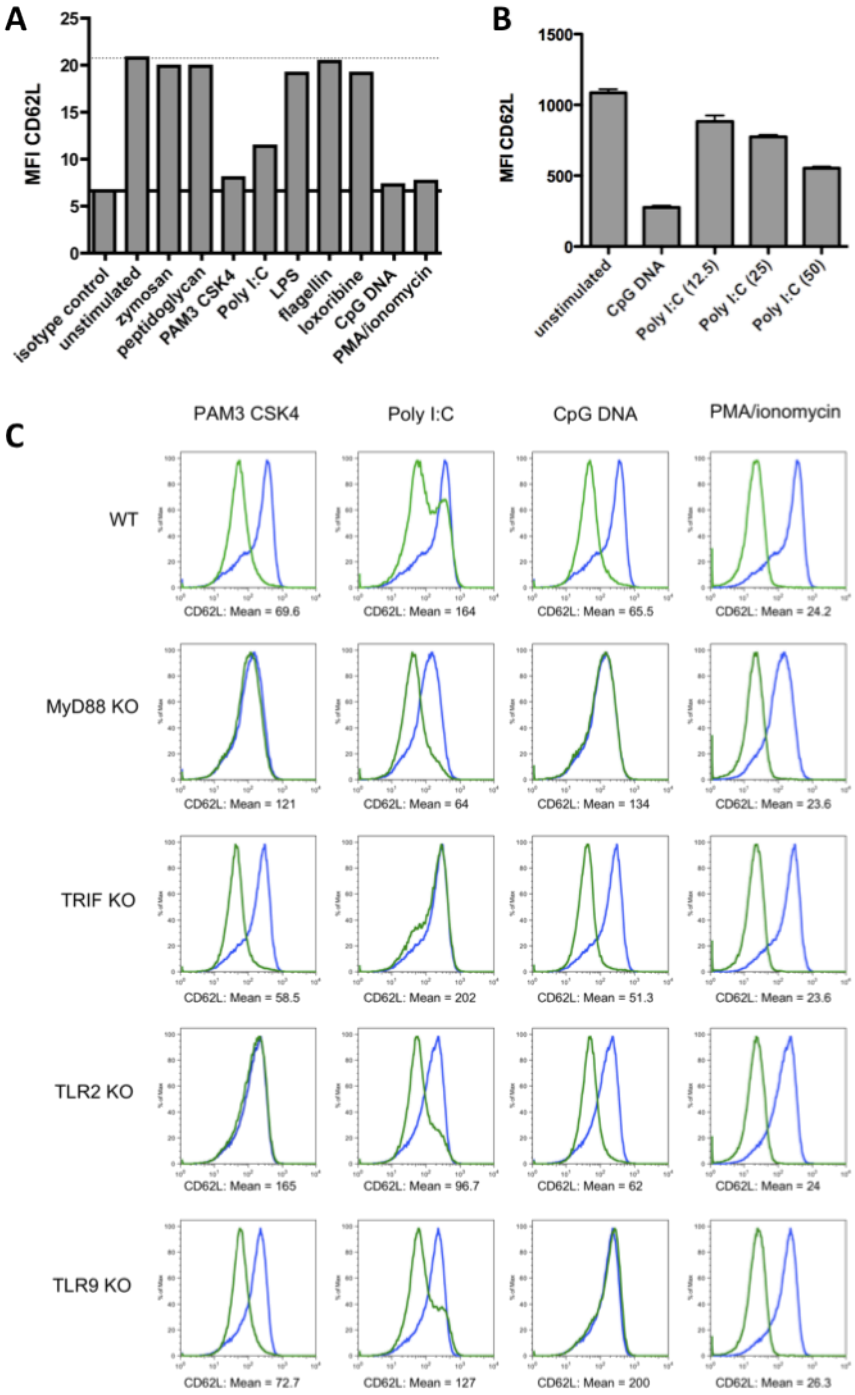

Figure 3.2: Loss of CD62L expression on B cells in response to some TLR ligands. Purified splenic B cells from C57BL/6 (A-C), MyD88$^{-/-}$, TRIF$^{-/-}$, TLR2$^{-/-}$, and TLR9$^{-/-}$ mice (C) were cultured with a variety of TLR ligands for 4 hours. B cell expression of CD62L was analysed by flow cytometry. PMA/ionomycin is included as a positive control. KO = knockout. In (A) dotted line represents unstimulated, bold line represents isotype control. In (B) the number in brackets indicates concentration of Poly I:C in µg/mL. In (C) unstimulated is in blue, and TLR stimulated in green. Data are representative of four independent experiments.

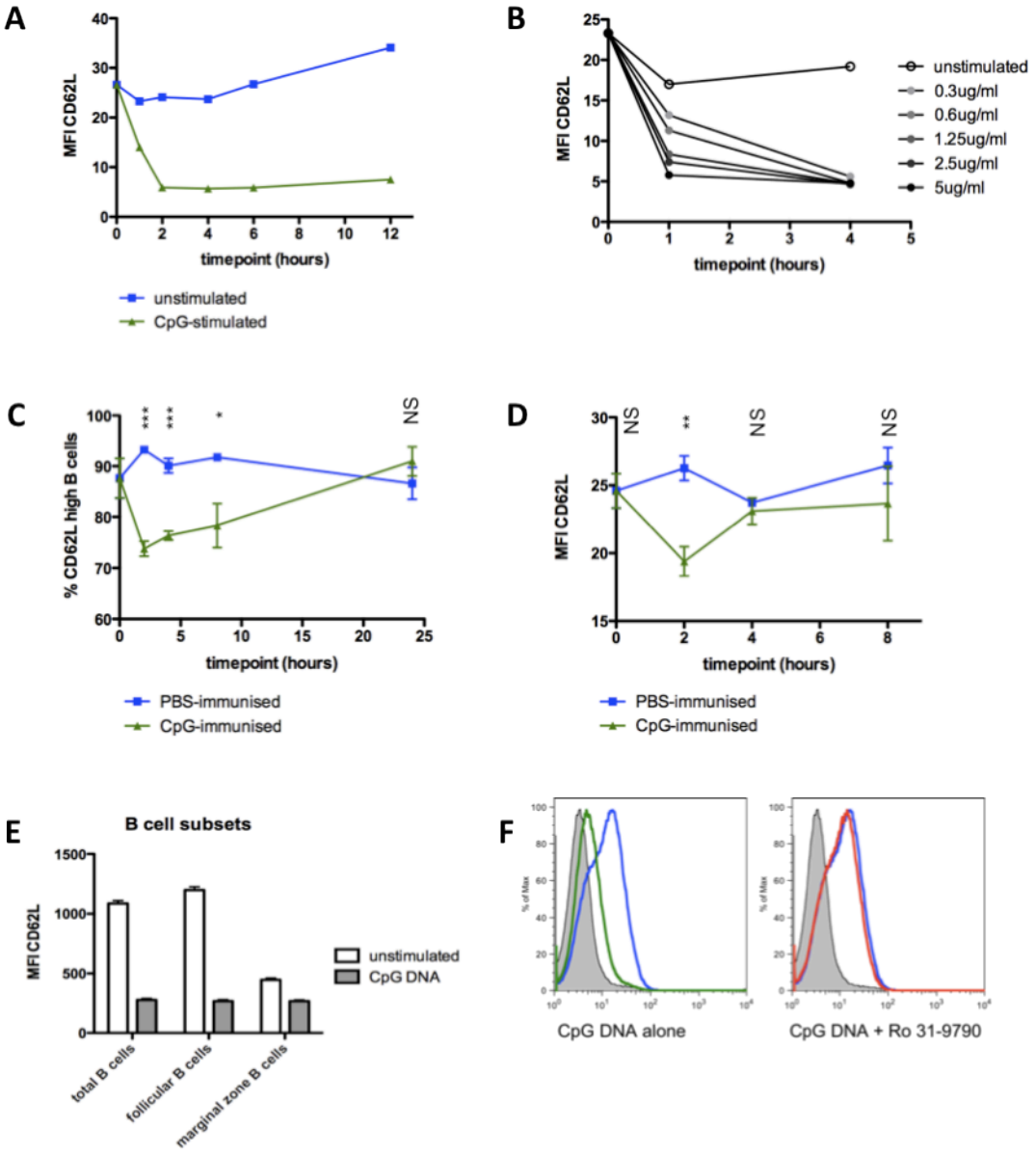

Figure 3.3: Loss of CD62L expression by B cells stimulated with CpG DNA is rapid and due to shedding from the cell surface. (A) Purified naïve B cells were cultured with 5 μg/mL CpG DNA for up to 12 hours then analysed for CD62L expression. (B) Purified naïve B cells were cultured with various concentrations of CpG DNA for up to 4 hours then stained for CD62L. (C & D) C57BL/6 mice were injected with 20μg CpG DNA and bled 2, 4, 8, and 24 hours later. Lymphocytes were isolated from the blood and B cells analysed for CD62L expression by % $CD62L^{hi}$ B cells (C) and MFI (D). Significance values are given for individual time-points, calculated by *t*-test. (E) Purified naïve B cells were stimulated with CpG DNA and B cell subset expression of CD62L analysed. (F) Purified naive B cells were cultured with CpG DNA for 4 hours with or without the addition of 50 μg/mL metalloprotease inhibitor Ro 31-9790. The isotype control is shaded, unstimulated in blue, CpG stimulation alone in green, and CpG + Ro 31-9790 is in red. In all cases, B cells were stained for expression of CD62L and analysed by flow cytometry. In (C & D) error bars indicate SEM, with 5 mice per group. Data is representative of 2-3 independent experiments.

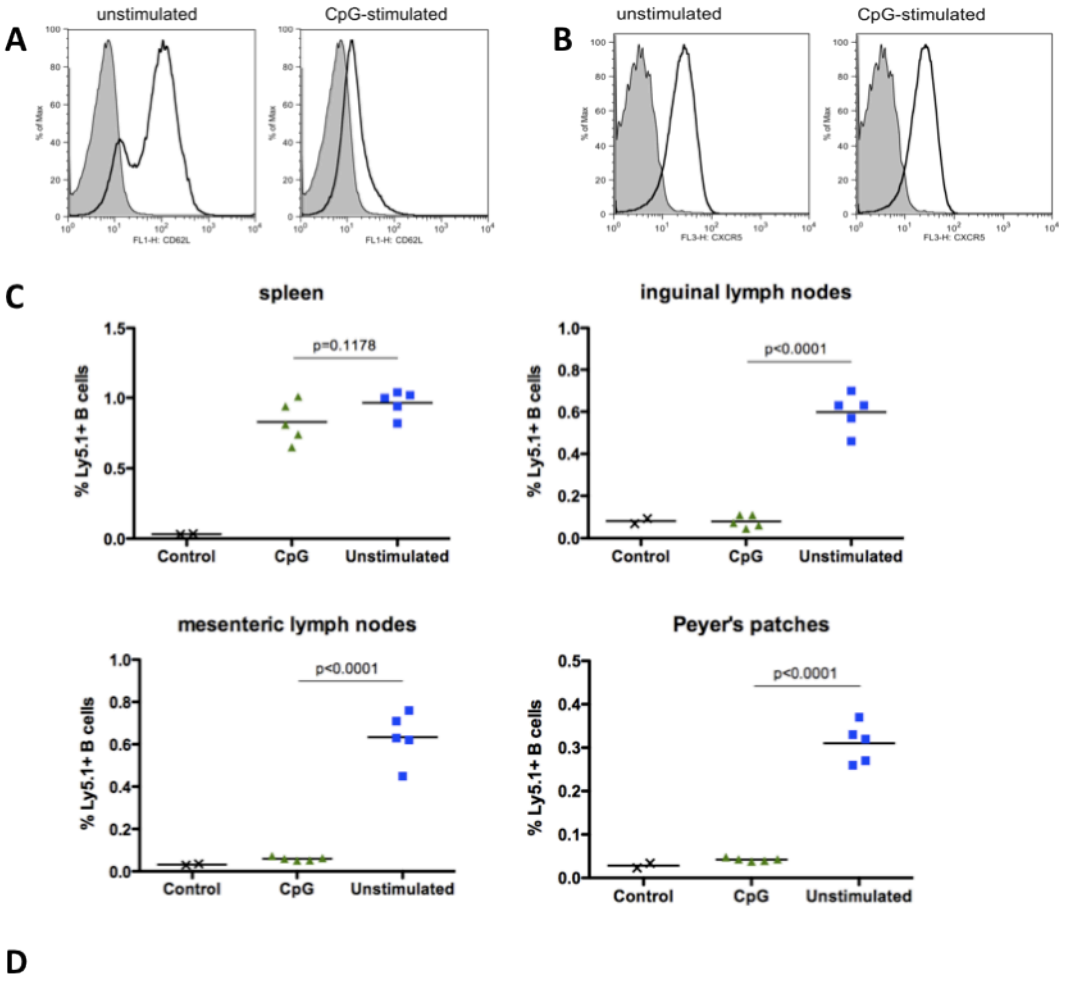

Figure 3.4: CpG-stimulated B cells are excluded from the lymph nodes and Peyer's patches. Purified Ly5.1⁺ B cells were cultured with 5μg/mL CpG DNA for 4 hours or left unstimulated. CD62L expression (A) and CXCR5 expression (B) were analysed. After washing, five million cells were transferred into C57BL/6 recipient mice. The following day (~18 hours after transfer) organs were taken and donor cells identified (C). The control mice did not receive cell transfer so indicates background staining. Significance values were calculated using the Student's *t*-test. (D) Spleen sections were stained with IgM (red) and Ly5.1 (green). Left is unstimulated B cells, right is CpG stimulated B cells. T = T cell zone, B = B cell follicle. Taken at x20 magnification. Data represents 4 independent experiments.

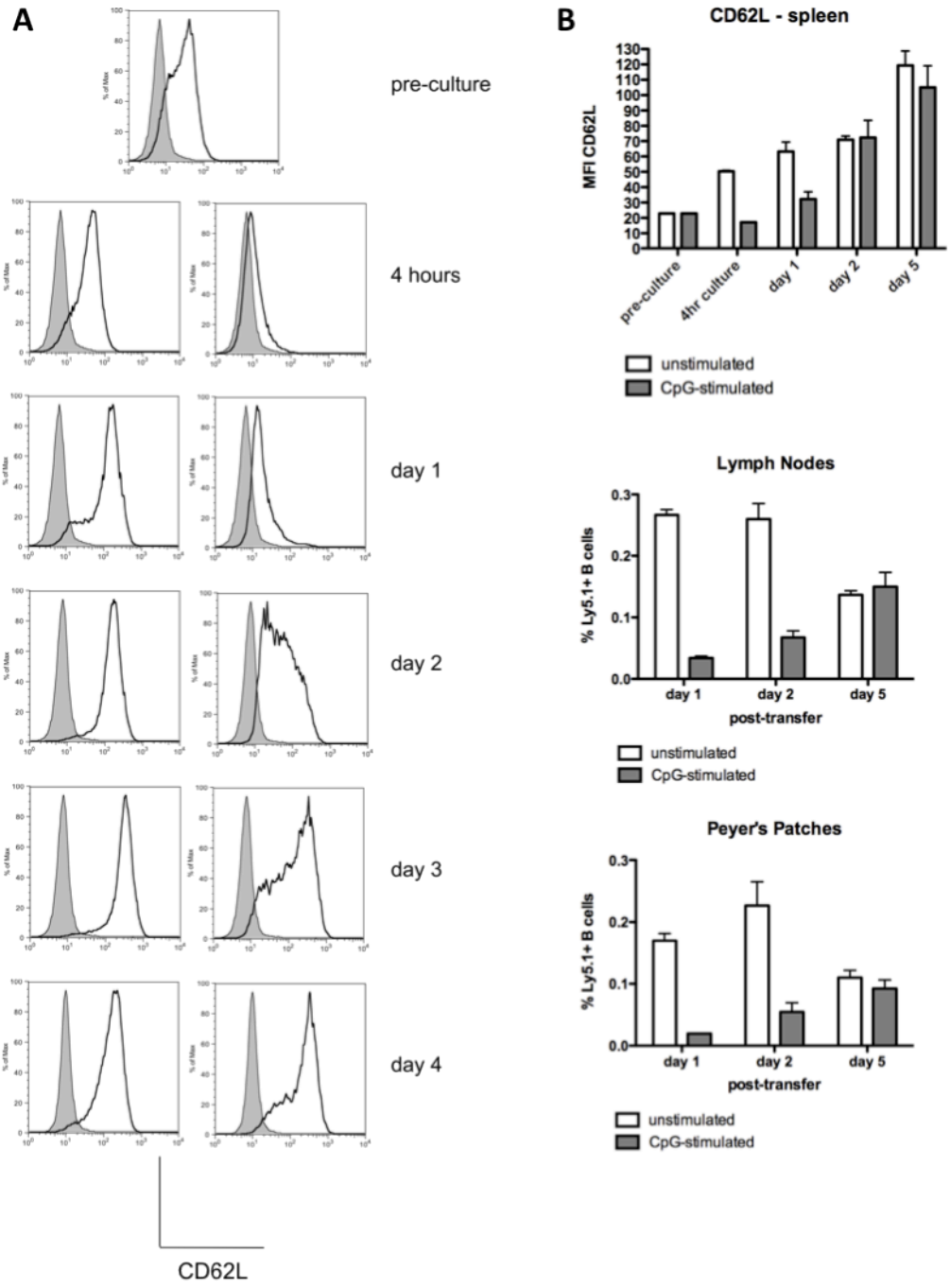

Figure 3.5: Pattern of CD62L recovery by B cells *in vitro* and *in vivo*. B cells were stimulated with CpG DNA for 4 hours *in vitro*. (A) Cells were harvested, washed and plated out again in fresh medium. Samples were taken up to 4 days later and analysed for B cell expression of CD62L. Left = unstimulated, right = CpG-stimulated. (B) After washing, 5 million cells were transferred into Ly5-distinct mice. Over the following days, organs were removed, donor cells identified (middle, bottom) and CD62L expression levels of splenic donor B cells analysed (top). Error bars show SEM, with 4 mice per group. Data represents 2-3 independent experiments.

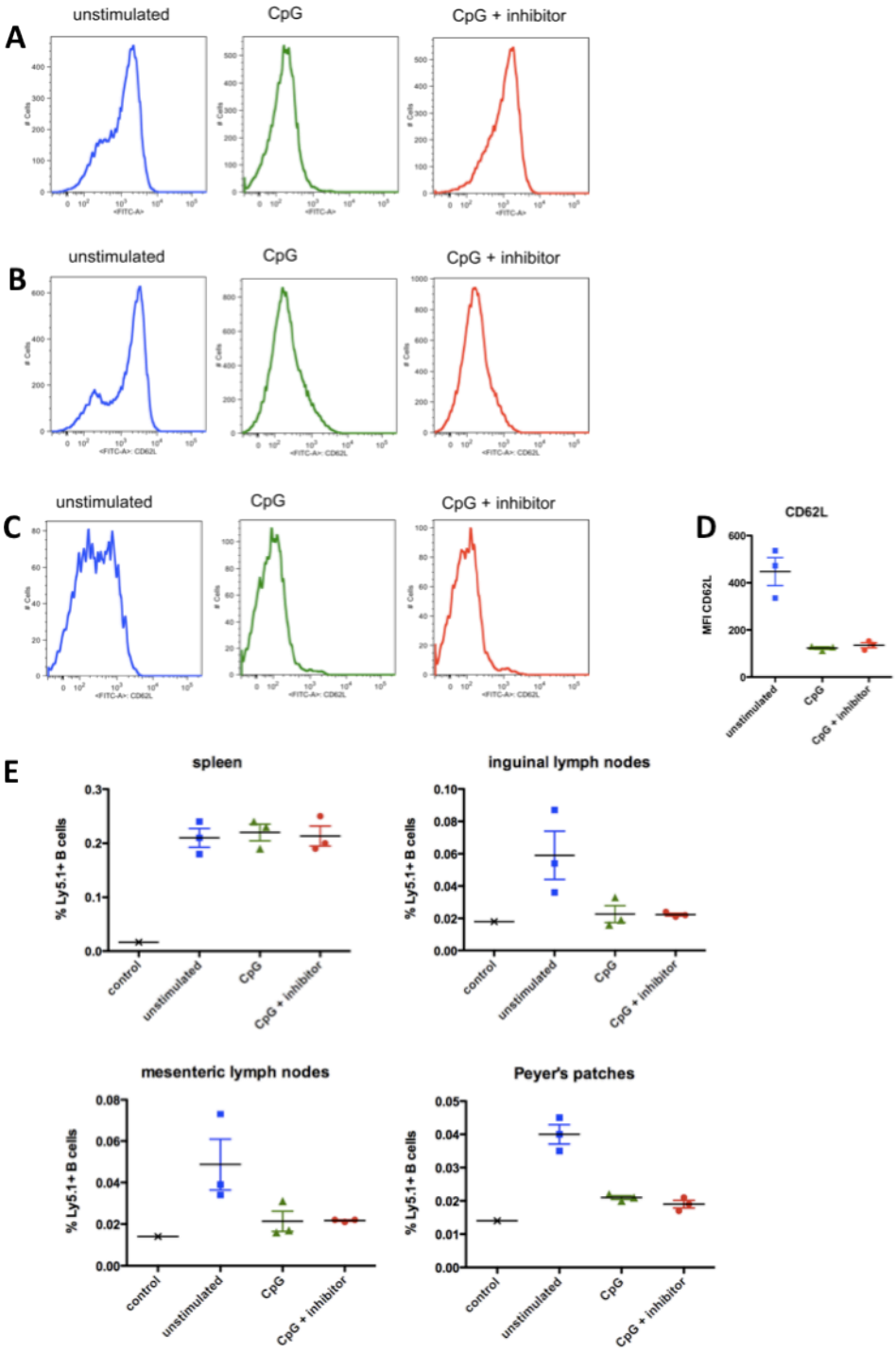

Figure 3.6: B cells stimulated with CpG DNA in the presence of the inhibitor later shed CD62L, and are excluded from lymph nodes and Peyer's patches. Purified Ly5.1$^+$ B cells were cultured with CpG DNA either with or without the inhibitor Ro 31-9790 (A). After culture, cells were either washed and left *in vitro* for a further 4 hours (B), or they were transferred into C57BL/6 mice for 4 hours (C), (D) and (E). Organs were then removed from recipient mice and donor cells identified both for their expression of CD62L (C) and (D), and for their localisation (E).

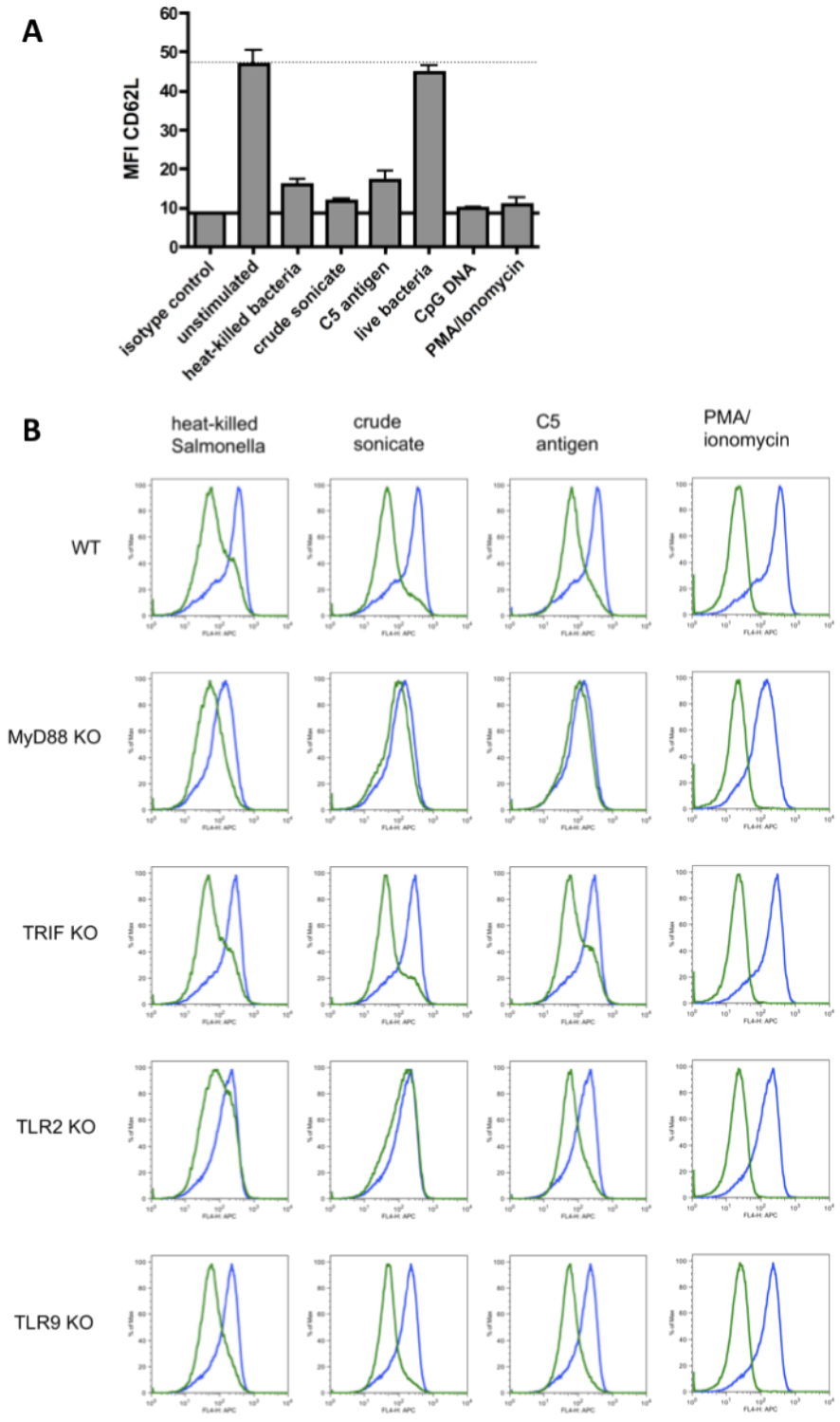

Figure 3.7: B cells shed CD62L when stimulated with antigens from *Salmonella*. Purified naïve B cells from C57BL/6 (A, B), MyD88$^{-/-}$, TRIF$^{-/-}$, TLR2$^{-/-}$, and TLR9$^{-/-}$ mice (B) were cultured with a variety of antigens from *S. typhimurium* for 4 hours. B cell expression of CD62L was analysed by flow cytometry. In (A) dotted line represents unstimulated, bold line represents isotype control. Error bars indicate SEM. In (B) blue line represents unstimulated, green line shows stimulated cells.

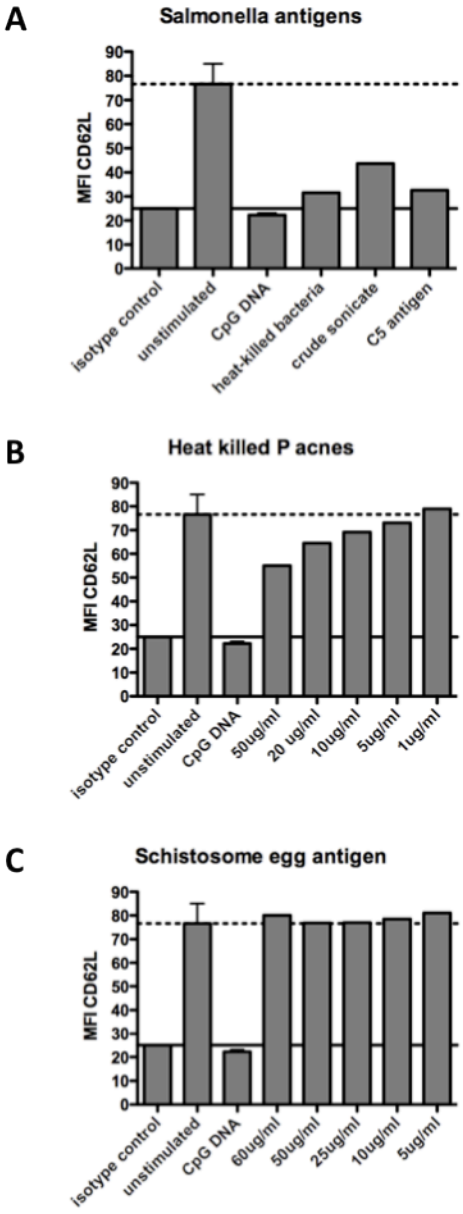

Figure 3.8: B cells also shed CD62L in response to the Gram-positive bacteria *P. acnes*, but not when stimulated with Schistosomal egg antigen. Purified naïve B cells from C57BL/6 mice were stimulated *in vitro* for 4 hours with *S. typhimurium* antigens (A), heat-killed *P. acnes* (B) or Schistosomal egg antigen (SEA) (C). In all cases the dotted line represents unstimulated, and the bold line represents the isotype control. Stimulation with CpG DNA is included as a control. Error bars indicate SEM. Data is representative of 2 experiments.

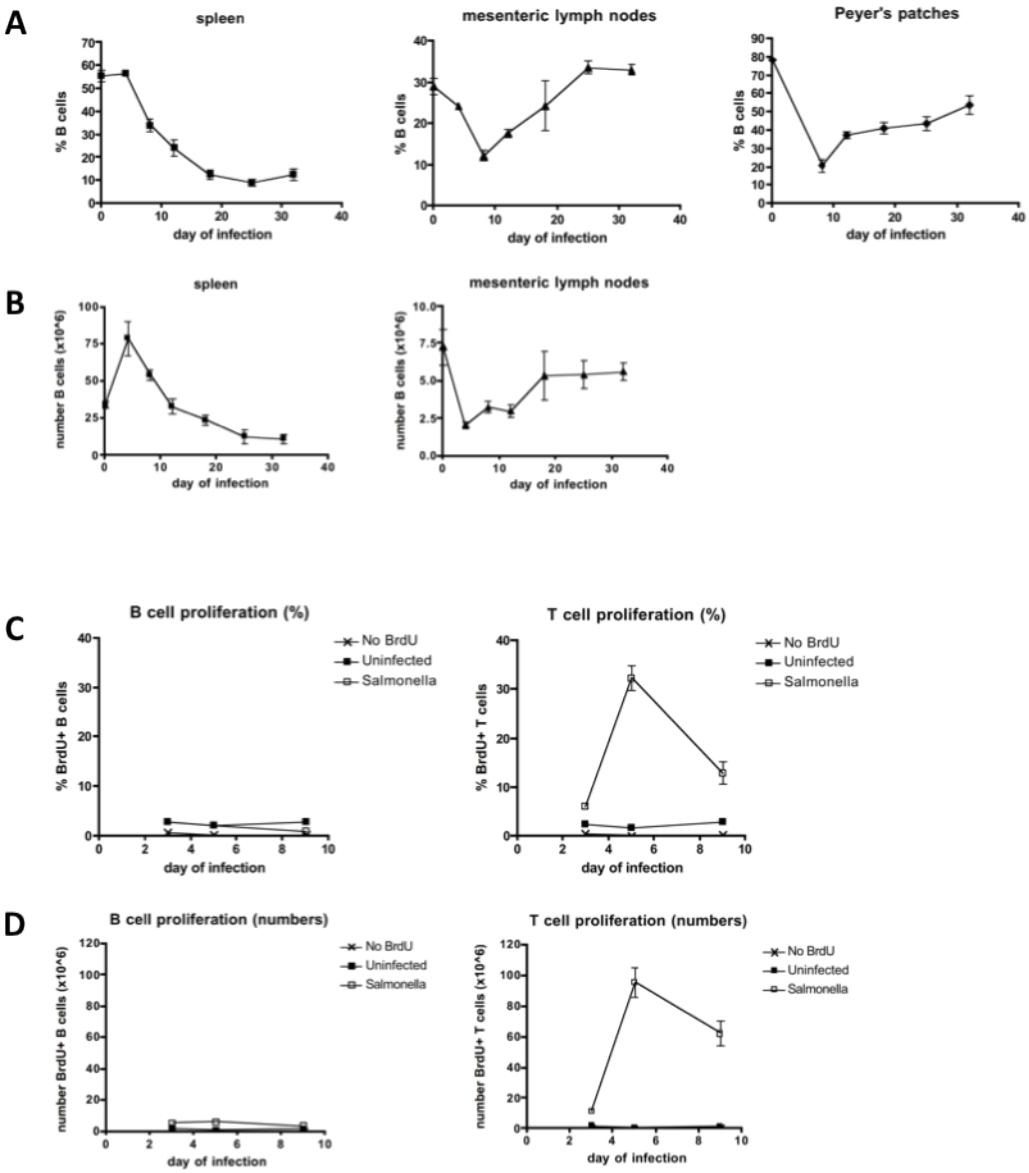

Figure 3.9: Altered localisation of B cells during *S. typhimurium* infection. C57BL/6 mice were infected with the attenuated SL3261 strain of *S. typhimurium*. Spleens, mesenteric lymph nodes and Peyer's patches were taken at various times during infection and percentages (A) and absolute numbers (B) of B cells identified. Some mice were injected (at either day 2, 4, or 8) with 2 mg BrdU i.p. and splenocytes analysed the following day for percentages (C) and absolute numbers (D) of proliferating cells. Error bars indicate SEM, with 4 mice per group.

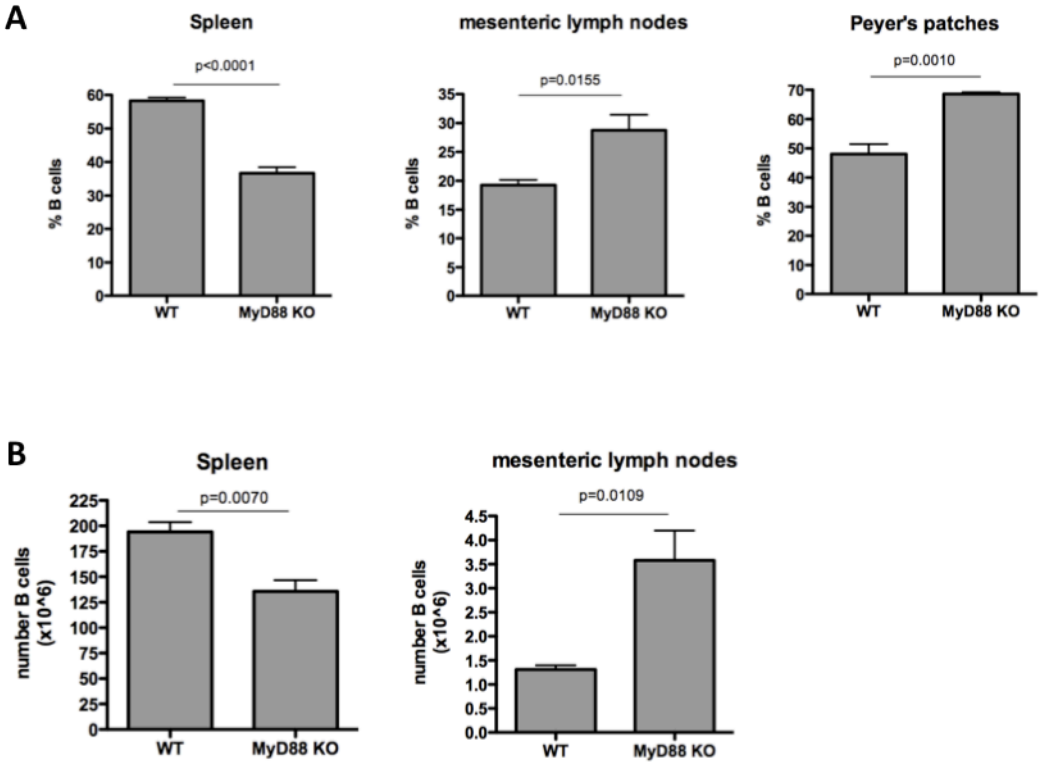

Figure 3.10: TLR-deficient mice show a reduced accumulation of B cells in the spleen during *S. typhimurium* infection. C57BL/6 and MyD88$^{-/-}$ mice were infected with the attenuated SL3261 strain of *S. typhimurium*. Spleens, mesenteric lymph nodes and Peyer's patches were taken on day 7 of infection and percentages (A) and absolute numbers (B) of B cells identified. Error bars indicate SEM, with 4 mice per group. Significance values were calculated using the Student's *t*-test. Data is representative of 2 experiments.

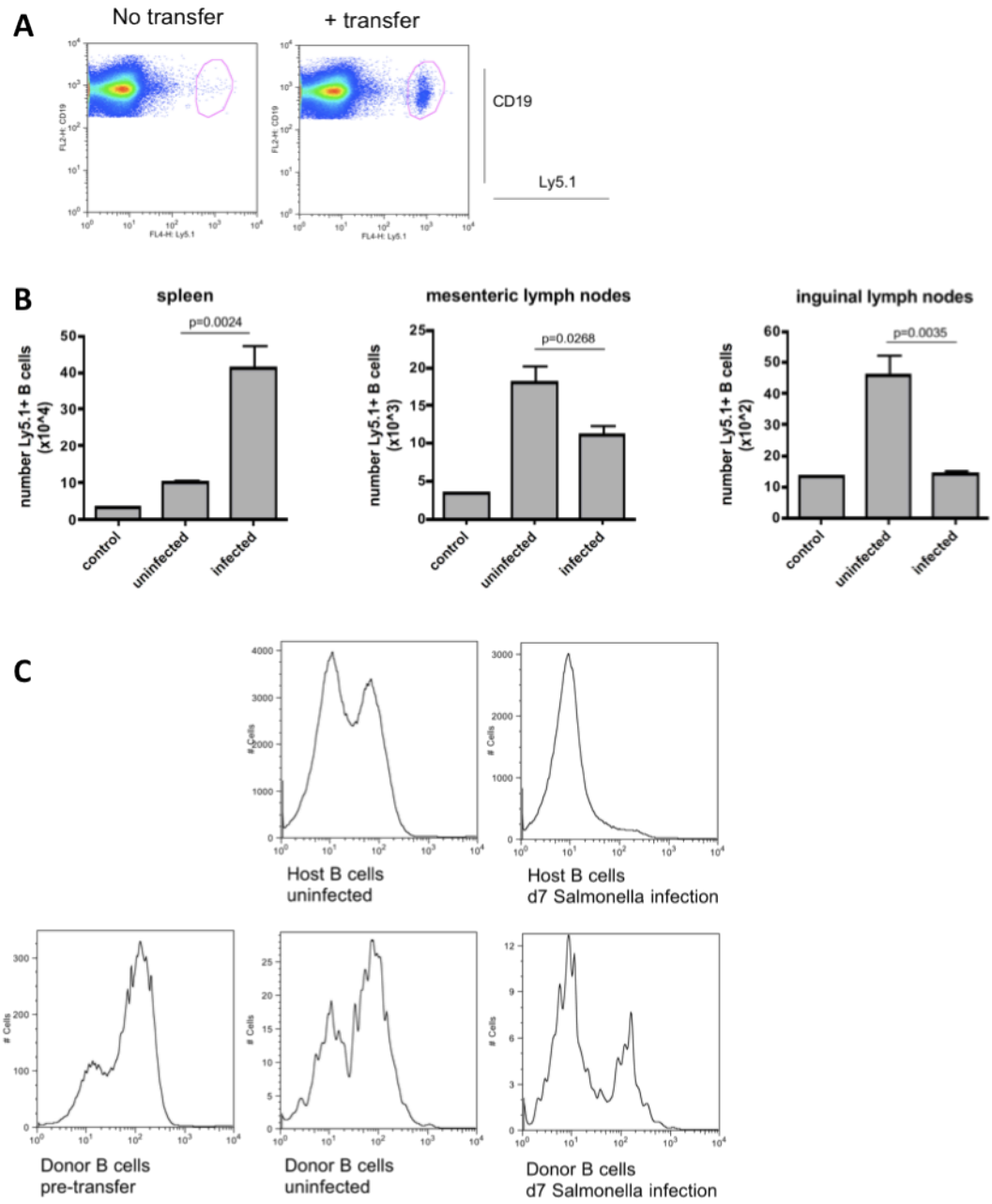

Figure 3.11: CD62L^{hi} B cells shed and migrate to the spleen, not lymph nodes, when transferred into *Salmonella*-infected mice. CD62L^{hi} cells from the blood of Ly5.1^{+} mice were transferred into either uninfected or day 6 *Salmonella*-infected C57BL/6 mice. The following day, spleens and lymph nodes were removed from recipient mice and donor cells identified. Example staining is shown in (A), with no transfer on left and cell transfer on right. Numbers of donor B cells in spleens and lymph nodes is shown in (B) CD62L expression of splenic B cells was also analysed (C). Error bars show SEM, with 5 mice per group. Data is representative of 3 independent experiments. The student's *t*-test was used to calculate significance values.

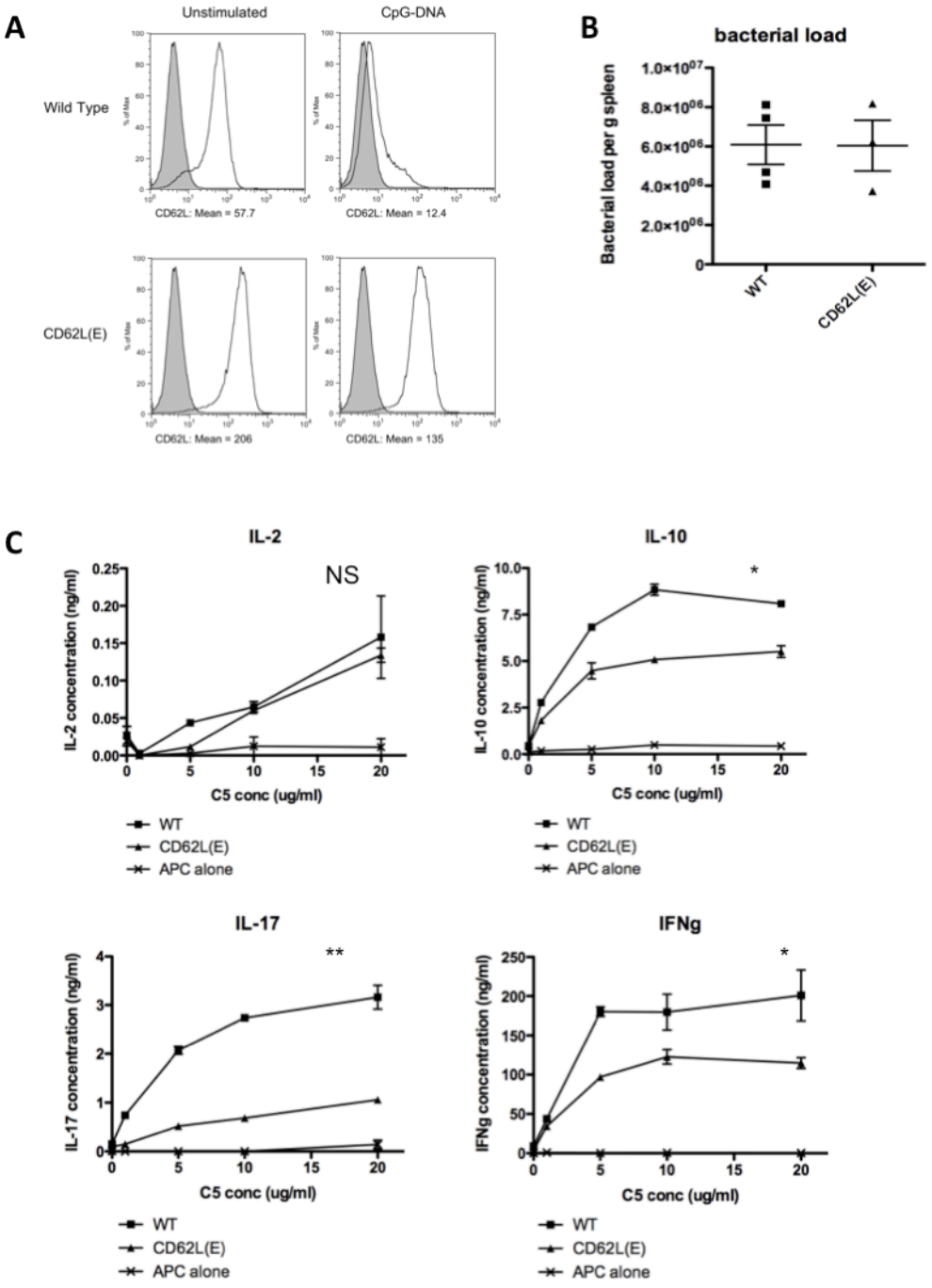

Figure 3.12: When B cells are unable to shed CD62L, primary T cell responses are impaired during *S. typhimurium* infection. Stimulation of B cells from CD62L(E) chimeric mice with CpG DNA confirmed that they do not shed CD62L (A). CD62L(E) chimeras were infected with the SL3261 attenuated strain of *S. typhimurium*. On day 4 of infection, spleens were removed and bacterial load determined (B). T cell restimulation cultures were set up *in vitro*, and T cell cytokine responses analysed (C). Two-way ANOVAs were performed to provide statistics in (C).

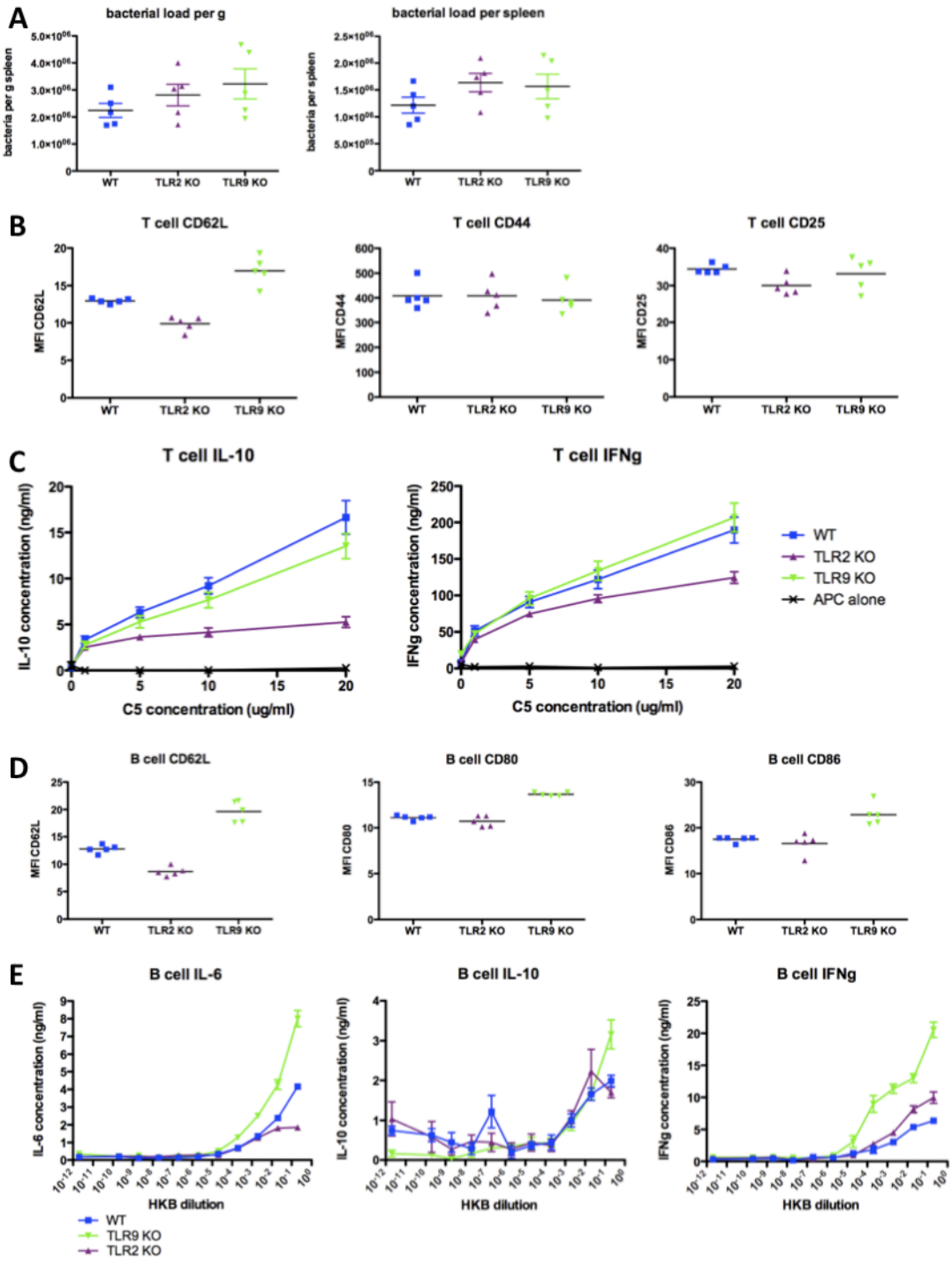

Figure 3.13: TLR2$^{-/-}$ and TLR9$^{-/-}$ mice show impaired primary immune responses to *S. typhimurium*. TLR2$^{-/-}$ and TLR9$^{-/-}$ mice were infected with *S. typhimurium.* At the peak of the primary response on day 7 of infection, spleens were removed and bacterial load calculated (A). T and B cells were analysed by flow cytometry for activation markers (B & D). T and B cells were purified and restimulated *in vitro* with C5 antigen and heat-killed bacteria, respectively, and assayed for cytokine production (C & E). Data are representative of two independent experiments.

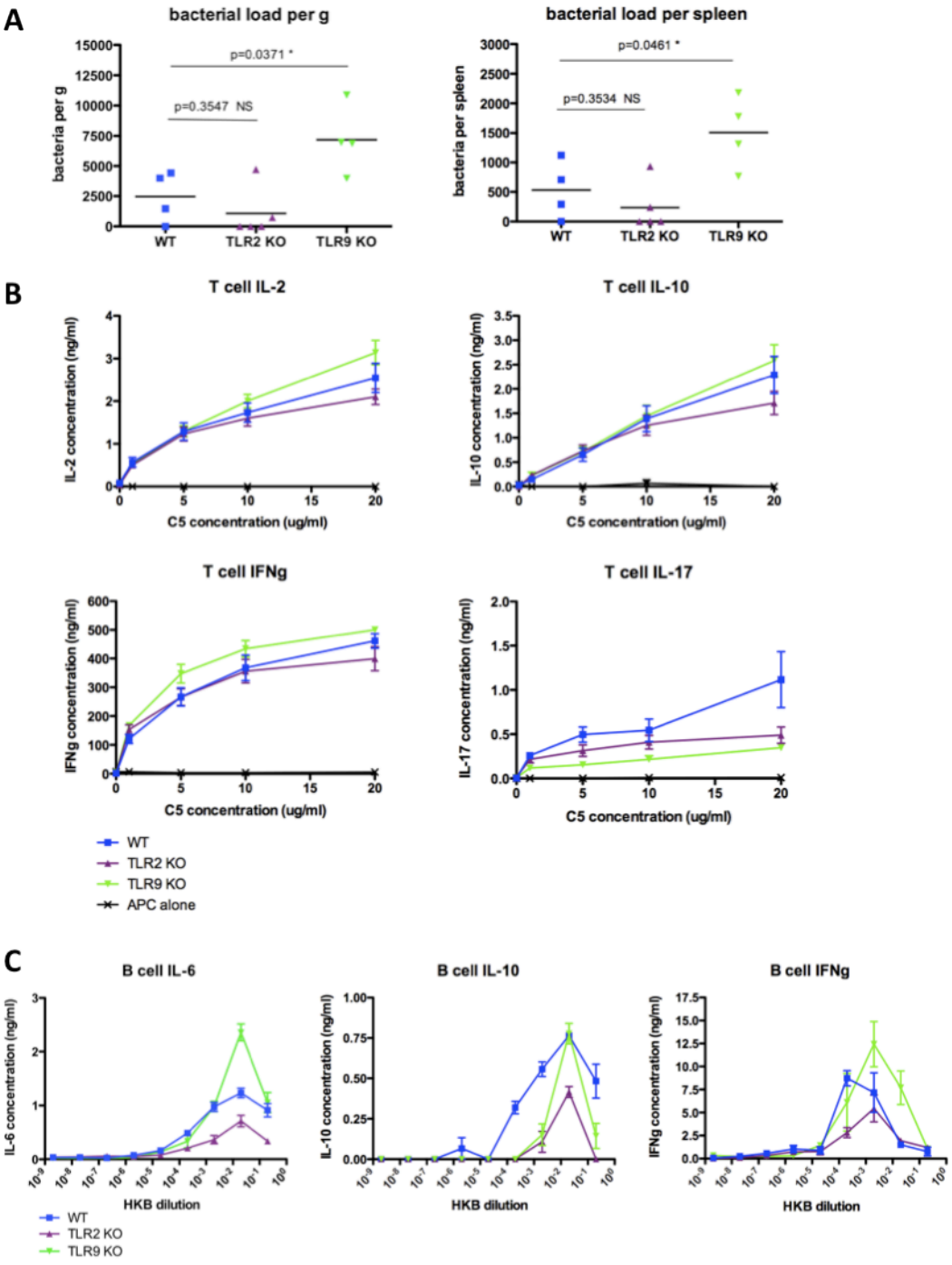

Figure 3.14: TLR2$^{-/-}$ and TLR9$^{-/-}$ mice exhibit normal T cell memory responses following *S. typhimurium* infection. Eight weeks after infection with *S. typhimurium*, spleens were removed and bacterial load calculated (A). T and B cells were purified and restimulated *in vitro* with C5 antigen and heat-killed bacteria, respectively, and assayed for cytokine production (B & C). Data represent two independent experiments.

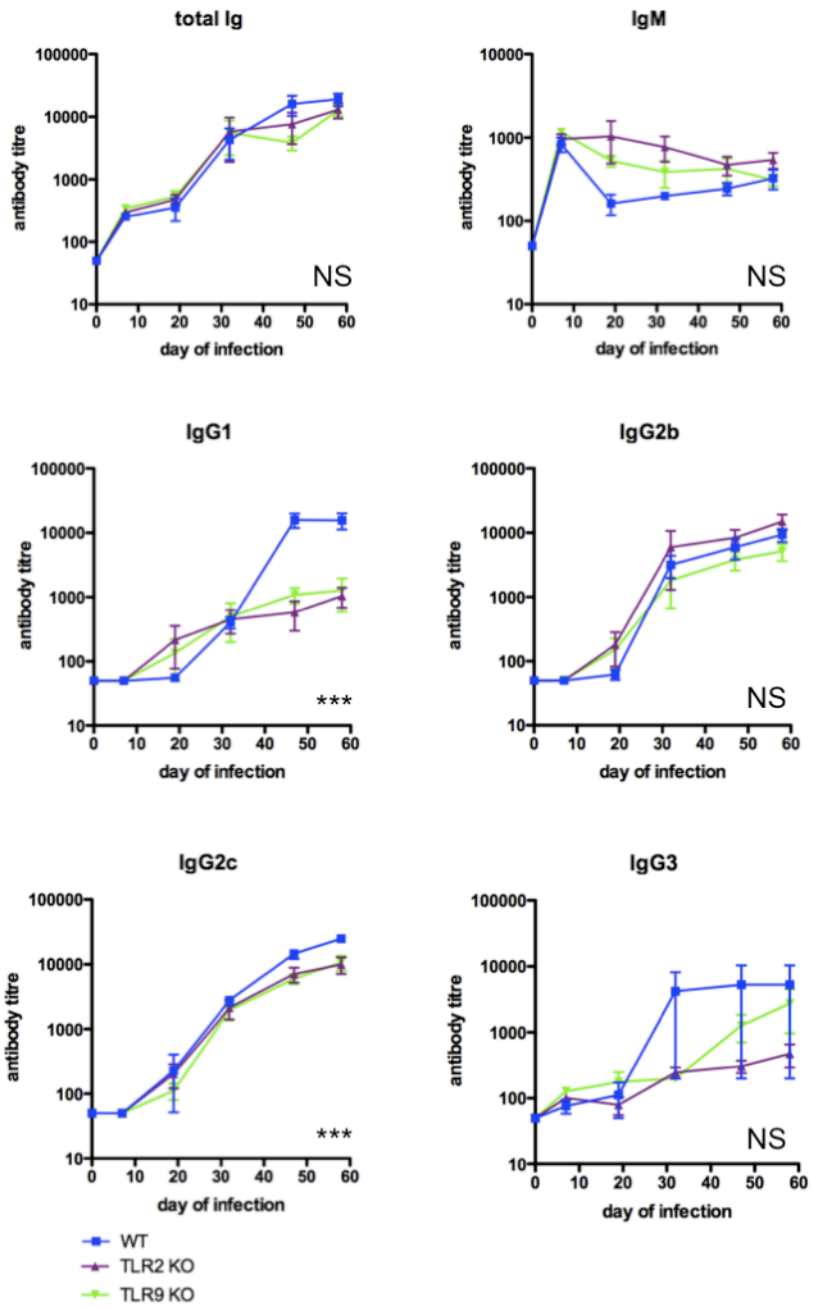

Figure 3.15: TLR2$^{-/-}$ and TLR9$^{-/-}$ mice show impaired IgG1 and IgG2c responses to *S. typhimurium*. Sera was collected from TLR2$^{-/-}$ and TLR9$^{-/-}$ mice throughout the infection, and antigen-specific antibody levels determined. Data are representative of two independent experiments. Two-way ANOVA was performed comparing WT to each of the knockout mice. In all cases NS = not significant, *** = $p<0.005$. Statistics apply to both knockout groups.

CHAPTER 4: *S. typhimurium*-induced changes in the spleen include the accumulation of antigen-presenting macrophages and the loss of marginal zone B cells

Introduction

The data presented so far using the *Salmonella typhimurium* murine infection model reveal significant changes in the B cell population early in infection due to TLR-induced alterations in surface CD62L expression. The subsequent effects on B cell migration resulted in a 2- to 3-fold increase in B cell numbers in the spleen during the initial few days of infection, as a result of influx from other lymphoid organs.

In addition to changes in the B cell population, it has previously been reported that the spleen undergoes profound changes to other immune cell populations during *Salmonella* infection. The most obvious phenotype of these changes is the splenomegaly induced by this infection, which is thought to be due mainly to the infiltration of macrophages and neutrophils [287,288], although as we saw in chapter 3, B cells also contribute. Macrophages, members of the reticuloendothelial system, are not only the cells in which the bacteria live and divide [197], but are also essential for the early control of the exponential growth phase of this bacterial infection [287]. Without this early control of bacterial growth, mortality rates are significantly increased [289].

The normal site of entry for *Salmonella* is via the oral route, and the invasion of the M-cells in the gut epithelium. From there, the bacteria pass through the Peyer's patches and mesenteric lymph nodes, and enter the bloodstream [201]. In the infection model used here, bacteria are injected intravenously, and the infection is immediately systemic. In both cases, systemic bacteria mean that the spleen is the major site of immune defence. The structure of the spleen enables the innate and adaptive arms of the immune response to come together and remove any blood-born pathogens they encounter. Macrophages are particularly important in this process. However, the clearance of *Salmonella* and the generation of protective immunity are dependent, not only on innate cells such as macrophages, but also on adaptive B and T cell responses [201]. IFNγ production by T cells and natural killer cells is necessary to enhance bacterial killing by innate cells residing in the spleen [201].

Furthermore, as already mentioned above, both T cell memory responses and B cell antibody production are generated, and involved in protective immunity [201]. Thus the spleen is the major site of bacterial accumulation, and is epicentre of the battle against this infection.

Here, the splenic changes induced by *S. typhimurium* infection are analysed in more detail by means of flow cytometry and immunohistology. The increasing macrophage population is investigated, as is the impact of infiltrating cells on splenic architecture, and the role of TLRs. Additionally, one of the early observations is the loss of the marginal zone population of B cells within the first few days of infection. I go on to consider the fate of these cells, and the downstream effects of losing these cells on the entry of blood-borne particles into the white pulp regions of the spleen.

Results

Infection with *S. typhimurium* causes splenomegaly and changes to lymphocyte population numbers within the spleen

Infection with *Salmonella typhimurium* is known to cause splenomegaly in mice [206]. Using spleen weight as a measure of splenomegaly, the data presented in figure 4.1A reveal that the onset of splenomegaly was rapid and severe. By day 7 of infection, spleen weight had increased by around 6-fold, and by day 12 reached a plateau at ~0.8g. In MyD88$^{-/-}$ mice this initial increase in spleen weight was reduced in comparison to wild type mice (figure 4.1B), suggesting that splenomegaly is partially, although not wholly, dependent on TLR stimulation. The time-course did not extend as far in the MyD88$^{-/-}$ mice so it was not possible to determine whether the onset of splenomegaly was simply delayed in the absence of MyD88 signalling, or whether the peak of spleen weight was reduced.

Looking at the kinetics of bacterial growth and contraction in wild type mice, splenic bacterial load, shown per gram (figure 4.1C) and per spleen (figure 4.1D), peaked around day 8, with bacteria being reduced to very low levels around 4 weeks after infection. However, a few bacteria still remained even 8 weeks after infection, suggesting that complete clearance of bacteria and the development of sterilising immunity is a relatively slow process in this infection model.

As mentioned in figure 3.9, B cell proportions and numbers within the spleen were found to change drastically during *S. typhimurium* infection. This is shown again in figures 4.1E & F, extending the time-course further. The percentage of B cells within the spleen decreased drastically, constituting only ~10% of live cells by day 30, compared to 50-60% in uninfected mice (figure 4.1E). Following the initial increase, absolute numbers of B cells were also reduced at this time-point (figure 4.1F). Furthermore, the proportion of CD4^{+} T cells within the spleen was reduced during the early stages of infection, up until day ~30 (figure 4.1G). However, when absolute numbers of T cells were calculated, T cell numbers were seen to be increased throughout infection (figure 4.1H). This increase is likely due to T cell division, as was seen in figure 3.9 when BrdU incorporation was studied. B and T cell numbers returned to normal levels around 80 days post-infection, indicating that the changes in lymphocyte populations within the spleen during *Salmonella* infection were inherently long-lived. The return of lymphocyte numbers in the spleen to pre-infection levels appeared to correlate with the clearance of bacteria.

Macrophage influx disrupts splenic architecture early in infection

The splenomegaly associated with *Salmonella* infection is likely caused by the influx of immune cells, probably macrophages [287,288]. To confirm the identity of these cells and further investigate the changes within the spleen, immunohistological analysis of infected spleen sections was performed. The representative photographs shown in figure 4.2 confirm that, by day 8 of infection, a large proportion of cells within the spleen were macrophages, as identified by CD11b staining (red). In uninfected mice (day 0), the $CD11b^+$ cells were found exclusively in the red pulp, surrounding the IgD^+ B cell follicles (blue areas). Pre-infection, macrophages were fairly dispersed throughout the red pulp, with few CD11b bright cells. By day 1 of infection, there were many more $CD11b^+$ cells within the red pulp, suggesting either an early influx of macrophages or an upregulation of this molecule on existing cells. Looking at day 4- and day 8-infected mice, there was a clear increase in $CD11b^+$ cell numbers, with $CD11b^+$ cells appearing in clumps in the red pulp region. Moreover, these cells appeared to have infiltrated the white pulp, as there were more cells staining red in the IgD^+ B cell follicles (blue), while the B cell areas appeared to be fragmenting at the later time-points. Thus, by this early stage of infection, the white pulp regions are being disrupted by infiltrating macrophages.

Further investigation suggests that these infiltrating macrophages are presenting antigen (figure 4.3). On day 0, the macrophages, identified by F4-80 staining (green), were focussed in the red pulp surrounding the areas of white pulp, in a similar pattern to the CD11b staining seen on day 0 in figure 4.2. In uninfected mice (day 0), the white pulp, consisting of the B cell follicles and T cell zones, exhibited MHC class II^+ cells (blue). These were B cells within the follicles and dendritic cells within the T cell zone, both of which have the capacity to present antigen. The $F4\text{-}80^+$ macrophages in the red pulp were MHC class II^- in the uninfected mice (i.e. green not blue). Progressing through the pictures of day 1, day 4, and day 8 infected mice, it can be seen that the macrophage population increased (more green), and also that these macrophages had increased expression of MHC class II (more green-blue double-positive cells). By day 8, these MHC class II^+ macrophages were found to be widespread throughout the spleen, with the areas of white pulp less distinguishable. Together, these data indicate that, during *Salmonella* infection, antigen-presenting macrophages influx into the spleen. Additionally, splenic architecture, in terms or red and white pulp regions, is severely disrupted, which may be due to the infiltrating macrophages.

Marginal zone B cells are lost in the first few days of infection

In addition to the influx of macrophages into the infected spleen, it has already been noted above that the white pulp regions are disrupted, and that the B cell population also undergoes significant changes. To investigate the changes to the B cell regions in more detail, immunohistological analysis of infected spleen sections, together with flow cytometry, were used to visualise B cell subsets.

By staining for CD21 and CD23 by flow cytometry, it was possible to distinguish between marginal zone B cells ($CD21^{hi}$ $CD23^{int\text{-}lo}$) and follicular B cells ($CD21^{int\text{-}hi}$ $CD23^{hi}$) within the spleen. In uninfected mice, marginal zone B cells constitute ~5% of B cells (figure 4.4A, far left, gated cells). The data presented in figure 4.4A reveal that this population of B cells, visible as a separate population on day 0, is either lost, or changes phenotype, early in infection. Although still visible on day 1, by days 4 and 8 this population is no longer distinguishable from follicular B cells. Also, the expression of CD23 by the large population of follicular B cells was reduced, even by day 1 of infection, while marginal zone B cells also appeared to have down-regulated expression of this molecule (figure 4.4A). Thus, from the flow cytometry data, it is not possible to determine whether marginal zone B cells disappear (by death, differentiation, or migration out of the spleen) or simply alter their phenotype, in terms of CD21 and CD23 expression, such that they can no longer be identified by flow cytometry. Sections from infected spleens were therefore analysed in an attempt to determine the fate of this cell population.

Marginal zone B cells can be identified by histology as IgM^{+} IgD^{-} cells, in contrast to follicular B cells that express both these markers. In uninfected mice the border of marginal zone B cells is clearly visible surrounding the follicles (figure 4.4B, day 0, red cells surrounding the purple follicular B cells). By day 1 of infection, this population looks to have dispersed, with few IgM^{+} IgD^{-} cells remaining *in situ*. On days 4 and 8 of infection, there is no distinguishing border to the follicles, as the marginal zone population of B cells no longer exists. By this stage, macrophages were infiltrating the white pulp (as seen in figures 4.2 & 4.3), contributing to the disrupted nature of the follicles. Therefore, it seems apparent that the marginal zone B cells do not simply alter CD21 and CD23 expression, making them undetectable by flow cytometry, but disappear completely from their usual position surrounding the white pulp regions of the spleen.

The absence of MyD88 signalling delays, but does not prevent, the loss of marginal zone B cells

Having established that marginal zone B cells are lost within 1-3 days of *S. typhimurium* infection, I wished to investigate whether this process was dependent on TLR stimulation. To do this, MyD88$^{-/-}$ mice were infected with *S. typhimurium*, and splenic B cell populations analysed by histology and flow cytometry, as in figure 4.4 above.

By flow cytometry, marginal zone B cells were clearly distinguishable from follicular B cells, by CD21 and CD23 expression, up to day 4 of infection of MyD88$^{-/-}$ mice (figure 4.5A). By day 8 of infection, a small population of marginal zone B cells looks to still be present. This is in contrast to wild type mice, in which this population was entirely lost by day 4 (figure 4.4A). Thus the loss of marginal zone B cells in MyD88$^{-/-}$ mice appears to be delayed by around 4 days. Additionally, follicular B cell reduction in CD23 expression appeared delayed in the absence of MyD88 signalling (figure 4.5A), suggesting that this, too, is partially dependent on TLR stimulation.

Immunohistological analysis provided more insight into the delayed loss of marginal zone B cells in MyD88$^{-/-}$ mice (figure 4.5B). On day 1 of *S. typhimurium* infection, when marginal zone B cells were already lost in wild type mice, there was a clear border of IgM^{+} IgD^{-} marginal zone B cells around the follicle (red cells around the purple follicular B cells). By day 4, this population was beginning to fragment, but was still visible. By day 8, however, only the remnants of this population remained. Together, the data presented in figure 4.5 conclude that the loss of the marginal zone population of B cells is delayed, but not prevented, in MyD88-deficient mice. Therefore, a component of the loss of this population is mediated by TLR signalling. This begs the question of what is happening to this population of cells. One hypothesis would be that marginal zone B cells differentiate into plasma cells following TLR stimulation. This theory is further investigated below.

An early extrafollicular plasma cell response develops by day 4 of *S. typhimurium* infection

In an attempt to identify the fate of the marginal zone B cell population, observations were made on the differentiation of plasma cells in the early stages of infection. Staining for IgM on infected spleen sections is a means, not only of identifying B cell follicles, but also of visualising IgM-secreting plasmablasts and plasma cells, which appear as very bright cells. The photographs presented in figure 4.6 reveal the presence of plasmablasts / plasma cells by

day 4 of infection (see arrows), which appeared to be producing IgM, but did not express IgG (data not shown). These IgM-secreting cells were located out-with the white pulp, in the red pulp region, rather than within GCs in B cell follicles, and thus are termed an extrafollicular plasma cell response. Again, the pictures presented in figure 4.6 demonstrate the disruption of the follicles by days 4 and 8 of infection, when marginal zone B cells are lost and the plasma cell response is most apparent. In order to quantify the development of these plasma cells and investigate the involvement of TLR stimulation, further analysis by flow cytometry was required.

MyD88$^{-/-}$ and CD1d$^{-/-}$ mice show impaired early plasma cell differentiation and IgM production during *S. typhimurium* infection

In order to quantify the early extrafollicular plasma cell response in *Salmonella*-infected mice, flow cytometry for the B cell markers B220 and CD138 was used. Example staining is shown in figure 4.7A. Plasmablasts, the precursors of plasma cells, are identified as B220^{+} CD138^{+} cells (right hand gate), while fully differentiated plasma cells are B220$^{int\text{-}lo}$ CD138^{+} (left hand gate). Both these cell types are capable of antibody secretion and therefore IgM-secreting plasmablasts and plasma cells were revealed by immunohistology in figure 4.6 above. By flow cytometry, plasmablast numbers were elevated at days 4 and 8 of infection in wild type mice, while plasma cells were only readily detectable in day 8-infected mice (figures 4.7B, circles). These plasmablasts and plasma cells appeared to be secreting IgM, as detectable levels of *Salmonella*-specific IgM were present in wild type mice on both day 4 and day 8 (figure 4.7C, circles), while *Salmonella*-specific IgG was not detected at this time-point (data not shown).

Given the above results that marginal zone B cell loss is delayed in MyD88$^{-/-}$ mice, I wished to determine whether plasma cell differentiation and/or IgM production was also delayed in these mice. This will provide insight into whether marginal zone B cells are likely to be the source of the IgM-secreting plasma cells found in wild type mice. In addition to looking at the early plasma cell responses in MyD88$^{-/-}$ mice, I also made use of CD1d$^{-/-}$ mice, which do not possess marginal zone B cells. Therefore, if the theory that marginal zone B cells differentiate into IgM-secreting plasma cells in response to TLR stimulation is correct, then one would expect MyD88$^{-/-}$ mice to have delayed plasma cell differentiation and IgM production, and CD1d$^{-/-}$ mice to have significant impairments in these functions.

The data displayed indicate that both MyD88$^{-/-}$ and CD1d$^{-/-}$ mice have reduced plasmablast numbers when compared to wild type mice, throughout the time-course of the experiment (figure 4.7B, left). Furthermore, plasma cell numbers were also reduced in MyD88$^{-/-}$ mice at day 8, while in CD1d$^{-/-}$ mice plasma cells were virtually absent (figure 4.7B, right). *Salmonella*-specific IgM was also diminished in both MyD88$^{-/-}$ and CD1d$^{-/-}$ mice (figure 4.7C). Taken together, these data indicate that early plasma cell differentiation and IgM production was reduced in MyD88$^{-/-}$ mice and significantly impaired in CD1d$^{-/-}$ mice. Therefore, the loss of the marginal zone B cell population in *S. typhimurium* infection correlated with the generation of IgM-secreting plasma cells. Thus it seems possible that the early extrafollicular plasma cell response was as a result of marginal zone B cell differentiation following TLR stimulation.

Staining of B cells *in vivo* is reduced during *S. typhimurium* infection

Due to the location of the marginal zone within the spleen, directly adjacent to the marginal sinuses, cells within the marginal zone are among the first to encounter blood-born antigen [2]. Indeed, marginal zone B cells have been shown to capture such blood-borne particles [252]. Here, I use an *in vivo* staining technique, by injecting fluorescently labelled antibodies, to further explore the loss of marginal zone B cells during *S. typhimurium* infection.

When fluorescently labelled antibodies against B cell markers are injected into mice, they are predominantly taken up by the marginal zone B cell population [252]. Here, anti-CD21 FITC and anti-CD19 PE were injected i.v. into recipient (uninfected) mice and, 20 minutes later, splenic B cell subsets analysed for binding by flow cytometry. Anti-CD21 FITC should be bound preferentially by marginal zone B cells, as this cell population expresses greater levels of CD21 on their surface. Anti-CD19 PE, however, has the ability to bind both marginal zone and follicular B cells, with no preference for either subset, *in vitro*. Here, 40-45% of follicular B cells bound (either) antibody in 20 minutes of exposure *in vivo*, while for marginal zone B cells the figure was much higher – around 65-70% (figure 4.8A). This confirms previous findings that marginal zone B cells are the first subset of B cells to encounter systemic particles [252].

As marginal zone B cells are lost during *S. typhimurium* infection (and these cells express highest levels of CD21), a fall in the number of B cells binding the anti-CD21 FITC antibody during infection would be expected. This is exactly the case, in that the proportions

of B cells binding anti-CD21 FITC in 20 minutes *in vivo* was significantly reduced following injection on days 1, 4, and 7 of infection (figure 4.8B). However, it was not known what effect the loss of marginal zone B cells would have on anti-CD19 PE binding during infection. One might expect binding of anti-CD19 PE to decrease also, due to the loss of marginal zone B cells. Alternatively, binding of anti-CD19 PE may be expected to increase, for two reasons. Firstly, early in infection, B cell numbers in the spleen have been shown to increase due to influx from other lymphoid organs (as presented in chapter 3). Secondly, the loss of marginal zone B cells may result in the exposure of follicular B cells to blood-borne particles. The results presented in figure 4.8C indicate that, during infection, anti-CD19 PE binding by B cells was also reduced, although to a lesser extent than binding of anti-CD21 FITC. These results suggest that, although marginal zone B cells are lost during infection, particles from the blood (in this case fluorescently labelled antibodies) do not have free access to follicular B cells. Thus it appears that a 'barrier' remains in place in the marginal zone region during infection, despite the loss of the marginal zone B cell population.

Labelled antibodies continue to accumulate in the marginal zone during infection, and do not enter the follicles

The data presented in figure 4.8C above suggest that, despite the loss of marginal zone B cells during infection, blood-borne particles do not have access to the follicles. In order to further investigate the maintenance of this 'barrier' in the marginal zone region, spleen sections from mice injected with anti-CD19 PE were analysed, to identify the location of injected antibody within the spleens of infected mice.

In figure 4.9 it can be seen that, in uninfected mice, the anti-CD19 PE antibody (red) was found to accumulate in the marginal zone. Dull staining was seen in the red pulp region, surrounding the B cell follicles, perhaps due to non-specific binding by macrophages. Meanwhile staining appeared strongest at the marginal zone, presumably due to binding by marginal zone B cells. Across all time-points of infection, it appears that the antibody had concentrated in regions around the follicles, in the marginal zone. Even in day 8-infected spleens, when marginal B cells had been lost and the follicles had partially broken up, antibody still accumulated around the follicles. The follicles themselves appeared as black voids, with no antibody binding (highlighted by 'F' in the pictures), indicating that antibody had not infiltrated these regions. These data strengthen the argument that, although marginal zone B cells are lost during infection, a barrier remains intact between the red pulp and white pulp areas of the spleen, and systemic particles accumulate in this region.

Marginal zone metallophilic macrophages become partially fragmented during *S. typhimurium* infection, but remain around the follicles

Another cell type found in the marginal zone is the marginal zone metallophilic macrophage, which can be identified by staining for MOMA-1 (metallophilic macrophage antibody). This population is also thought to be involved in the removal of antigens from the bloodstream [290]. Previous data suggests that marginal zone B cells play a role in the generation and/or maintenance of this cell type [15]. Therefore, it was uncertain whether marginal zone metallophilic macrophages would be affected by the loss of marginal zone B cells during *S. typhimurium* infection. Furthermore, identifying any changes to the distribution of these cells during infection will provide insight into the retention of the 'barrier' between the red pulp and white pulp regions.

It was found that, during infection, the marginal zone metallophilic macrophage population became partially fragmented but was not lost (figure 4.10). In uninfected mice (day 0), the marginal zone metallophilic macrophages (green) can be seen between the follicular and marginal zone B cells (identified by IgM staining, red). By days 4 and 8 of infection, when the marginal zone B cells had been lost, the marginal zone metallophilic macrophages were still seen surrounding the follicular B cell population, although appeared slightly dispersed. Thus their presence in the marginal zone region was not dependent on marginal zone B cells. Therefore, these cells may form part of the barrier that remains around the white pulp when marginal zone B cells are lost, and function to prevent particles from the bloodstream from entering the follicles.

Discussion

The data presented here confirm that antigen-presenting macrophages influx into the spleen during the first week of *S. typhimurium* infection, and that the white pulp regions become disrupted at this time. The initial splenomegaly, together with the loss of marginal zone B cells, is partially dependent on TLR signalling. However, despite the loss of the marginal zone B cell population during infection, a physical barrier to blood-borne particles remains between the red and white pulp regions. Furthermore, an early extrafollicular plasma cell response develops in *S. typhimurium* infection. Due to the evidence of TLR-induced differentiation of IgM-secreting plasma cells, and the lack of these plasma cells in $CD1d^{-/-}$ mice that lack a marginal zone, I speculate that the origin of these plasma cells is likely to be the marginal zone B cell population.

Macrophage influx into the spleen during *S. typhimurium* infection

The data presented in figures 4.2 & 4.3 confirm that the major cell-type infiltrating the spleen during infection was macrophages, as determined by their expression of CD11b and F4-80. This influx of macrophages was rapid, with numbers of $CD11b^{+}$ cells appearing elevated after just 24 hours of infection (figure 4.2). Alternatively, the increase in CD11b staining may be as a result of upregulation of this molecule by macrophages already present in the red pulp of the spleen. Indeed, TLR stimulation has previously been shown to induce such an upregulation both in macrophages [291] and neutrophils [292]. Therefore, the presence of bacteria is likely to induce upregulation of surface CD11b on macrophages in the *S. typhimurium* infection model, as well as the influx of monocytes from the bloodstream and subsequent differentiation into functional macrophages. Also, some subsets of murine dendritic cells have been shown to express CD11b [293], and they, together with neutrophils, may be responsible for some of the CD11b staining seen here in figure 4.2.

Furthermore, the data displayed in figure 4.1B suggest that splenomegaly is partially dependent on TLR signalling, as the initial increase in spleen weight was reduced, but not absent, in $MyD88^{-/-}$ mice. Both the increase in numbers of newly differentiated macrophages in the spleen, and the influx of B cells from other lymphoid organs (as outlined in chapter 3) show dependence on TLR stimulation, and were likely to have contributed to the rapid and severe splenomegaly identified in the first week or so of infection.

Loss of marginal zone B cells

In addition to changes in the innate cells of the spleen, adaptive immune cells, such as B cells, also underwent alterations in terms of cell number, subsets and localisation, during *S. typhimurium* infection. One of the most striking changes to the B cell population was the loss of the marginal zone B cell subset. From the histology pictures, this cell population appeared dispersed in wild type mice by day 1 of infection, and was unidentifiable by flow cytometry by day 4 (figure 4.4). One explanation for the differences in the timescale of marginal zone B cell loss between the flow cytometry and histology results is that, by day 1, marginal zone B cells may have migrated away from the marginal zone into the red pulp and so not be visible by histology in the marginal zone region, but still identifiable by flow cytometry via the expression of CD21 and CD23.

The loss of marginal zone B cells was seen to be delayed by around 4 days in MyD88$^{-/-}$ mice (figure 4.5). This loss of marginal zone B cells *in vivo* following injection of heat-killed *E. coli* or TLR ligands has been reported previously [294,295]. Furthermore, the loss of marginal zone B cells during infection has been shown in various models, such as relapsing fever caused by *Borrelia crocidurae*, where this population was reduced 2-fold by day 6 [296], and *Trypanosoma brucei,* where analysis on day 10 of infection revealed this population to be absent [297]. There are three possible explanations for the loss of marginal zone B cells during infection: migration, death or differentiation. Due to the knowledge that marginal zone B cells are non-circulating in mice [262], migration of these cells out of the spleen seems unlikely. However, early data by Gray *et al* on the loss of marginal zone B cells reports that these cells migrate in an intra-splenic manner to the B cell follicles, for the delivery of antigen to follicular dendritic cells [294]. More recent data also indicates a role of marginal zone B cells in the transport of antigen into the follicles [252], and so migration of these cells into the follicles is one plausible explanation for their loss. Alternatively, marginal zone B cells may be lost by apoptosis. Indeed, the authors using the *T. brucei* system attributed the loss of marginal zone B cells to be due mainly to apoptosis, as apoptotic cell markers such as Annexin V and 7AAD were elevated [297]. However, in the *B. crocidurae* system, the authors imply that the loss of marginal zone B cells is as a result of differentiation into IgM^{+} plasma cells [296]. Here, I propose that the TLR-induced loss of marginal zone B cells in *S. typhimurium* infection is due to differentiation into IgM-secreting extrafollicular plasma cells.

Marginal zone B cell differentiation into plasma cells

The data presented show that the loss of marginal zone B cells occurred at approximately the same time as the generation of plasmablasts within the spleen, between days 1 and 4 of infection (figures 4.4 & 4.7). This, together with the finding that the early plasma cell response was virtually absent in $CD1d^{-/-}$ mice that lack marginal zone B cells (figure 4.7), suggests that differentiation into plasma cells is the likely fate of marginal zone B cells. However, it should be noted that $CD1d^{-/-}$ mice also have a deficiency in invariant natural killer T cells (iNKT cells) [250]. As iNKT cells have been shown to 'help' B cell antibody responses [298,299,300], this may be an alternative explanation for the lack of early IgM production in the $CD1d^{-/-}$ mice. Alternatively, reduced numbers of B1 cells would explain the lack of IgM production, as well as the lower numbers of splenic plasmablasts in naïve mice seen in figure 4.7B. However, data from both our own laboratory (S. Brown, T.A. Barr & D. Gray, unpublished observations) and a published report [301] suggests B1 cell numbers to be normal in $CD1d^{-/-}$ mice.

Additionally, the loss of marginal zone B cells was delayed (figure 4.5), and the early plasma cell response reduced (figure 4.7), in the absence of MyD88 signalling, indicating a role for TLR stimulation. TLR stimulation of B cells is known to result in the differentiation of plasma cells in a T cell-independent manner [125], with MyD88-deficient mice showing reduced steady-state levels of serum antibody [127]. Looking specifically at marginal zone B cells, they are thought to be poised for plasma cell differentiation, making ~6-fold more IgM than follicular B cells in response to LPS stimulation *in vitro* [125], and doing so in shorter periods of time [255]. Moreover, several other studies have reported the differentiation of plasma cells from marginal zone B cells, in a *Borrelia* infection study [296], and in an antigen-loaded *Streptococcus pneumoniae* model [162]. Further data suggests that this differentiation of marginal zone B cells into plasma cells involves an interaction with blood-derived dendritic cells, by-passing the need for T helper cells [302]. Thus, it seems a feasible explanation that TLR stimulation of marginal zone B cells would result in IgM^{+} plasma cell differentiation within the first week of *S. typhimurium* infection.

Early production of IgM that is capable of binding *Salmonella* antigens

TLR-dependent differentiation of plasmablasts and plasma cells in the spleen was apparent by days 4 and 8 of infection, respectively. This correlated with an increase in serum IgM that was capable of binding *Salmonella* antigens (figure 4.7). These IgM-secreting plasma cells were located primarily out-with the follicles, in the red pulp region (figure 4.6), and thus constitute an extrafollicular plasma cell response. Due to the polyclonal nature of TLR stimulation, this plasma cell response is likely to have occurred in a T cell-independent manner, as antigen-specific T cell help for B cells seems unlikely at this early stage of infection. Thus the antibody produced would be expected to represent the diverse specificities of the marginal zone BCRs, and therefore constitute 'natural' or cross-reactive IgM.

Marginal zone B cells are the main source of cross-reactive IgM in the spleen. Although capable of opsonisation and neutralisation, IgM functions mainly to activate the complement system, thus acting as a kick-start to the immune response. Marginal zone B cells, together with peritoneal B1 cells, are thought to be responsible for the initial wave of IgM production in response to blood-borne particulate antigen [162]. Such IgM has been shown to be vital in immune responses to bacteria, with mice expressing a mutant form of IgM, that cannot be secreted, showing increased mortality in a peritonitis model [281]. Data from previous studies also highlights the importance of early TLR-induced IgM production in infection; in *Borrelia hermsii* infection, TLR-induced IgM production is essential in controlling bacterial growth very early in infection [303], and an impairment in TLR signalling leads to delayed IgM production which, in turn, results in more severe bacteraemia [303]. Therefore, the early extrafollicular plasma cell response and IgM production seen in *S. typhimurium* infection is one of the first components of the innate immune response against the bacterial infection, confirming the role of marginal zone B cells in innate immunity.

The early extrafollicular plasma cell response in *S. typhimurium* infection

Extrafollicular plasma cell responses can occur in a T cell-dependent or -independent manner, and the resulting antibody that is generated is of low affinity, as the B cells have not undergone somatic hypermutation within a GC. An early extrafollicular plasma cell response has been reported previously with regards to *S. typhimurium* infection [206]. Similar to my own data, the authors reported that the extrafollicular plasma cell response was detectable by day 3 of infection. However, the remainder of their data differed significantly from my own findings. The authors found some of the resulting plasma cells to

be class switched, secreting IgG2c, and this aspect was, therefore, strongly dependent on the presence of T cells [206]. In contrast, the plasma cells indentified here in figure 4.6 had an IgM^+ phenotype and had not switched to IgG (data not shown), suggesting a T cell-independent mechanism. Importantly, published data shows the extrafollicular antibody response (including low affinity IgM) to play a role in preventing the colonisation of splenic macrophages by *Salmonella,* following pre-incubation of bacteria with serum [206], highlighting its importance in this infection model.

Marginal zone B cells are the first B cell subset in the spleen to encounter systemic antigen

Here, I make use of an *in vivo* staining technique to study the binding of fluorescently labelled antibodies by cells in the spleen, and the effects of the loss of marginal zone B cells on antibody entry into the follicles. Looking firstly in uninfected mice, a much greater proportion of marginal zone B cells bound the antibodies (either anti-CD21 FITC or anti-CD19 PE) than follicular B cells (figure 4.8), indicating that marginal zone B cells were first to access blood-borne particles. One discrepancy in the data presented is that, by flow cytometry, ~40% of follicular B cells were found to have bound anti-CD19 PE (figure 4.8A), while the histology data shows virtually no staining within the follicles (figure 4.9, day 0). The likely explanation for the differences in these findings is that further binding of anti-CD19 PE may have occurred during preparation of the samples for flow cytometry (i.e. mashing of the spleens), which disrupted splenic architecture and may have allowed antibodies present in the red pulp to bind follicular B cells. Interestingly, the histology pictures reveal dim anti-CD19 PE staining in the red pulp of uninfected mice (figure 4.9). One possible explanation for this is that macrophages in this region may have bound the antibody non-specifically, perhaps through Fc receptors.

An elegant study by Cinamon and colleagues [252] revealed the role of marginal zone B cells in capturing blood-borne antigen and delivering it into the follicles. Using the same *in vivo* staining technique that I use here, the authors provide evidence that marginal zone B cells continuously shuttle between the marginal zone and follicular regions in uninfected mice, delivering antigen to follicular dendritic cells [252]. My data presented here certainly confirm that marginal zone B cells are the first B cell subset in the spleen to access systemic labelled antibodies. The loss of these shuttling marginal zone B cells may be a further explanation for the decrease in anti-CD19 PE binding during *Salmonella* infection (figure 4.8C).

Despite the loss of the marginal zone B cell population during *S. typhimurium* infection, a physical barrier to blood-borne antigen was retained in the marginal zone region. While the bright staining of the marginal zone region was seen throughout all time-points of infection (figure 4.9), there was virtually no staining of B cells in the follicles. This suggests that, not only were fluorescently labelled antibodies prevented from entering the follicles, but also the injected antibodies continued to accumulate in the marginal zone despite the loss of marginal zone B cells.

Marginal zone metallophilic macrophages are maintained during infection and may capture the injected antibodies in the marginal zone

The marginal zone metallophilic macrophage population, although partially dispersed, was retained in the marginal zone, despite the loss of marginal zone B cells (figure 4.10). This provides evidence, contrary to published data [15], that marginal zone B cells are not essential for the maintenance of this population of macrophages. In agreement with my data, previous studies showing the loss of marginal zone B cells following injection with TLR ligands [295], and in *Borrelia* infection [296], both indicate that marginal zone metallophilic macrophages are maintained. This cell type is known to be involved in the early innate response in the spleen, secreting type I interferons during viral infection [304]. Furthermore, they have been implicated in the generation of antibody responses to T cell-dependent particulate bacterial antigens [305]. As marginal zone metallophilic macrophages do not express MHC class II and therefore cannot present antigen [306], the likely role for these cells in the development of T cell-dependent antibody responses is as an intermediate cell type, perhaps capturing antigen and passing it on to professional APCs, such as dendritic cells, or even marginal zone B cells. Further data in support of antigen capture by marginal zone metallophilic macrophages, from Aichele and colleagues, indicates that marginal zone metallophilic macrophages, together with marginal zone macrophages, are essential for trapping particulate antigen from the bloodstream, but are dispensable for antigen presentation and the development of T cell responses [290]. Therefore these marginal zone metallophilic macrophages certainly play an immune role, and may be responsible for binding the labelled antibody (perhaps recognising the foreign structure generated in rats, or the PE region, or simply via Fc receptors) and trapping it in the marginal zone region during *S. typhimurium* infection, thus preventing its entry into follicles.

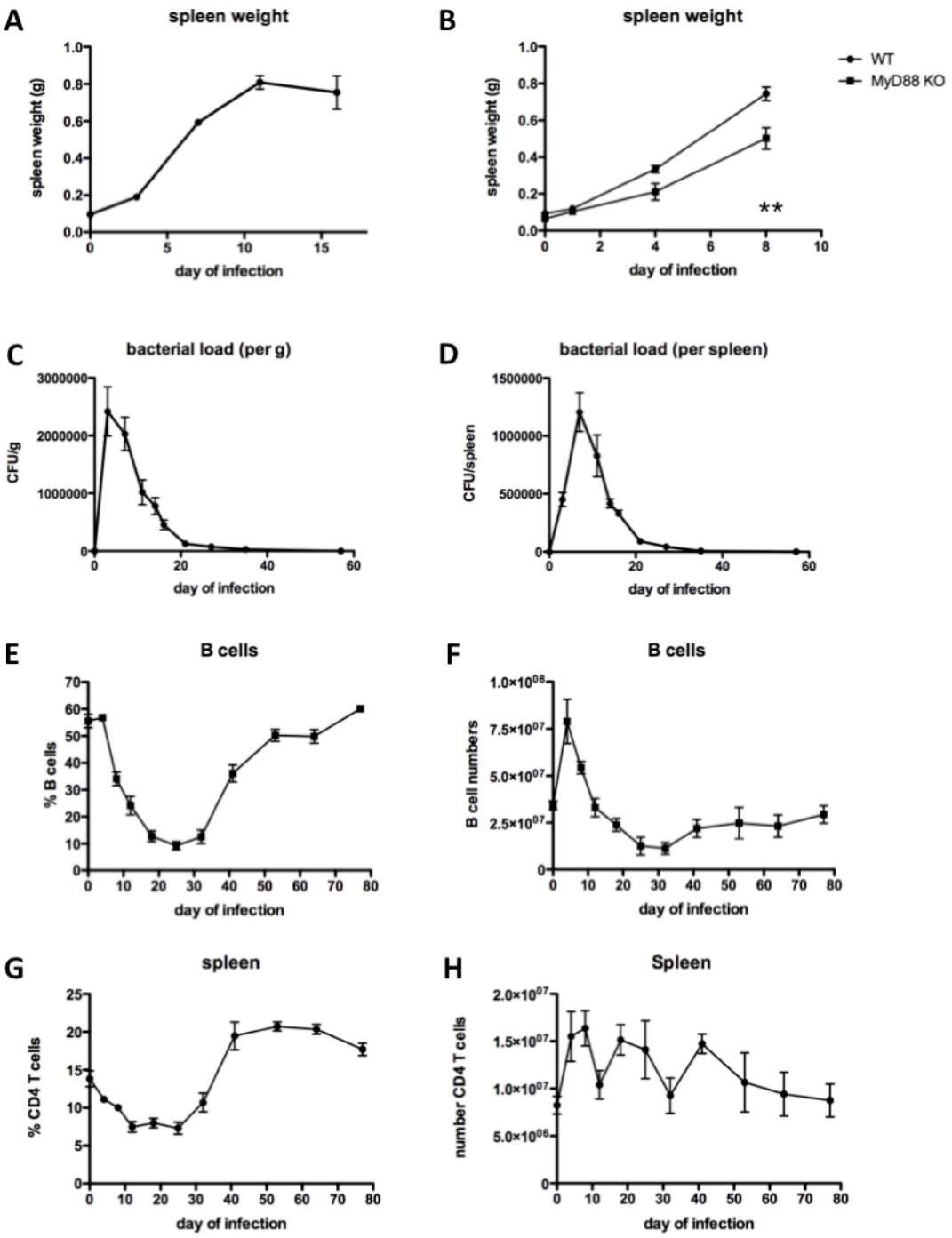

Figure 4.1: Infection with *S. typhimurium* causes splenomegaly and changes to lymphocyte population numbers within the spleen. C57BL/6 (A-H) or MyD88$^{-/-}$ (B) mice were infected with *S. typhimurium* on day 0. Spleen weight (A-B), splenic bacterial load per gram (C), splenic bacterial load per spleen (D), B cell percentages (E) and absolute numbers (F), and T cell percentages (G) and absolute numbers (H) were analysed throughout infection. Error bars indicate SEM, with at least 5 mice per group. In (B) statistical analysis was performed using a two-way ANOVA. ** = p-value of <0.1.

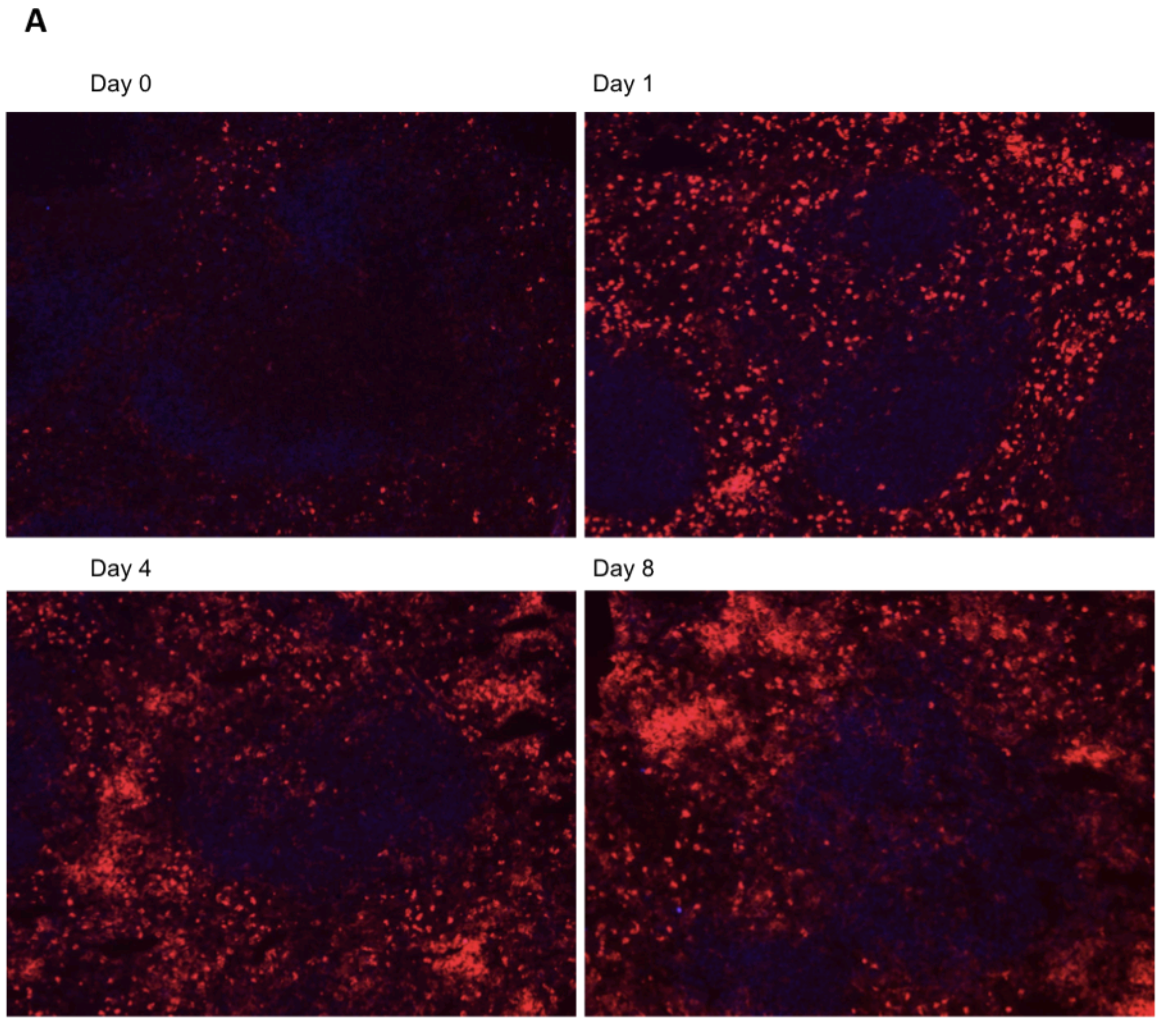

Figure 4.2: Macrophage influx disrupts splenic architecture early in infection. Spleen sections from day 1, day 4, and day 8 *Salmonella*-infected mice, together with uninfected mice (day 0), were stained for CD11b (red) and IgD (blue) to identify macrophages and B cells, respectively. Pictures are representative of at least 3 mice per timepoint, and of 2 independent experiments. Taken at x20 magnification.

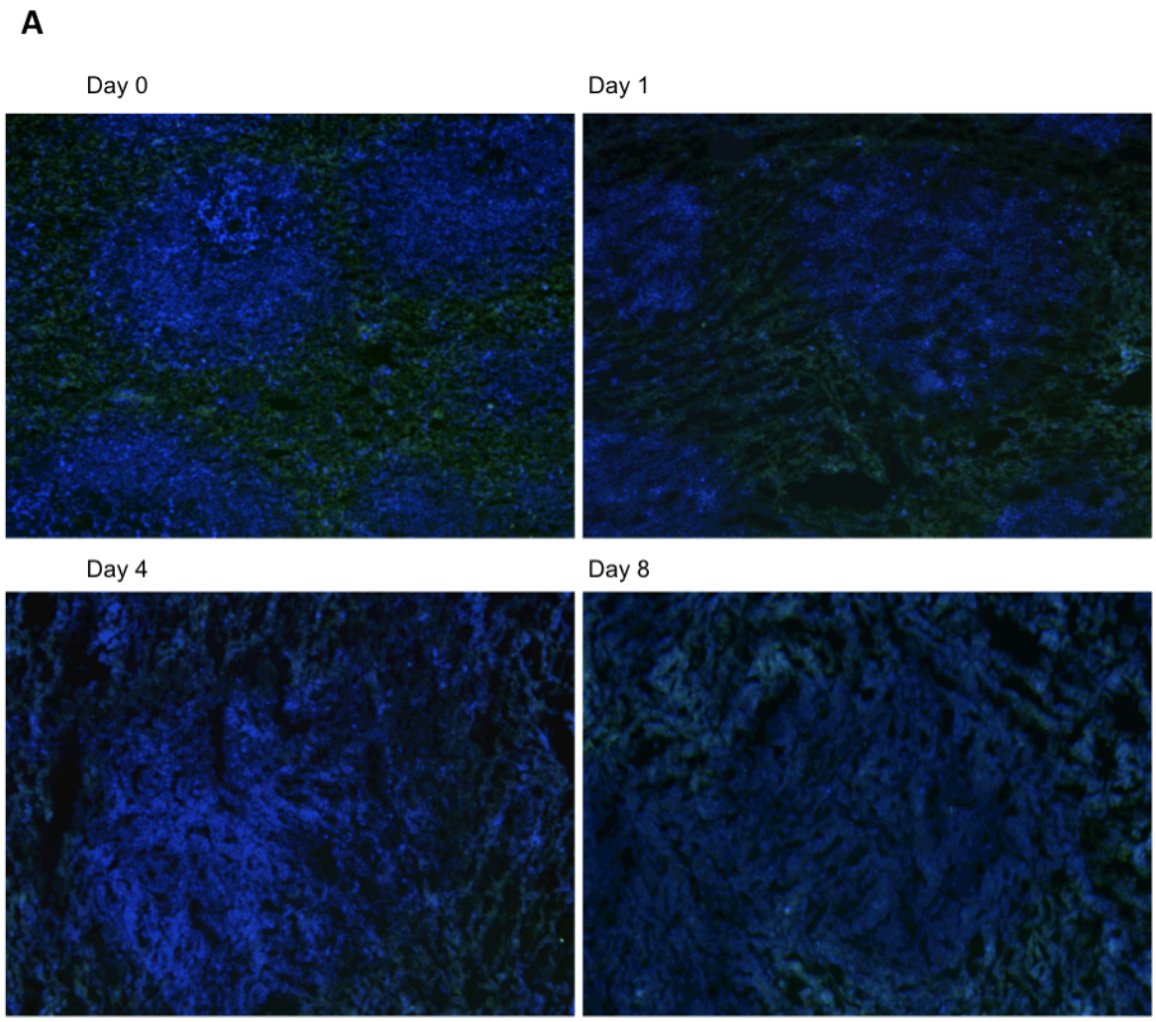

Figure 4.3: The macrophages found in the infected spleen are capable of presenting antigen. Spleen sections from day 1, day 4, and day 8 *Salmonella*-infected mice, together with uninfected mice (day 0), were stained for F4-80 (green) and MHC class II (blue) to identify macrophages and their antigen-presenting capacity. Pictures are representative of at least 3 mice per timepoint, and of 2 independent experiments. Taken at x20 magnification.

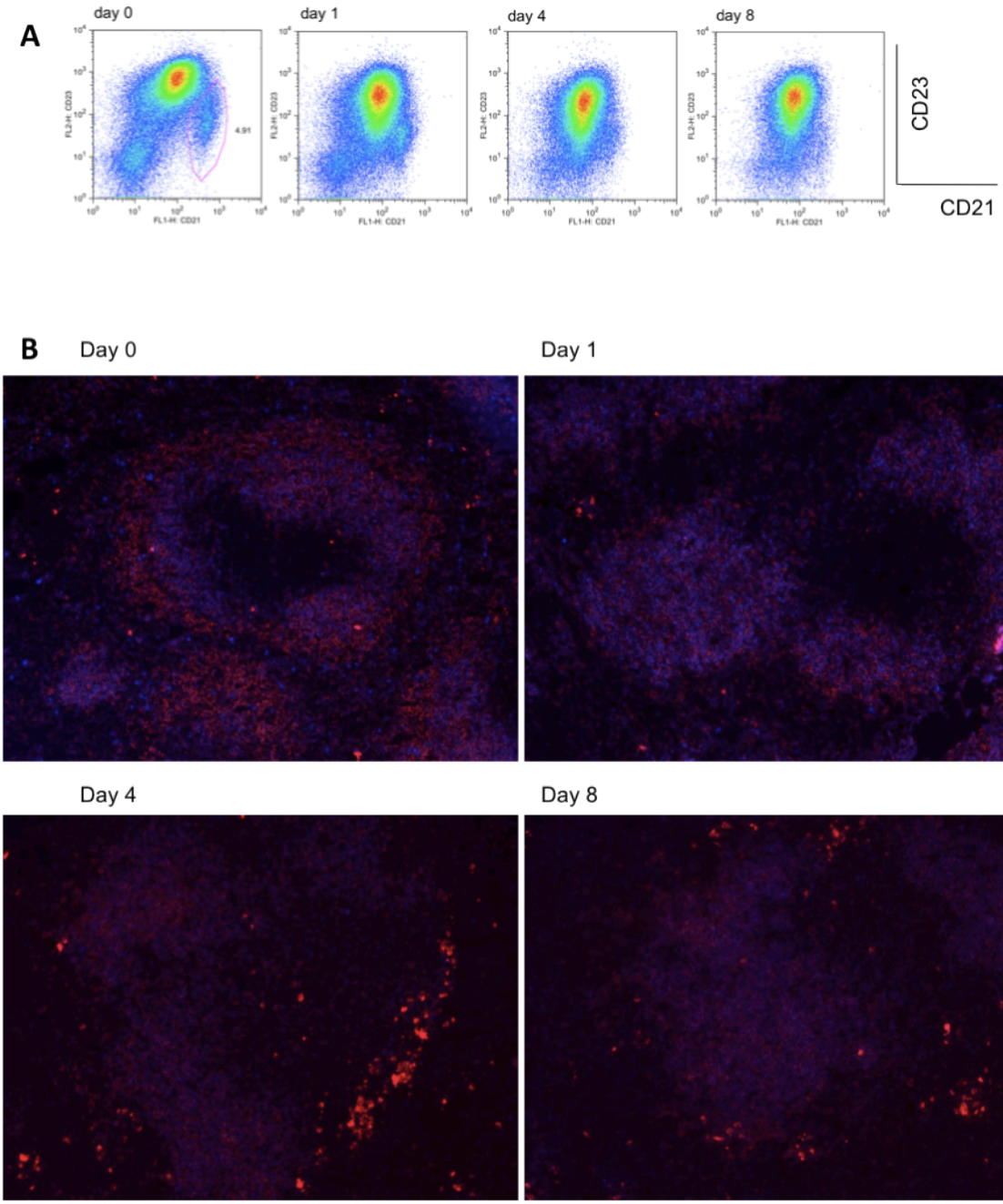

Figure 4.4: Marginal zone B cells are lost during the first few days of infection. C57BL/6 mice were infected with *S. typhimurium* on day 0, and spleens analysed on days 1, 4, and 8 of infection. The marginal zone B cell population was identified by CD21 and CD23 expression by flow cytometry (A), and IgM (red) and IgD (blue) expression by histology (B). In (B) the marginal zone population is identified as IgM^+ IgD^- cells (red only) surrounding the B cell follicles, while follicular B cells express both IgM and IgD so appear purple. Taken at x20 magnification.

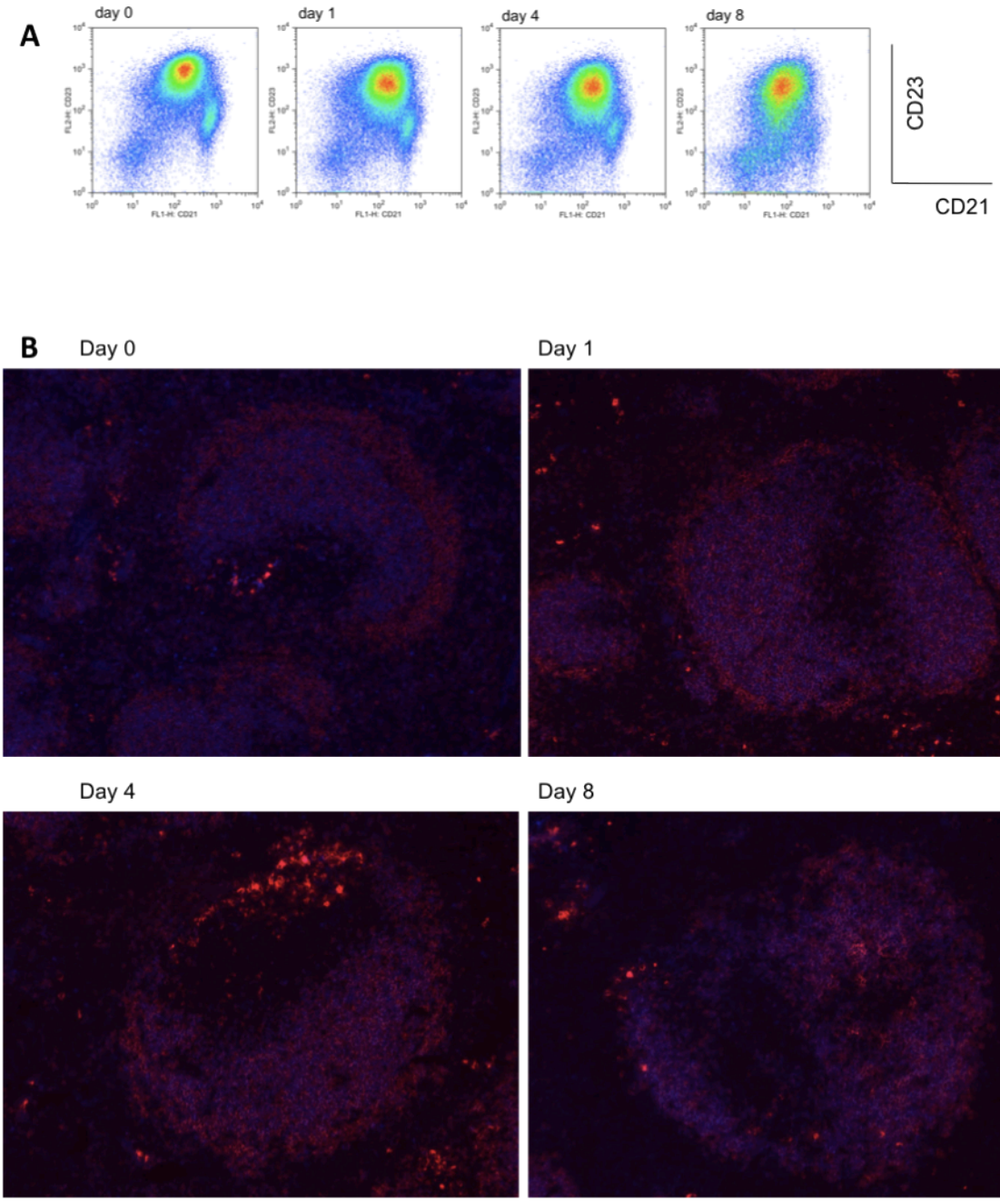

Figure 4.5: The absence of MyD88 signalling delays, but does not prevent, the loss of marginal zone B cells. MyD88$^{-/-}$ mice were infected with *S. typhimurium* on day 0. Spleens were analysed on days 1, 4, and 8 of infection for the marginal zone population as determined by CD21 and CD23 expression by flow cytometry (A), and IgM (red) and IgD (blue) expression by histology (B). In (B) the marginal zone population is identified as IgM^{+} IgD^{-} cells (red only) surrounding the B cell follicles. Follicular B cells express both IgM and IgD, so appear purple. Taken at x20 magnification.

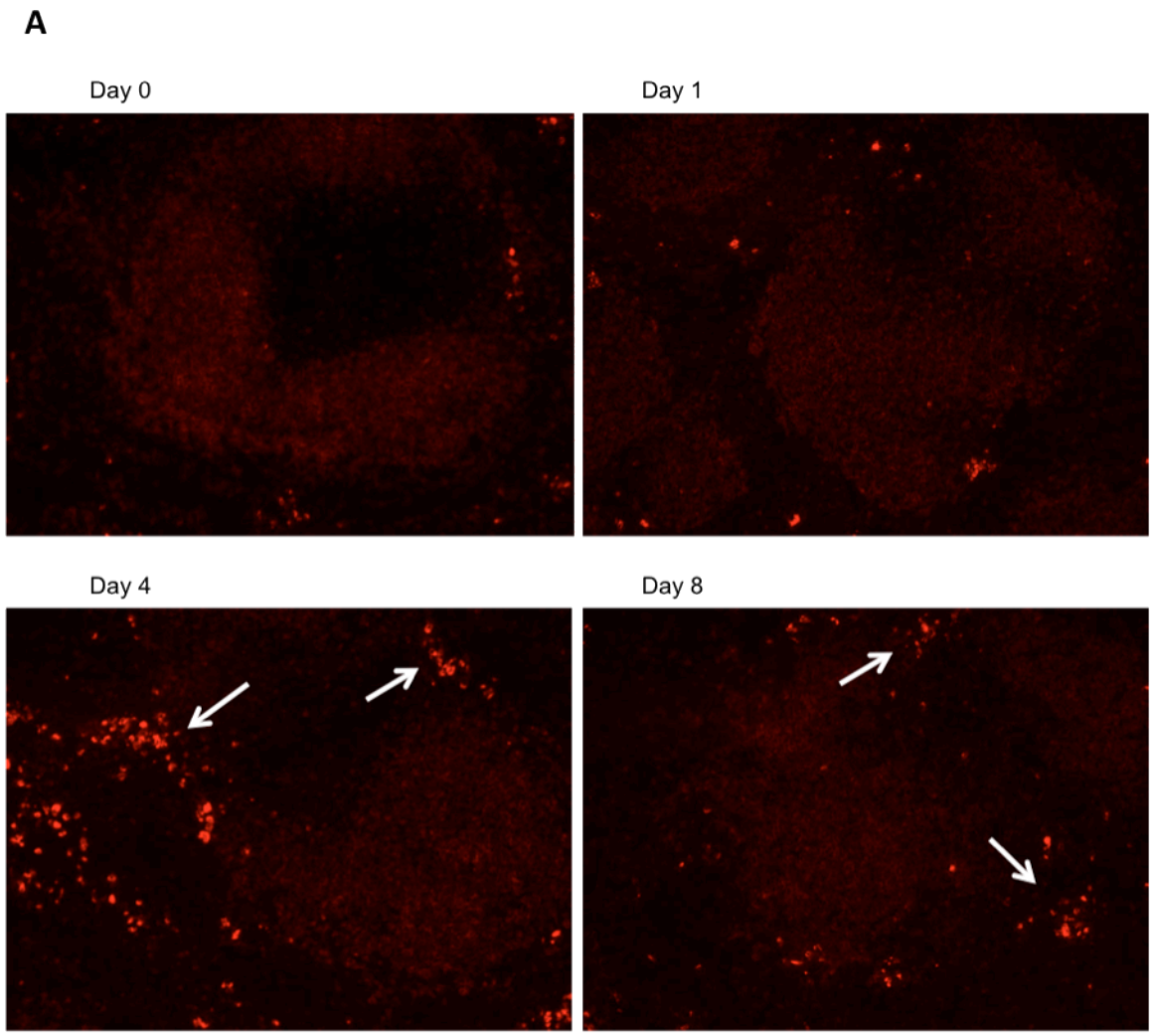

Figure 4.6: An early extrafollicular plasma cell response develops by day 4 of *S. typhimurium* infection. C57BL/6 mice were infected with *S. typhimurium* on day 0. Spleen sections from different days of infection were stained with IgM (red) to identify IgM-secreting plasma cells (bright cells, highlighted by arrows). Pictures are representative of at least 3 mice per timepoint, and of 2 independent experiments. Taken at x20 magnification.

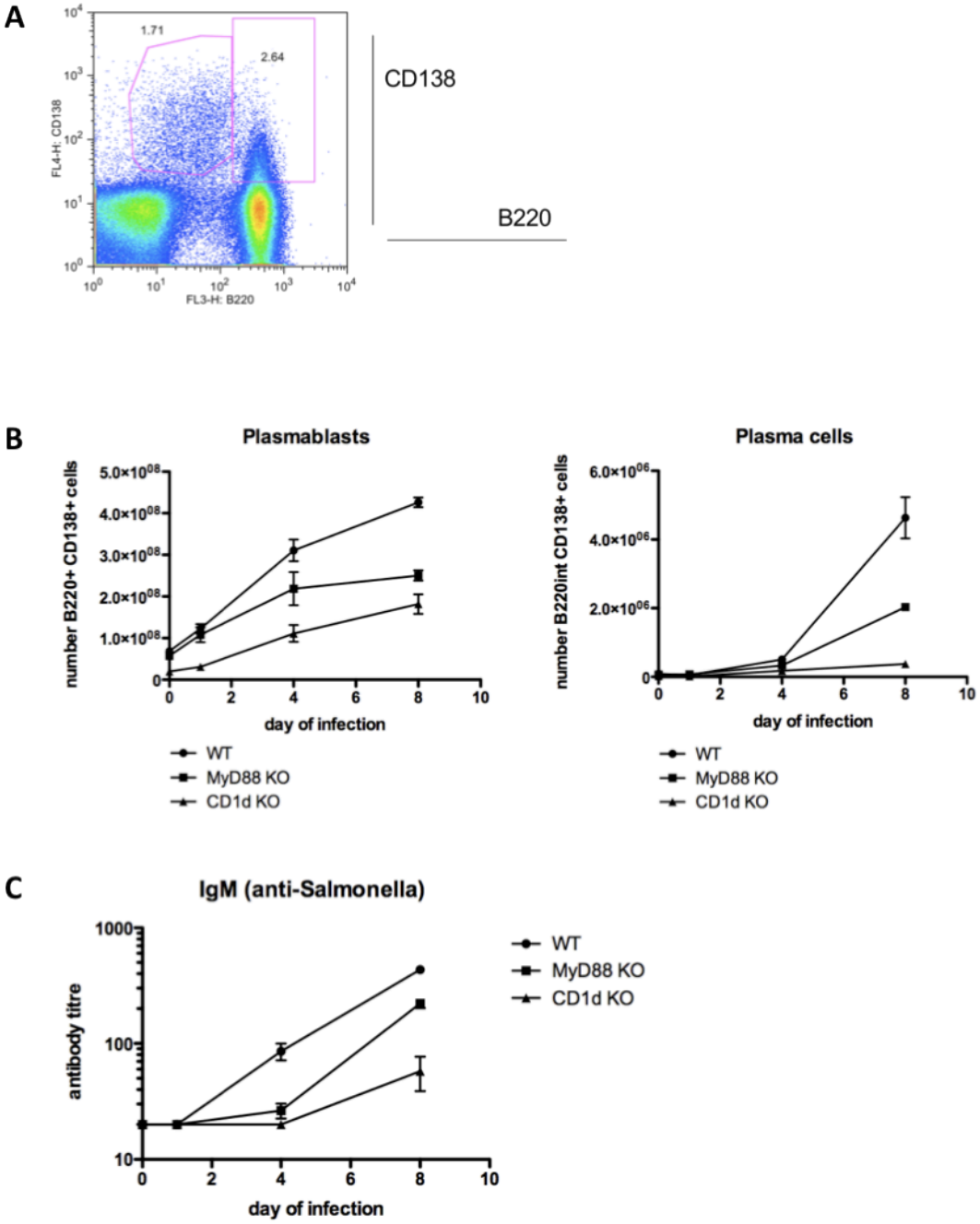

Figure 4.7: MyD88$^{-/-}$ and CD1d$^{-/-}$ mice show impaired early plasma cell differentiation and IgM production during *S. typhimurium* infection. C57BL/6, MyD88$^{-/-}$, and CD1d$^{-/-}$ mice were infected with *S. typhimurium* on day 0. Spleens were collected on days 1, 4, and 8 of infection, and plasmablasts (B220^{+} CD138^{+}) and plasma cells (B220^{int} CD138^{+}) identified by flow cytometry (B). Example staining is shown in (A). Serum was analysed for *Salmonella*-specific IgM (C). Error bars indicate SEM with 4 mice per group.

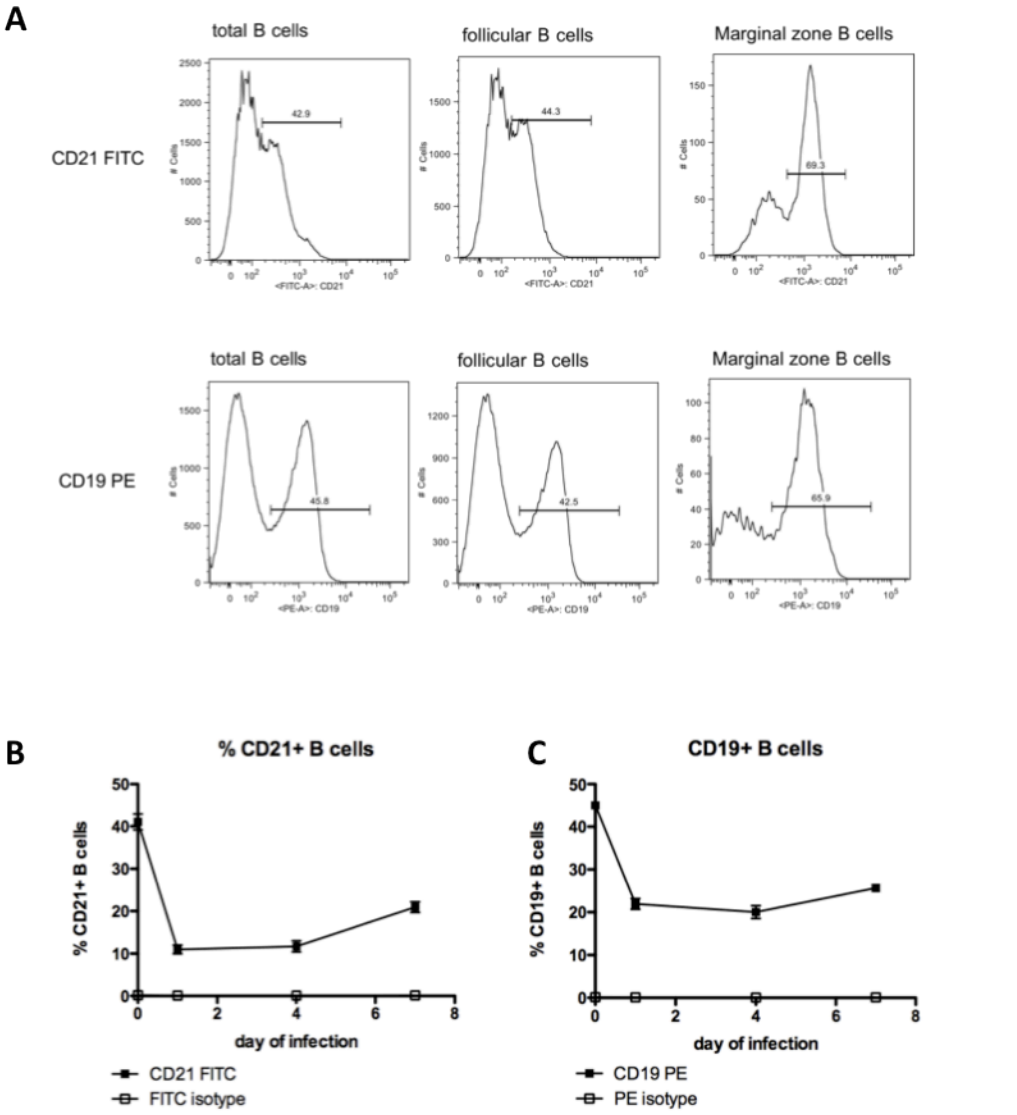

Figure 4.8: Staining of B cells *in vivo* is reduced during *S. typhimurium* infection. C57BL/6 mice were infected with *S. typhimurium* on day 0. On days 0, 1, 4, and 7 mice were injected with 1µg anti-CD21 FITC and 1µg anti-CD19 PE i.v. Spleens were removed 20 minutes post-immunisation and analysed for antibody binding. (A) Representative histograms of anti-CD21 FITC (top) and anti-CD19 PE (bottom) binding *in vivo* by total, follicular and marginal zone B cells in uninfected mice. (B) Binding of anti-CD21 FITC and (C) anti-CD19 PE *in vivo* by total B cells during *S. typhimurium* infection.

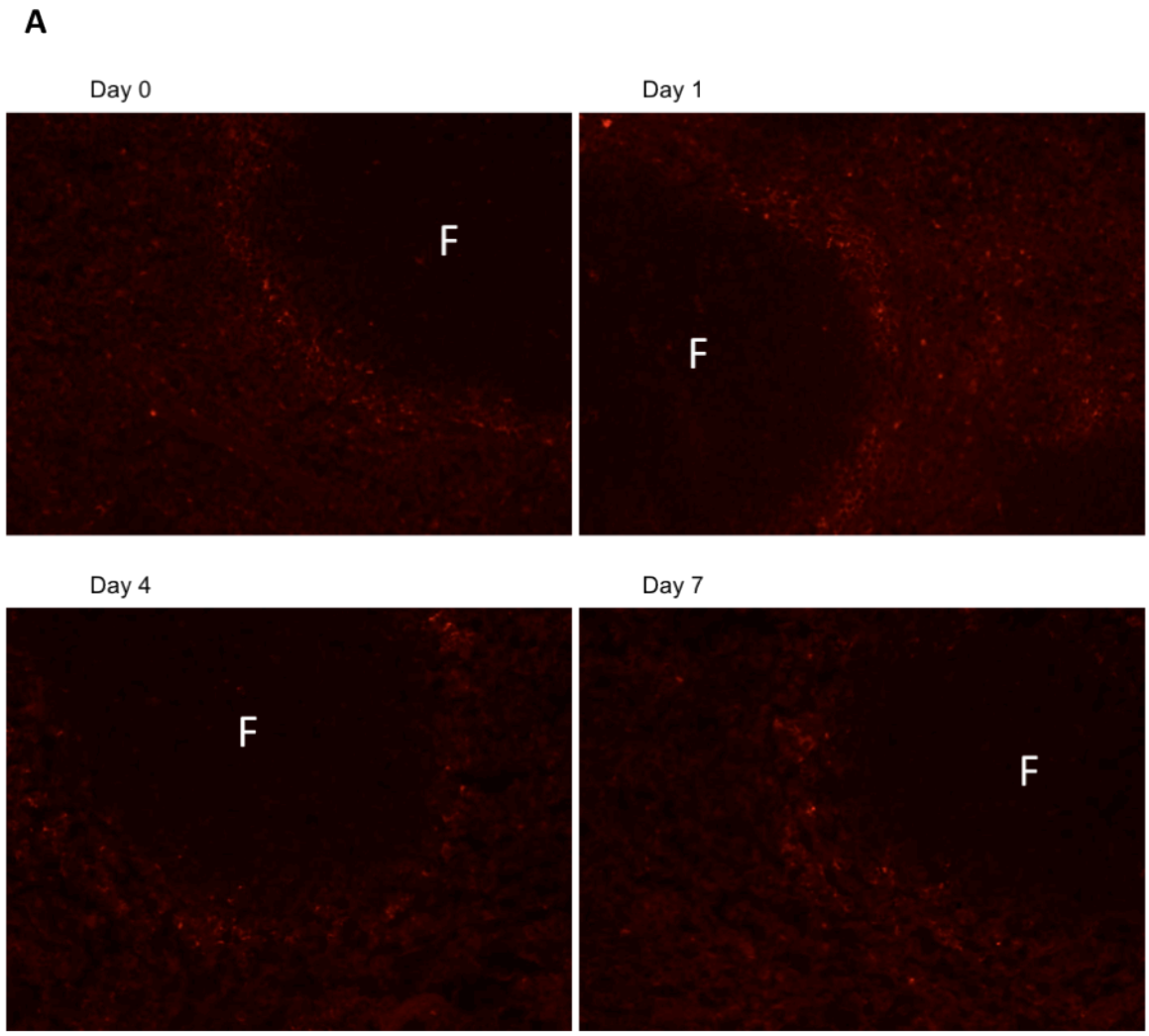

Figure 4.9: Labelled antibodies continue to accumulate in the marginal zone during infection, and do not enter the follicles. Mice were infected with *S. typhimurium* on day 0. On days 0, 1, 4, and 7, they were injected with 1µg anti-CD19 PE i.v. Spleens were removed 20 minutes post-immunisation and tissue sections analysed for antibody binding (A). Pictures are representative of at least 3 mice per timepoint, and of 2 independent experiments. Taken at x20 magnification. F = B cell follicles.

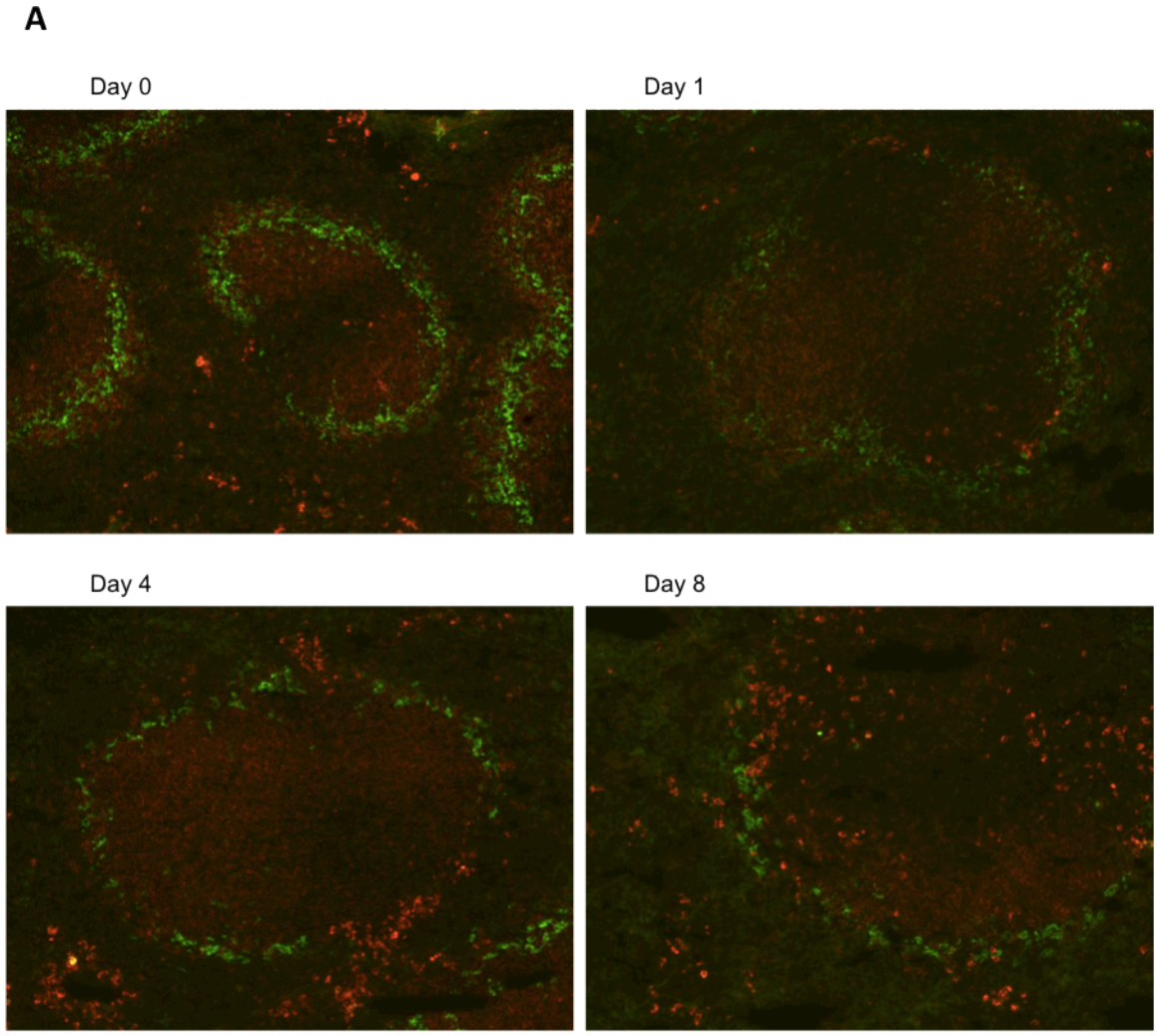

Figure 4.10: Marginal zone metallophilic macrophages become partially fragmented during *S. typhimurium* infection, but remain around the follicles. Spleen sections were taken on days 0, 1, 4, and 8 of infection and stained for MOMA-1 (green) and IgM (red) to detect marginal zone metallophilic macrophages and B cell follicles, respectively (A). Pictures are representative of at least 3 mice per timepoint, and of 2 independent experiments. Taken at x20 magnification.

CHAPTER 5: The role of B cells in the generation of T cell memory and T follicular helper cell populations - use of the *Salmonella typhimurium* infection model

Introduction

The data presented so far reveal the innate responses of whole populations of B cells in response to TLR stimulation. In *Salmonella typhimurium* infection, I have shown that these TLR-induced changes to B cells include the shedding of CD62L, and subsequent alterations in migration patterns, and the differentiation of marginal zone B cells into IgM-secreting plasma cells. These rapid responses of B cells, which occur within the first few days of infection, contribute to the innate defence. In addition to these innate functions, B cells have the capacity to present cognate antigen via MHC class II, following endocytosis through their BCR. This antigen presentation by B cells, together with their ability to secrete cytokines, means they have the potential to drive T helper cell differentiation, and thus direct the adaptive T cell response.

Here, I investigate the role of B cells in influencing adaptive immune responses *in vivo*, specifically, in the differentiation of $CD4^+$ T cells. To do this, I again make use of the *S. typhimurium* infection model, as well as a peptide immunisation strategy (see chapter 6). In the *S. typhimurium* infection model, antigen-specific T helper cell responses are analysed by measuring cytokine production following *in vitro* restimulation. As the immune response to this infection is characterised by a strong Th1 response and IFNγ production [201], this cytokine is most indicative of the *in vivo* $CD4^+$ T cell response to this infection.

In order to further dissect the specific requirement for B cells in the generation of $CD4^+$ T cell responses, I use anti-CD20 B cell depletion antibodies. This antibody, approved for use in humans in the form of the drug Rituximab, is used to efficiently deplete B cells in lymphoma patients [219]. Here, I use a murine clone of anti-CD20 to deplete B cells in mice at various times throughout the immune response (in this case following *S. typhimurium* infection) and follow the generation of T helper cell responses.

There are several advantages of the anti-CD20 depletion system over the use of B cell-deficient mice. Firstly, in the mice used (normal C57BL/6 mice) the T cells have developed in the presence of B cells. Therefore, their immune system and lymphoid tissues are normal, unlike B cell-deficient mice which have been shown to have abnormal T cells [216]. However, it cannot be guaranteed that T cells remain normal after B cell depletion. Additionally, these mice have normal levels of 'natural' serum antibody (before depletion), which is known to be involved in early immune responses [281]. Importantly, this system allows the control of the presence or absence of B cells during an immune response. For example, in some experiments presented below, B cells were depleted on day 10 of infection. The initial priming of the immune response therefore occurred in a B cell-sufficient environment, with B cells absent during the later stages of infection. Conversely, mice depleted of B cells on day -7 (i.e. before infection) lacked B cells throughout the immune response, and should resemble B cell-deficient μMT mice.

I, therefore, use anti-CD20 depletion antibodies in the *S. typhimurium* infection model to further dissect the role of B cells in generating $CD4^+$ T cell responses. Specifically, I focus on the involvement of B cells in T cell memory generation. It has previously been shown, both in the *S. typhimurium* infection model [154,155] and in other infections [152,153], that T helper cell memory is impaired in B cell-deficient mice. However, the exact role of B cells in influencing T cell memory generation remains unknown. Previous data indicates that B cell expression of MHC class II is required for efficient T cell memory generation [142], indicating that direct contact between cognate B and T cells is essential. This would suggest that B cells are required to provide a specific signal that other APCs, such as dendritic cells, are unable to supply. This may be a specific signalling molecule expressed only by B cells, or alternatively, a signal that other APCs can express, but that is not of the correct quantity, quality or 'context' for T cell memory to be generated. Thus, by depleting B cells on different days of infection, I aim to determine the window of time in which B cells are required for T cell memory generation. It should be noted that, although the data presented discusses the role of B cells in the generation of memory T cells, the fact that B cells are thought to also play a role in the maintenance of T cell memory should not be ignored [116]. As B cell depletion is fairly long-lived, the distinction between generation and maintenance of memory T cells proves difficult.

In addition to analysing the generation of T cell memory, I also investigate the effects of B cell depletion on the $CD4^+$ T cells most intimately associated with B cells in the follicular regions; the T_{FH} cells. B cells are critically dependent on 'help' from T_{FH} cells for the GC reaction to occur, and the subsequent differentiation of class switched effector and memory cells [54]. The secretion of IL-21 by such T_{FH} cells is thought to aid the differentiation of plasma cells, while the high expression levels of co-stimulatory molecules by T_{FH} cells ensures B cell survival and differentiation [54]. The location of this T cell subset within the follicles allows direct contact with B cells, and thus it seems likely that B cell depletion will affect this cell population.

Therefore, using anti-CD20 B cell depletion in *S. typhimurium* infection, I aim to investigate the role of B cells in the generation and maintenance of T_{FH} cells, and analyse at what time-point antigen presentation by B cells is required for T cell memory generation.

Results

CD20 expression by B cells

The B cell depletion antibody targets the surface molecule CD20, which is expressed only by B cells. Firstly, B cells from different organs were analysed for their expression of this molecule (figure 5.1A). B cells from the spleen, lymph nodes and peritoneal cavity were found to express an intermediate level of CD20, while expression of CD20 by B cells in the bone marrow was lowest. Interestingly, the Peyer's patches were found to have two distinct populations of B cells, which differed in their expression of CD20 (figure 5.1A). These cells were further analysed in order to determine the nature of their differences. In figure 5.1B it can be seen that the $CD20^{hi}$ population expressed higher levels of CD40 and CD80, and lower levels of CD62L than the $CD20^{lo}$ population, suggesting that they are in a more activated state. The $CD20^{hi}$ cells were analysed for GL7 and IgD expression, to determine if they are GC B cells with a $GL7^{+}$ IgD^{-} phenotype. The $CD20^{hi}$ cells appeared to have more of a GC phenotype, in that they expressed higher levels of GL7 and lower levels of IgD than the $CD20^{lo}$ population (figure 5.1C). By analysing this in a different way, it was clear that by gating on the $GL7^{+}$ IgD^{-} GC B cells, they expressed higher levels of CD20 then the $GL7^{-}$ IgD^{+} non-GC B cells (figure 5.1D). Therefore, these $CD20^{hi}$ B cells are likely activated cells, some of which are undergoing the GC reaction.

B cell subsets in the spleen were also analysed for their surface expression levels of CD20. Figure 5.2 shows that marginal zone B cells ($CD21^{hi}$ $CD23^{int\text{-}lo}$) were found to express higher levels of CD20 than follicular B cells ($CD21^{int\text{-}hi}$ $CD23^{hi}$) (figure 5.2A), while B1 cells ($B220^{int}$ $CD5^{int}$) expressed greater levels than B2 cells ($B220^{hi}$ $CD5^{lo}$) (figure 5.2B). All B cell subsets expressed levels of CD20 above isotype control levels.

Together, the data from figures 5.1 & 5.2 indicate that B cell subsets, and B cells from different tissues, express varying levels of CD20. However, in all cases, B cells expressed CD20 to some degree (above isotype control levels), and therefore should be depleted by the anti-CD20 depletion antibody.

B cell depletion is efficient with immunisation, and lasts upwards of 5 weeks

In order to determine the efficiency and timescale of B cell depletion *in vivo*, a depletion experiment was performed, in which mice were treated with a single dose of anti-CD20 depletion antibody. Mice were subsequently immunised the following day, and B cell numbers followed over time in various lymphoid tissues. The data presented in figure 5.3A reveal that B cells numbers were vastly reduced even by day 3 post-treatment in all organs analysed, and this reached baseline by day 10 (red line). In the spleen, the major site of B cell localisation, B cell numbers constituted less than 0.5% by day 10 post-treatment, indicating efficient depletion. Non-depleted mice showed an increase in B cell numbers in the peritoneal cavity, as would be expected following the i.p. immunisation (blue line). In B cell-depleted mice, however, this increase did not occur, and B cell numbers reached baseline by day 3 post-treatment. Interestingly, the population of B cells that remained in the bone marrow were found to be $CD20^-$ (see figure 5.11B later). A population of B cells was also seen to remain in the Peyer's patches, constituting around 15% of live cells, although these cells were not further investigated. However, B cell numbers in the Peyer's patches were still reduced, as starting levels in uninfected mice were ~60-70%. Looking at B cell subsets within the spleen, both marginal zone and follicular B cells were fully depleted by day 10 post-treatment, although the decline of marginal zone B cells appeared slower than that of follicular B cells (figure 5.3B).

B cell repopulation was not seen in any organ investigated during the 5-week time-course of this experiment (except for one mouse which showed ~8% B cells in the lymph nodes at day 38, figure 5.3A), indicating that depletion was surprisingly long-lived. Antigen-specific antibody responses following boosting (i.e. day 38 post-treatment) were also analysed in these mice (figure 5.3C). All antibody isotypes were reduced in the depleted mice when compared to non-depleted mice, but some isotypes, specifically IgG1, appeared significantly higher in depleted mice than naïve unimmunised mice, suggesting that they mounted a partial antigen-specific antibody response.

It is clear, therefore, that anti-CD20-mediated B cell depletion is both efficient and long-lasting. Importantly, depletion was effective with immunisation, allowing this system to be used to follow antigen-specific immune responses following immunisation or during infection.

T cell memory is impaired in B cell-deficient mice following *S. typhimurium* infection

As mentioned above, one of the aims of this project was to analyse the role of B cells in the generation of $CD4^+$ T cell memory. Firstly, I wanted to confirm that B cell-deficient mice have impaired T cell immunity following *S. typhimurium* infection, as has previously been studied [154,155]. T helper cell cytokine production following *in vitro* restimulation with *Salmonella* C5 antigen was used as a measure of memory. In these cultures, irradiated whole spleen cells were used as APCs, and thus both dendritic cells and B cells were present as antigen presenters. However, antigen-specific/primed B cells are absent in these cultures, as T cells from infected mice were positively selected prior to culture, and thus B cells were excluded. IFNγ is the 'hallmark' Th1 cytokine, and its production, together with IL-2, is most representative of T cell memory to *Salmonella.* The data presented in figure 5.4 reveal that B cell-deficient (μMT) mice had significantly impaired T cell IL-2, IL-10, IFNγ, and IL-17 recall responses to *Salmonella* antigen 12 weeks post-infection when compared to wild type mice. These data confirm that B cell-deficient mice have an impairment in T cell memory, and that the *S. typhimurium* infection model is a suitable system for investigating T cell memory.

B cell-depleted mice show normal primary T cell responses to *S. typhimurium*

In order to investigate the timing of the involvement of B cells in the generation of T helper cell responses, B cells were depleted at different times during *S. typhimurium* infection. The protocol used is outlined in figure 5.5. Briefly, mice were treated with a single dose of anti-CD20 B cell depletion antibody on either day -7, day 2, or day 10. Control groups of mice received an isotype control on the same days. All mice were infected with *S. typhimurium* on day 0. The primary (day 7) and memory (week 12) T cell responses were assayed. At these time-points, splenic bacterial load was measured, and T cell responses analysed by means of *in vitro* restimulation, and activation marker expression directly *ex vivo*. B cell numbers were also analysed to determine depletion status.

Looking at the primary time-point, it was confirmed that B cells had been depleted from the spleens of both the day -7 and day 2 depleted groups, but not the isotype control-treated groups (figure 5.6A). Percentages of B cells in the spleen of the day 2 depleted group were <0.5%, indicating that B cells were fully depleted by 5 days after treatment. Splenic bacterial load, both per gram and per spleen, was found to be equivalent in the non-depleted and depleted mice (figure 5.6B), indicating that the absence of B cells did not impact on the

early control of bacterial growth. By isolating the $CD4^+$ T cell population, these cells were analysed for the activation markers CD62L, CD44, and CD25. The data in figure 5.6C reveal that T cells from mice depleted on day -7 appeared less activated (i.e. express more CD62L, less CD44 and less CD25) than the isotype-treated controls. Mice depleted on day 2, however, appeared to have normal levels of T cell activation markers. This would suggest that T cell priming is slightly impaired when B cells are absent at the initiation of the immune response.

When restimulated *in vitro*, T cell cytokine production was largely equivalent across the depleted and non-depleted groups (figure 5.6D). Certainly, no impairment in IFNγ, the typical Th1 cytokine, was identified, while T cell IL-10 production appeared slightly enhanced in both the B cell-depleted groups. T cell IL-17 production appeared slightly reduced in the day -7 depleted group. However, IL-17 levels were low at this early stage of infection, so no strong conclusions on the role of B cells in Th17 cell priming can be made. IL-2 production by T cells is undetectable at this early stage (data not shown). Together, these data indicate that the early Th1 response was largely normal in B cell-depleted mice, which supports published data that B cells are not required for driving primary T cell responses [145,146].

Mice depleted of B cells on day -7 or day 2 of *S. typhimurium* infection show impaired T cell memory generation

In addition to analysing the primary T helper cell response, B cell-depleted animals were analysed 12 weeks post-infection to look at bacterial clearance and memory T cell presence. This experiment aimed to determine the timing of the involvement of B cells in the generation of T cell memory, in the *S. typhimurium* infection model.

As can be seen in figure 5.7A, in depleted groups the B cells had repopulated the spleen by this late time-point. Interestingly, B cells had not fully repopulated the spleens of two of the mice in the day -7 depleted group. The kinetics of B cell repopulation following depletion during infection are discussed later (see figure 5.11). Meanwhile, splenic bacteria had almost been cleared in all of the groups of mice, with just a few viable bacteria remaining (figure 5.7B). The depletion of B cells did not therefore affect the clearance of this pathogen, despite the lack of antibody and impaired T helper cell responses.

$CD4^+$ T cell cytokine production following restimulation with *Salmonella* antigen was assayed, as a measure of T cell memory, in mice depleted of B cells at different times during infection. It is clear from the data presented in figure 5.7C that the day -7 and day 2 depleted groups show impaired T cell IL-2 and IFNγ responses, the main Th1-associated cytokines. This is indicative of impaired memory generation when B cells were depleted on day -7 or day 2 of infection. T cell IL-17 production was also defective in the day -7 and day 2 depleted groups, suggesting Th17 memory was also impaired in these groups. In all cases, cytokine production by T cells from the day 10 depleted group was equivalent to that of the non-depleted group, indicating normal memory generation. It should be noted, however, that although T cell cytokine production is reduced in the day -7 and day 2 depleted groups in comparison to non-depleted mice, levels are above that of naïve T cells, suggesting that some memory is formed, even in the absence of B cells.

T cell IL-10 production, seen in figure 5.7C, was equivalent in the depleted and non-depleted groups. Interestingly, this IL-10 production by infected mice was also equivalent to levels produced by naïve T cells, suggesting that T cell IL-10 production in response to *Salmonella* antigen in culture is not a memory response, and therefore that IL-10 production by T cells cannot be utilised as a measure of memory in this model. Together, the data presented in figure 5.7C highlight a role for B cells during the first ~10 days of infection for efficient T helper cell memory generation.

Antibody responses are reduced in depleted groups, while B cell cytokine responses after repopulation appear normal

The *Salmonella*-specific serum antibody responses were measured in B cell-depleted and non-depleted mice 12 weeks post-infection. Unsurprisingly, antibody responses (total *Salmonella*-specific immunoglobulin) were reduced in mice depleted on days -7 or 2 (figure 5.8A). Mice depleted on day 10 of infection had strong antibody responses, but this was still reduced when compared to isotype control-treated mice.

As mentioned above, B cells had repopulated the spleens of depleted mice by 12 weeks post-infection (see figure 5.7A). These B cells were isolated, stimulated *in vitro*, and cytokine production analysed, in order to determine if they were capable of responding to the bacterial antigen, and not refractory in any way. Figure 5.8B shows that B cell IL-6, IL-10 and IFNγ production was largely equivalent across both depleted and non-depleted groups. B cell

production of IFNγ was particularly variable at this time (figure 5.8B, far right), and minimal in comparison to levels of T cell-derived IFNγ. Indeed, the levels of cytokine produced by B cells 12 weeks post-infection were comparable with that produced by naïve B cells (figure 5.8B). This would imply that B cells from infected mice do not possess cytokine memory, as was discussed in chapter 3.

B cells are required for T follicular helper cell generation and maintenance

The data presented in figure 5.7 indicate a role for B cells during the first ~10 days of infection for the generation of T helper cell memory. However, the exact function of B cells in driving T cell memory formation remains unknown. As the B cell follicles are the most likely site of B-T cell interaction, T cells with the T_{FH} phenotype were investigated during *Salmonella* infection. These T_{FH} cells can be identified by several different ways according to the unique markers they express. Here, I identified T_{FH} cells by flow cytometry either by ICOS and CXCR5 expression, or by PD-1 and CXCR5 expression. Example staining and gating of T_{FH} cells, for each method of identification, is given in figure 5.9A. It was found that, during the early stages of *S. typhimurium* infection in B cell-sufficient mice, the T_{FH} cell population in the spleen expanded up until day 7, before reaching a plateau (figures 5.9B & C, blue line). B cell-deficient μMT mice lacked this population of T cells entirely (figures 5.9B & C, purple line). By treating mice with anti-CD20 B cell depletion antibody on day 2, the numbers of T_{FH} cells rose slightly above μMT levels, but did not really get the chance to establish, and remained at low levels. Meanwhile, treating with anti-CD20 on day 10 of infection resulted in the initial expansion of this population, which was then rapidly lost. In both cases, by day 16 of infection the T_{FH} cell population had been completely abolished (figure 5.9B and C, red lines). These data indicate that B cells are essential for both the generation and maintenance of T_{FH} cells during *S. typhimurium* infection, and suggests that B cells may provide a survival niche or signal for the T_{FH} cell population.

A large proportion of T follicular helper cells appear to be Th1 effector cells

These T_{FH} cells, found in large numbers during the early stages of *S. typhimurium* infection, precede the helper function, as GCs do not appear in this model until ~4 weeks [206]. Therefore, these early T_{FH} cells were further analysed for their expression of the Th1-associated transcription factor, Tbet, and the activation marker, CD44, to determine if they have a Th1 phenotype. Figures 5.10A & B show that, by day 7 of infection, around 70% of the T_{FH} cell population were $CD44^{hi}$ and expressing Tbet, suggesting that they are activated Th1 cells. While at the same time-point only around 10% of non-T_{FH} cells expressed these

markers. Thus at this early stage of infection, when T_{FH} cell numbers were increasing, a greater proportion of T_{FH} cells had this Th1 effector cell phenotype than non-T_{FH} cells (figure 5.10B), indicating either that T cells expressing the Th1 master regulator are over-represented in the T_{FH} cell subset, or that T_{FH} cells begin to express Th1 markers.

Further data confirming that these T_{FH} cells are Th1 effector cells is shown in figure 5.10C, from Dr Tom Barr's work. These data show that, by gating on either $IFN\gamma^+$ or $IFN\gamma^-$ T cells identified by intracellular staining in naïve or day 7-infected mice, the $IFN\gamma^+$ T cells present in large numbers on day 7 of infection have an $ICOS^+$ $CXCR5^+$ T_{FH} cell phenotype. In other words, the IFNγ-producing T cells at this early stage of infection are predominantly of the T_{FH} cell phenotype. It should be noted, however, that many more T cells within the spleen express Tbet than secrete IFNγ. Together, the data presented in figure 5.10 highlight the plasticity between the Th1 and T_{FH} cell populations. The data further imply that a large proportion of T cells with the T_{FH} cell phenotype on day 7 of infection are antigen-specific Th1 effector cells, responding to the pathogen.

B cell repopulation is enhanced when B cells are depleted during established *S. typhimurium* infection

The kinetics of B cell repopulation in uninfected and *Salmonella*-infected mice were analysed, to determine the effects of immune activation on the efficacy of anti-CD20-mediated B cell depletion. To do this, mice were treated with a single dose of anti-CD20 B cell depletion antibody on day 0. Mice were either infected with *S. typhimurium* before depletion (day -7), after depletion (day 7), or left uninfected. B cell numbers in the spleen, lymph nodes and bone marrow were analysed in the weeks following depletion. It appears that by depleting B cells before infection, B cell repopulation was delayed in comparison to depletion during infection (figure 5.11A). In other words, when B cells were depleted after *Salmonella* infection had already established, they returned sooner. These data also agree with that seen in figure 5.7A, where two mice in the day -7 depleted group had not fully repopulated B cells in the spleen 12 weeks after infection, while B cell repopulation was complete in both the day 2 and day 10 depleted groups.

Additionally, this experiment provided interesting information on the B cell populations within the bone marrow. In naïve bone marrow there appeared to be 2 distinct populations of B cells when CD19 was plotted against CD20 (figure 5.11B, far left, see gates). These are likely to be $CD19^+$ $CD20^+$ mature B cells, and $CD19^+$ $CD20^-$ immature pro-B cells. When

mice were treated with anti-CD20 B cell depletion antibody, only one of these populations (the $CD19^+$ $CD20^+$ mature B cells) was depleted (figure 5.11B, second from the left). Non-depleted mice infected with *S. typhimurium* underwent profound changes in their bone marrow, and the $CD19^+$ $CD20^-$ B cell population was lost while only the $CD19^+$ $CD20^+$ population remained (figure 5.11B, second from the right). Anti-CD20 treatment combined with *S. typhimurium* infection resulted in the loss of both B cell populations in the bone marrow (figure 5.11B, far right). These data reveal that the changes in lymphocyte subsets induced by *S. typhimurium* infection are not restricted to the spleen (as outlined in chapter 4), but lymphocytes in the bone marrow, too, are altered. These data also explain that seen in figure 5.11A, where in the bone marrow anti-CD20 treatment alone (square symbols) did not efficiently deplete the B cell population, as by gating on $CD19^+$ cells included the $CD20^-$ pro-B cell population that resisted depletion.

Discussion

Levels of CD20 expressed by B cell subsets

CD20 expression by B cells was found to vary depending on the organ and subset from which they were isolated (figures 5.1 and 5.2). While expression of CD20 by B cells from the spleen and lymph nodes was similar, in the bone marrow CD20 expression levels were much lower. This is likely due to the presence of immature pro-B cells in the bone marrow, which express the B cell marker CD19 but do not yet express CD20 [220,228]. In the Peyer's patches, a population of B cells was found to express high levels of CD20 (although a further $CD20^-$ population, which was resistant to depletion, may also be present). Upon further investigation, these $CD20^{hi}$ cells were found to be in a more activated state, and resemble GC B cells. As the Peyer's patch B cells are involved in IgA production for gut immunity, they are thought to have large numbers of GCs [307]. Although published data indicates that GC B cells maintain surface expression of CD20 [228], I have found no data suggesting they express this molecule at higher levels. However, there is evidence to suggest that signalling through CD20 functions in rescuing GC B cells from apoptosis [308], so it would make sense that these cells therefore express CD20 at higher levels, explaining the results seen here in figure 5.1. These $CD20^{hi}$ B cells were also found in small numbers in the spleen and lymph nodes, where the number of B ells undergoing the GC reaction in naïve mice is lower. CD20 expression levels on B cells in the peritoneal cavity were similar to B cells from the spleen. Thus there appears no reason that this population of B2 cells should be resistant to depletion, as has previously been suggested [309].

B cell depletion kinetics

Depletion of B cells from the spleen, lymph nodes, blood and peritoneal cavity following immunisation was both efficient and long-lived (figure 5.3). However, populations of B cells were found to remain in both the bone marrow and Peyer's patches. The population of $CD19^+$ cells that remained in the bone marrow was found to be $CD20^-$ and are therefore likely to be immature pro-B cells. The B cell population in the Peyer's patches that was resistant to depletion was not further investigated. However, assuming that these cells are $CD20^-$, they may be $CD19^+$ $CD20^-$ plasmablasts, on their way to becoming $CD19^-$ $CD20^-$ fully differentiated plasma cells [228], although few B cells in the Peyer's patches appeared $CD20^-$ before depletion (figure 5.1A). Alternatively, these cells may be GC B cells, which are more resistant to depletion than follicular B cells [241]. As mentioned above, Peyer's patches, together with mesenteric lymph nodes, have large numbers of GCs for the

generation of IgA-secreting plasmablasts, which then migrate to the lamina propria and maintain gut immunity [307,310]. A more detailed analysis of this population would be required to confirm the phenotype of these resistant Peyer's patch B cells.

B cell numbers reached baseline levels in the blood, bone marrow and peritoneal cavity by 3 days post-depletion, while in the spleen, lymph nodes and Peyer's patches, baseline levels had been reached by day 10 (figure 5.3). These data therefore indicate that depletion takes 3-10 days. The data in figure 5.6A allow the more accurate analysis of the time interval required for B cell depletion, as mice depleted on day 2 of infection had <0.5% B cells in the spleen 5 days later. Thus it can be concluded that B cell depletion takes around 3-5 days. This interval of 3-5 days for B cells to be depleted should be kept in mind when analysing results from mice treated on different days on infection. For example, mice treated on day 2 of infection will still have some, although significantly less, B cells on day 5.

B cell subset depletion

The depletion kinetics of B cells within the spleen appeared to differ depending on the subset analysed. The data in figure 5.3B indicate that follicular B cell numbers were rapidly diminished, while the loss of the marginal zone B cell population was delayed. This is in agreement with previously published data, which shows marginal zone B cells to be more resistant to depletion than follicular B cells [241]. This result was surprising as marginal zone B cells expressed higher levels of surface CD20 than follicular B cells (figure 5.2), and are known to be the first B cell subset in the spleen to access circulating antibodies (see chapter 4), and thus one might have expected the marginal zone population to be depleted first. These data therefore suggest that marginal zone B cells have an innate resistance to depletion. Thus, the susceptibility or resistance to depletion does not appear to correlate with surface expression of CD20. One possible explanation for the resistance of marginal zone B cells is that the induction of apoptosis, one of the mechanisms by which B cells are depleted [224], may be less efficient in these cells, either due to survival factors in the marginal zone or characteristics of the long-lived marginal zone cells themselves.

It should be noted that all data presented in figure 5.3A relates to $CD19^{+}$ B cells. B1 cells ($B220^{int}$ $CD5^{int}$) found predominantly in the peritoneal cavity were not included in this analysis. Therefore the kinetics of depletion (and repopulation) of these cells in this model remain unknown. However, some published data provides insight into these cells, stating that they are more resistant to depletion than splenic B cells [240,309]. This may be due to

an innate resistance mechanism, similar to marginal zone B cells, or due to reduced access to depletion antibodies as a result of their non-circulatory status. A study by Hamaguchi *et al* went some way to answering this question. By adoptively transferring splenic B cells into the peritoneal cavity the authors found these cells to be similarly resistant to depletion, suggesting that the reason for their resistance is that lack of antibody access to this site [309]. Although my data does not address the resistance of the B1 cell population within the peritoneal cavity, conventional $CD19^+$ B2 cells in this site were efficiently depleted (figure 5.3A).

The duration of B cell depletion

B cell depletion was surprisingly long lasting, with numbers still at basal levels for the duration of the initial depletion experiment, upwards of 5 weeks post-depletion (figure 5.3A). The anti-CD20 depletion antibody used was the 18B12 clone of the IgG2a isotype, which should therefore follow an exponential decay cycle, with a half-life of 6-8 days [311]. Unfortunately, circulating anti-CD20 levels were not analysed here. Analysing such serum IgG2a would perhaps reveal how long after treatment this antibody remains in circulation *in vivo,* and would help establish the timescale of its effectiveness. The initial report, by the authors who made this particular clone of anti-mouse CD20, shows B cell numbers to be on the increase ~4 weeks post-depletion, with numbers returning to non-depleted levels around 7-8 weeks post-treatment [242]. Thus, B cell depletion seen here appears to last longer than previously reported, despite giving the same dose of anti-CD20 via the same route. The difference in longevity of depletion seen here may be due to the mouse strain used. However, analysis ~11-12 weeks post depletion revealed B cell numbers in the spleen to have returned to non-depleted levels (figure 5.7A). Furthermore, these B cells that returned to the spleen continued to express CD20 on the cell surface at similar levels to pre-depletion (data not shown), and so should not be resistant to further depletion. This would suggest that no selection for $CD20^-$ B cells has taken place after this single does of anti-CD20, as has been suggested in a previous study following long-term treatment in humans [312]. Additionally, the repopulating splenic B cells responded to heat-killed bacterial antigen *in vitro* in a similar way to non-depleted B cells and naïve B cells (figure 5.8B), indicating that they are capable of cytokine production, and not refractory.

B cell repopulation in *S. typhimurium* infection

Interestingly, the kinetics of B cell repopulation appeared to be accelerated in mice with established *S. typhimurium* infection, in comparison to mice depleted of B cells before infection (figure 5.11A). In other words, depletion before infection was longer lived than depletion during infection. This would suggest that the pathogen, or the immune response to it, is causing B cells to repopulate the lymphoid tissues at a faster rate. There are several possible explanations for this. B cell depletion may be less effective during an ongoing immune response, perhaps due to the activated state of the cells. Indeed GC B cells have been shown to be more resistant to depletion than both follicular and marginal zone B cells [241]. However, the data presented in figure 5.11A suggest that this is not the case, as B cells reached basal levels of <0.5% before repopulation, even when depleted during infection. Alternatively, anti-CD20 may decay and be removed from the circulation at a faster rate during infection. The increase in number and activation status of splenic macrophages will result in a greater phagocytic capacity, and may be more efficient at removing particles from the bloodstream. The removal of anti-CD20 from circulation would therefore allow the regeneration of mature B cells from their precursors in the bone marrow sooner. However, as this antibody is generated in mice [240], it should not appear as a foreign particle, and therefore whether or not enhanced degradation or removal is likely, I'm unsure. A more likely explanation is that infection may increase B cell maturation from their precursors in the bone marrow, and enhance recruitment of such cells to the spleen. This increase in B cell maturation and proliferation, as well as apoptosis, in both the bone marrow and spleen during infection may be 'mopping up' the anti-CD20 antibodies.

Further investigation of the bone marrow of B cell-depleted and *S. typhimurium* infected mice revealed interesting changes to B cell populations in this site (figure 5.11B). Anti-CD20 depletion alone depleted only mature B cells ($CD19^+$ $CD20^+$), whereas in *S. typhimurium* infection the population of pro-B cells ($CD19^+$ $CD20^-$) was lost. B cell depletion combined with *S. typhimurium* infection resulted in the loss of both populations of B cells from the bone marrow. This decrease in pro-B cell numbers in the bone marrow during *S. typhimurium* infection has previously been reported [313]. The authors attributed the loss of this population to be due to either increased apoptosis, as a result of direct colonisation of these cells by the bacteria, or elevated rates of B cell maturation. While the exact mechanism of loss of pro-B cells from the bone marrow requires further investigation, these data clearly highlight that the bone marrow, in addition to the spleen (see chapter 4), undergoes profound changes to lymphocyte populations during this bacterial infection.

These changes may be induced by the presence of bacteria, as *Salmonella* has been shown to live within the B cell [313] and phagocyte [314] populations of the bone marrow, or as a result of increased maturation and recruitment of bone marrow cells to the spleen [204].

Due to the loss of the B cell precursors from the bone marrow during infection, one might expect B cell repopulation to be delayed in infected mice. However, as discussed above, the opposite was true, and B cell repopulation was in fact enhanced by infection. This may be due to the more rapid turnover and maturation of B cells and their precursors during infection, and subsequent recruitment to the spleen.

Serum antibody levels following depletion

As the mice used for B cell depletion were immuno-sufficient C57BL/6 mice, natural antibody was present in the serum before depletion. Furthermore, existing long-lived plasma cells situated in the bone marrow, which are $CD20^-$, should remain unaffected by anti-CD20 treatment, and therefore serum antibodies specific for previously encountered antigen should also be present. As mentioned in the introduction to this chapter, these existing levels of serum antibody are one of the advantages of this B cell depletion system over the use of B cell-deficient mice. However, these levels of circulating antibody have been shown to drop following repeated anti-CD20 treatment in humans, with both total IgM [315] and class-switched IgG [316,317] affected. While the reduction in IgM levels is likely caused by the loss of splenic marginal zone and peritoneal B1 B cells, the loss of IgG is thought to be due to the death of long-lived plasma cells, as, due to the depletion of memory B cells, they are no longer replenished from the memory B cell pool [167]. Unfortunately, antibody levels in unimmunised B cell-depleted mice were not measured here, so the effects of a single dose of anti-CD20 in mice on serum antibody levels remain unknown. However, the data presented here show antibody responses to 'new' antigens, encountered when B cells are depleted, to be impaired (figures 5.3C & 5.8A).

Antigen-specific antibody production following B cell depletion

One interesting observation from my data was that, in the initial B cell depletion experiment with DNP-KLH immunisation, DNP-specific antibodies in B cell-depleted mice, although reduced in comparison to non-depleted mice, were significantly above levels in naïve mice, despite anti-CD20 treatment one day before immunisation (figure 5.3C). This antigen-specific antibody was predominantly of the IgG1 isotype, which would suggest a T cell-dependent mechanism, although T cell-independent IgG production has been reported in a

viral infection model [318]. The presence of antigen-specific class switched antibody in these immunised mice, which were depleted 1 day prior to immunisation, was unexpected. Serum was taken at the end-point of the experiment (day 37 post-treatment, which was 6 days post-boost), at which time B cell numbers were still at basal levels. Therefore, antibody production in response to the boost seems unlikely, so this antigen-specific antibody must have been produced during priming. As depletion of B cells takes 3-5 days, this may have allowed time for B cell activation and IgG-secreting plasmablast/plasma cell differentiation, which are $CD20^-$ and resist depletion.

Additionally, with anti-CD20 depletion in *Salmonella* infection, antigen-specific antibody was found, 12 weeks post-infection, in the day 10-depleted group (figure 8A). Again, these data indicate early production of antigen-specific antibody in this system. However, previous reports suggest the GC reaction doesn't occur until late in this infection, around 4-5 weeks [206]. Thus the presence of such antigen-specific antibody in B cell-depleted mice was unexpected.

Together, the presence of antigen-specific antibody in B cell-depleted mice, in both the DNP-KLH immunisation system and in *Salmonella* infection, suggests early production of class-switched antibody before B cell depletion was completed. These data leave us with unanswered questions as to how, if this antibody was produced during the first few days of immune priming, was it still present 5 weeks (in the DNP-KLH immunisation system) or 12 weeks (in the *Salmonella* model) later: Were long-lived IgG1-secreting plasma cells generated within the first few days of the immune response? Another explanation would be that, as B cell depletion was not complete (0.1-0.5% $CD19^+$ cells remain in the spleen, ~15% $CD19^+$ remain in the Peyer's patches), antigen-specific activated B cells might be in some way resistant to depletion, and therefore selected for survival. As mentioned above, B cells that have entered the GC reaction are thought to be more resistant to depletion than either follicular or marginal zone B cells [241]. However, again this seems an unlikely explanation, as the numbers of $CD19^+$ cells found in the spleens of day -7 and day 2 depleted mice appeared equivalent (<0.5%), although the Peyer's patches were not analysed in this particular experiment. Furthermore, B cell-deficient μMT mice also show 'background' $CD19^+$ cell staining in the spleen (data not shown), presumably due to non-specific binding by other cell types, so how much of the remaining CD19 staining in depleted mice is real B cell staining is unknown. Thus the development of this antigen-specific antibody despite B cell depletion required further investigation, and is discussed further later, in chapter 6.

B cell involvement in primary T helper cell responses

Whether or not B cells play a role in the initial priming of T cell responses remains a topic of dispute. While some authors report an impairment in primary T cell proliferation in the absence of B cells [142,143], others state that B cells are dispensable at this early stage [145,146]. Here, the use of anti-CD20-mediated B cell depletion allowed further analysis of the role of B cells in early T cell differentiation. Initially, T cells isolated on day 7 of infection from B cell-depleted mice appeared to be in a less activated state, in terms of the cell surface activation markers CD62L, CD44 and CD25 (day -7 group, figure 5.6C). However, production of IFNγ, the main Th1-associated cytokine, was not impaired in either the day -7 or day 2 depleted groups (figure 5.6D). If anything, IFNγ production by T cells was higher in the B cell-depleted groups in comparison to the non-depleted groups. This enhanced Th1 response in the absence of B cells has been reported previously, and may be due to the absence of B cell-derived IL-10 and subsequent increase in IL-12 production by dendritic cells [319]. Interestingly, this primary T cell IFNγ production was normal in B cell-depleted groups, despite the loss of the T_{FH} cell population (figure 5.9), which contains some cells of the Th1 phenotype (figure 5.10). Thus although some T_{FH} cells have a Th1 phenotype and secrete IFNγ, the loss of this population during the primary response does not result in impaired production of IFNγ by the whole splenic T cell population.

Further to the Th1 response, IL-17 production by T cells in the day -7 depleted group appeared reduced when compared to the other groups (figure 5.6D), which may point to a role of B cells in priming the early Th17 response. Indeed, *in vitro* data suggests B cells are capable of supporting Th17 cell differentiation [320]. However, as IL-17 levels are low at this early stage of infection, it is impossible to draw any conclusions on the role of B cells in Th17 cell differentiation from this data.

Conversely, IL-10 production by T cells from depleted mice appeared elevated. Enhanced IL-10 production would suggest a more regulatory phenotype, but as IFNγ production was also increased, this seems counter-regulatory. Instead, IL-10 production may originate from the Th1 cells themselves, as Th1 effectors have also been shown to secrete IL-10 as a mechanism of self-regulation [321], and thus reflect the greater Th1 response. In summary, B cell-depleted mice show fairly normal primary T cell responses to *S. typhimurium,* and thus the involvement of B cells in T cell priming appears minimal.

B cells are required for the generation of T cell memory

It was firstly confirmed, with the use of B cell-deficient μMT mice, that T cell memory was significantly impaired following *Salmonella* infection in the absence of B cells (figure 5.4). T cell production of IL-2, IL-10, IL-17 and IFNγ twelve weeks post-infection were all significantly impaired in the μMT mice. These data are in agreement with previous findings in the same infection model [154,155], where B cell-deficient mice were shown to lack protective immunity, as mortality rates were significantly increased following challenge. The authors demonstrate that the lack of protective immunity is likely due to the lack of T cell-derived IFNγ [154,155]. Therefore, here, the severe impairment in T cell IFNγ production in μMT mice is likely to confer the lack of protective immunity.

The use of anti-CD20-mediated B cell depletion allowed me to control the presence or absence of B cells, and investigate the timing of their involvement in the generation of memory T cells, by depletion on different days of infection. Th1 cell memory, as identified by IL-2 and IFNγ production, was significantly impaired when B cells were depleted on day -7 or day 2 of infection, whereas normal memory was generated with B cell depletion on day 10 (figure 5.7C). Similarly, IL-17 production was also reduced in the day -7 and day 2 depleted groups, but not when treated with anti-CD20 on day 10. However, even in the two groups with impaired T cell memory, production of IL-2, IL-17 and IFNγ was higher than that produced by naïve mice. These data therefore suggest that memory is not an 'all or nothing' concept, and, although reduced in the day -7 and day 2 B cell-depleted groups, it was not entirely absent. It would have been interesting to then challenge these groups of mice with the virulent C5 strain, and establish whether the impairment in T cell memory, especially IFNγ production, in the day -7 and day 2 depleted groups correlates with a lack of protective immunity. Interestingly, IL-10 production by T cells was equivalent in all groups, including the naïve mice, indicating that this is not a memory response. Therefore, IL-10 production by T cells in this system cannot be used as a measure of T cell memory.

The data presented indicate a role for B cells in the generation of T cell memory, but do not determine the nature of this role. Previous data shows that the addition of immune serum does not rescue protection when B cell-deficient mice are challenged with the virulent strain [154], suggesting that antigen presentation, rather than antibody production, is required. The transfer of immune serum to depleted mice, here, would be required to confirm that lack of antigen-specific antibody is not the cause of the impairment in T cell memory. Importantly, these data provide strong evidence for the requirement of B cells during the first ~10-15 days

(taking into account the time it takes for B cells to be depleted) of infection for the efficient generation of T cell memory. Given that this infection takes 4-6 weeks to be cleared, and GC formation and switched antibody production doesn't occur until 1 month after infection [206] (and T.A. Barr, S. Brown, T. Slocombe & D. Gray, unpublished data), this result was unexpected. Furthermore, my result is contradictory to previous reports that B cells are not involved in antigen presentation until late in immune responses, either because they cannot prime naïve T cells [139], or because the numbers of cognate B cells capable of presenting antigen are too low before proliferation in the GC [133]. These results therefore leave us with the question as to what it is that B cells are doing between days 2 and 10 of infection that is impacting on T cell memory generation. This concept is discussed in greater detail below, and in the final discussion in chapter 7.

The generation and maintenance of T follicular helper cells is dependent on the presence of B cells

In addition to functioning as APCs for the generation of T cell memory, B cells were found to be essential for both the generation and maintenance of T_{FH} cells (figure 5.9). During *S. typhimurium* infection, the T_{FH} cell population expanded in non-depleted mice, whether through proliferation or increased migration to the follicles remains undetermined. Baseline levels of T_{FH} cells were lower in uninfected μMT mice, while the expansion of this population during infection did not occur, suggesting that B cells are required for their generation and/or maintenance. The use of anti-CD20 allowed a fuller investigation into the dependence of this population on B cells. Depletion of B cells on day 2 of infection resulted in the initial increase in T_{FH} cell numbers, but these cells were rapidly lost following anti-CD20 treatment. Meanwhile, depletion on day 10 allowed normal expansion of T_{FH} cells, but again this population was lost. The rapid loss of T_{FH} cells within a few days after B cell depletion suggests that B cells provide a survival niche or signal for the maintenance of this population. Together, these data show that B cells are required for both the expansion and maintenance of this population during *S. typhimurium* infection.

Previously published data comments on the role of B cells in T_{FH} cell presence and function. B cell numbers, for example, have been shown to correlate well with the number of T cells situated in the follicle [75]. The authors show the accumulation of T cells in the follicles following immunisation to be dependent on dendritic cells, and their expression of CD40 and OX40-ligand, together with T cell expression of CXCR5 [75]. However, neither the expression of CD40 or MHC class II by B cells is necessary for the migration of T cells to

the follicles [75]. The absence of ICOSL expression by B cells results in significantly decreased numbers of T_{FH} cells following KLH immunisation, although numbers are not reduced to levels seen in B cell-deficient mice [40]. Thus, my data highlight that B cells are not only required for the expansion of the T_{FH} cell population during an immune response, but are also essential for their maintenance under steady-state conditions. Whether this is solely dependent on B cell expression of ICOSL, or whether other signals are involved, remains to be investigated.

B-T cell interaction in the follicles

Activated Th1 cells, identified by Tbet expression and IFNγ production (figure 5.10), were over-represented in the T_{FH} cell compartment during the initial week of infection. In other words, a large proportion (~70% on day 7 of infection) of T_{FH} cells appeared to be activated Th1 cells. This would suggest, therefore, that many of these cells are antigen-specific T cells responding to the infection, although antigen-specificity is not assayed directly here. Other members of the laboratory have proved that the increase in cells of the T_{FH} cell phenotype by flow cytometry correlates with an increase in T cell staining within the follicles (T.A. Barr, S. Brown & D. Gray, unpublished data), confirming that these cells enter the B cell regions of the spleen. This migration of newly activated T cells into the follicles has been shown previously, and is due to the rapid upregulation of CXCR5 expression by T cells upon activation [322]. Therefore, what is currently identified with these markers as a T_{FH} cell population may, in the early stages following activation, be a transient phase that activated T helper cells go through. During this time, antigen-specific T cells would have the opportunity to interact with B cells in the follicles. I predict that these early T_{FH} cells, seen clearly during *S. typhimurium* infection, will be different in gene expression and function from the bona fide T_{FH} cells that help select B cells in the GC. Because GCs form only beyond day 40 during *Salmonella* infection [206], there is a separation of these early T_{FH} cells from those that go on to inhabit GCs. Thus, the *Salmonella* infection model is ideal for dissecting the heterogeneity of the T_{FH} cell population. This matter is discussed more extensively in the final discussion presented in chapter 7.

Could T follicular helper cells be memory precursors?

The presence or absence of T_{FH} cells correlated with the generation of T cell memory. Specifically, by depleting B cells on day 2 of infection, the T_{FH} cell population did not expand, and T cell memory was not generated. Conversely, B cell depletion on day 10 of infection resulted in the initial expansion of T_{FH} cells until the plateau phase was reached,

before these cells were lost, and memory generation was normal (figures 5.7 & 5.9). I propose that these T_{FH} cells with a Th1 phenotype found during the first ~1-3 weeks after infection are antigen-specific T cells that interact with B cells within the follicle, and receive the signal necessary for memory generation. Therefore, these cells with the transient T_{FH} phenotype, or a proportion of them, may be memory precursors. The dependence of T cell memory generation on the presence of B cells would be explained by the fact that T_{FH} cells are also dependent on B cells. With B cell depletion on day 10 of infection, having normal numbers of T_{FH} cells for the initial ~10-12 days appears to be enough for T cell memory to be generated.

However, this theory is purely speculative, and my data does not directly link the T_{FH} cell population to the generation of memory cells. Clearly, this apparent correlation between T_{FH} cells and T cell memory generation requires further investigation. In order to more directly link T_{FH} cell expansion during infection to memory cell development, one experiment would be to prevent the expansion of T_{FH} cells, and note the effect on memory generation. As CXCR5 expression by T cells is required for the accumulation of T cells in the follicles after immunisation [75], then migration to the follicles can be prevented using CXCR5-deficient T cells. The use of either $CXCR5^{-/-}$ T cell transfers, or making chimeras in which the T cell population alone is deficient in CXCR5, would prevent the migration of such T cells to the follicles, and may inhibit the B-T cell interaction required for T cell memory generation. It would therefore be interesting to see if the development of T cell memory is impaired in such systems.

Disadvantages of the B cell depletion system

Although anti-CD20 B cell depletion has been used here as a better alternative to the use of B cell-deficient mice, this system is not without its drawbacks. Firstly, B cell depletion early in the immune response (on days -7 or 2 of infection) resulted in an impairment in antigen-specific antibody production (figure 5.8A). Therefore, the data presented do not rule out a role of antigen-specific antibody on influencing T cell responses. Immune serum transfer into these mice would be required to prove that the lack of T cell memory (and T_{FH} cell development) is not as a result of diminished antibody levels, as has been done previously in B cell-deficient mice [154]. Furthermore, depleted mice receive a massive dose (0.25mg) of anti-CD20 i.v., and thus have unnaturally high levels of circulating IgG2a of this particular specificity. Binding of this antibody to B cells results in their deletion by a variety of mechanisms, including antibody-dependent cellular cytotoxicity, complement-dependent

cytotoxicity and activation of the apoptotic pathway [223]. This process of removing ~60% of splenocytes is likely to impact upon other the other immune cells involved, such as phagocytes, and could therefore have a knock-on effect on the generation of immune responses to pathogens. However, there is no doubt that the advantages of this system outweigh the drawbacks, and thus the data presented here provides great insight into the specific role B cells are playing in the generation of T cell responses *in vivo*.

Implications for Rituximab treatment in human patients

The use of anti-CD20 to analyse the effects of B cell depletion on the generation of T helper cell responses generated several interesting results. B cells were found to be important in the generation and maintenance of T_{FH} cells, and in the generation of T cell memory. These results therefore have important implications for human patients undergoing Rituximab treatment. The data presented suggest that T cell memory responses to antigens encountered when B cells are depleted will be severely impaired. Moreover, existing T helper cell memory may also be lost with long-term B cell depletion, as B cells have been shown to be involved in the maintenance of such memory [116]. Antibody responses to antigens encountered during anti-CD20 treatment will also be impaired. Thus patients undergoing anti-CD20 treatment are unlikely to gain immunity to any infectious agents or vaccine antigens encountered during the time of depletion, while existing immune memory, in terms of both T cells and antibody, is also at risk. Furthermore, the observation that B cell repopulation was enhanced following depletion during ongoing *S. typhimurium* infection implies that anti-CD20-mediated B cell depletion may be less effective, in terms of duration of depletion, in patients with ongoing immune responses. Although the data here was generated in an infection model, the same may well be true for ongoing autoimmune responses, such as Rheumatoid Arthritis and SLE, that Rituximab is used as a treatment for [228]. Indeed, in mice models of autoimmune diseases, B cell depletion by anti-CD20 is less effective [240]. Thus, the data presented in this chapter using anti-CD20-mediated B cell depletion may have significant implications for Rituximab treatment in human patients.

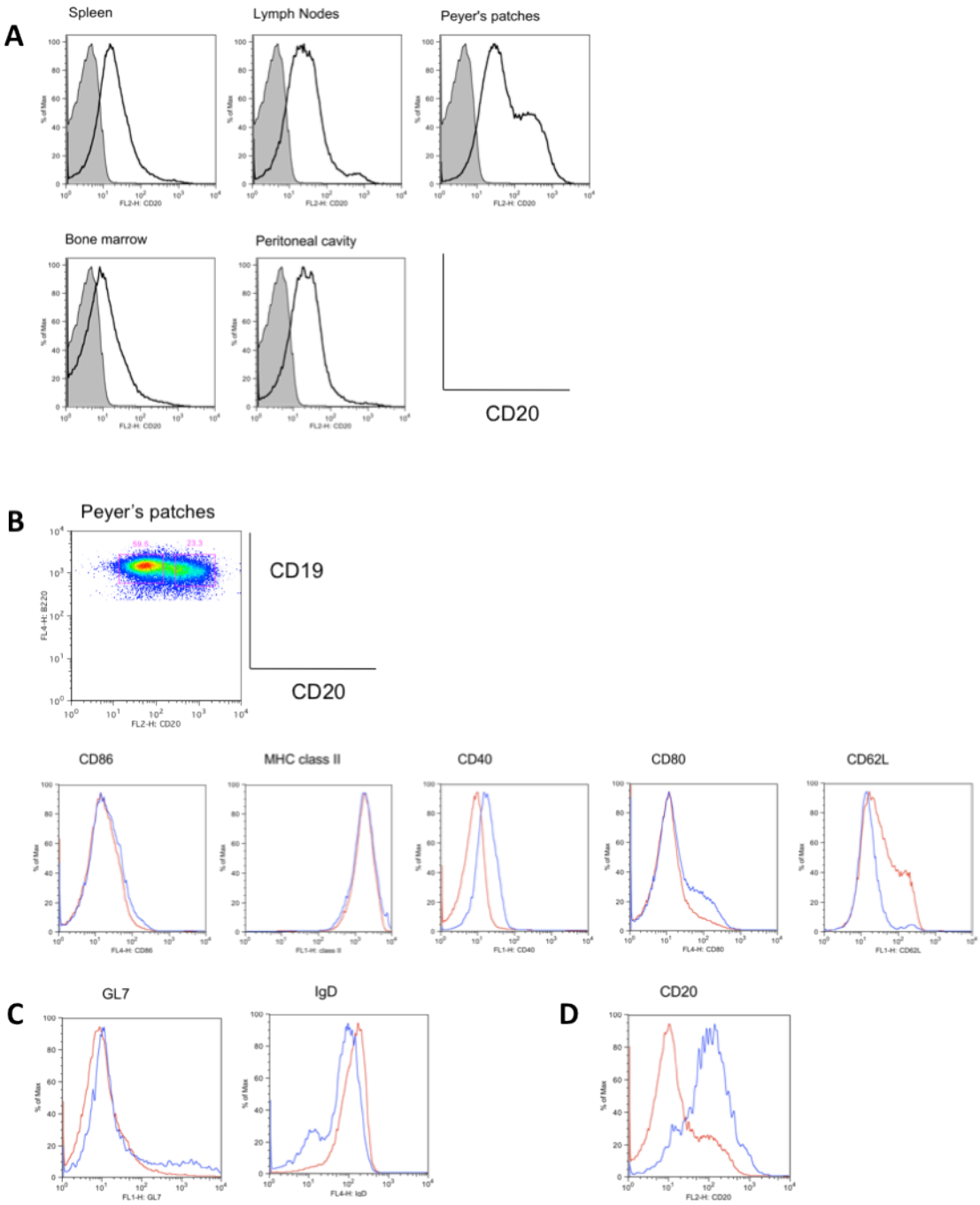

Figure 5.1: B cells from different organs express varying levels of CD20. Organs were removed from naïve C57BL/6 mice and stained for B cell expression of CD20 by gating on $CD19^+$ cells (A). Shaded line represents isotype control, and bold line indicates B cell CD20 levels after gating on $CD19^+$ cells. The two populations of B cells in the Peyer's patches that differ in their expression of CD20 (B, top) were analysed further by staining for expression of activation markers as shown in (B, bottom). These two populations were analysed further for expression of GL7 and IgD to determine if they are germinal centre B cells (C). In (B) and (C) blue = $CD20^{hi}$ and red = $CD20^{int}$ B cells. (D) Gating on $GL7^+$ germinal centre B cells, blue, or $GL7^-$ non-germinal centre B cells, red, their CD20 expression was determined. Data represents 3 individual mice.

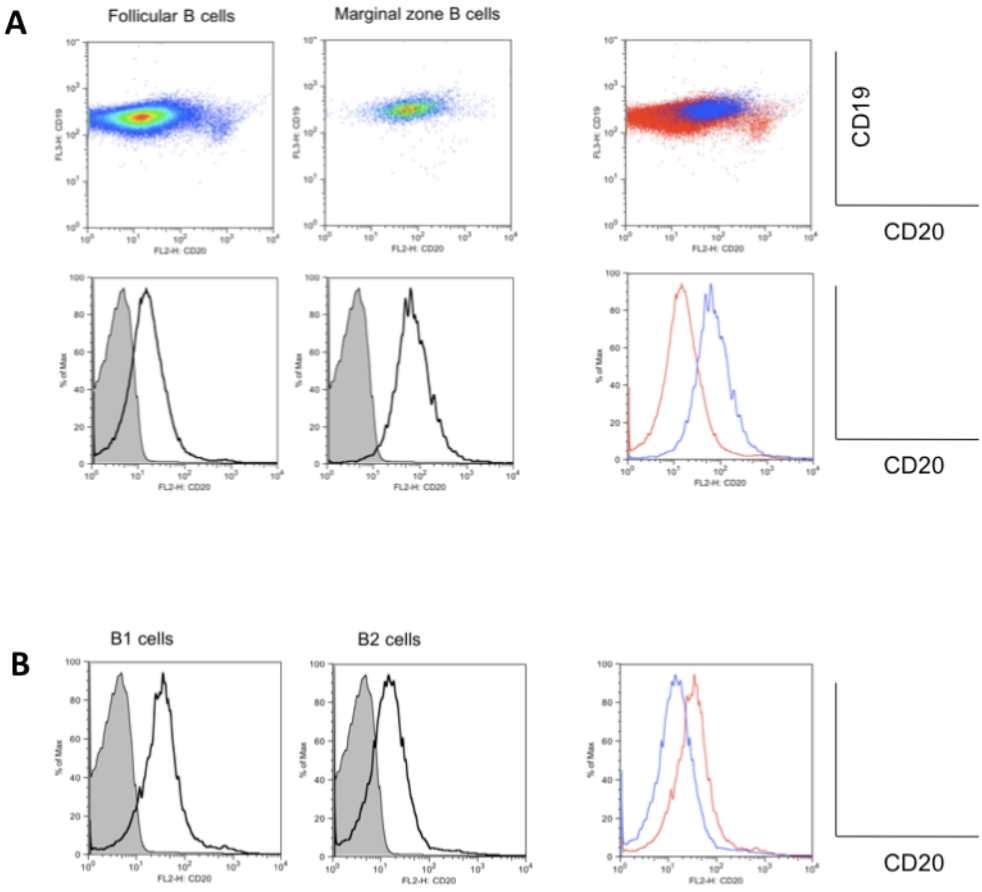

Figure 5.2: B cell subsets express varying levels of CD20. B cell subsets in the spleen were analysed for expression of CD20. (A) Follicular B cell (red) and marginal zone B cell (blue) expression of CD20. (B) B1 cell (red) and B2 cell (blue) expression of CD20. In both cases shaded line indicates isotype control, and bold line shows B cell CD20 expression. Data is representative of 3 individual mice.

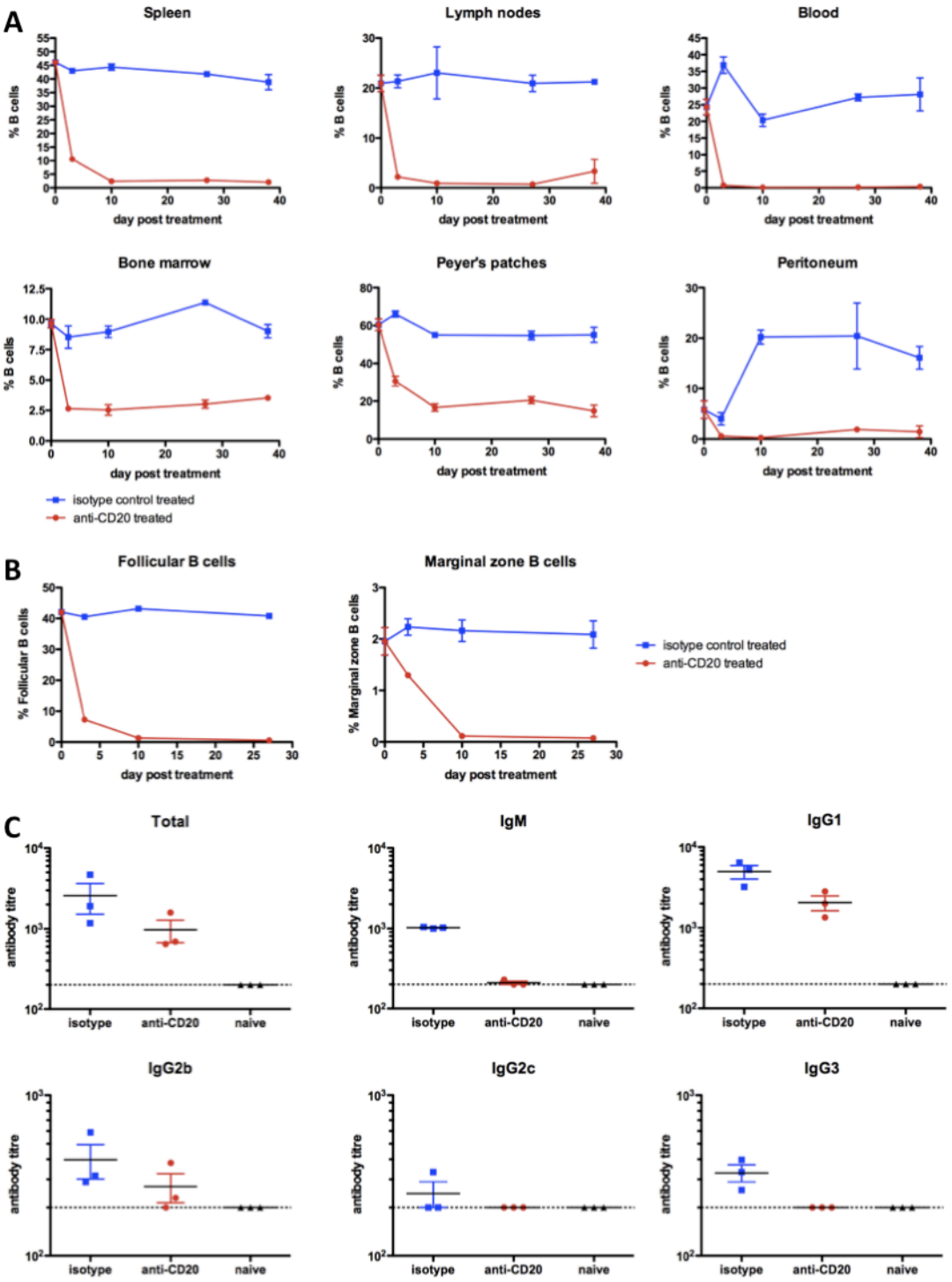

Figure 5.3: B cell depletion is efficient with immunisation and lasts upwards of 5 weeks. C57BL/6 mice were given a single dose of 250µg anti-CD20 or isotype control i.v. on day 0. On day 1, mice were immunised with DNP-KLH/Alum i.p. Where appropriate, mice were boosted with DNP-KLH/Alum i.p. and s.c. on day 31. Samples were taken on days 3, 10, 27, and 38 and analysed for B cells in different organs (A). Splenic B cell subsets were identified (B). Sera was taken on day 37 and analysed for DNP-specific antibody isotypes (C). In all cases blue = isotype control treated, red = anti-CD20 treated. In (C) the dotted line indicates the limit of detection.

A

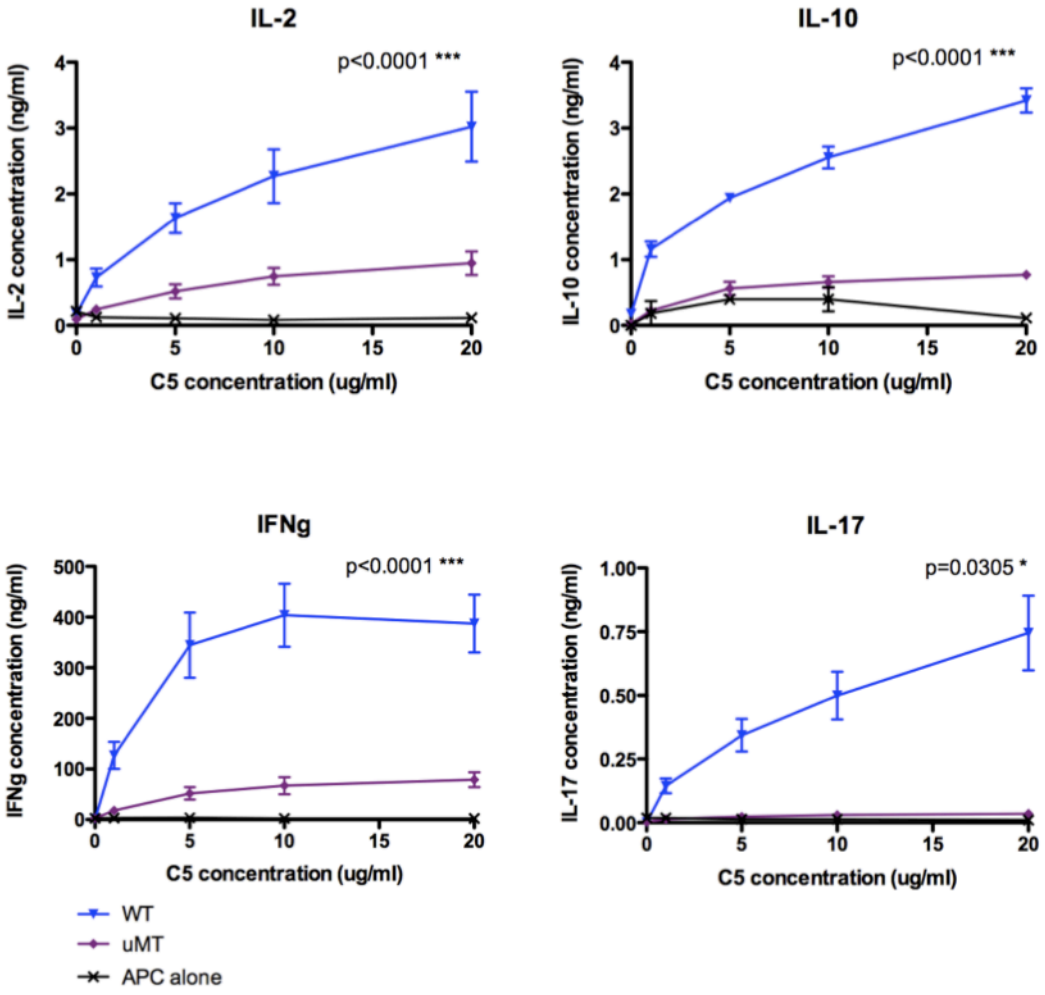

Figure 5.4: T cell memory is impaired in B cell-deficient mice following *S. typhimurium* infection. C57BL/6 and μMT mice were infected with *S. typhimurium*. Twelve weeks later splenic T cell cytokine responses were measured following *in vitro* restimulation with C5 antigen. Irradiated whole spleen cells were used as APCs in culture. IL-2, IL-10, IL-17 and IFNγ production was analysed. Two-way ANOVA was performed, comparing wild type to μMT mice, with p-values given in the figure. Error bars indicate SEM with 4 mice per group.

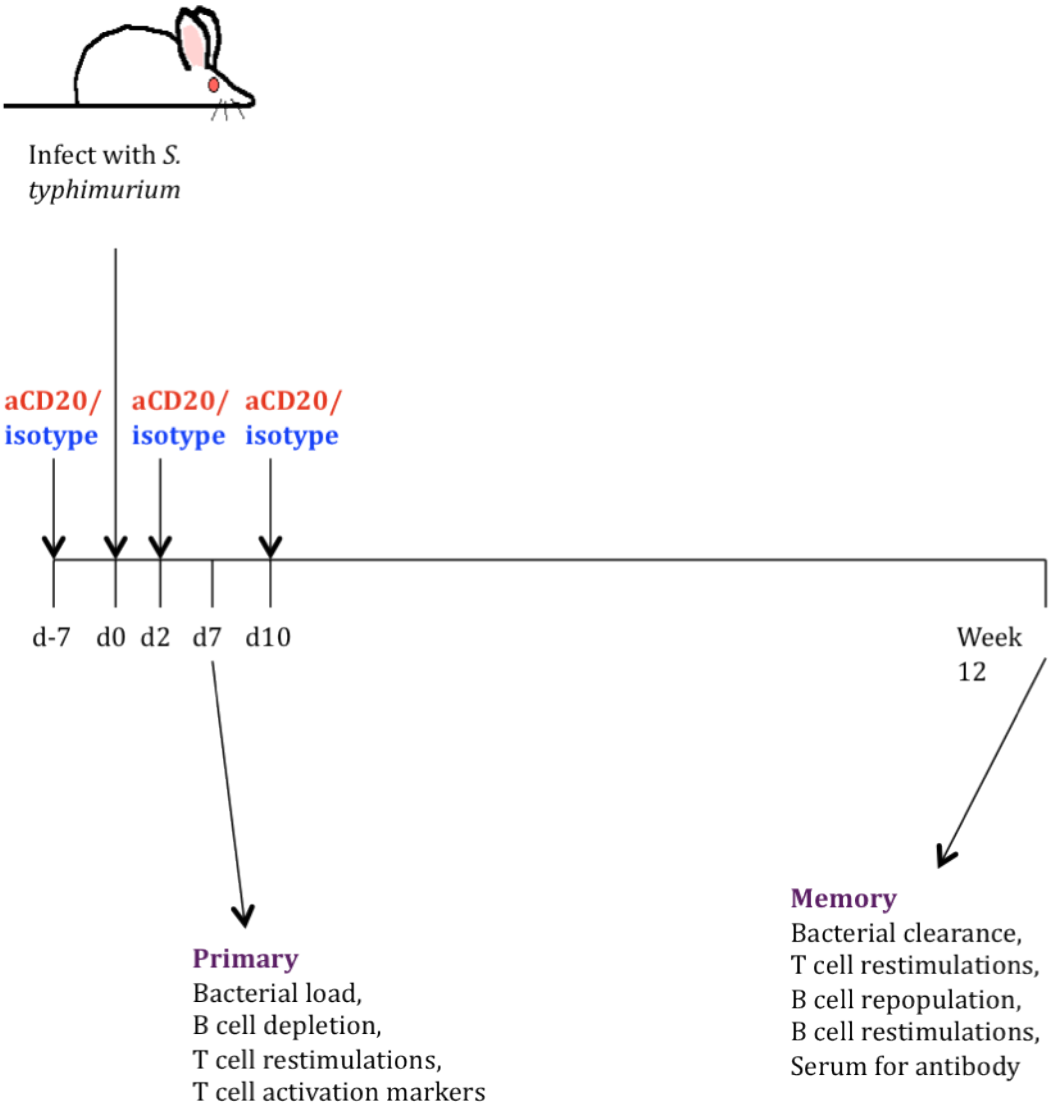

Figure 5.5: Protocol for anti-CD20 depletion and T cell analysis in *S. typhimurium* infection. Mice were infected with *S. typhimurium* on day 0. Three groups of mice each received a single dose of anti-CD20 depletion antibody (or the relevant isotype control antibody) on either day -7, day 2, or day 10 of infection. Mice were taken on either day 7 (primary) or week 12 (memory) for analysis.

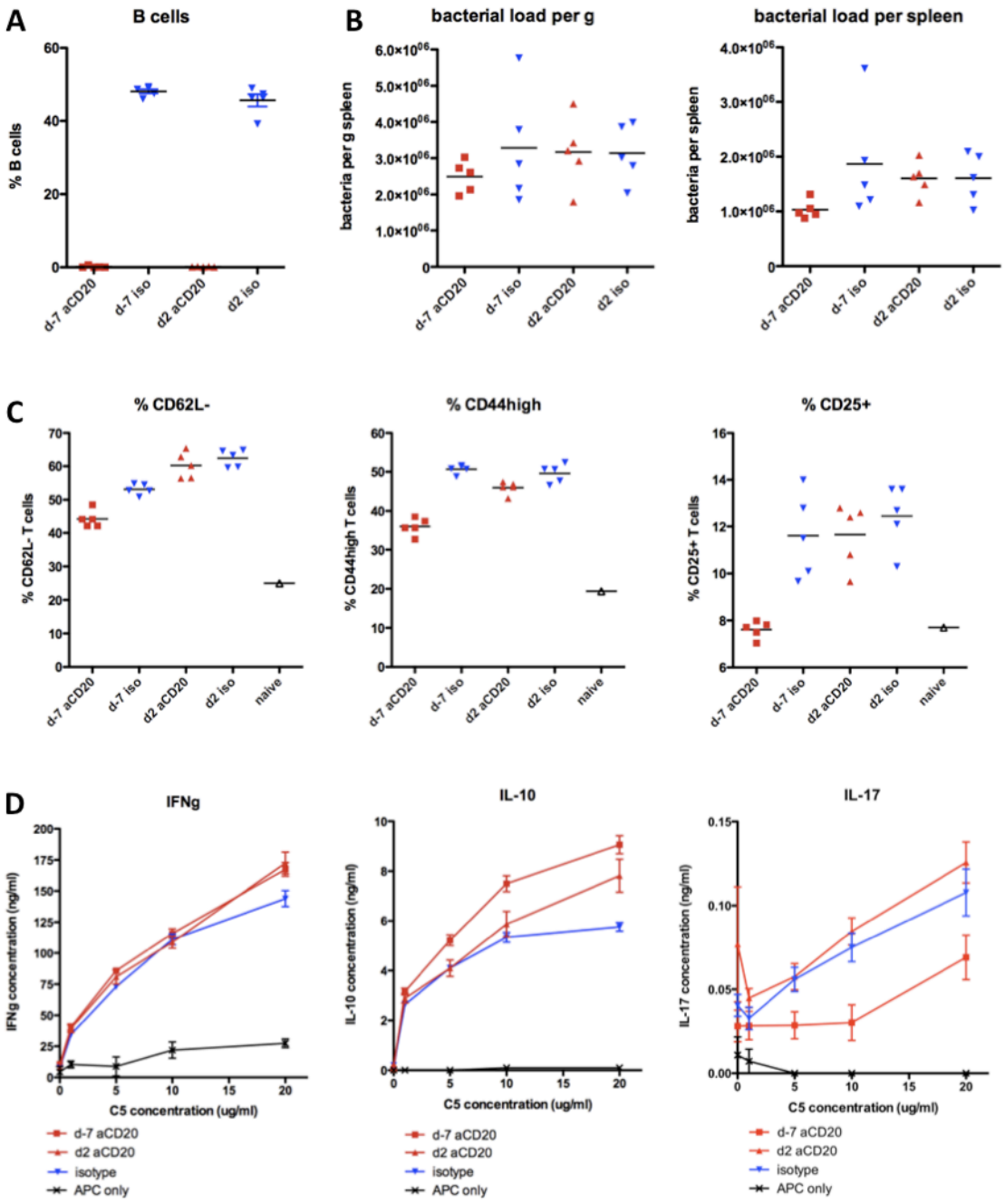

Figure 5.6: B cell-depleted mice show normal primary T cell responses to *S. typhimurium*. C57BL/6 mice were infected with *S. typhimurium* and given a single dose of anti-CD20 or isotype control on either day -7 or on day 2. On day 7 of infection, B cell depletion (A) and bacterial load (B) were analysed. T cells were analysed for the activation markers CD62L, CD44 and CD25 (C). T cell cytokine production following *in vitro* restimulation was assayed (D), where error bars indicate SEM with 5 mice per group. Isotype control treated groups were combined in (D). Data represents 3 independent experiments.

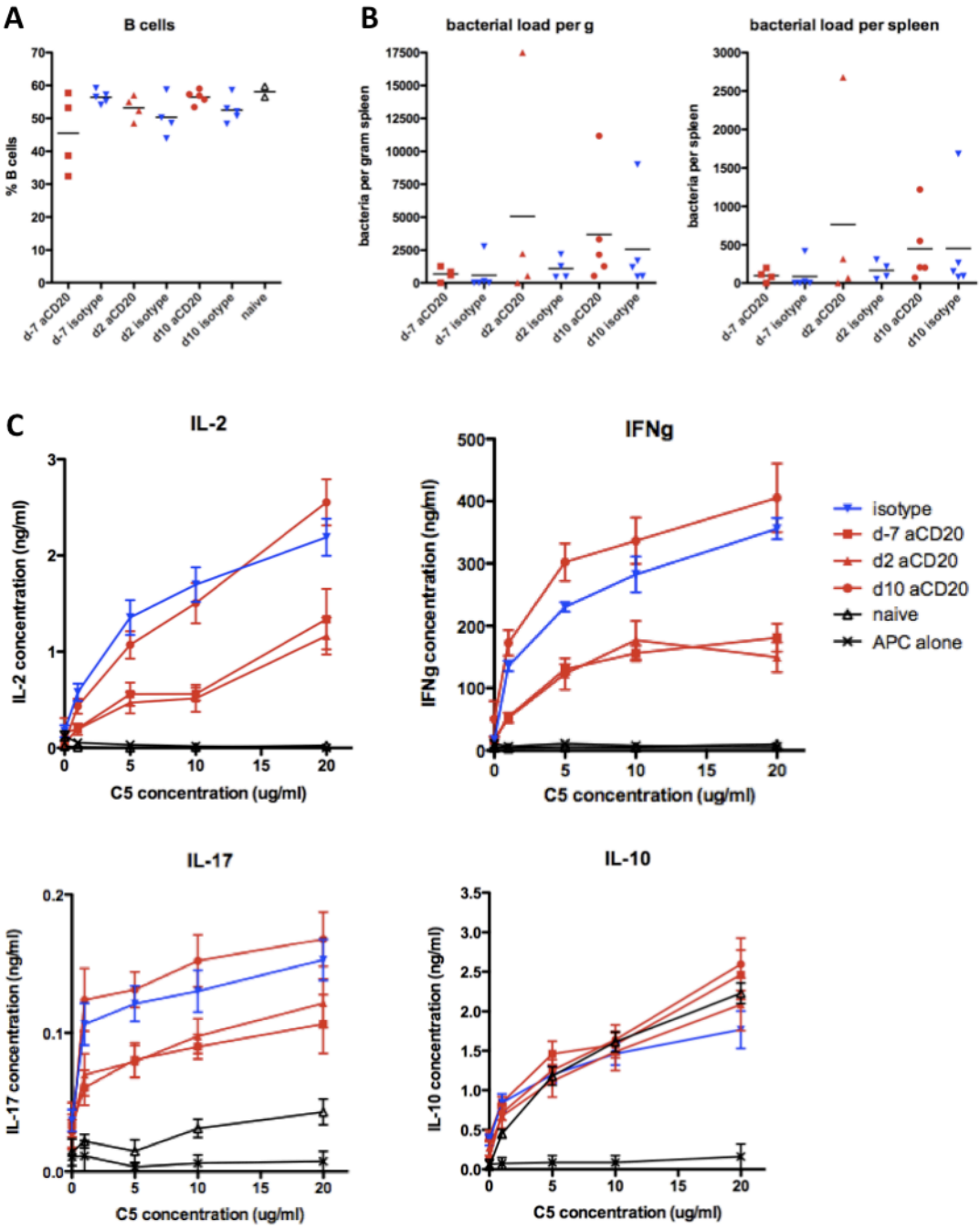

Figure 5.7: Mice depleted of B cells on day -7 or day 2 of infection show impaired memory T cell generation. C57BL/6 mice were infected with *S. typhimurium* and given a single dose of anti-CD20 or isotype control on either day -7, day 2, or day 10 of infection. Twelve weeks post-infection, mice were analysed for B cell repopulation (A) and bacterial load (B). T cell cytokine production was measured following *in vitro* restimulation (C). The three isotype control treated groups were combined in (C). Error bars indicate SEM, with 4-5 mice per group. Data is representative of 3 independent experiments.

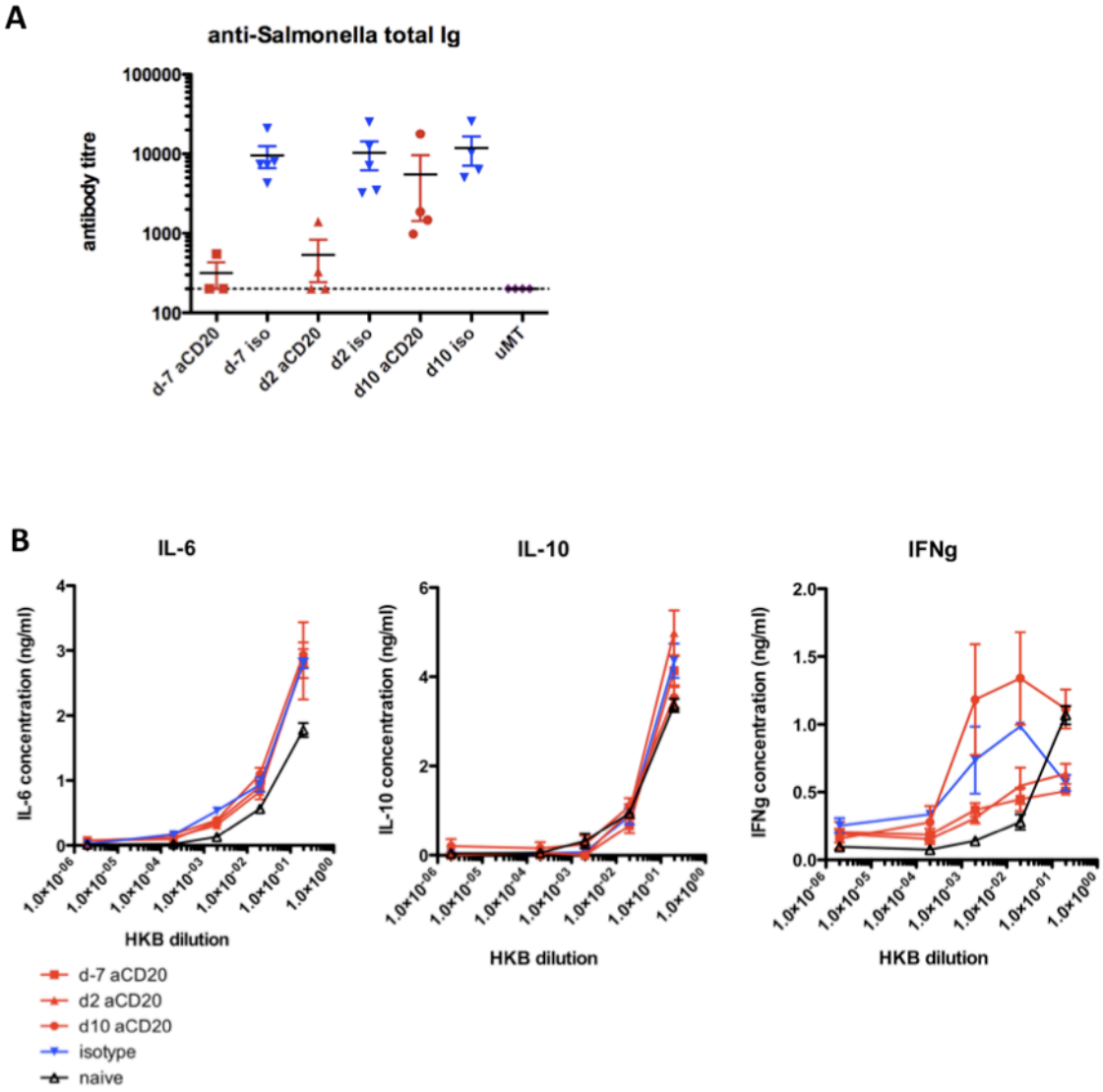

Figure 5.8: Antibody responses are reduced in depleted groups, while B cell cytokine responses after repopulation appear normal. C57BL/6 mice were infected with *S. typhimurium* and given a single dose of anti-CD20 or isotype control on either day -7, day 2, or day 10 of infection. (A) Serum was collected from the mice 12 weeks post-infection, and *Salmonella*-specific antibody titres (total immunoglobulin) measured. Dotted line represents the limit of detection. (B) Twelve weeks post-infection B cells were restimulated *in vitro* with heat-killed *Salmonella* and their cytokine response measured after 5 days of culture. The three isotype control treated groups were combined. Error bars indicate SEM. HKB = heat-killed bacteria.

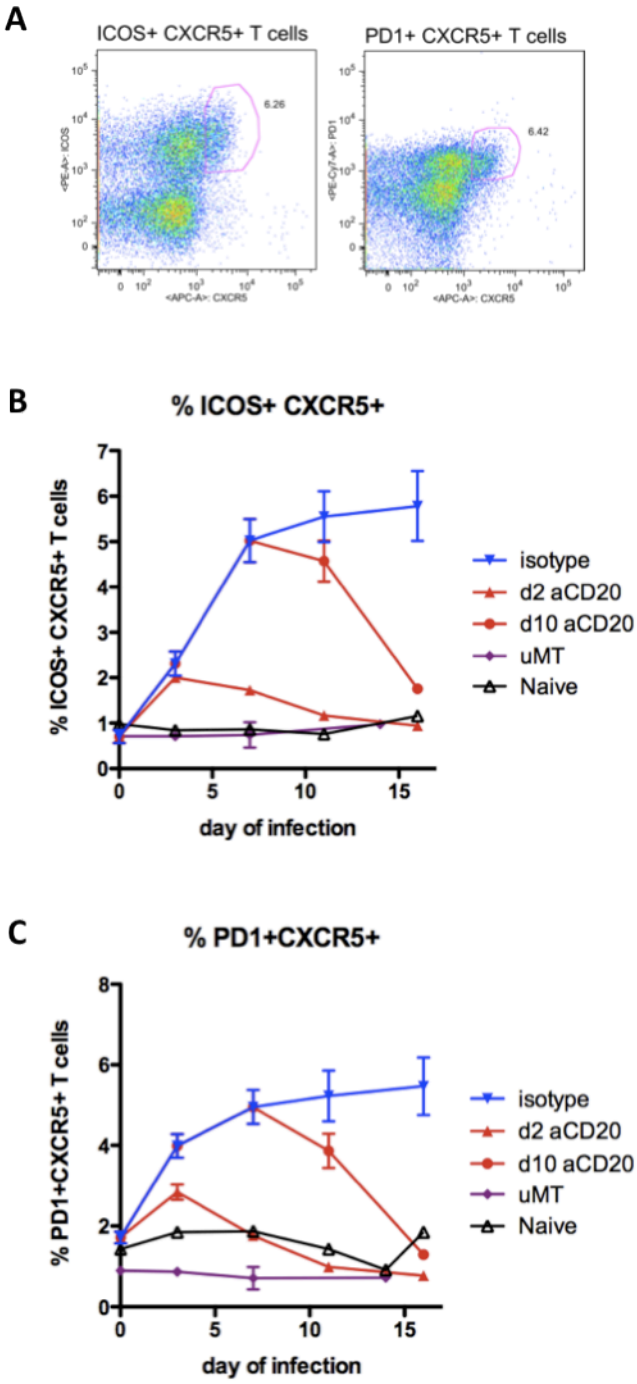

Figure 5.9: B cells are required for T follicular helper cell generation and maintenance. C57BL/6 mice were infected with *S. typhimurium* on day 0. Mice were treated with a single dose of anti-CD20 on either day 2 or day 10 of infection (red), or isotype control on day 2 only (blue). Spleens were removed on days 3, 7, 11 and 16, and T follicular helper cells identified by either ICOS and CXCR5 expression (B) or PD1 and CXCR5 expression (C). Error bars indicate SEM with 3-4 mice per group. Example staining and gating is shown in (A).

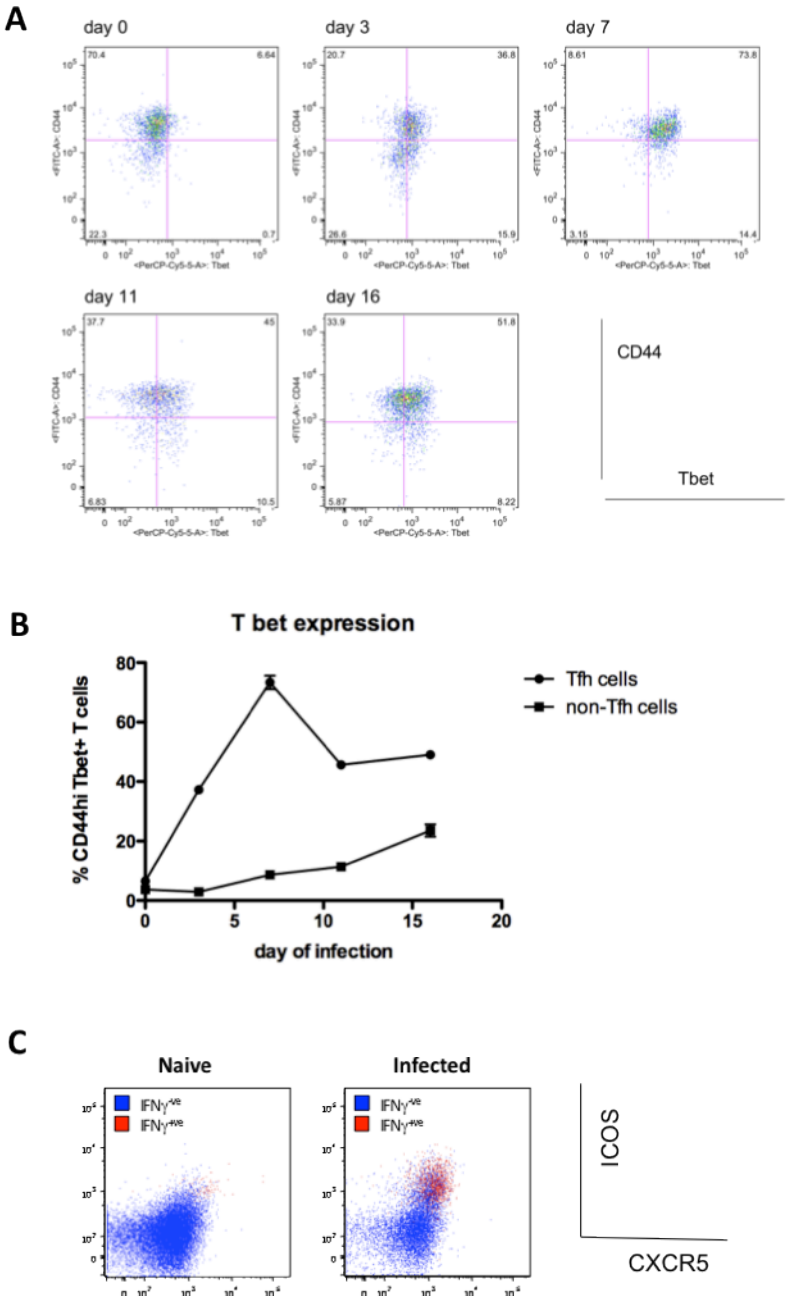

Figure 5.10: A large proportion of T follicular helper cells appear to be Th1 effector cells. (A & B) The T follicular helper cells identified in non-depleted mice as $PD1^{+}CXCR5^{+}$ in figure 5.9C were further analysed for Tbet and CD44 expression. Representative dot-plots from each time-point are shown in (A), with $\%CD44^{hi}Tbet^{+}$ cells shown in (B), for both T follicular and non-T follicular helper cells. Error bars indicate SEM. (C) $IFN\gamma^{+}$ (red) and $IFN\gamma^{-}$ (blue) T cells, identified by intracellular staining in naïve and day 7-infected mice, were further characterised for their expression of the T_{FH} cell markers ICOS and CXCR5. Data in figure (C) is courtesy of Dr Tom Barr.

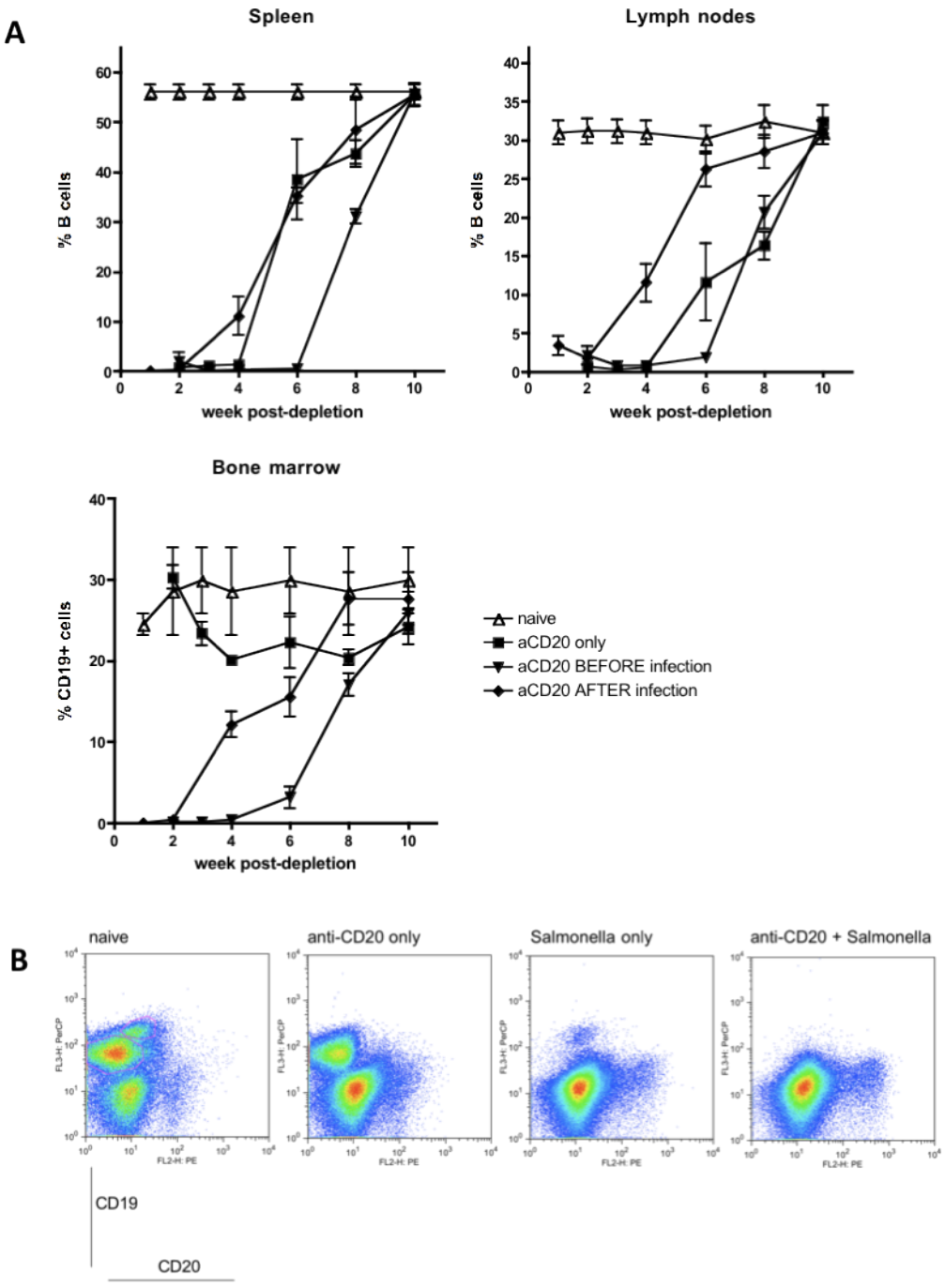

Figure 5.11: B cell repopulation is enhanced when B cells are depleted during established *S. typhimurium* infection. (A) C57BL/6 mice were given a single dose of anti-CD20 on day 0 and either infected with *S. typhimurium* on day-7 (diamond), day 7 (inverted triangle), or left uninfected (square). Spleens, lymph nodes and bone marrow were removed at various time-points after depletion and analysed for presence of B cells. Error bars indicate SEM. (B) Bone marrow was analysed for B cells by staining for CD19 and CD20 on day 7 of *Salmonella* infection, either with or without B cell depletion on day -7.

CHAPTER 6: The role of B cells in the generation of T cell memory - use of MHC class II tetramers

Introduction

The results from the use of anti-CD20-mediated B cell depletion in the *S. typhimurium* infection model revealed a role for B cells as APCs in the initial ~10 days of infection for the efficient generation of T helper cell memory. However, using the *S. typhimurium* infection model for the analysis of T helper cell memory has its limitations, namely that the presence or absence of memory is measured by splenic T cell restimulations with antigen for 3 days of culture, and the subsequent measure of cytokine production. In effect, a single aspect of T cell memory function is being measured, rather than the identification of the memory T cells themselves. In order to more directly quantify the presence of antigen-specific memory T cells, I make use of MHC class II tetramers in a peptide immunisation system.

As mentioned in the main introduction, MHC class II tetramers are a useful tool for identifying antigen-specific T cells directly *ex vivo* following immunisation with the peptide of interest [214]. Tetramers are composed of 4 biotinylated MHC class II molecules with the peptide, in this case the H19env peptide, covalently attached. These complexes are then bound by PE-labelled Streptavidin [323]. An annotated diagram of an MHC class II tetramer is shown in figure 6.1A. The tetramer complex mimics an APC, binding the TCR of antigen-specific cells, and thus these cells show up positive for PE by flow cytometry. One of the major advantages of using MHC class II tetramers to measure T cell responses is that the antigen-specific cells are being directly visualised, rather than being measured by function. In addition, the use of flow cytometry allows the phenotype of tetramer$^+$ T cells to be analysed by other cell markers, for example, to determine their activation status.

The kinetics of T cell expansion and decline following immunisation with the H19env peptide have been characterised by a previous member of the laboratory, Megan MacLeod [215]. Following immunisation with H19env peptide in CFA subcutaneously, for example, the peak of antigen-specific T cell numbers in the spleen and draining lymph nodes is around day 9. Thereafter, T cell numbers decline until a stable memory pool is reached. Such memory cells could be identified in the spleen, albeit in small numbers, up to ~200 days after priming [215]. This method of identifying memory T cells has been used successfully in the

past in MHC class II-B cell chimeras (MHC class $II^{B-/-}$). In these mice, the B cell compartment does not express MHC class II and thus cannot present antigen to $CD4^+$ T cells. Using tetramers, it was found that T helper cell memory was severely reduced in these MHC class $II^{B-/-}$ chimeras following peptide immunisation [142]. Therefore, MHC class II expression by B cells, and thus antigen presentation, is required for the generation of memory T helper cells [142].

Here, I aim to more fully investigate the role of B cells in the development of T helper cell memory using the peptide immunisation system and detecting antigen-specific T cells directly using tetramers. To do this, I use anti-CD20 treatment to deplete B cells on different days before or after immunisation, and analyse the effects on T cell memory development, in a similar way to in the *S. typhimurium* model, in chapter 5. The results presented in chapter 5, above, showed memory to be deficient after B cell depletion on day -7 or day 2 of *S. typhimurium* infection. If the reduction in cytokine production in such groups equates to a reduction in numbers of antigen-specific T cells present, rather than reduced capacity, then here I expect early depletion of B cells to result in reduced numbers of $tetramer^+$ T cells six weeks after peptide immunisation, at the memory time-point. Additionally, the tetramer system allows the antigen-specific T cells generated in B cell-deficient or -depleted mice to be analysed for expression of cell surface markers, such as activation markers, and so I will determine any differences between T cell responses that develop in the presence or absence of B cells.

In addition to further investigating memory generation in B cell-deficient and -depleted mice, I want to characterise the role of TGFβ in regulating T helper cell responses *in vivo*, in order to determine the effects of the lack of TGFβ-mediated regulation on the effector and memory responses. The MHC class II tetramer system is ideal for doing this, as the antigen-specific T cell response can be measured directly. The TGFβ family of cytokines influence a wide variety of cells within the body, including immune cells, regulating cell behaviour. Specifically, TGFβ influences T helper cell subset differentiation, by the induction of $FoxP3^+$ iTreg cells (or Th17 cells when IL-6 is present, or Th9 cells when IL-4 is present) [32]. Recently, a genetically modified strain of mice has been generated, in which all T cells express a mutant form of the TGFβ receptor that is unable to transmit the signal intracellularly (called CD4-dnTGFβRII mice) [43]. Thus, both $CD4^+$ and $CD8^+$ T cells in these mice are unable to respond to TGFβ signalling. The resulting effects on the cytotoxic T effector cell response during infection have been studied in detail. The authors report the

peak of $CD8^+$ T cell numbers at the primary response to be significantly increased in the absence of TGFβ signalling on T cells, followed by a delayed decline of this population [324]. The effector function of these $CD8^+$ effector T cells, however, was unaffected by the lack of TGFβ signalling. The report concludes that TGFβ influence on cytotoxic T cells regulates the contraction phase, by the induction of apoptosis [324]. Therefore, here, I aim to establish whether or not TGFβ mediates the same effects on $CD4^+$ T cells, following immunisation with the H19env peptide. Specifically, does the lack of T helper cell regulation by TGFβ lead to an enhancement in differentiation of short-lived effector cells during the primary response? And is subsequent memory generation impaired? The theory, therefore, is that in the absence of TGFβ-mediated regulation of $CD4^+$ T cells, a greater primary effector response soon after priming may be uncontrolled, resulting in the inability to generate long-lived memory cells.

In summary, I make use of MHC class II tetramers to follow antigen-specific T helper cell responses *in vivo*. By doing so, I more fully explore the requirement of B cells for T helper cell priming and memory development, and investigate the role of TGFβ signalling in T cells in the regulation of the effector response, as well as memory generation.

Results

Identification of antigen-specific T cells using MHC class II tetramers

MHC class II tetramers are a useful method of identifying *in vivo*-generated endogenous antigen-specific T cells, following immunisation with peptide. Example staining and gating of cells, stained with the tetramer, is outlined in figure 6.1B (left to right). Briefly, a live lymphocyte gate was set using forward and side scatter, and then B cells, macrophages and dead cells were removed from analysis by gating out B220-, F4-80- and Propidium Iodide (PI)-positive cells. This excluded all non-T cells that may have bound the tetramer in a non-specific manner, and therefore helped to reduce the number of false-positive readings. After gating on $CD4^+$ T cells, tetramer-positive cells were then viewed, usually against a T cell activation marker such as CD44 (figure 6.1B, left to right). $Tetramer^+$ T cells were consistently found to be in an activated $CD44^+$ state. Typical staining at the primary response generated ~0.3% $tetramer^+$ T cells in the spleen (figure 6.1B, far right, top), while after boosting ~1% of T cells were likely to be $tetramer^+$ (figure 6.1B, far right, bottom). The use of tetramers was, therefore, an efficient method of detecting antigen-specific T cells directly *ex vivo*, and allowed the further characterisation of these cells using other cell surface markers.

Test of different immunisation strategies for the efficient detection of antigen-specific T helper cell responses

Initially, different peptide immunisation strategies were tested in order to generate a visible population of antigen-specific T cells, detected using MHC class II tetramers. The primary and boost time-points were analysed for the presence of tetramer-binding T cells in the spleen and draining (inguinal) lymph nodes. The two immunisation strategies used were as follows: strategy A – priming with peptide in CFA s.c. followed by boosting with peptide in LPS s.c. and i.p., and strategy B – primed with activated peptide-pulsed dendritic cells i.v. and boosted with peptide in CFA s.c. The data presented reveal that, at the primary time-point on day 8, $tetramer^+$ T cells were readily detectable in the spleens of both groups of mice (figure 6.2A, left), suggesting that both immunisations were inducing a splenic T cell response. The group receiving the peptide immunisation in CFA s.c. (strategy A) also showed a strong T cell response in the draining lymph nodes (figure 6.2A, right). However, the group immunised with peptide-pulsed dendritic cells i.v. (strategy B) did not have increased numbers of $tetramer^+$ T cells in the inguinal lymph nodes when compared to background staining in naïve mice (figure 6.2A, bottom). Thus both immunisation strategies

induced a strong primary T cell response in the spleen, with tetramer$^+$ T cells clearly visible. Immunising with peptide emulsified in CFA by the subcutaneous route also induced a strong T cell response in the draining lymph nodes, so for analysing lymph node responses this method has clear advantages over the use of peptide-pulsed dendritic cells.

The data presented in figure 6.2B (left) show that, following boosting at week 6, mice treated with strategy B (boosted with H19env peptide in CFA) had much greater numbers of antigen-specific T cells in the spleen than mice immunised with strategy A (boosted with LPS). Indeed, in the group boosted with LPS, tetramer$^+$ T cell numbers in the spleen were barely above that in naïve mice (figure 6.2B, left). In the inguinal lymph nodes, the numbers of tetramer$^+$ T cells were comparable between the two treatment groups (figure 6.2B, right). Together, these data show that immunisation strategy B (priming with peptide-pulsed dendritic cells, boosting with peptide in CFA) induced a much greater splenic T cell response after boosting than strategy A (priming with peptide in CFA, boosting with LPS).

However, the use of peptide-pulsed dendritic cells for priming in immunisation strategy B has several drawbacks. Firstly, due to immunising i.v. there was no primary draining lymph node response (figure 6.2A, right). Secondly, as I wanted to use this model to analyse the role of B cells as APCs in both the early and late phases of the response, using antigen-loaded dendritic cells may have bypassed antigen presentation by B cells, and thus may be an artificial model. Therefore, for all subsequent immunisations below, I used peptide in CFA as a primary immunisation, and boosted with peptide-pulsed dendritic cells.

B cell-depleted mice show largely normal primary T cell expansion following peptide immunisation

The aim of optimising the peptide immunisation strategy for the generation of strong T cell responses *in vivo,* and the visualisation of such responses directly *ex vivo* using MHC class II tetramers, was to then combine this system with anti-CD20-mediated B cell depletion, and analyse the generation of T cell memory. Thus, I wish to determine whether B cells are required for T helper cell responses in peptide/adjuvant immunisations in the same way as during *S. typhimurium* (see chapter 5). The immunisation and depletion protocol used was similar to that used in chapter 5 above, and is outlined in figure 6.3. Briefly, groups of mice were treated with a single dose of the anti-CD20 depletion antibody on either day -7, day 2, or day 10. The wild type (WT) group received the anti-CD20 isotype control on day 2, and represents the non-depleted group. B cell-deficient μMT mice were also included. All mice

were immunised on day 0 with peptide emulsified in CFA, via the subcutaneous route. Where appropriate, mice were boosted 6 weeks post-immunisation with peptide-pulsed dendritic cells i.v. Spleens and draining (inguinal) lymph nodes were removed on day 9 (primary), week 6 (memory), and 5 days post-boost (boost) to detect antigen-specific T cell numbers using MHC class II tetramers.

On day 9 after immunisation, the percentages and absolute numbers of tetramer$^+$ T cells in the spleen was approximately equivalent across all the groups (figure 6.4A), although there is clearly large variation. Certainly, there were no significant differences between groups. Thus B cell deficiency, by either depletion or in μMT mice, did not result in an impairment in T cell expansion in the spleen during priming. Similarly, in the draining lymph nodes, there were no statistically significant differences between the percentages or numbers of antigen-specific T cells in different experimental groups (figure 6.4B). However, there was a general trend for the numbers of tetramer$^+$ T cells in the draining lymph nodes of μMT mice to be lower compared to in wild type mice (figure 6.4B, purple symbols versus blue symbols), although this did not reach statistical significance. The trend for lower T cell responses in the draining lymph nodes in the absence of B cells was also apparent in B cell-depleted mice (figure 6.4B, red symbols). Therefore, although T cell priming appears normal in the spleen, there may be slight reduction in T cell expansion in the draining lymph nodes in the absence of B cells. Due to a broad distribution of frequency of tetramer$^+$ T cells, larger group sizes would have improved statistical analysis.

Early depletion of B cells impairs memory T cell responses in the draining lymph nodes

Detecting antigen-specific memory T helper cells 6 weeks post-immunisation in immunised versus unimmunised (naïve) mice was possible (see figure 6.12 below). However, due to the variability within groups and the extremely low numbers of tetramer$^+$ T cells, the use of MHC class II tetramers for the detection of significant differences in memory generation between anti-CD20 treatment groups proved unsuccessful (data not shown). Either very large group sizes or a tetramer enrichment protocol [325] would have been required to detect any differences between B cell-depleted and non-depleted groups. Therefore, I decided to boost the response using peptide-pulsed dendritic cells, and analyse T cell numbers on day 5 post-boost as representative of memory. However, one should bear in mind that this boost data also contains cells undergoing a primary response.

The results presented in figure 6.5A reveal that B cell-deficient μMT mice had much higher proportions of tetramer$^+$ T cells in the spleen than wild type mice after boosting (figure 6.5A, left, purple versus blue symbols). However, when absolute numbers were calculated, antigen-specific T cell numbers were equivalent in the wild type and B cell-deficient mice (figure 6.5A, right). Looking at B cell-depleted mice, the group depleted on day -7 showed reduced numbers and percentages of tetramer$^+$ T cells in the spleen, while mice depleted on day 2 or day 10 had normal levels of antigen-specific T cells (figure 6.5A). In the draining lymph nodes, however, mice depleted of B cells on day -7 or day 2, together with μMT mice, all had significantly reduced T cell responses. Meanwhile, mice depleted of B cells on day 10 had normal numbers of tetramer$^+$ T cells in the draining lymph node (figure 6.5B). This reduction in the boost T cell response in the draining lymph nodes of B cell-deficient mice, and mice depleted of B cells on day -7 or day 2, implies an impairment in T cell memory. Interestingly, boost T cell responses in the spleen appeared more normal in the B cell-deficient (and -depleted) mice, suggesting that splenic memory was normal. Together these data imply that, in the absence of B cells, the impairment in T cell memory, in terms of numbers of antigen-specific T cells, is most apparent in the draining lymph nodes but relatively normal in the spleen.

The boost data presented in figure 6.5 were from one experiment out of three. Data from the other two experiments (shown in appendix 1) did not show such significant differences between B cell-deficient and -sufficient groups, although on the whole the general trends remained. Therefore, in order to get a more accurate picture of antigen-specific T helper cell responses in the anti-CD20 treated groups, I pooled the boost data from all three experiments, and analysed it to detect significant differences between groups. To do this, I used a general linear model ANOVA, and Tukey's multiple comparison test. This method of analysis adjusted the data to take into account the variation between experiments. The results from such analysis are presented in table 6.6. The table displays the p-value and summary results from comparing each treatment group to the wild type group. In other words, the wild type group was seen as the positive control, and each other group was compared to it, and it was determined whether or not the treatment group was significantly different to the positive control. Starting with naïve mice, the results show that the boost response in both the spleen and draining lymph nodes of wild type mice was significantly greater than the numbers of tetramer$^+$ T cells in naïve mice (table 6.6). Moreover, the boost response in wild type mice was greater than the primary (wild type or μMT) response, indicating that memory had been generated. Importantly, in B cell-deficient μMT mice,

although the percentage of tetramer$^+$ T cells in the spleen differed to wild type mice, the numbers of antigen-specific T cells in the spleen after boosting was equivalent to in wild type mice (i.e. not significant). However, the T cell response in the lymph nodes of μMT mice was significantly reduced compared to the wild type response, suggesting that T cell memory in the lymph nodes was impaired, but splenic responses were normal. Looking at the effects of B cell depletion on the T cell boost response, anti-CD20 treatment on day 2 or day 10 resulted in normal T cell responses in both the spleen and lymph nodes (table 6.6). However, depletion of B cells on day -7 caused a reduction in the numbers of tetramer$^+$ T cells identified in the lymph nodes post-boost. As in the μMT group, splenic responses in the day -7 treatment group were normal.

In summary, by pooling the data from the 3 experiments, I found that B cell depletion on day -7 resulted in impaired T cell boost responses in the lymph nodes, similar to in B cell-deficient mice. B cell depletion on day 2 or day 10, however, did not result in such an impairment. Again, these data highlight a possible reduction in T cell memory in the lymph nodes in the absence of B cells, whereas responses appeared normal in the spleen. The data highlights an early requirement for B cells in the efficient generation of CD4$^+$ T cell memory.

Mice depleted of B cells on day 2 or day 10 possess unexpectedly high levels of antigen-specific antibody

As mentioned in chapter 5, I was surprised to find that mice depleted of B cells one day prior to immunisation with DNP-KLH mounted antigen-specific antibody responses that were significantly above naïve levels (figure 5.3C). In order to further characterise the antibody response in immunised B cell-depleted mice, serum was collected throughout the time-course of the above B cell depletion peptide immunisation experiment (figures 6.4 & 6.5). The results shown in figure 6.7A indicate that B cell-sufficient wild type mice mounted a strong antibody response against the peptide (blue line), a response which was absent in μMT mice (purple line). Interestingly, antibody levels reached the plateau by day 9 post-immunisation in wild type mice, suggesting a rapid B cell antibody response. Mice treated with anti-CD20 on day -7 only began to produce detectable levels of antigen-specific antibody after boosting, when B cells had repopulated (red squares). The group of mice depleted of B cells on day 2 post-immunisation had equivalent levels of peptide-specific antibody to wild type mice on day 9 (red triangles). Thereafter, serum levels of antigen-specific antibody in the day 2-depleted group dropped more rapidly than in wild type mice,

and indeed levels were significantly lower than in wild type mice. However, the levels of antigen-specific antibody in this day 2 depleted group remained surprisingly high, even at time of boosting. Meanwhile, peptide-specific antibody levels in mice treated with anti-CD20 on day 10 were similar to wild type levels throughout the course of the experiment (red circles). In terms of total anti-H19env antibody, levels in the day 10 treatment group were not significantly different to those in wild type mice (figure 6.7A). In all groups, the majority of this peptide-specific antibody was of the IgG1 isotype (figure 6.7B), suggesting an involvement for T cells. Together, these data show that mice depleted of B cells on day 2 or day 10 mount substantial and long-lived peptide-specific IgG1 antibody responses.

Tetramer$^+$ T cells found in the spleens of B cell-deficient mice are in a highly activated state

The hypothesis was that B cell-deficient mice have impaired T cell memory generation, and therefore I expected these mice to have significantly lower numbers of antigen-specific T cells after boosting. In fact, as can be seen in figure 6.5A above, although responses in the lymph nodes appeared reduced, μMT mice had normal numbers of tetramer$^+$ T cells in the spleen on day 5 post-boost. As I did not expect to find these cells in the spleen, I analysed them further to determine if they were different, in terms of activation marker expression, to those found in wild type mice. Both at the primary and boost responses, the antigen-specific T cells found in μMT mice had significantly elevated levels of CD44 in comparison to those in wild type mice (figure 6.8B, with representative staining shown in figure 6.8A). Furthermore, the tetramer$^+$ T cells isolated from μMT mice expressed lower levels of surface CD62L after both priming and boosting (figure 6.8C). Together, this would suggest that T helper cells from μMT mice are in a highly activated state, a phenotype that is most striking following boosting. Interestingly, the antigen-specific T cells found in B cell-depleted mice also have this more activated phenotype after boosting, in terms of their expression of CD44 (figure 6.8D), although levels expressed by T cells from B cell-depleted mice remained significantly lower than in μMT mice. This highly activated phenotype appeared restricted to activated T cells following immunisation, and was not a characteristic of the total T cell population in naïve μMT mice (figure 6.8E). Therefore, I went on to examine the primary and boost T cell responses in μMT mice further, to determine if the highly activated antigen-specific T cells generated differ from those in wild type mice in other ways, such as function.

Th1 and Th17 cell priming appears normal in the absence of B cells

In order to establish whether or not antigen-specific T cells in μMT mice, with the highly activated phenotype, had the same effector cell capacity as those in wild type mice, I further analysed T cells *ex vivo* at both the primary and boost time-points for their Th1 and Th17 phenotype. To do this, I stained for the transcription factors Tbet (Th1) and Rorγt (Th17), and performed intracellular cytokine staining for the typical Th1-and Th17-associated cytokines, IFNγ and IL-17, respectively. Such analysis will provide insight into the functional ability of effector T cells generated in μMT mice.

Firstly, at the peak of the primary response on day 9 post-immunisation, expression of the Th1 cell transcription factor, Tbet, and the Th17 cell transcription factor, Rorγt, by splenic T cells were equivalent in wild type and μMT mice (figure 6.9A). Furthermore, cytokine production, as determined by intracellular staining for IFNγ and IL-17, was normal in the absence of B cells (figure 6.9B). Although there were trends for lower responses in the μMT mice, these did not reach statistical significance, and therefore we have to conclude that responses were normal. Together, these data support the tetramer$^+$ T cell numbers data, above (figure 6.4), that initial T cell priming following peptide immunisation is not dependent on the presence of B cells. Thus, even though T helper cells generated in the spleen at the primary response on day 9 after immunisation had a highly activated phenotype, in terms of higher CD44 levels and lower expression of CD62L (figure 6.8), they were neither impaired nor hyper-active in their effector cell differentiation, as measured by transcription factor expression, or their cytokine producing ability. Thus, at this early time-point, T cell priming in terms of effector responses appears normal μMT mice.

Splenic Th1 and Th17 responses after boosting are equivalent in wild type and B cell-deficient mice

Although T cell priming is not dependent on antigen presentation by B cells, it has already been established that B cells are required for T cell memory generation. Here, however, I found the numbers of tetramer$^+$ T cells in the spleen after boosting to be normal, suggesting that splenic memory was normal (figure 6.5A, above). These cells differed from those in wild type mice, in that they appeared to have a significantly more activated phenotype, as they expressed higher levels of CD44 and lower levels of CD62L (figures 6.8B & C). I therefore wanted to know if these cells, detectable in large numbers in the spleen after boosting, were capable of cytokine production and effector cell differentiation.

The data presented in figure 6.10A reveal that, after boosting, Tbet and Rorγt expression by splenic T cells was normal in μMT mice. Additionally, production of IFNγ and IL-17 by splenic T cells was also equivalent in the wild type and μMT groups (figure 6.10B). These data suggest that the antigen-specific T cells found in μMT mice after boosting are equally capable of effector cell differentiation and IFNγ and IL-17 secretion, compared to wild type cells, despite their differences in activation marker expression. Additionally, these data imply that splenic T cell memory in these B cell-deficient mice was normal. Interestingly, by gating on the cytokine-positive T cells, it can be seen in figure 6.10C that, again, these antigen-specific T cells expressed higher levels of CD44. In other words, the highly activated T cells found in B cell-deficient mice were functional as cytokine-producing effector cells. The reason for their variation in expression of cell surface activation markers, therefore, remains unknown.

T cell division and effector responses are significantly impaired in the lymph nodes of B cell-deficient mice at the boost response

The MHC class II tetramer staining data presented in figure 6.5B above indicate that, in the absence of B cells, antigen-specific T cell numbers at the boost were significantly lower in the lymph nodes, but normal in the spleen, in this model. To further dissect this difference between splenic and lymph node responses in μMT mice, I used a BrdU incorporation system to investigate the expansion of T helper cells after boosting. To do this, mice were injected with BrdU i.p. for three consecutive days prior to analysis. Spleens and draining (inguinal) lymph nodes were then removed on day 5 post-boost and BrdU uptake measured.

Figure 6.11A shows that T cell division in the spleen of immunised μMT mice was not significantly different from that in immunised wild type mice, although it did appear slightly reduced. In the lymph nodes, however, T cell division was significantly reduced in μMT mice (figure 6.11B). In fact, T cell division in the lymph nodes of immunised μMT mice was lower than that seen in naïve wild type mice, suggesting that constitutive turnover of T cells may be deficient in the μMT lymph nodes, although analysis of a naïve μMT control group would be required to confirm this. Additionally, Th1 and Th17 effector cell responses appeared lower in the lymph nodes of B cell-deficient mice after boosting. This was demonstrated by the reduced numbers of Tbet- and Rorγt-expressing T cells in the draining lymph nodes at this time (figure 6.11C). Together, these data confirm that T cell responses at the boost were reduced in the lymph nodes of B cell-deficient mice, suggesting decreased T cell memory generation at this site.

Antigen-specific memory T cells do not appear to reside in the bone marrow or express Ly6C

In addition to investigating memory T cell generation in μMT mice, I wanted to use MHC class II tetramers to analyse the localisation of such memory T helper cells in wild type mice. A recent report by Tokoyoda *et al* [97] suggested that the main site of localisation of memory $CD4^+$ T cells to be the bone marrow, and that memory cells resting there express the surface marker Ly6C. I therefore analysed the spleen, lymph nodes and bone marrow for the presence of tetramer-binding T cells during the primary response on day 9, 6 weeks later at the memory time-point, and on day 5 post-boost. Due to the extremely low numbers of $CD4^+$ T cells present in the bone marrow (~2%), it was necessary to pool bone marrow from mice within the immunised or naïve groups, and perform $CD4^+$ T cell sorts prior to tetramer staining, in order to enrich the T cell population.

From the data presented, it can be seen that, although a large percentage of T cells in the bone marrow appeared to be antigen-specific at the primary and boost time-points (figure 6.12A), when multiplied up to absolute numbers, this accounted for very few of the total number of $tetramer^+$ T cells (figure 6.12B). Similarly, at the memory analysis, the number of antigen-specific T cells in the bone marrow constituted a very small proportion of the total number of $tetramer^+$ T cells (figure 6.12B). It appeared, instead, that the spleen and (draining) lymph nodes were the major sites of localisation of the antigen-specific T cells 6 weeks after immunisation (figure 6.12B).

Furthermore, the antigen-specific memory T cells identified, either in the bone marrow or the spleen, did not appear to be expressing the memory 'marker' Ly6C (figures 6.12C & D). Instead, ~80% of the $tetramer^+$ cells identified at the memory time-point, either in the spleen or bone marrow, appeared to be Ly6C-negative (figure 6.12D). It should be noted, however, that the numbers of cells identified 6 weeks post-immunisation were small, making it difficult to phenotype these cells accurately. However, I provide evidence, here, contrary to the above-mentioned report, and I would argue that, in this system, antigen-specific T helper cells do not appear to reside in the bone marrow at the memory phase, or express Ly6C. Thus, Ly6C does not, in my opinion, appear to be a marker for memory T helper cells, as has been suggested [97].

T cells from naïve CD4-dnTGFβRII mice appear to be in a more activated state

One of the most striking characteristics of antigen-specific T helper cells isolated from μMT mice following peptide immunisation was that they appeared in a highly activated state, in terms of surface activation markers. Specifically, they expressed greater levels of CD44, and lower levels of CD62L (figure 6.8). One possible explanation for this activated state is that the lack of B cell-derived regulatory cytokines might be resulting in an activated T cell phenotype. One such regulatory cytokine is TGFβ.

As mentioned above, the use of MHC class II tetramers is an ideal method of following antigen-specific T cells following immunisation. Following reports on the influence of TGFβ on regulating effector $CD8^+$ T cell responses [324]; I wanted to use this peptide immunisation system to follow the $CD4^+$ T cell response in CD4-dnTGFβRII mice. These mice express a dominant negative (dn) form of the TGFβRII under the control of the CD4 promoter. This mutant form of the TGFβ receptor possesses a truncated intracellular tail, and therefore cannot transmit TGFβ signalling. T cells in these mice are unable to respond to TGFβ. Using the peptide immunisation system, I aim to determine the role of TGFβ in the regulation of effector $CD4^+$ T cell responses, including effector cell regulation and memory generation, following peptide immunisation.

Initially, naïve CD4-dnTGFβRII T helper cells were analysed for their activation status using a series of cell surface markers. Figure 6.13 shows that T cells from naïve CD4-dnTGFβRII mice had a more activated phenotype than T cells from wild type mice. This was demonstrated by higher expression of CD44 and Ly6C, and lower expression of CD62L (figures 6.13A & B). These mice appeared to have greater numbers of short-lived effector T cells (with a $KLRG1^{hi}$ IL-$7R\alpha^{lo}$ phenotype), as illustrated by the higher expression of KLRG1 and lower expression of IL-7Rα by the total $CD4^+$ T cell population (figure 6.13C). Furthermore, splenic T cell turnover in naïve mice, measured by Ki67 staining, was elevated in T cells that cannot respond to TGFβ (figure 6.13D). Due to the involvement of TGFβ in the differentiation of Treg cells [32], the numbers of $FoxP3^+$ T cells in the spleen were measured, and found to be equivalent in the CD4-dnTGFβRII and wild type mice (figure 6.13E). This suggests that TGFβ is not required for Treg cell generation, confirming a previous report in these mice [52]. Splenocytes were isolated from naïve mice, and stained for intracellular cytokines. The data shows that T cells from the CD4-dnTGFβRII mice had

much greater production of IFNγ than T cells from naïve wild type mice (figure 6.13F), suggesting higher levels of Th1 cell priming.

CD4-dnTGFβRII mice show enhanced priming in the lymph nodes, and a biased Th1 response in the spleen

The $CD8^+$ T effector cell response has been shown to be elevated in the CD4-dnTGFβRII mice at the peak of the primary response [324]. In this study, I immunised both wild type and CD4-dnTGFβRII mice with peptide in CFA, and measured antigen-specific T cell numbers in the spleen and draining lymph nodes at the peak of the primary T cell response, on day 9. The results shown in figure 6.14A indicate that antigen-specific T cells in the spleen were reduced in CD4-dnTGFβRII mice, while numbers in the draining lymph nodes were elevated. This shows that, in the absence of TGFβ signalling in T cells, expansion of T cells within the draining lymph nodes was enhanced, whereas the T cell response in the spleen was reduced. T cells from the spleen had a significant Th1 bias, producing more IFNγ than wild type cells, but not producing IL-17 (figure 6.14B). Therefore, during the primary response, the T cells in the spleen of the CD4-dnTGFβRII mice appeared to not only be having a reduced response in terms of $tetramer^+$ T cell numbers, but were also making a different type of effector response. Meanwhile, similar to in $CD8^+$ T cells [324], effector T cell numbers were elevated at the site of priming, in this case in the draining lymph nodes.

CD4-dnTGFβRII mice may possess more antigen-specific T cells in the spleen six weeks after immunisation, and continue to display a biased Th1 phenotype

Six weeks after immunisation, the numbers of $tetramer^+$ T cells in the spleen and draining lymph nodes were measured. As can be seen in figure 6.15A, the CD4-dnTGFβRII mice appeared to have increased numbers of antigen-specific T cells in the spleen at this late time-point, although the small group sizes make statistical analysis difficult. In the draining lymph nodes, however, there was no significant difference between the numbers of $tetramer^+$ T cells in the wild type and CD4-dnTGFβRII mice (figure 6.15A, bottom). These data highlight the elevated numbers of antigen-specific T cells in the spleen, but does not indicate whether they are true memory cells, or a runaway effector response. Again, similar to at the primary response, in the absence of TGFβ signalling, splenic T cells mounted a strong Th1 response characterised by IFNγ secretion, but did not produce IL-17 (figure 6.15B). This Th1 bias was not restricted to immunised mice, but the naïve CD4-dnTGFβRII mouse also displayed excessive IFNγ production (figure 6.15B), suggesting that it is not an antigen-specific response.

In the absence of TGFβ signalling in T cells the boost response, and therefore memory T helper cell generation, appears normal

Although antigen-specific T helper cells were present in the spleen in large numbers six weeks post-immunisation in the CD4-dnTGFβRII mice, it was not known whether T helper cell memory had been generated. To investigate the generation of memory in these mice, they were boosted with peptide-pulsed dendritic cells 6 weeks after priming, and the numbers of antigen-specific T cells analysed 5 days after boosting. The data presented in figure 6.16A demonstrate that the boost T helper cell response was normal in both the spleen and draining lymph nodes of the CD4-dnTGFβRII mice, indicating that memory T cell generation was not impaired in the absence of TGFβ signalling in T cells. In a similar manner to the primary and memory responses, splenic T cells from these mice exhibited a strong Th1 bias, with greater IFNγ production and an absence of IL-17 secretion (figure 6.16B). This IFNγ production was not antigen-specific, as naïve CD4-dnTGFβRII T cells produced comparable amounts (figure 6.16B). Together, these data suggest T cell memory generation and boost responses to be normal in absence of TGFβ signalling in T cells, indicating that TGFβ-mediated regulation of the $CD4^+$ T cell population is not necessary for these aspects of T cell function.

CD4-dnTGFβRII mice show impaired switched antibody responses, but increased production of IgM

Due to the excessive T cell activation and IFNγ production in the CD4-dnTGFβRII mice, I was intrigued as to the effects this would have on B cell antibody production. Th1 responses tend to promote IgG2a/c production by B cells (in an antigen-specific manner), and thus I expected the unregulated IFNγ production in the CD4-dnTGFβRII mice to induce a strong IgG2c response. The data shown in figure 6.17A, however, indicate that this is not the case. In fact, when TGFβ signalling was lacking on T cells, peptide-specific antibody responses were decreased (figure 6.17A, total Ig). Specifically, class switched antibody was impaired in these mice, as both IgG1 and IgG2b were reduced (figure 6.17A, IgG1 & IgG2b). Notably, IgG2c and IgG3 levels were at the limit of detection (data not shown). IgM responses, on the other hand, although reduced at the primary response on day 9, were elevated by the memory and boost time-points (figure 6.17A, IgM). Looking at IgM production on day 5 post-boost in more detail, the elevated IgM phenotype was not restricted to immunised CD4-dnTGFβRII mice, but naïve CD4-dnTGFβRII mice also had high levels of serum IgM capable of binding the H19env peptide (figure 6.17B). In summary, antigen-

specific class-switched antibody responses, namely IgG1 and IgG2b, were impaired when T cells were unable to respond to TGFβ. Conversely, IgM production was enhanced in these mice by 6-7 weeks after immunisation. The observation that naïve CD4-dnTGFβRII mice also had increased serum IgM by the later stages of the experiment suggests that the resulting IgM is simply cross-reactive, and not related to the peptide immunisation.

Together, the work using MHC class II tetramers to follow antigen specific T helper cells responses in CD4-dnTGFβRII mice revealed priming in the lymph nodes to be enhanced, whilst memory generation, and expansion after boosting, was normal. Furthermore, T cells in these mice were in a more activated state in terms of cell surface markers, and were predisposed to IFNγ production. Class-switched antibody production, meanwhile, was reduced, but cross-reactive IgM was elevated. These data highlight the involvement of TGFβ signalling in T cells on the modulation of Th1 responses in both naïve and immunised mice, and reveals the knock-on effect on B cell antibody production.

Discussion

The use of MHC class II tetramers for the analysis of antigen-specific T helper cell responses

MHC class II tetramers allow the direct analysis of *in vivo*-generated endogenous antigen-specific T cells. The main advantage of this system is that such antigen-specific T cells can be visualised directly by flow cytometry, and therefore phenotyped for other surface markers, such as the activation markers used here. However, the data presented in this chapter highlight the drawbacks of tetramers. Firstly, the presence of tetramer$^+$ T cells indicates only that T cells of that particular specificity exist, but does not provide information on their functional ability. Therefore, without further analysis, it is impossible to determine if tetramer$^+$ T cells are functional, cytokine-producing effector cells. Instead, they may be Treg cells, anergic tolerised cells, or cells in an inactive state. Unfortunately, due to the low success rate of *in vitro* restimulation cultures with the H19env peptide antigen (data not shown), measuring cytokine production by these antigen-specific T cells to determine their T helper cell subset phenotype proved difficult. Instead, I used two methods of determining the T helper cell phenotype in this system: transcription factor staining and intracellular cytokine staining. As the intracellular cytokine and transcription factor staining protocol was not combined with tetramer staining, and the intracellular cytokine staining utilised PMA restimulation (which results in TCR downregulation and is therefore not compatible with tetramer staining), the effector phenotype of the antigen-specific T cells was not directly measured. Therefore, the transcription factor and intracellular cytokine data presented reflects the total T helper cell phenotype. It is hoped that, as these analyses focus on activated CD44^{hi} cells, this will be representative of the antigen-specific T helper cell response, but short of using a cytokine-capture assay or sorting the tetramer$^+$ T cells for culture, this will be difficult to confirm.

A second drawback of the use of tetramers is the limit of detection. At 6 weeks post-immunisation, for example, tetramer staining was consistently higher in immunised mice compared to naïve mice (figure 6.12), so memory cells could be detected. However, detecting significant differences between experimental groups, such as the B cell depletion groups, was problematic due to the large variability within groups. To overcome this, very large group sizes would have been required, which was not feasible. Alternatively, a tetramer enrichment protocol, such as that used by Marc Jenkins [325], could have been used to visualise the small numbers of tetramer$^+$ T cells. Therefore, for all experiments I used

boost responses as a measure of memory, rather than detecting memory cells themselves. It should be noted, however, that this boost response will contain cells undergoing primary activation.

Ideally, I would want to combine the *S. typhimurium* infection model with the use of MHC class II tetramers, in order to reap the benefits from both systems. Thus, a strain of *S. typhimurium* expressing the H19env peptide (or another peptide that has corresponding tetramers available) would allow both the detection of antigen-specific T cells by flow cytometry, and the antigen-specific restimulation cultures to determine their subset phenotype. The development of a bacterial strain expressing a particular peptide is an ongoing topic of interest in our laboratory. In an attempt to overcome these issues, here, I measured the numbers of tetramer$^+$ T cells, together with transcription factor expression and intracellular cytokine staining by the total T helper cell population, and assumed that the whole population phenotype accurately reflected that of the antigen-specific cells.

Peptide immunisation strategy

Following a trial experiment to optimise the immunisation strategy for creating a clear population of tetramer$^+$ T cells (figure 6.2), in all subsequent experiments, mice were primed with the H19env peptide in CFA subcutaneously, and boosted with peptide-pulsed dendritic cells intravenously. Although some data suggests the injection of dendritic cells i.v. to led to tolerance rather than immunity [326], I did not find this. Instead, boosting with antigen-loaded dendritic cells i.v. resulted in the expansion of antigen-specific T cells, and the generation of a population that was significantly higher than in a primary immune response (figure 6.5, blue inverted triangle wild type response versus open diamond primary response). Furthermore, the injection of dendritic cells i.v. led to an increase in antigen-specific T cell numbers in the inguinal lymph nodes – the draining site of the primary immune response. This was surprising, as systemic cells do not have direct access to the lymph nodes like they do the spleen, and dendritic cell entry to the lymph nodes was thought to occur through the lymphatic system, rather than across high endothelial venules [327]. Thus, it remains unknown how systemic fully matured and activated dendritic cells would access the lymph nodes to drive T cell expansion at this site. As cells had been extensively washed before transfer, the injection of free antigen that could be picked up by local APCs seems unlikely.

Memory T helper cell characteristics

Having optimised the peptide immunisation system for memory T helper cell detection, the localisation of these memory cells was a topic of interest. As mentioned above, published data indicates that memory $CD4^+$ T cells are located preferentially in the bone marrow in mice, and express the cell surface marker, Ly6C [97]. In figure 6.12, however, I provide evidence that contradicts this published report. I found the memory cells located in the bone marrow to constitute a very small proportion of total antigen-specific memory T cells. Instead, the spleen and (draining) lymph nodes were the major sites of memory cell localisation (figure 6.12B). Furthermore, the memory cells located in both the spleen and bone marrow 6 weeks after priming did not express Ly6C, but instead were, for the most part, Ly6C-negative (figures 6.12C & D). It should be noted, however, that the memory cells detected were few in number, and required pooling from separate mice and enriching on a CD4 column, so it was difficult to show conclusively that the $tetramer^+$ T cells were not expressing Ly6C. The differences between my own data and the earlier report may be due to the system used. Tokoyoda and colleagues used two methods of memory cell detection: firstly a transgenic T cell transfer system and detection by Thy1 expression, and secondly, a protein antigen in CFA immunisation and detection of antigen-specific T cells by *in vitro* restimulation with antigen [97]. Here, by directly visualising antigen-specific memory T cells *ex vivo* following the immunisation of wild type mice, my tetramer system has distinct advantages over the use of transgenic cell transfers and restimulation assays for memory cell detection, and thus I believe my results on this matter to be more valid.

As the spleen and (draining) lymph nodes, rather than the bone marrow, were found to be the major sites of antigen-specific memory T cell localisation (figure 6.12B), I focussed on these sites for all other analysis of T cell memory. Due to the extremely small numbers of $tetramer^+$ T cells located in the bone marrow, I doubt I missed any significant populations of antigen-specific T cells by not analysing the bone marrow in the B cell depletion experiments.

T cell priming is not dependent on B cells

I have previously given evidence from the *S. typhimurium* infection model (figure 5.6) supporting published findings [145,146] that the initial priming of $CD4^+$ T cells was normal in B cell-deficient (and -depleted) mice, and thus B cells are dispensable for the primary T cell response. Here, I provided further data on this topic, and showed the numbers of antigen-specific T cells in both the spleen and draining lymph nodes to be normal in B cell-

deficient and -depleted mice (figure 6.4). Furthermore, the differentiation of Th1 and Th17 effector cells, expressing Tbet and Rorγt, respectively, was equivalent in B cell-deficient and -sufficient mice after priming (figure 6.9A). The numbers of IFNγ- and IL-17-producing cells, too, was normal in μMT mice during the primary response (figure 6.9B). Together, these data provide strong evidence, contradictory to some previous reports [142,143,144], that B cells are not required for $CD4^+$ T cell priming in this peptide immunisation system.

T cell memory generation in B cell-deficient mice

Previously, in the *S. typhimurium* infection model I showed T cell memory to be significantly impaired in B cell-deficient mice (figure 5.4). Here, by detecting antigen-specific T cells using tetramers, I found μMT mice to have normal numbers of antigen-specific T cells in the spleen after boosting, but significantly lower numbers in the lymph nodes (figure 6.5, table 6.6 & appendix 1). These data suggest that splenic memory in this system is normal in the absence of B cells, but memory in the lymph nodes shows a dependence on B cells. Furthermore, splenic T cell division, expression of Tbet and Rorγt, and production of IFNγ and IL-17 was normal in μMT mice after boosting (figures 6.10A, 6.10B & 6.11A). In the lymph nodes, however, T cell proliferation, as well as numbers of $Tbet^+$ and $Ror\gamma t^+$ T cells, was significantly reduced in B cell-deficient mice (figures 6.11B & C). Thus, I have provided strong evidence to suggest that, in this peptide immunisation system, T cell memory generation in the (draining) lymph nodes was significantly disrupted in the absence of B cells, while splenic memory developed normally. While the simplest explanation for the defect in lymph node memory is that B cells have been shown to be important APCs for driving T cell responses in this site [138], the alternative possibilities are discussed in greater detail below.

T cell memory generation in B cell-depleted mice

In the *S. typhimurium* infection model, I identified a requirement for B cells during the first ~10 days of infection for the development of T helper cell memory. Specifically, the depletion of B cells on day -7 or day 2 resulted in significantly impaired memory, whereas with depletion on day 10, memory generation was normal (figure 5.7). Meanwhile B cell-deficient μMT mice had a severe reduction in T cell memory (figure 5.4). Here, using the peptide immunisation system, μMT mice consistently had reduced T cell responses in the lymph nodes after boosting (figure 6.5, table 6.6 & appendix 1). However, the effects of anti-CD20-mediated B cell depletion on T cell memory development in this peptide immunisation system gave variable results. In one experiment (of three), the lymph node T

cell boost response was significantly impaired in the day -7 and day 2 treatment groups, and normal in the day 10 anti-CD20 treated group (figure 6.5). These data, therefore, gave similar results to in the *S. typhimurium* infection model, and pointed to a role of B cells in the first ~10 days of the immune response for T cell memory generation. However, in the other 2 repeats of this experiment (shown in appendix 1), there were no significant differences between the depleted and non-depleted groups. In these 2 experiments, the percentages of tetramer$^+$ T cells in the lymph nodes after boosting were lower than seen in the first experiment. While in experiment 1 around 0.5% of lymph node T cells bound the tetramer, in experiments 2 and 3, this figure was only ~0.3% (compare blue inverted triangles in figure 6.5B to appendix 1). Therefore, it appears that the immune response against the peptide was lower in experiments 2 and 3, making the detection of significant differences between groups more difficult, due to the low percentages of tetramer$^+$ T cells.

By pooling the results from all 3 experiments, the lymph node T helper cell response in the μMT group remained significantly reduced when compared to the wild type group (table 6.6). However, of the B cell-depleted groups, only anti-CD20 treatment on day -7 resulted in diminished T cell boost responses in the lymph node compared to the non-depleted group, whereas with treatment on day 2 or day 10 T cell boost responses were normal (table 6.6). As this pooled data analysis of the results from all 3 experiments is the most accurate interpretation of responses in B cell-depleted mice, this result is most valid. It therefore contrasts to results from the *S. typhimurium* model, where the day 2 treated group had impaired memory (figure 5.7). The simplest explanation for the presence or absence of memory in this day 2 treated group is that the kinetics of the immune response in the two models vary substantially. While *S. typhimurium* is an infection that takes around 4-6 weeks to clear, the immune response to peptide antigen is likely to be short-lived. Thus, the kinetics of both the T helper cell and B cell responses are likely to differ vastly between these two systems. For example, looking at the B cell response, while in *Salmonella* infection the class switched antibody response is slow to arise, reaching its peak around 4-5 weeks of infection (see figure 3.15), in the peptide immunisation model class switched antibody levels were high by day 9 (figure 6.7). These differences in the timing of antibody appearance reflect differences in the B cell response. Therefore, it may be that the kinetics of the B cell response dictate the timing of their involvement in T cell memory generation.

Splenic versus lymph node memory

The finding that splenic T cell memory appeared normal in μMT mice following peptide immunisation (figure 6.5A) contrasts to that from the *S. typhimurium* infection model, where splenic T cell memory was absolutely dependent on B cells (figure 5.4). One explanation, which may account for the differences between models, is that the antigens and route of administration differed vastly. On the one hand, *Salmonella* bacteria are a complex pathogen consisting of many available antigens, which result in a systemic infection and colonisation of the spleen. As seen in chapter 4, the spleen is the major site of the immune response, and becomes severely disrupted during this infection. In the peptide immunisation system, on the other hand, the much simpler peptide antigen was administered s.c. together with an adjuvant, making the draining lymph nodes the primary site of immune activation. Therefore, it appears that the lymphoid organ in which initial priming occurred was the one in which T cell memory showed a dependence on B cells.

It may be interesting to alter the method of peptide immunisation, by varying the route. Perhaps the reason for the differences in splenic versus lymph node T cell memory in the tetramer system is due to the peptide immunisation strategy used. As mentioned above, splenic memory was impaired following systemic *S. typhimurium* infection in μMT mice, whereas this was not the case following antigen in CFA s.c. immunisation. Notably, in addition to initially priming the draining lymph nodes, administration of CFA s.c. results in an antigen depot, which may result in chronic T cell stimulation in this region [328]. Perhaps, if the peptide antigen became rapidly systemic, with the spleen, rather than the lymph nodes, as the major site of priming, the effects on splenic T cell memory generation may differ. Additionally, the B cell response to protein versus peptide antigen is known to differ, and B cells have been shown to preferentially present protein rather than peptide antigen [147,148]. Thus, the use of a protein antigen, in addition to being more physiological, may alter B cell antigen presentation and impact upon the development of a memory T cell population. Furthermore, tetramers could be used, here, to detect memory generation after priming with peptide-pulsed dendritic cells in μMT mice. It would be intriguing to determine the effects of B cell deficiency on memory generation after this type of immunisation. Clearly T cell memory was generated following priming with peptide-pulsed dendritic cells (figure 6.2B), but it would be interesting to determine if this memory was dependent on the presence of B cells, as B cell antigen presentation is likely to be minimal.

A further alternative, which may explain the impairment in lymph node but not splenic memory in this system, is that the reduction in T cell responses in the lymph nodes may be due to an innate defect in lymph node architecture or function, as a result of their development without B cells being present. However, the fact that lymph node boost responses were also reduced in B cell-depleted mice (figure 6.5), which developed normally in a B cell-sufficient host and possess B cells at the time of boosting due to B cell repopulation, this seems an unlikely explanation.

Antigen-specific splenic T cells generated in μMT mice appear highly activated, in terms of surface marker expression, but function normally

As mentioned above, the numbers of antigen-specific T cells found in the spleen of μMT mice after boosting were equivalent to those in wild type mice. However, such T cells differed in phenotype from those generated in wild type mice in that they appeared to be in a more activated state. Specifically, expression of CD44 was significantly higher on μMT tetramer$^+$ T cells, while expression of CD62L was lower (figure 6.8). This was also the case at the primary response, although to a lesser extent (figures 6.8B & C). However, despite this activated phenotype of antigen-specific splenic T cells, their expression of Tbet and Rorγt, as well as their production of IFNγ and IL-17, was normal at both the primary (figure 6.9) and boost (figure 6.10) responses. Thus, although the antigen-specific T cells generated in μMT mice differed in surface marker phenotype from those in wild type mice, they did not appear to differ in terms of Th1/Th17 effector cell generation or cytokine-producing capacity. This leaves us with the question as to why antigen-specific T cells in μMT mice expressed higher levels of CD44 and lower levels of CD62L.

The adhesion molecule CD44 has been implicated in the regulation of survival of antigen-activated T helper cells of the Th1 phenotype into the memory phase [329]. The authors report that signalling through CD44 on Th1 effector cells regulates cell death by both limiting Fas-mediated apoptosis and promoting cell survival pathways [329]. In μMT mice, here, the Th1 effector cells may have upregulated expression of CD44 in an attempt to overcome the lack of the B cell-mediated signal required for memory development. However, this is purely speculative, and I can provide no evidence to support this theory. Indeed, this may not be correct, as the phenotype of increased CD44 expression seemed to not be restricted to Th1 cells, but IL-17-producing effector Th17 cells also had higher levels of surface CD44 (figure 6.10C). Therefore, the reason for the increased expression of CD44, and reduced expression of CD62L, on tetramer$^+$ T cells found in B cell-deficient mice

remains unknown. A further possible explanation is that the lack of B cell-derived TGFβ in regulating T cell function may result in this activated phenotype, a concept that is discussed more fully later. Interestingly, the increased expression of CD44 on tetramer$^+$ T cells was also apparent, to a lesser extent, on T cells from B cell-depleted mice (figure 6.8D), indicating that this phenomenon is not due to innate deficiencies in T cells generated in μMT mice.

Peptide-specific antibody responses in B cell-depleted mice

Despite the early depletion of B cells, the day 2 anti-CD20 treated group mounted unexpectedly large antigen-specific antibody responses, of the IgG1 isotype, following peptide immunisation (figure 6.7). The development of antigen-specific antibody responses in mice depleted of B cells soon after (or before) immunisation was also seen after DNP-KLH immunisation (figure 5.3C). However, such antigen-specific antibody was not seen in the day 2 depleted group following *S. typhimurium* infection (figure 5.8A).

The explanations for the presence of antigen-specific class switched antibody in B cell-depleted mice were discussed in chapter 5 above. To expand that discussion further, it appears that the production of antigen-specific class switched antibody was limited to peptide or protein immunisation and, in both cases, was predominantly of the IgG1 isotype. The time-course of antibody levels after peptide immunisation showed maximum serum IgG1 levels to be reached by day 9 post-immunisation in day 2-depleted, day 10-depleted, and non-depleted groups (figure 6.7B). As B cells take ~3-5 days to be efficiently depleted, they will have reached baseline levels in the day 2-depleted group around 7 days after immunisation. This presence of B cells for the initial 7 days appears enough for IgG1 antibody levels to reach high levels (figure 6.7B).

These data highlight two interesting points: Firstly, the production of such large amounts of antigen-specific IgG1 in the initial ~7 days after immunisation raises the issue of T cell dependence. T cell-independent IgG has been reported in a viral infection model [318], indicating that the IgG1 found here may occur in either a T cell-dependent or -independent manner. T cell ablation would help in clarifying the requirement for T cells. The second point raised by these data is that, at time of boosting 6 weeks post-immunisation, peptide-specific IgG1 levels remained surprisingly high in the day 2-depleted group, although they did appear to decay more rapidly than in B cell-sufficient mice (figure 6.7). If IgG1-secreting plasma cells had been generated in the initial ~7 days, these cells would have

resisted depletion. However, as early extrafollicular plasma cells are thought to only have a lifespan of 3-5 days [330], the longevity of the antibody seen here suggests the generation of long-lived plasma cells. This raises the intriguing possibility of the early generation of long-lived plasma cells that resist depletion by anti-CD20. However, as long-lived plasma cells are thought to differentiate after the GC reaction [330], this would suggest the GC reaction to have occurred by day 9 post-immunisation (when antibody levels reached the plateau), which seems unlikely. The analysis of the affinity of such IgG1 antibody, indicating affinity maturation, together with the timing of the GC reaction in this particular immunisation strategy, would help to clarify if the antibody was generated pre- or post-GC.

Interestingly, recent data studying long-lived plasma cells following anti-CD20 treatment concludes that, during periods of B cell depletion when memory B cells are absent, long-lived plasma cell numbers, together with serum antibody levels, remain constant, indicating that long-lived plasma cells are inherently long-lived and do not require the memory pool for replenishment [330]. Therefore, if long-lived plasma cells had been generated by day 9, they would have maintained serum antibody levels for the course of this experiment. However, the possibility of long-lived plasma cell generation by day 9 post-immunisation is a topic which requires further investigation. If true, this phenomenon has broader implications in both the vaccine field, and in the use of anti-CD20 in humans.

The role of TGFβ in regulating $CD4^+$ T cells in naïve mice

One striking observation from the $tetramer^+$ T cells isolated from μMT mice was that they appeared in a highly activated state in terms of surface markers, in that they expressed higher levels of CD44 and lower levels of CD62L in comparison to T cells isolated from wild type mice (figure 6.8). One possible explanation for this higher state of activation may be the lack of B cell-derived TGFβ. Indeed, such B cell-derived TGFβ has been shown to induce/expand Treg cells *in vivo* [331]. Thus, T helper cell responses were measured in CD4-dnTGFβRII mice, which possess T cells that are unable to respond to TGFβ, using the peptide immunisation system. Naïve CD4-dnTGFβRII mice have been shown in the past to spontaneously develop an autoimmune disease at around 3-4 months of age, characterised by the infiltration of inflammatory immune cells into multiple organs, and the presence of circulating autoimmune antibodies [43]. This observation alone points to a role of TGFβ signalling in T cells in the control of anti-self immune reactions. The onset of autoimmunity may explain the death of some animals in my own experiments by week 6 post-immunisation, which is why group sizes after boosting were small (figure 6.16).

The data presented in figure 6.13 reveal the T helper cell phenotype in naïve CD4-dnTGFβRII mice. Such T cells displayed a more activated, effector phenotype (in terms of surface expression of activation and effector markers), with greater levels of division (measured by Ki67 staining). The increase in CD44 expression and diminished CD62L expression resembled that seen in the B cell-deficient mice (figure 6.8), thus B cell-derived TGFβ may be playing a role, although this was not assayed directly. As these mice were unimmunised naïve mice that should not have underlying infection (although such mice could be undergoing a response to commensal bacteria), this suggests a role for TGFβ signalling in T cells in homeostasis. Indeed, previous reports suggest TGFβ signalling in naïve T cells to regulate tolerance and promote survival [332]. Furthermore, T helper cells from naïve CD4-dnTGFβRII mice showed signs of Th1 activation, as characterised by their enhanced production of IFNγ. Both the Th1 bias, which regulates Th17 cells [37], and the lack of TGFβ signalling, which is required in conjunction with IL-6 for Th17 cell differentiation [32], explain the complete loss of IL-17 production by T cells from the CD4-dnTGFβRII mice (figures 6.14B, 6.15B & 6.16B). The lack of Th17 cell differentiation is likely to impact on immune responses against extracellular bacteria and fungi, especially at mucosal sites [32], and thus may impact on survival rate if encountered with such pathogens.

Interesting, despite evidence indicating TGFβ involvement in the differentiation of inducible FoxP3$^+$ Treg cells [32,49], the total numbers of FoxP3$^+$ splenic T helper cells were equivalent in wild type and CD4-dnTGFβRII mice (figure 6.13E). This evidence supports previous findings in these mice that Treg cell numbers are normal in the absence of TGFβ signalling in T cells [52]. During an immune reaction, however, a proportion of antigen-activated T cells are thought to differentiate into Treg cells in the periphery [32]. Therefore, although total splenic Treg cell numbers were unaffected in CD4-dnTGFβRII mice, these mice likely lack the ability to generate antigen-activated iTreg cells during infection. This deficiency may impact on the control of antigen-specific effector T cells.

The role of TGFβ in regulating CD4$^+$ T cell responses following peptide immunisation

TGFβ has been shown to influence CD8$^+$ T cell responses during viral infection, by limiting the peak effector response by the induction of apoptosis [324]. In this study, I used CD4-dnTGFβRII mice to follow the antigen-specific T helper cell response using tetramers. Primary T cell expansion in the draining lymph nodes appeared enhanced, with tetramer$^+$ T

cell numbers higher than in wild type mice (figure 6.14A, bottom). This concurs with the data from the $CD8^+$ T cell response, in that the peak of $CD8^+$ T cell division was also enhanced in these mice. However, the numbers of $tetramer^+$ T helper cells in the spleen at the peak of the primary response appeared reduced in CD4-dnTGFβRII mice, following peptide immunisation (figure 6.14A, top). Therefore, the unregulated effector response appeared localised to the draining lymph nodes. The reason for the reduced numbers of antigen-specific T cells in the spleen is not obvious. Perhaps, either the T cells themselves, or the initiating APC, are remaining in the lymph node as opposed to trafficking to the spleen. However, the role of TGFβ signalling in influencing the migration of these cells is unknown, and not investigated here.

Six weeks post-immunisation, the numbers of tetramer-binding T cells in the draining lymph nodes were equivalent in wild type and CD4-dnTGFβRII mice. However, in the spleen there appeared to be elevated numbers of $tetramer^+$ T cells (figure 6.15), although statistical analysis was difficult due to small group sizes. This increase in $tetramer^+$ T cells in the spleen may be due, either to enhanced memory generation, or a lag in decline of the effector response. Data on the $CD8^+$ T cell responses indicate a lag in the decline of antigen-specific effector cells in the absence of TGFβ signalling in T cells [324]. Therefore, a lag in decline of effector cell numbers due to the lack of TGFβ-induced apoptosis seems a likely explanation for the elevated numbers of antigen-specific T helper cells seen at the memory time-point. However, even if TGFβ is involved in the control of the decline phase of $CD4^+$ effector T cells, other mechanisms of control must exist, as antigen-specific T cell numbers in the spleen underwent a decline phase between day 9 and week 6 (compare figures 6.14A & 6.15A).

Antigen-specific T cell numbers after boosting were normal in the CD4-dnTGFβRII mice (figure 6.16). This therefore suggests that both memory generation and T cell re-activation are not dependent on TGFβ signalling in T cells. These data contrast to my original hypothesis that an enhanced primary effector response may be detrimental to memory development. However, clear distinction between effector and memory T helper cells following immunisation was difficult. Here, $CD4^+$ T cell memory generation appeared normal in the absence of TGFβ signalling in T cells, as the boost response was normal (figure 6.16). Indeed, the normal development of T cell memory has previously been reported in the $CD8^+$ T cell compartment in these CD4-dnTGFβRII mice [324], indicating that neither $CD4^+$ not $CD8^+$ T cell memory generation requires TGFβ signalling in T cells.

Interestingly, here, although elevated numbers of antigen-specific T cells were seen in the draining lymph nodes after priming (figure 6.14A), excessive T cell expansion was not seen on day 5 post-boost (figure 6.16A). It may be that boost responses do not require TGFβ-mediated control, or that the time-point analysed was earlier than the peak of the response. Alternatively, the lack of significant differences between groups at this time-point may simply be due to small group sizes, as a result of some mice dying before the completion of the experiment.

Furthermore, it should be noted that the above data describes the effects of the lack of signalling through the TGFβ receptor in all T cells, but does not distinguish between the role of TGFβ-induced apoptosis of effector cells, and TGFβ-induced differentiation of an inducible Treg cell population. Additionally, one should bear in mind that the impairment in TGFβ signalling also exists in the $CD8^+$ T cell population of these mice.

Lack of TGFβ signalling in T cells impacts on antibody production

With the increased T helper cell activation and IFNγ production in the spleen (figure 6.14B), I expected to find increased levels of the Th1-associated antibody isotypes, IgG2c/b [333]. Instead, the CD4-dnTGFβRII mice had decreased levels of class switched IgG1 and IgG2b circulating antibody (figure 6.17A), and very low levels of IgG2c, which were at the limit of detection (data not shown). The predominance of IgG1 production in response to peptide immunisation had been noted before by myself (figure 6.7B) and others [334], and occurred despite the Th1-biased environment. This antibody response data indicates an impairment in T cell help for B cells in the CD4-dnTGFβRII mice. Perhaps the highly activated state of T helper cells in these mice (or their Th1 bias) makes them less efficient at helping B cells, explaining the reduction in antigen-specific class switched antibody. It would therefore be interesting to measure the numbers of T_{FH} cells in these CD4-dnTGFβRII mice.

The increase in IgM, capable of binding H19env peptide, seen at the memory and boost time-points in the CD4-dnTGFβRII mice, was not as a result of immunisation, as it was also present in naïve mice (figure 6.17B). These naïve mice were, by this late stage in the experiment, around 13 weeks old (3^+ months). This is around the time of the onset of autoimmune disease, which leads to death of these animals [43]. It would be interesting therefore to determine whether this cross-reactive IgM, found in both naïve and immunised CD4-dnTGFβRII mice of this age, is also capable of binding self-antigens.

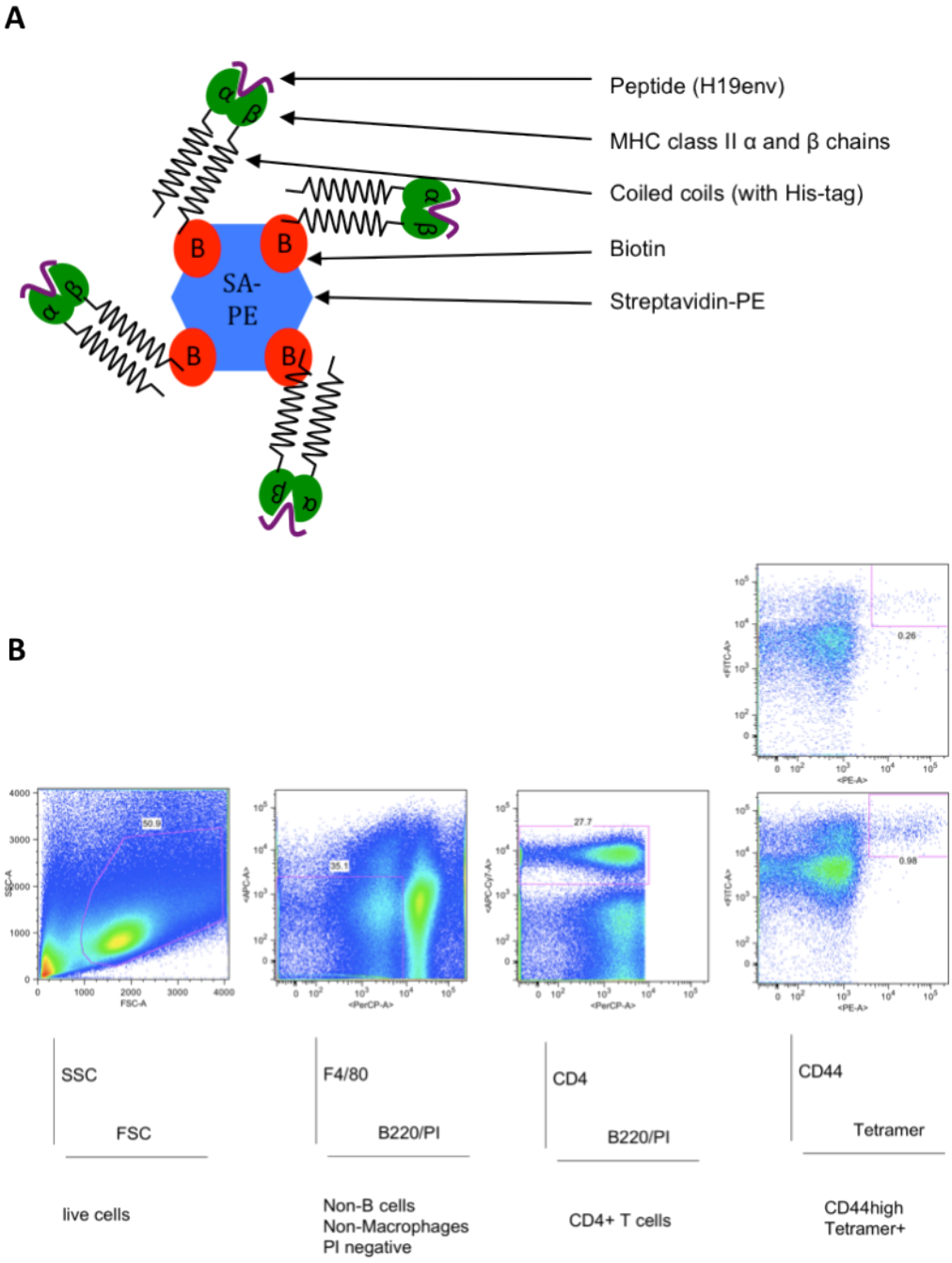

Figure 6.1: Identification of antigen-specific T cells using MHC class II tetramers. (A) Illustrated diagram of the structure of an MHC class II tetramer complex. (B) Tetramer staining analysis. From left to right, first a lymphocyte gate is set using forward (FSC) and side (SSC) scatter. F4/80$^+$, B220$^+$ and PI$^+$ cells are subsequently excluded. The CD4$^+$ T cell population is then gated, and finally T cells are analysed by tetramer binding versus CD44 expression. The cells of interest are in the top right quadrant. Top right plot shows example of primary response (~0.3%), while bottom right shows a boost response (~1%).

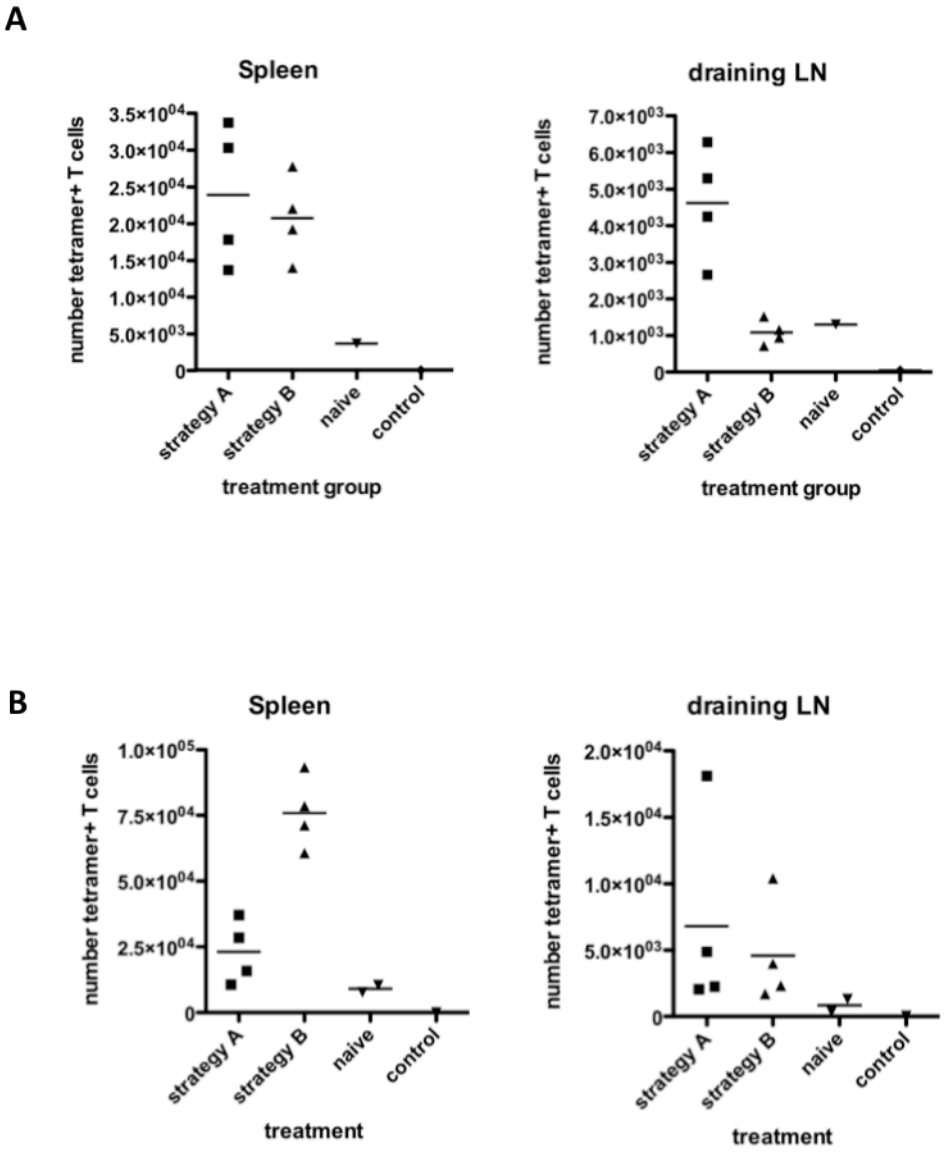

Figure 6.2: Test of different immunisation strategies for the efficient detection of antigen-specific T helper cell responses. Two groups of C57BL/6 mice were immunised by different methods, and their T cell responses assayed by tetramer staining flow cytometry at the primary response on day 8 (A) and on day 5 after boosting (B). Strategy A was immunised with peptide in CFA s.c. then boosted with peptide in LPS i.p. and s.c. 5 weeks later, while strategy B was immunised with peptide-pulsed dendritic cells i.v. then boosted with peptide in CFA s.c. In both (A) and (B), spleen data is on the left, with draining lymph node data on the right. The horizontal line represents the mean. Control represents staining with the tetramer bound by an irrelevant peptide.

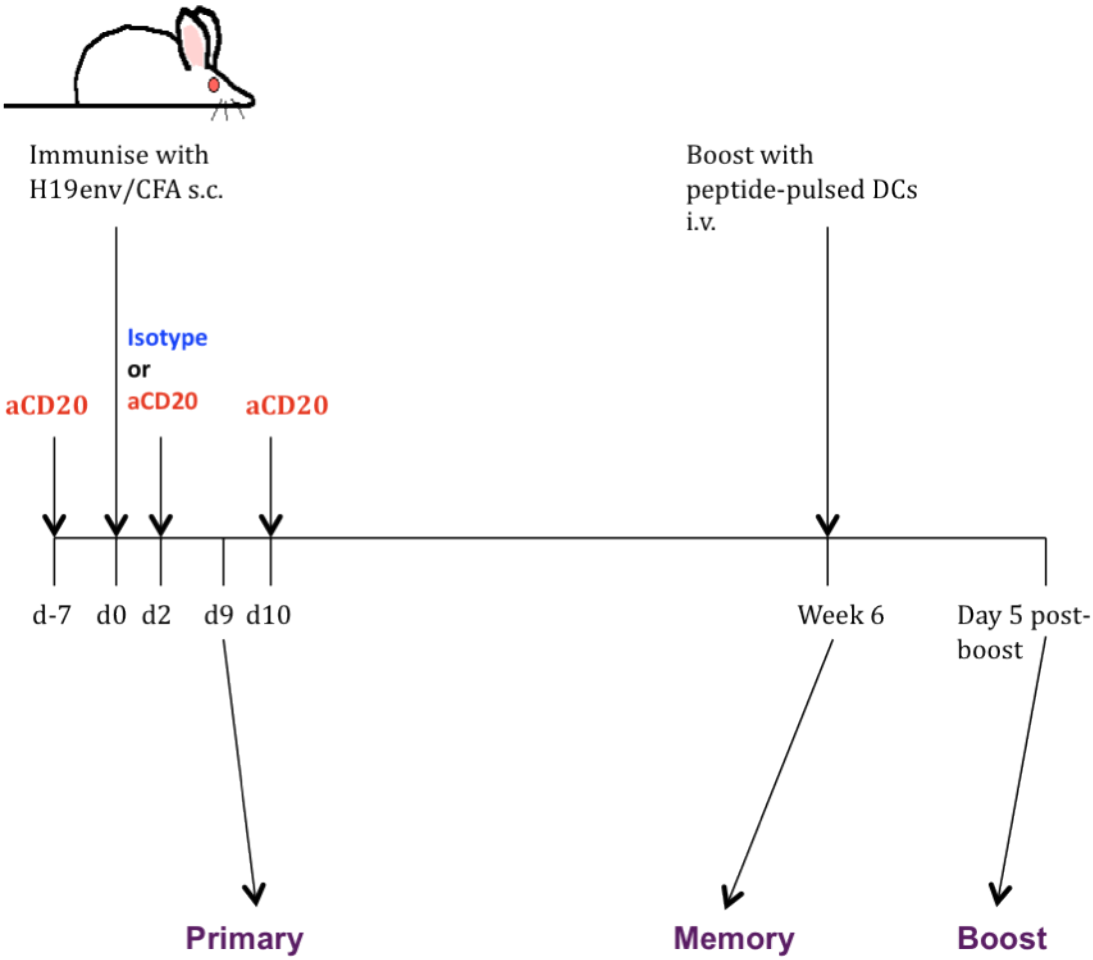

Figure 6.3: Protocol for anti-CD20 B cell depletion and the detection of T cell responses using MHC class II tetramers. Mice were immunised with H19env peptide emulsified in CFA subcutaneously on day 0. Three groups of mice each received a single dose of anti-CD20 depletion antibody on either day -7, day 2, or day 10. The wild type group received the anti-CD20 isotype control on day 2, and represents the non-depleted control group. Where appropriate mice were boosted with peptide-pulsed dendritic cells i.v. 6 weeks after primary immunisation. Mice were taken on either day 9 (primary), week 6 (memory), or day 5 post-boost (boost) to analyse the T cell response using MHC class II tetramer staining.

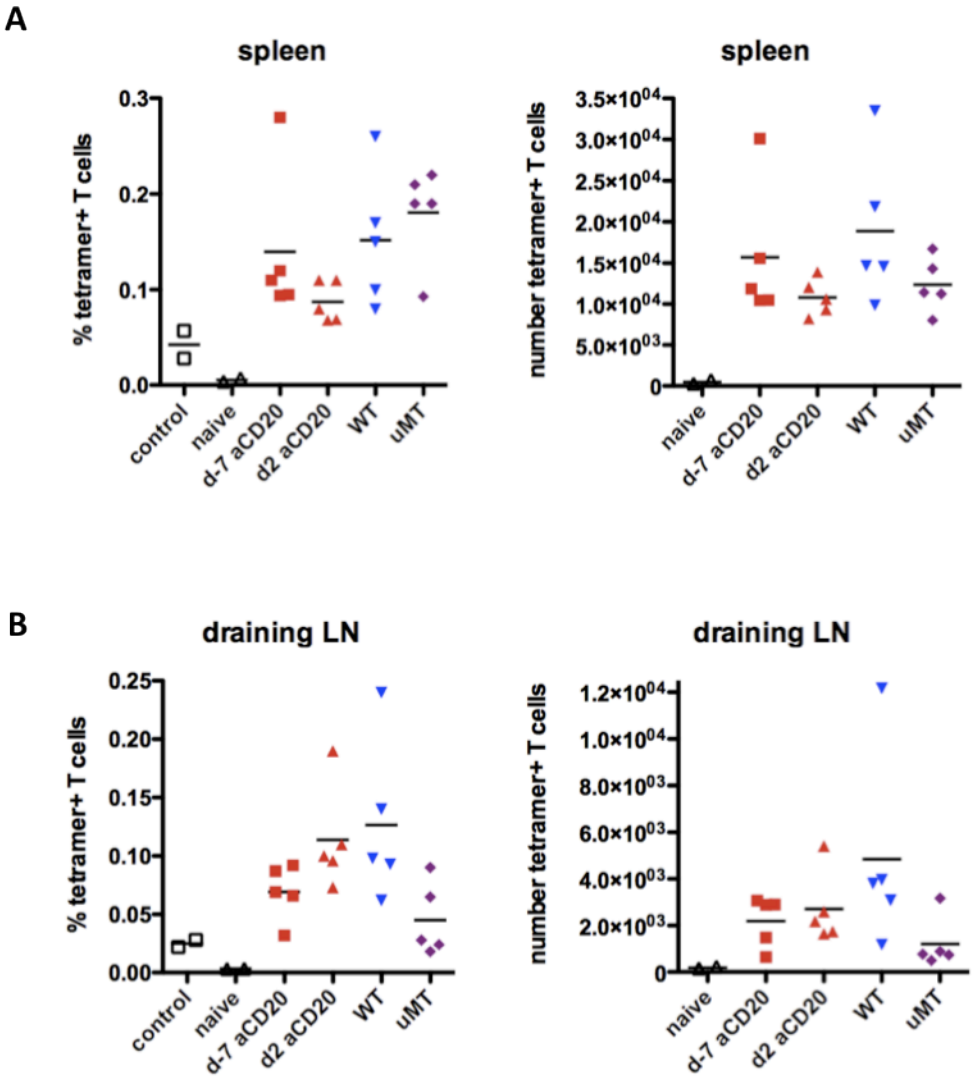

Figure 6.4: B cell-depleted mice show largely normal primary T cell expansion following peptide immunisation. C57BL/6 or μMT mice were immunised with H19env peptide in CFA s.c. on day 0. Some C57BL/6 mice were treated with anti-CD20 on either day -7 or day 2. The wild type group received the anti-CD20 isotype control on day 2 (i.e. non-depleted). On day 9, at the peak of the primary response, spleens (A) and draining lymph nodes (B) were analysed for tetramer binding to identify the percentages (left) and absolute numbers (right) of antigen-specific T cells. Control indicates staining with the tetramer containing an irrelevant peptide. Data represents 3 independent experiments.

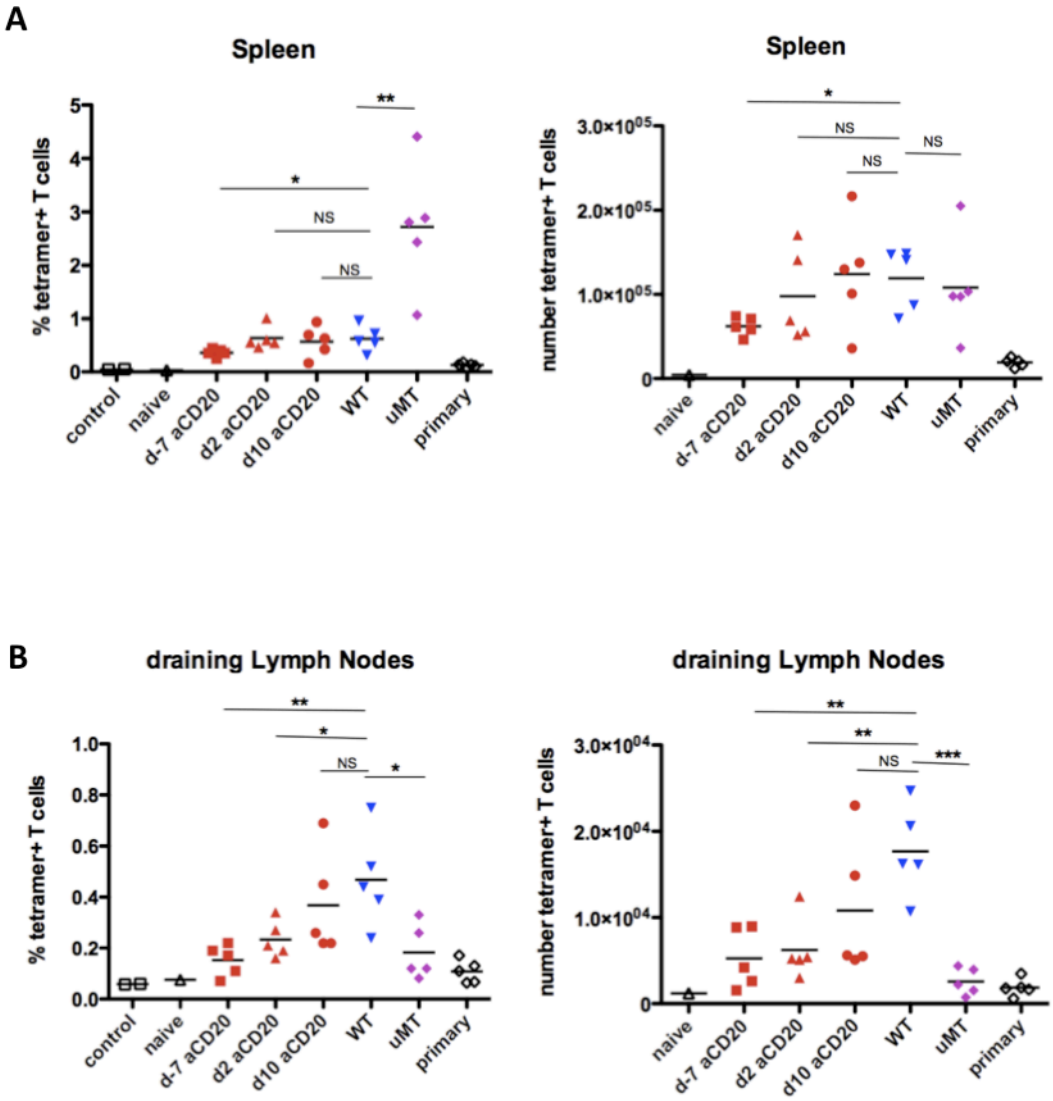

Figure 6.5: Early depletion of B cells impairs memory T cell responses in the draining lymph nodes. Six weeks after priming mice were boosted with peptide-pulsed dendritic cells i.v. On day 5 post-boost, spleens (A) and draining lymph nodes (B) were analysed for antigen-specific T cells using tetramer staining. Percentages (left) and absolute numbers (right) of tetramer$^+$ T cells are shown. Control represents tetramer containing an irrelevant peptide. The horizontal line represents the mean. The Student's *t*-test was used to calculate significance values. p=0.01 to 0.05 *, p= 0.001 to 0.01 **, p<0.001 ***, NS = not significant (p>0.05).

	Spleen %		Spleen numbers		LN %		LN numbers	
	P-value	Summary	P-value	Summary	P-value	Summary	P-value	Summary
Naïve	0.0000	***	0.0000	***	0.0000	***	0.0000	***
WT primary	0.0000	***	0.0000	***	0.0000	***	0.0000	***
µMT primary	0.0003	***	0.0000	***	0.0000	***	0.0000	***
µMT	0.0000	***	0.9222	NS	0.0462	*	0.0000	***
d-7 aCD20	0.9991	NS	0.9531	NS	0.0266	*	0.0396	*
d2 aCD20	0.9987	NS	1.0000	NS	0.7953	NS	0.4106	NS
d10 aCD20	0.9998	NS	0.9895	NS	0.9928	NS	0.7858	NS

Table 6.6: Statistical analysis of data pooled from the three B cell depletion tetramer experiments. Mice were immunised with peptide in CFA subcutaneously, and boosted with peptide-pulsed dendritic cells 6 weeks later. On day 5 post-boost, spleens and draining lymph nodes were removed and the percentages and absolute numbers of tetramer$^+$ cells measured. The data from 3 identical experiments was pooled and analysed using a General Linear Model ANOVA (Tukey's multiple comparison test) to adjust the means. The p-values presented in the table above represent comparisons between each experimental group (e.g. day -7 anti-CD20) to the wild type group (positive control). The p-value summaries given are as follows: p=0.01 to 0.05 *, p= 0.001 to 0.01 **, p<0.001 ***, NS = not significant (p>0.05).

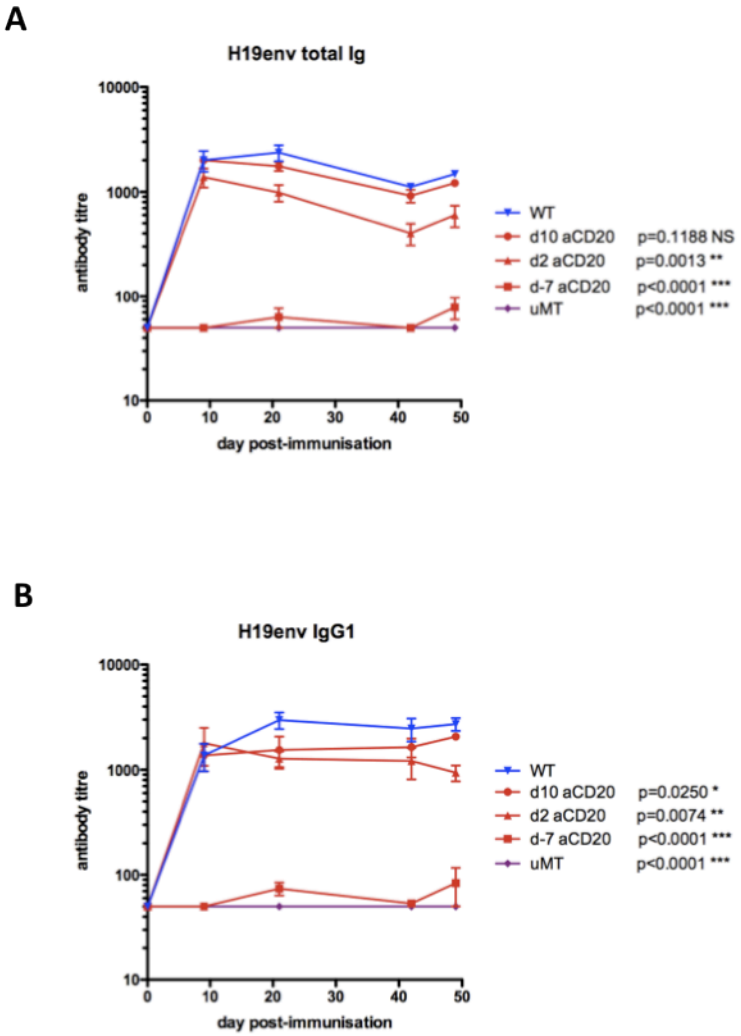

Figure 6.7: Mice depleted of B cells on day 2 or day 10 possess unexpectedly high levels of antigen-specific antibody. Serum was collected throughout the time-course of the experiment, from mice primed with peptide in CFA and boosted with peptide-pulsed dendritic cells 6 weeks later. Antigen-specific antibody responses against the H19env peptide were determined in the depleted and non-depleted mice. (A) Total anti-H19env antibody. (B) IgG1 anti-H19env antibody. Error bars indicate SEM with 5 mice per group. All statistics were calculated using the two-way ANOVA (comparing each treatment group to the wild type non-depleted group group), and significance values are displayed in the figure. Data represents 3 independent experiments.

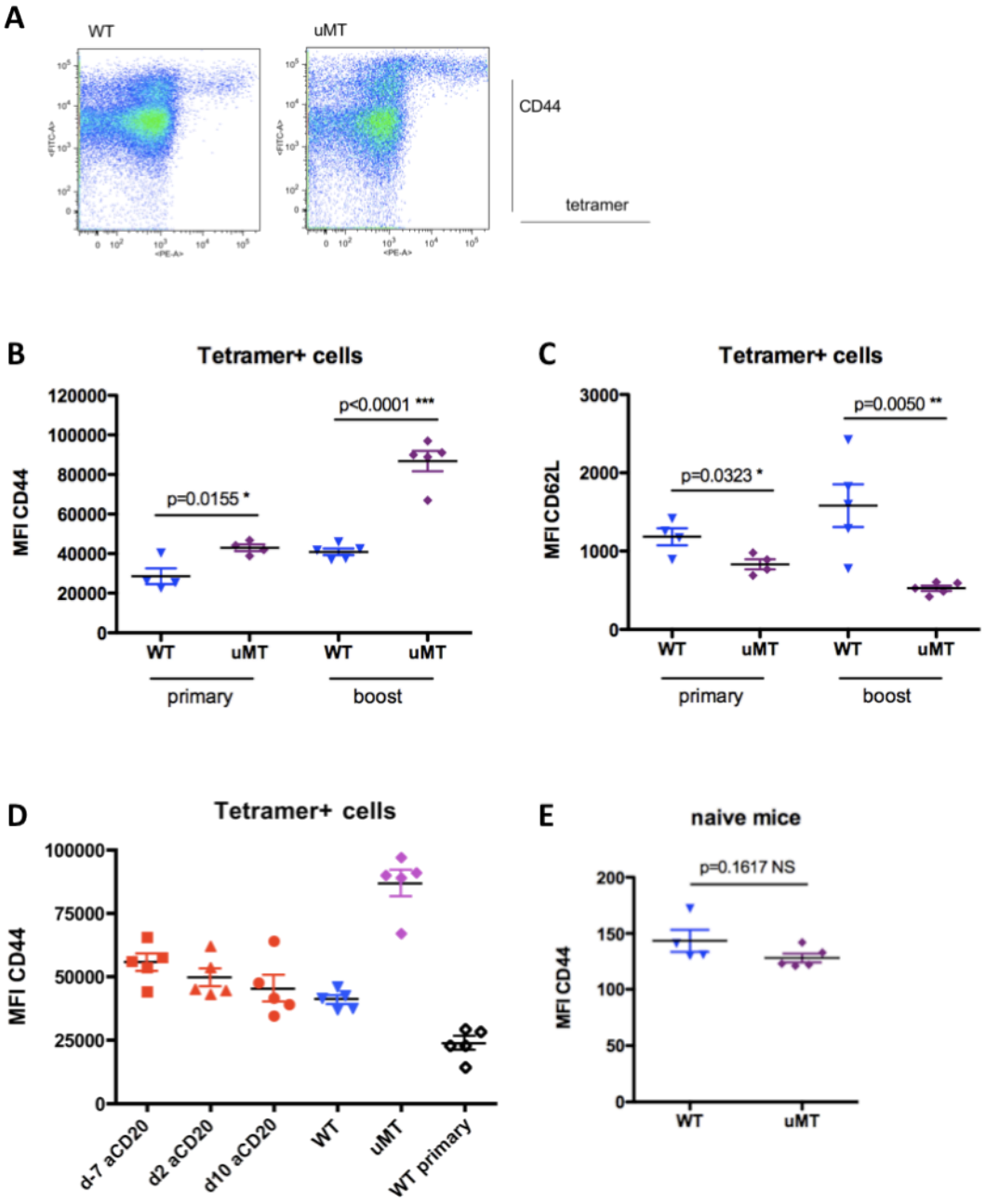

Figure 6.8: Tetramer⁺ T cells found in the spleens of B cell-deficient mice are in a highly activated state. (A) Example staining of T cells from wild type and μMT mice after boosting, showing tetramer binding by CD44 expression. (B) Expression of CD44 and (C) CD62L by T cells from wild type and μMT mice at the primary (left) and boost (right) analysis. (D) Tetramer⁺ T cell expression of CD44 by T cells from B cell-deficient and B cell-depleted groups on day 5 after boosting. (E) CD44 expression by total splenic T cells in naïve wild type and μMT mice. The Student's *t*-test was used to calculate significance values where shown. Data is representative of 2-3 independent experiments.

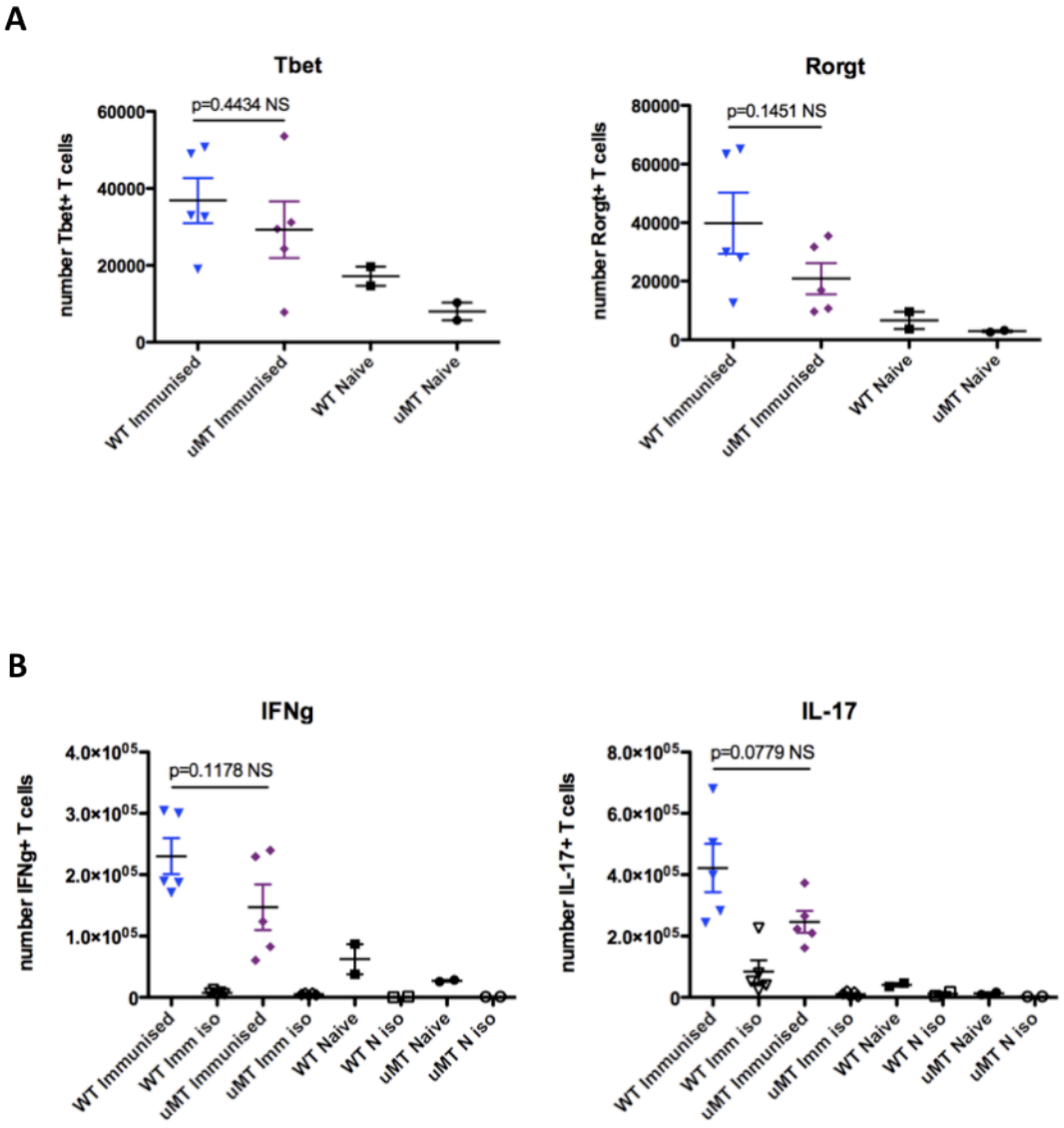

Figure 6.9: Th1 and Th17 cell priming appears normal in the absence of B cells. Wild type and μMT mice were immunised with peptide in CFA s.c. or left unimmunised. (A) Splenocytes from day 9 post-immunisation were analysed directly *ex vivo* for expression of the Th1 and Th17 transcription factors, Tbet and Rorγt, respectively. (B) Splenocytes were restimulated with PMA/ionomycin for 4 hours *in vitro* and $CD4^+$ T cells assayed for intracellular IFNγ and IL-17. Statistical analysis was performed using the Student's *t*-test. Data is representative of 2 experiments. Rorgt = Rorγt, IFNg = IFNγ, NS = not significant, iso (in B) = isotype control staining.

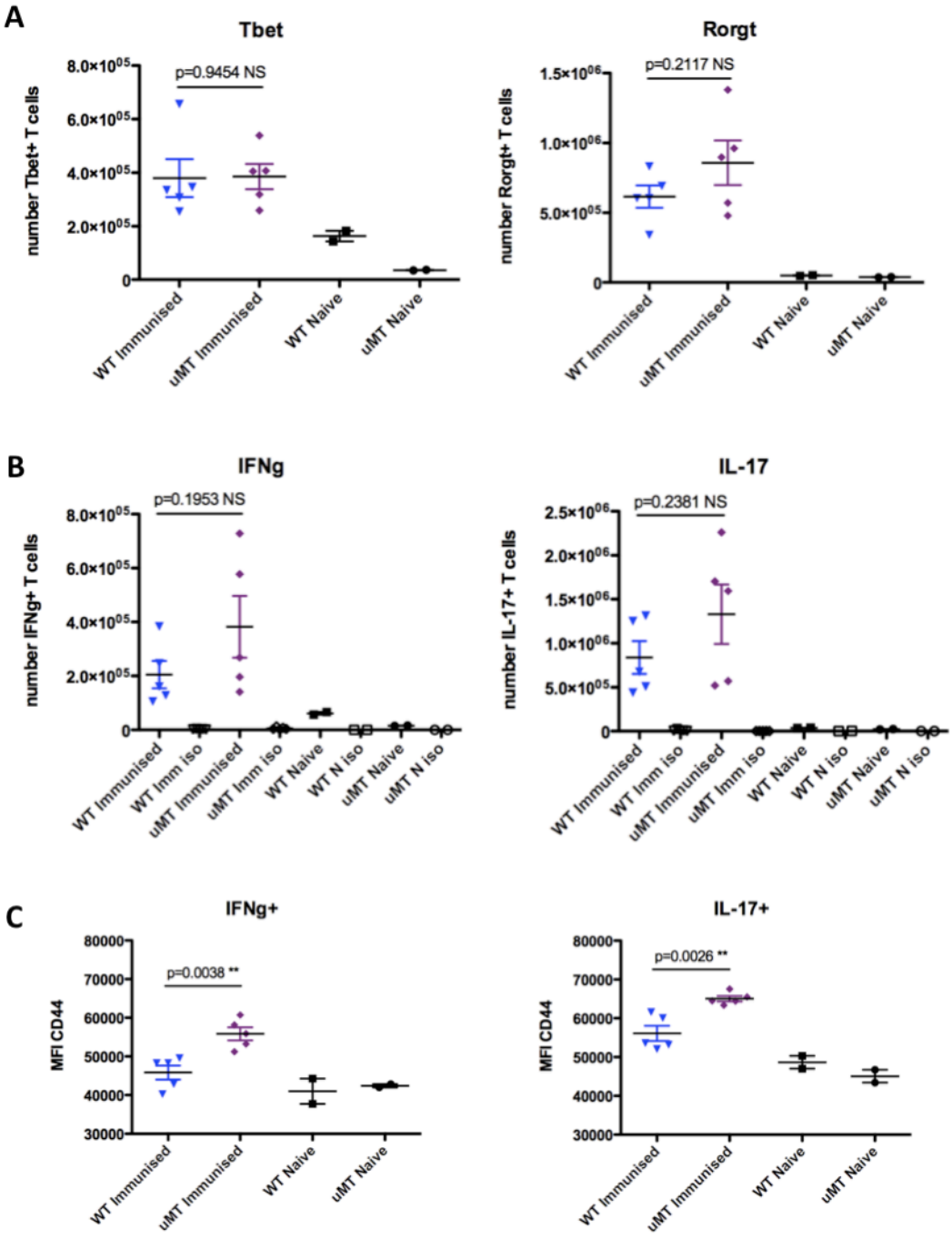

Figure 6.10: Splenic Th1 and Th17 responses after boosting are equivalent in wild type and B cell-deficient mice. Splenocytes were removed on day 5 post-boost from wild type and μMT mice. (A) Cells were stained directly *ex vivo* for the transcription factors Tbet and Rorγt. (B) Splenocytes were cultured for 4 hours with PMA/ionomycin and T helper cells stained for intracellular IFNγ and IL-17. (C) Cytokine-positive T cells identified in (B) were further analysed for their expression of CD44. The Student's *t*-test was used to calculate p-values.

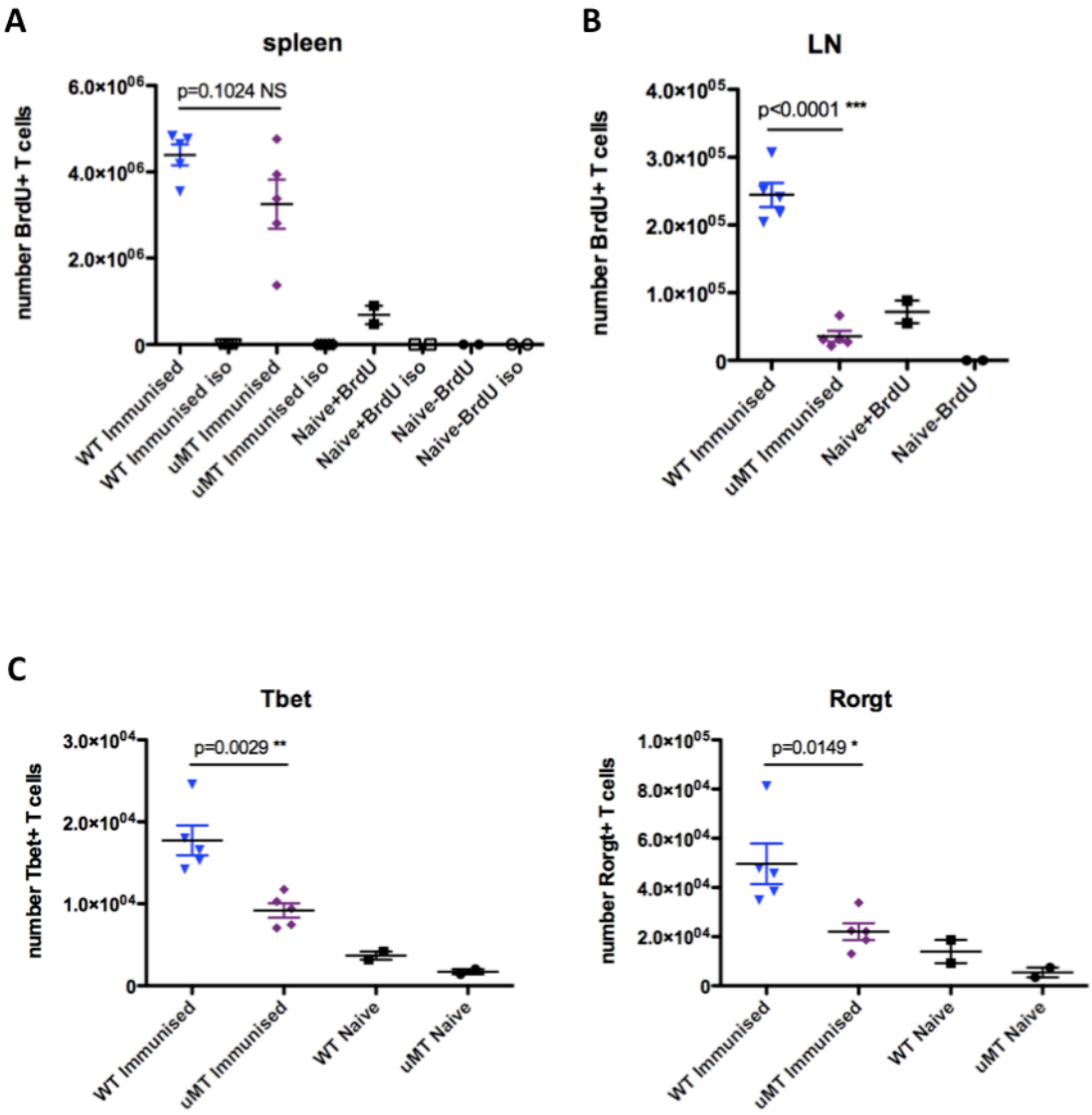

Figure 6.11: T cell division and effector responses are significantly impaired in the lymph nodes of B cell-deficient mice at the boost response. Immunised wild type and μMT mice were boosted with peptide-pulsed dendritic cells 6 weeks after priming. (A & B) Mice were injected with BrdU i.p. for 3 consecutive days immediately before harvesting on day 5 post-boost (i.e. on days 2, 3, and 4 post-boost). T cells from the spleen (A) and lymph nodes (B) were assayed for their incorporation of BrdU. (C) T cells from the draining lymph nodes were analysed directly *ex vivo* for the transcription factors Tbet and Roryt on day 5 post-boost. In (A) iso = isotype control staining.

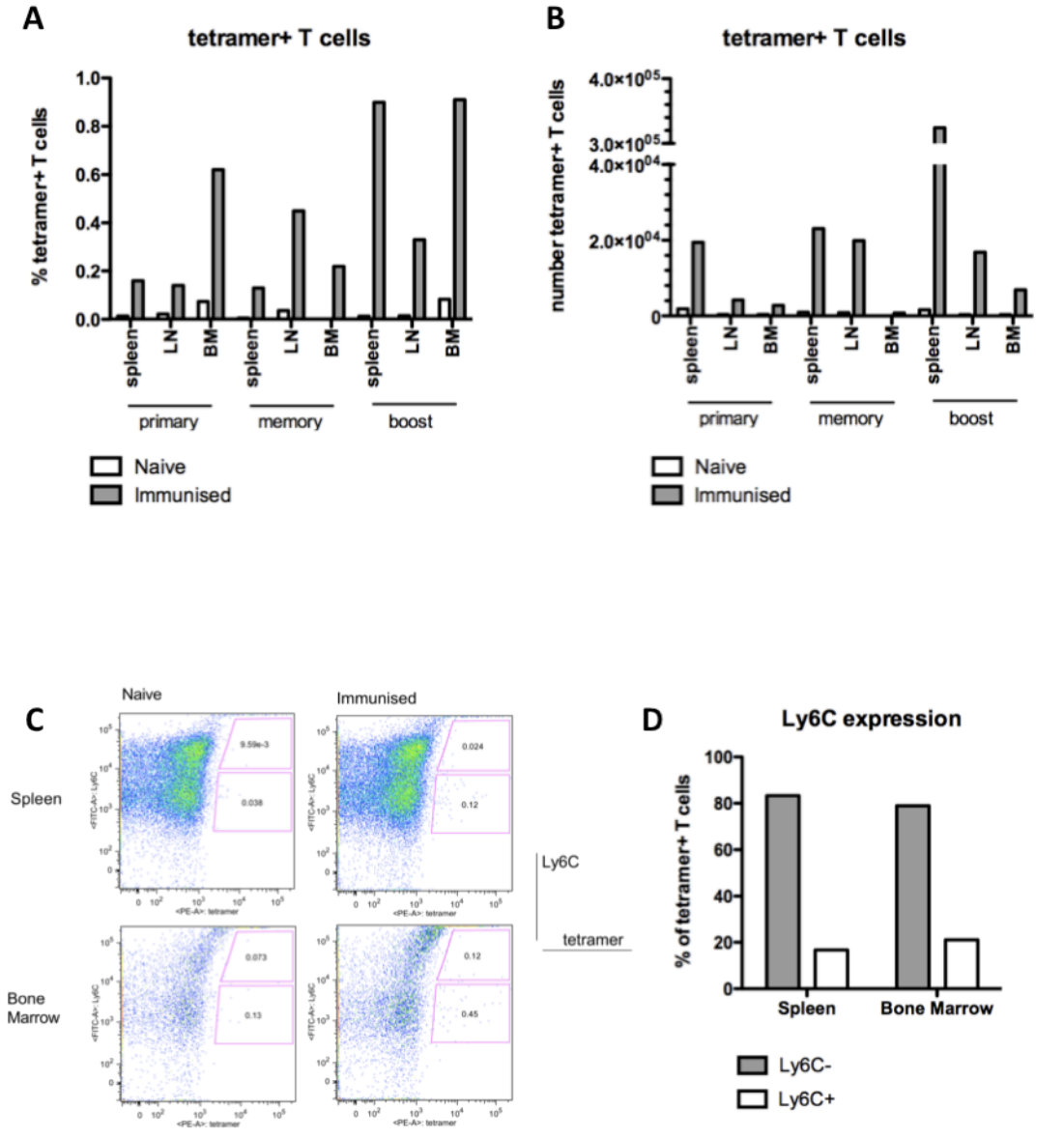

Figure 6.12: Antigen-specific memory T cells do not appear to reside in the bone marrow or express Ly6C. (A & B) The localisation of antigen-specific T cells in immunised wild type mice was analysed at the primary, memory and boost timepoints, by looking in the spleen, draining lymph nodes (LN) and bone marrow (BM). The percentages (A) and absolute numbers (B) of tetramer$^+$ T cells in these organs are shown. Absolute numbers in the bone marrow represents the cells from the femur, tibia and humerus of both legs from each mouse. (C & D) At the memory timepoint, the tetramer$^+$ T cells in the spleen and bone marrow were further analysed for their expression of Ly6C. Representative plots are shown in (C), while percentages of tetramer$^+$ T cells that are Ly6C$^-$ and Ly6C$^+$ are shown in (D).

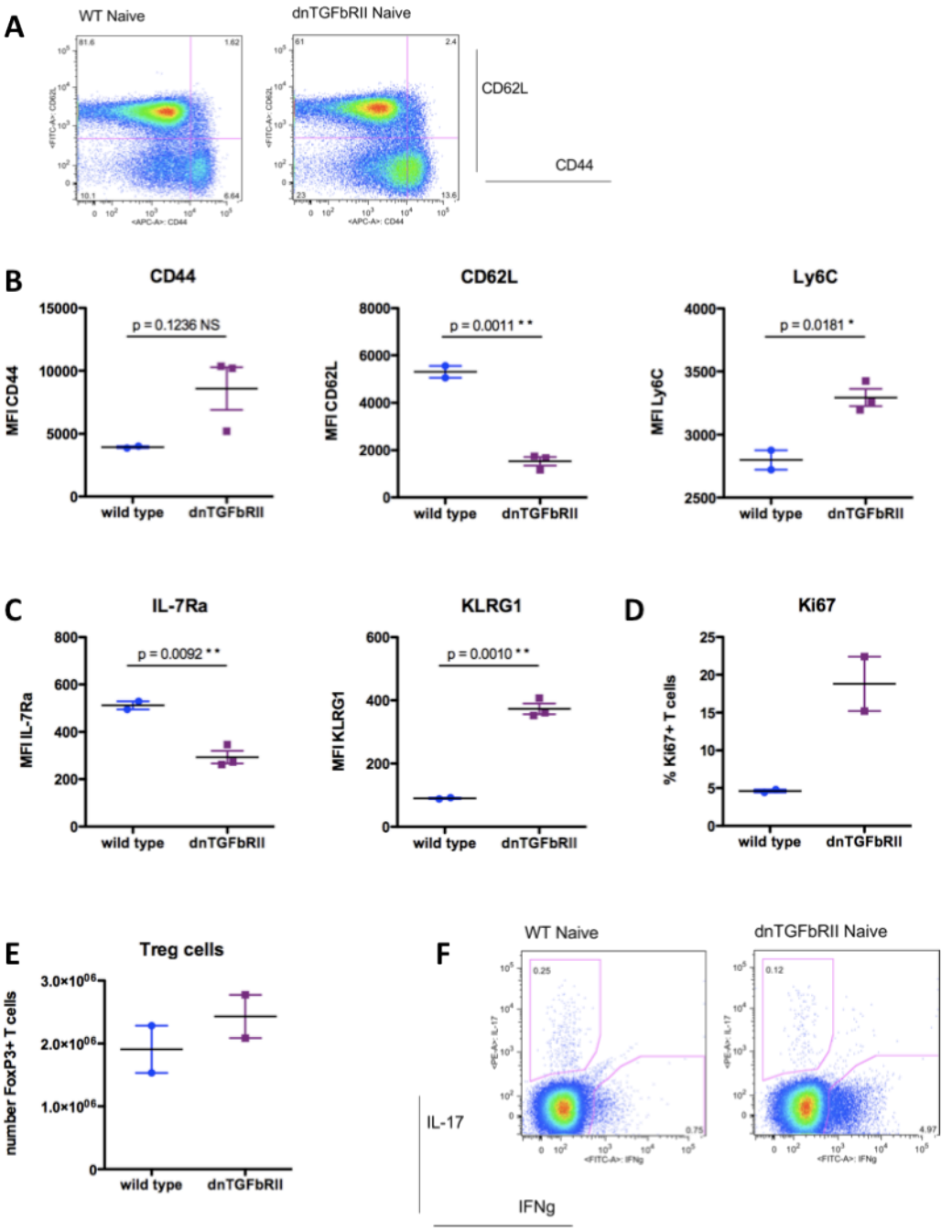

Figure 6.13: T cells from naïve CD4-dnTGFβRII mice appear to be in a more activated state. Splenic T helper cells from naïve wild type and CD4-dnTGFβRII mice were analysed for their activation status. (A) Example staining of CD44 and CD62L expression. (B) Expression of CD44, CD62L and Ly6C by $CD4^+$ T cells. (C) IL-7Rα and KLRG1 expression. The numbers of dividing $Ki67^+$ splenic T cells (D) and $Foxp3^+$ Treg cells (E) were determined. (F) Splenocytes were restimulated with PMA and ionomycin and analysed for T cell IFNγ and IL-17 production. Data in (F) represents 3 mice of each strain. The Students *t*-test was used to calculate significance values in (B) and (C).

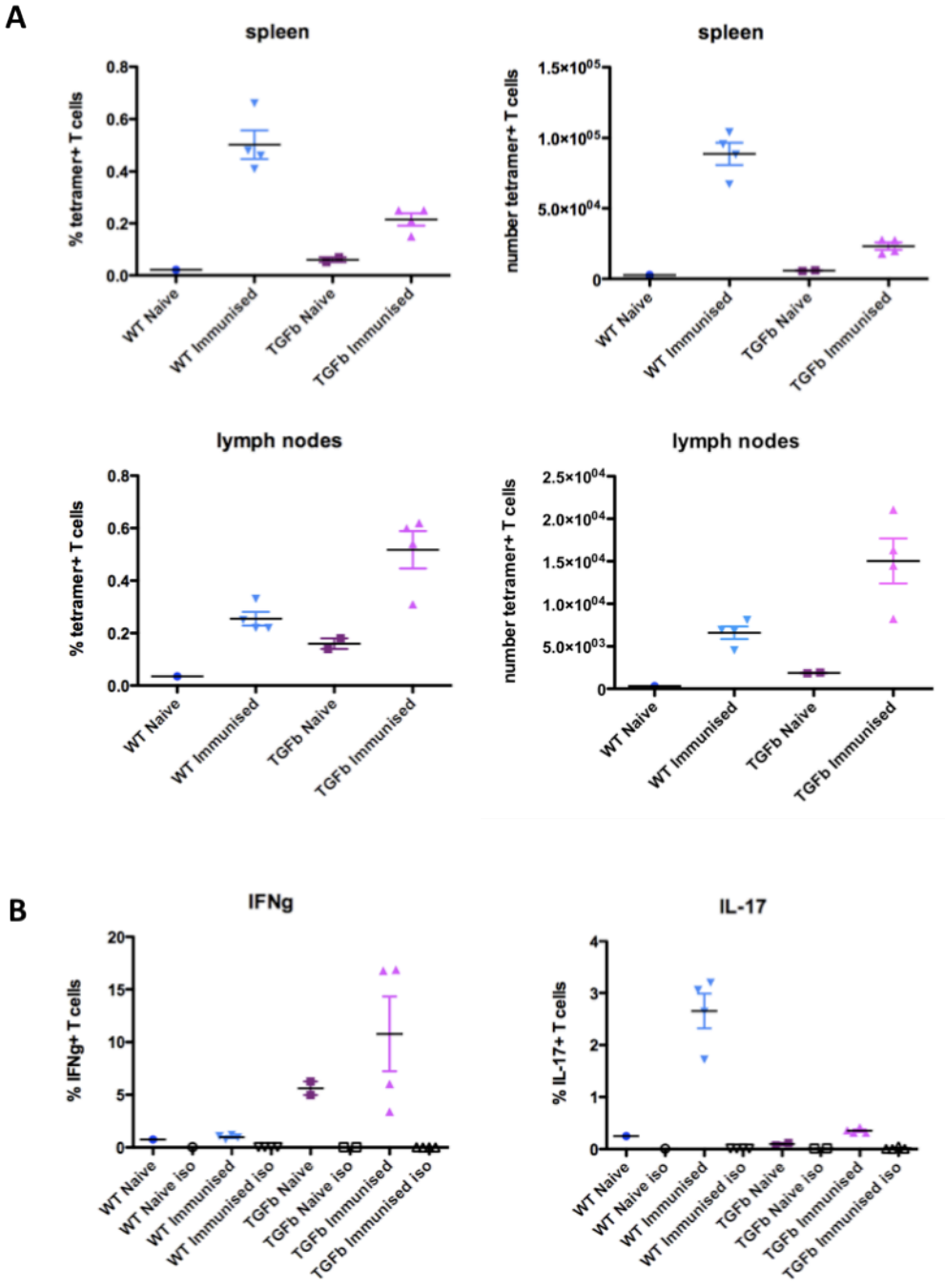

Figure 6.14: CD4-dnTGFβRII mice show enhanced priming in the lymph nodes, and a biased Th1 response in the spleen. Wild type and CD4-dnTGFβRII mice were immunised with H19env peptide in CFA s.c. On day 9 post-immunisation spleens and draining lymph nodes were removed and antigen-specific T cells identified by tetramer staining (A). Splenocytes were restimulated with PMA and ionomycin for 4 hours and T cell IFNγ and IL-17 responses measured (B). In all cases TGFb = CD4-dnTGFβRII mice, while in (B) iso = isotype control staining.

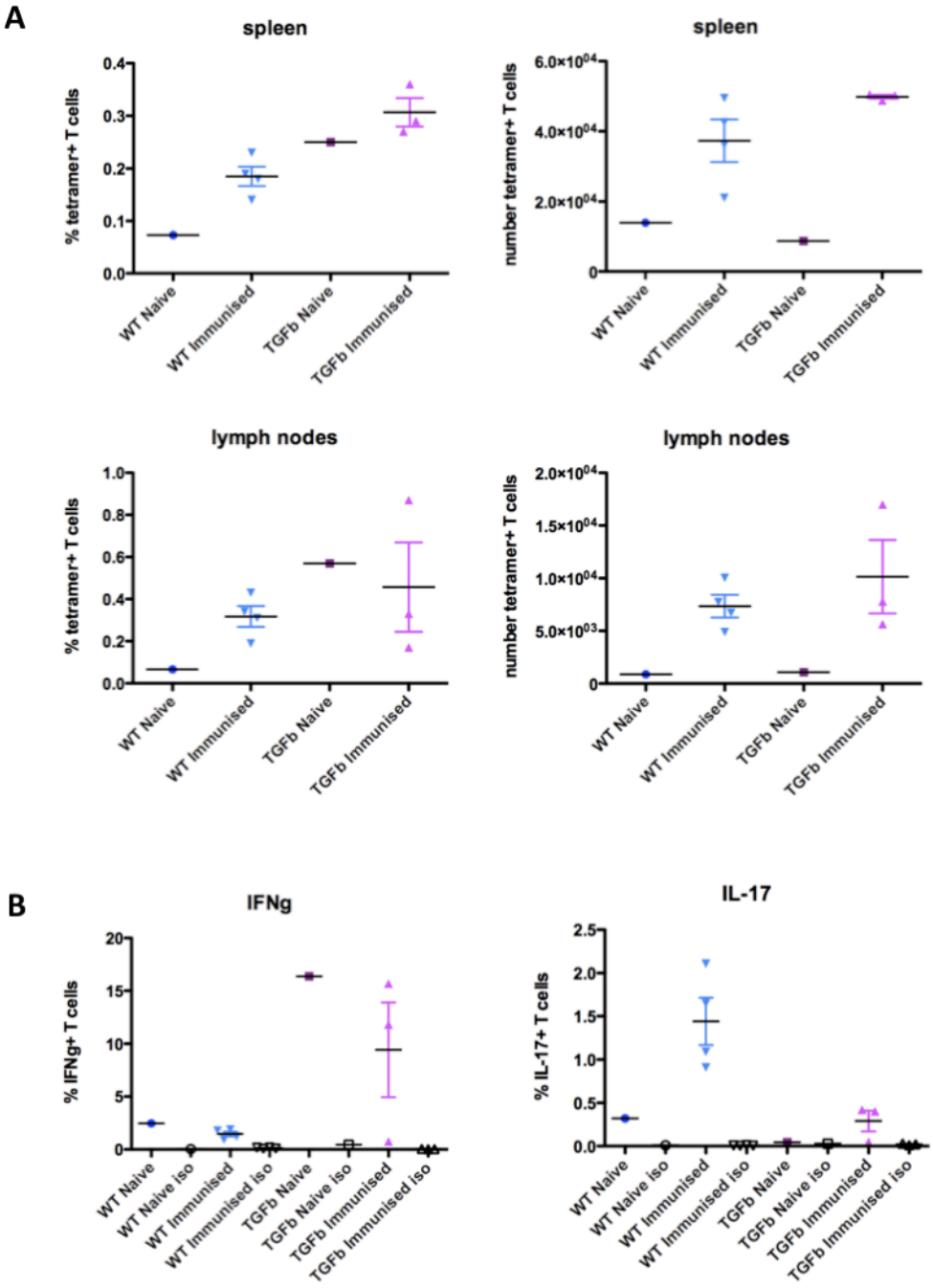

Figure 6.15: CD4-dnTGFβRII mice may possess more antigen-specific T cells in the spleen 6 weeks after immunisation, and continue to display a biased Th1 phenotype. Six weeks after priming the memory T cell response in CD4-dnTGFβRII mice was analysed by tetramer staining of spleens and draining lymph nodes (A). Splenocytes were restimulated with PMA and ionomycin for 4 hours and T cell IFNγ and IL-17 responses measured (B). In all cases TGFb = CD4-dnTGFβRII mice, while in (B) iso = isotype control staining. Statistical analysis was not performed due to small group sizes.

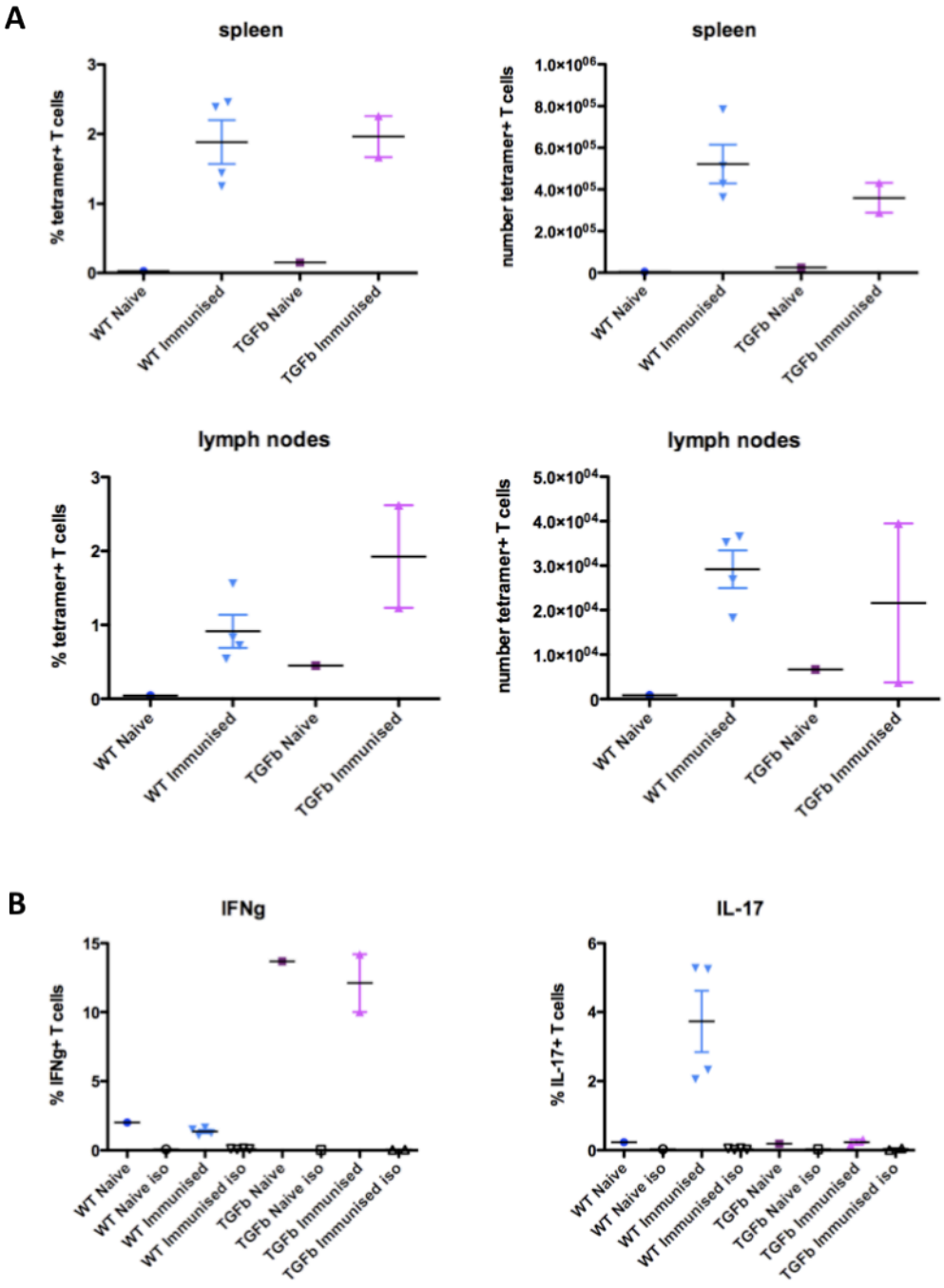

Figure 6.16: In the absence of TGFβ signalling in T cells the boost response, and therefore memory T helper cell generation, appears normal. CD4-dnTGFβRII mice were boosted with peptide-pulsed dendritic cells 6 weeks after priming, and 5 days later spleens and draining lymph nodes were removed. Antigen-specific T cells were identified by tetramer staining (A). Splenocytes were restimulated with PMA and ionomycin for 4 hours and T helper cell IFNγ and IL-17 responses measured (B). In all cases TGFb = CD4-dnTGFβRII mice, while in (B) iso = isotype control staining. Statistical analysis was not performed due to small group sizes.

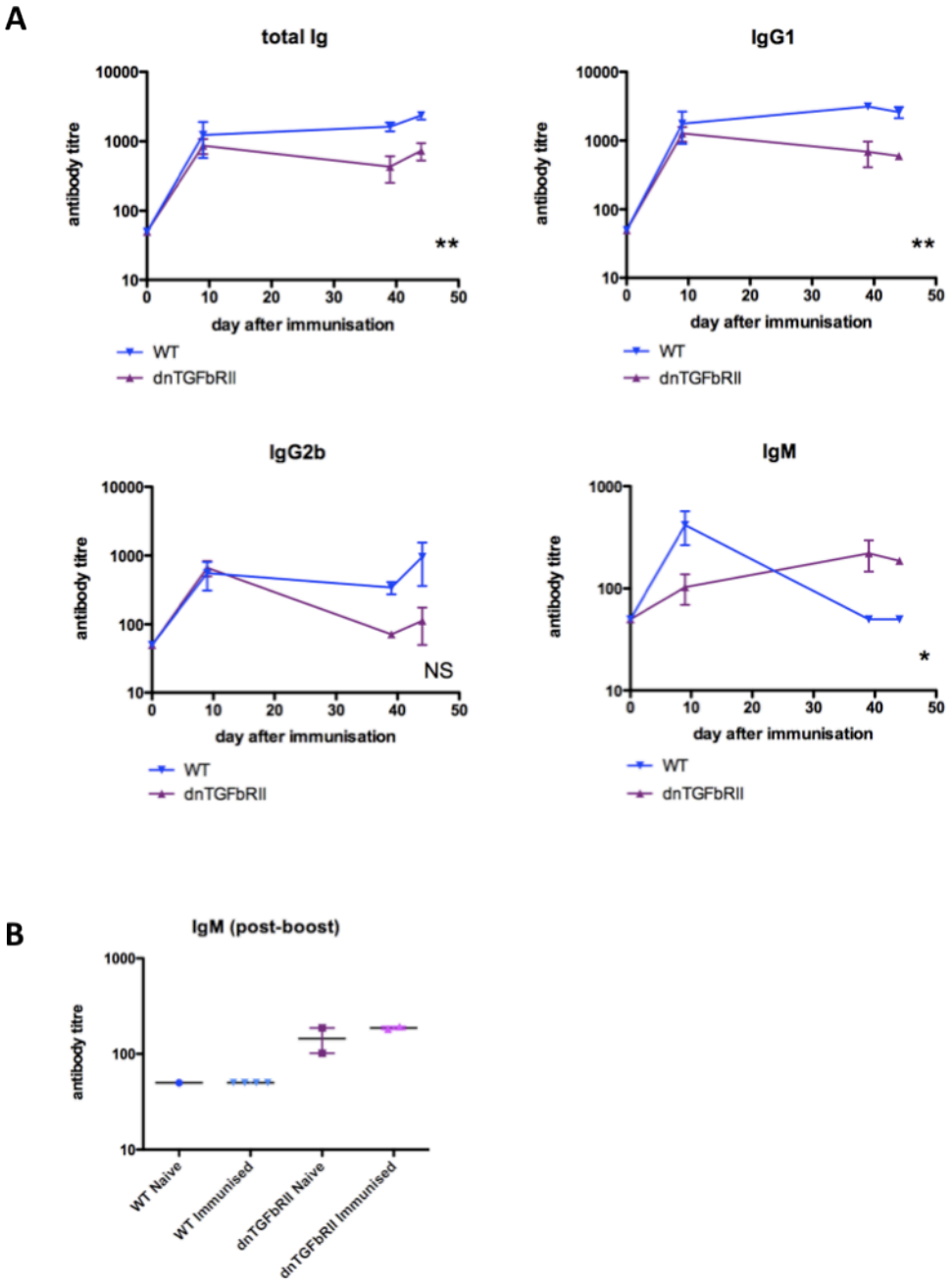

Figure 6.17: CD4-dnTGFβRII mice show impaired switched antibody responses, but increased production of IgM. Serum was collected from wild type and CD4-dnTGFβRII mice pre-immunisation and at the primary, memory and boost timepoints. Antigen-specific antibody responses against the H19env peptide were determined for each of the subclasses shown (A). Levels of IgG2c and IgG3 were at the limit of detection (data not shown). IgM levels post-boost were analysed in greater detail to include the levels in age-matched naïve mice (B). In (A) significance values were calculated using the two-way ANOVA, and are indicated in the graphs. NS = not significant.

CHAPTER 7: Final Discussion and Summary

Overview

Clearly, the generation of immune responses against invading microorganisms is a vital phenomenon that continuously protects the host from pathogen-mediated damage. These responses must be tightly regulated, to prevent both anti-self reactions and excessive immunopathology, whilst ensuring the removal of the infectious agent. The early and rapid response of innate cells induces activation of the adaptive immune response, which is slower to develop. Usually, the activation of both the innate and adaptive arms of the immune system are required for the clearance of infections and the generation of memory cells. These memory B and T lymphocytes, part of the adaptive immune response, are the fundamental mechanism of long-lasting immunity to future infection, and the reason for the efficacy of vaccines.

In this study I focussed on the responses of a particular lymphocyte subset, the B cell, which was traditionally thought of as an adaptive cell, functioning mainly by secreting large amounts of antibody. Here, however, I have demonstrated the important roles that B cells play in both the innate and adaptive arms of immune defence, and suggest that their position at the interface of innate and adaptive immunity ensures efficient adaptive immune cell activation and memory generation.

Innate responses of B cells

In this PhD, I have shown that B cells have the ability to respond rapidly to signals received directly from invading organisms, through TLRs. Signalling through these innate receptors, expressed to varying degrees on all subsets of B cells [124], resulted in changes to whole populations of B cells, independent of their BCR specificity. The effects of TLR stimulation of B cells were found to be many and varied, and are discussed, together with the knock-on effects on the adaptive immune response, in detail here.

The marginal zone population of B cells, situated within the spleen adjacent to the marginal sinuses, is one of the first cell types to access systemic antigen [2]. In *S. typhimurium* infection, I identified significant and rapid changes to this population of B cells, which were partially dependent on their expression of the adaptor protein, MyD88, indicating a role for TLR signalling (chapter 4). Specifically, marginal zone B cells were lost entirely by day 4

of infection in wild type mice, a phenotype also seen following injection with heat-killed bacteria and TLR ligands [294,295]. The likely fate of this population of marginal zone B cells is the differentiation into IgM-secreting plasma cells in the red pulp, and the generation of an early extrafollicular plasma cell response. Interestingly, although the resulting IgM specificity likely reflects the variation in BCR specificities within the marginal zone B cell population, the differentiation of these plasma cells correlated with an increase in serum IgM that was capable of binding *S. typhimurium* antigens (chapter 4). As IgM is a potent activator of the complement system, and such complement can lead to lysis of bacteria [281], this IgM production is likely to directly aid pathogen killing, as has been reported in *Borrelia* infection [303]. The early differentiation of effector B cells from the marginal zone population following TLR stimulation not only aids bacterial killing directly, but will also no doubt help stimulate adaptive immune cell activation, as is discussed further below.

In addition to changes within the marginal zone population of B cells, follicular B cells, too, are directly affected by TLR stimulation. The stimulation of all B cells by TLR ligands, specifically through TLR2, TLR3, and TLR9, resulted in the shedding of the cell surface adhesion molecule, CD62L (chapter 3). During *S. typhimurium* infection, this TLR-mediated alteration in CD62L expression led to changes in B cell migration within the host. B cell populations no longer localised to sites that require CD62L for entry, namely the lymph nodes and Peyer's patches, and accumulated in the spleen during the first week of infection. Altered trafficking of B cells, in a non-specific manner to the spleen, likely enhanced the exposure of B cells to bacterial antigen, increasing the potential for activation of cognate cells, which in turn have the ability to drive T helper cell activation. Therefore, TLR-induced shedding of CD62L is likely to influence the activation of the $CD4^+$ T cell subset of the adaptive immune response.

B cells are positioned at the interface of innate and adaptive immunity

The activation of B cells through innate receptors such as TLRs will likely influence the developing adaptive immune response. The early production of cross-reactive IgM by TLR-stimulated marginal zone B cells during *S. typhimurium* infection, for example, likely had several effects on the initiation of the adaptive immune response, in addition to the direct complement-mediated killing mechanism discussed above. Firstly, as the resulting IgM was capable of binding *S. typhimurium* antigens (chapter 4), there was potential for the direct binding of bacteria, with the induction of phagocytosis by splenic macrophages, and possibly dendritic cells, expressing the high affinity Fcα/μ receptor [335]. The ongoing stimulation

of these cells by TLRs and other innate receptors will enhance antigen presentation of the phagocytosed bacterial antigen, allowing subsequent activation of $CD4^+$ and $CD8^+$ T cells. Secondly, as B cells themselves express the Fcα/μ receptor [335], uptake of IgM-coated bacteria will likely also enhance antigen presentation to T helper cells by B cells. Thus the early activation of the $CD4^+$ T cell response is likely influenced by the innate responses of B cells, a concept that has recently been reported in the *S. typhimurium* infection model [151], although my own data from day 7 of infection reported T cell cytokine responses to be normal in the absence of B cells (figure 5.6).

The involvement of TLRs at the interface of innate and adaptive immunity has long been recognised [336,337]. In particular, stimulation of B cell TLRs has been shown to induce significant changes in B cells that result in increased antigen presenting capacity, which in turn impacts upon T helper cell activation. These changes include the upregulation of surface MHC class II, which preferentially present cognate antigen taken up through the BCR [135], upregulation of co-stimulatory molecules, such as CD80, CD86 and CD40 [124], and the secretion of cytokines capable of inducing T helper cell differentiation [124]. Thus, the early innate activation of B cells by TLR ligands not only aids antibody production, which can impact upon the activation of other cell types, but also helps in the initiation of the adaptive immune response by focussing B cell migration to the spleen, inducing their activation, and increasing antigen presentation to T cells. Thus, the early innate responses of B cells following TLR stimulation promote both B and T cell activation.

Conflicting evidence on the innate roles of B cells in *Salmonella* infection

Here, I have summarised the innate functions of B cells in *S. typhimurium* infection, which include the accumulation of B cells in the spleen, an early plasma cell IgM response, and a potential for antigen presentation to $CD4^+$ T cells (chapters 3 & 4). Despite these observations, the absence of B cells (by B cell depletion of wild type mice) did not have a significant impact on splenic bacterial load at the peak of infection, on day 7 (figure 5.6B). Thus, one could conclude that these innate responses of B cells are not influencing the control of bacterial growth. However, I would argue that B cells might indeed be contributing to bacterial killing, be it directly or indirectly, but that the effects are either too small to detect by the assay used, or that there is a timing/kinetics issue, and perhaps looking only on day 7 of infection is not sufficient to detect such differences. I favour the latter explanation, and would investigate further by performing a day-by-day analysis of bacterial loads in wild type and B cell-deficient (or -depleted) mice.

Cognate roles of B cells in T cell differentiation

The TLR-induced changes to B cell phenotype significantly increases their antigen presenting ability. However, the precise role of B cells in $CD4^+$ T cell differentiation remains a topic of debate. Here, I showed that initial T cell priming occurred independently of B cells, both in terms of numbers of antigen-specific T cells and their effector phenotype (chapters 5 & 6). The efficient generation of T helper cell memory, however, was undoubtedly dependent on B cell presence (chapters 5 & 6). Specifically, B cells were necessary in the first ~10 days of *S. typhimurium* infection (chapter 5), or even earlier in the peptide immunisation system (chapter 6), for the development of $CD4^+$ T cell memory. This early dependence on B cells was unexpected, as B cells were not thought to be efficient at antigen presentation and influencing T cell responses until late in the immune response, either due to their inability to prime naïve T cells [139], or due to the low numbers of antigen-specific B cells present before proliferation in the GC [133]. However, the early requirement for B cells, identified here, points to their role in influencing T cell memory generation well before the GC reaction develops, as is discussed below.

Interestingly, I found another T helper cell population to be dependent on the presence of B cells, the T follicular helper cells. In chapter 5, I showed the numbers of T_{FH} cells to increase dramatically during the first week of *S. typhimurium* infection in B cell-sufficient mice, a phenomenon that was absent in μMT mice. Furthermore, following B cell depletion, the T_{FH} cell population was rapidly lost, within a few days, highlighting the role of B cells in the generation and/or maintenance of this population. The exact mechanism of this influence of B cells on T_{FH} cells remains unknown, but is perhaps a survival niche or signal. Potential candidates might be B cell expression of ICOSL, or B cell-derived IL-6 production.

Heterogeneity of the T_{FH} cell population

The population of $CD4^+$ T cells with the T_{FH} cell phenotype was found to expand rapidly during the early stages of *Salmonella* infection in wild type mice (chapter 5). A large proportion of these cells had a Th1 effector cell phenotype, as determined by their expression of the Th1 master regulator, Tbet, and their secretion of IFNγ (chapter 5). This observation, together with the reports that antigen-activated T cells upregulate CXCR5 and migrate into the follicles soon after activation [75], suggests that such T cells with the T_{FH} cell phenotype are antigen-specific T cells responding to the infection. Indeed, reports in the Th2 setting of helminth infection, show that the IL-4-producing T cells are localised within

the B cell follicles and express markers typical of T_{FH} cells [73,74], supporting the notion that antigen-activated effector T cells may gain the T_{FH} cell phenotype (or vice versa). Together, these data highlight the heterogeneity within the T_{FH} cell subset.

In the *Salmonella* infection model, it is known that the GC reaction, and the appearance of high affinity class-switched antibody, doesn't occur until relatively late in infection, at around week 4-5 after onset [206]. Thus, the early T_{FH} cells with a Th1 effector phenotype that appear during the first week of infection do not seem to be functioning as true helpers for the B cell response, in that they do not induce GC formation. This observation leaves us with the interesting possibility that there might be two waves of T_{FH} cells in this infection. Firstly, the early cells of the T_{FH} cell phenotype may simply be antigen-activated Th1 cells acquiring a transient $CXCR5^+$ phase and migrating through the follicles, whereas later, true T_{FH} cells that are specialised in helping B cells, aid the GC reaction and the differentiation of high affinity class-switched plasma and memory cells.

Clearly, the distinction between these two possible waves of T_{FH} cells is a topic of ongoing research in our laboratory. We aim to determine whether the 'early' and 'late' T_{FH} cells differ in their localisation within the follicles/GCs, gene expression profiles, and helper function. Using transcription factor identification, it may be possible to distinguish between these two potential populations of T_{FH} cells. In the helminth model, for example, it was shown that the Th2 effector cells located in the follicles expressed both the Th2-associated transcription factor GATA3, and the T_{FH} cell-associated transcription factor Bcl-6 [74]. Therefore, analysing the expression of the Th1-associated transcription factor, Tbet, as well as Bcl-6 in 'early' and 'late' T_{FH} cells in the *Salmonella* infection model may allow distinction. One might expect true 'late' T_{FH} cells to express only Bcl-6, whereas the 'early' T_{FH} cells, which were shown to express Tbet (chapter 5), may or may not also express Bcl-6.

The correlation between T_{FH} cells and memory generation

The results showing a requirement for B cells in the initial ~10 days of *S. typhimurium* infection contradicts previous thinking that B cells were only efficient at antigen presentation late in infection, or in the activation of memory T cells. However, the observation that the T cell-dependent GC response is slow to develop in the *Salmonella* model, with GCs and class switched antibody appearing around week 4-5 of infection [206], suggests that the B-T cell interaction necessary for T helper cell memory formation occurs well before the GC reaction.

Furthermore, the lack of the early expansion of the T_{FH} cell population during *S. typhimurium* infection in B cell-deficient mice, and the rapid loss of this population soon after B cell depletion, showed that the presence or absence of T_{FH} cells correlated well with the generation of T helper cell memory (chapter 5). Here, I raise the possibility that, in the first ~10 days of infection, B and T cells interact in the follicles and such T cells with the T_{FH} cell phenotype receive the signal(s) required for memory development. In other words, soon after immunisation / onset of infection, activated antigen-specific T cells gain the $CXCR5^+$ T_{FH} cell phenotype and migrate to the follicle, interact with antigen-presenting B cells, and receive the signal(s) necessary for memory development. Thus, in essence, such 'early' T_{FH} cells might be memory precursors and the reason for the early increase in CXCR5 expression might be for the migration to the follicle to receive the vital signal(s) from B cells.

The 'Big Picture' of T cell memory generation

As discussed in the main introduction (figure 1.3), there are several theories as to the differentiation pathway of memory T helper cells [77,81]. Recent data provides evidence that *in vitro*-derived effector T cells are capable of differentiating into memory T cells *in vivo* [338,339], and that *in vivo*-generated $IFN\gamma^+$ effector cells can form long-lived memory cells [340], supporting the linear model of memory development. Whereas data from our own laboratory shows memory cell development is capable *in vivo* without effector cell differentiation [215], suggesting a divergent model is likely. The model of memory cell differentiation is further complicated by the discovery of 'central' and 'effector' memory subsets in the $CD4^+$ T cell compartment [82]. How these subsets of memory cells fit into the pathway is unknown, and highlights the fact that many questions remain as to the differentiation processes that lead to memory development. Furthermore, at what stage along the differentiation pathway B cells are required, also remains unknown. However, the data presented in this thesis allow me to speculate on the likely model of the involvement of B cells in T cell memory differentiation.

The illustration shown in figure 7.1 summarises some of what is known about the differentiation of effector and memory T helper cells. Specifically it shows the B cell-independent differentiation of short-lived effector cells, which requires the transcription factor Blimp-1 [92]. The generation of T cell memory, on the other hand, is B cell-dependent. For simplicity, I have omitted central and effector memory cell subsets, as little is known about the differentiation of these cells. Importantly, figure 7.1 highlights the

requirement for a B-T cell interaction in memory T cell development, although the exact signal that B cells provide remains unidentified (represented by the question mark). Evidence from $CD8^+$ T cell differentiation reveals that Blimp-1 expression promotes the generation of short-lived effector cells, whilst inhibiting Bcl-6 expression [89,341]. Conversely, Bcl-6 has been implicated in both the differentiation and maintenance of memory $CD8^+$ T cells [90]. It is, therefore, possible that Bcl-6 may also control the differentiation of the memory population of $CD4^+$ T cells. Published reports show this transcription factor to control the development of T_{FH} cells in the T helper cell compartment [41,42]. Therefore, the involvement of the transcription factor, Bcl-6, in both $CD8^+$ T cell memory formation, and $CD4^+$ T_{FH} cell differentiation, strengthens my proposal, here, that T_{FH} cells may be memory cell precursors.

Could T_{FH} cells be memory precursors?

The diagram presented in figure 7.2 shows an updated version of the $CD4^+$ T cell memory generation model, incorporating my theory that T_{FH} cells, or a proportion of them, are potentially memory precursors. It is well documented that, soon after immunisation, antigen-activated T cells upregulate CXCR5 expression and migrate to the follicles [75,342]. These cells with the T_{FH} phenotype found in large numbers in the early stages of *S. typhimurium* infection have been found to express the Th1 transcription factor, Tbet, and secrete IFNγ (chapter 5). Due to the expansion of T_{FH} cells during the early stages of infection and their effector cell phenotype, these cells are likely to be antigen-specific T cells responding to infection, undergoing a transient acquisition of T_{FH} cell phenotype. As mentioned above, the transcription factor, Bcl-6, is known to be responsible for driving cells of the T_{FH} cell phenotype [41,42]. During this T_{FH} cell phase, these antigen-activated cells, located in the follicle, have the potential to interact with B cells and receive the relevant signal(s) necessary for memory differentiation. The observation that B cells are required during the first ~10 days of an immune response (chapters 5 & 6) certainly suggests that it is at this early stage that the B-T cell interaction required for memory generation occurs. However, the exact signal(s) that B cells are providing requires further investigation, and is discussed further below.

Unanswered questions

Despite my data going some way to identifying the timing of the involvement of B cells in T helper cell memory generation, there are many questions that remain. In fact, as with most projects, many more questions have arisen from the results presented. One of the questions

that is foremost in my mind is: what is the signal(s) that B cells are providing to T helper cells for the generation of memory? The fact that T helper cell memory is absent in μMT mice (chapters 5 & 6) suggests that B cells are providing a specific signal that other APCs, such as dendritic cells, cannot provide. Previous members of our laboratory have shown that direct contact between cognate B and T cells, requiring MHC class II expression by B cells, is required for memory generation [142], showing that B cell antigen presentation is essential. Additionally, IL-7 signalling is thought to be required for both the generation and maintenance of T helper cell memory [343], although the source of this IL-7 requires further investigation. Meanwhile, an interaction between CD40 and CD40L, on B and T cells respectively, is not essential for memory formation, but is vital for the re-activation of memory cells [215].

Recent (provisional) data from our laboratory strengthens the observed correlation between T_{FH} cells and memory. For example, MD4 mice, in which all B cells recognise Hen Egg Lysozyme and thus cannot take up and present other antigens, lack T_{FH} cells and do not generate T cell memory in the *Salmonella* infection model (T.A. Barr, S. Brown & D. Gray, unpublished data). Furthermore, the most recent data from our laboratory indicates T helper cell memory to be impaired, although not absent, when B cells lack expression of ICOSL (T.A. Barr, S. Brown & D. Gray, unpublished data). As ICOSL has also been shown to be involved in the generation of T_{FH} cells [40], these data, again, highlight a correlation between T_{FH} cell generation and memory cell development. Together, these data reinforce the theory that the early migration of activated T cells into the follicle may be the time of the B-T cell interaction necessary for memory development. Clearly, further investigation is required into the identity of the specific signal that B cells are providing for T helper cell memory differentiation.

Concluding remarks

Understanding the fundamental principles of immune activation and memory generation is essential for the production of vaccines with the highest possible efficacy. The data presented in this PhD thesis has expanded our knowledge of the roles that B lymphocytes play in such immune activation, and highlights the importance of an early interaction between B and T cells for efficient memory generation. The varied functions of B cells should not be underestimated, and this requirement for B cell antigen presentation should be considered during vaccine development, to ensure that T cell memory generation is optimal.

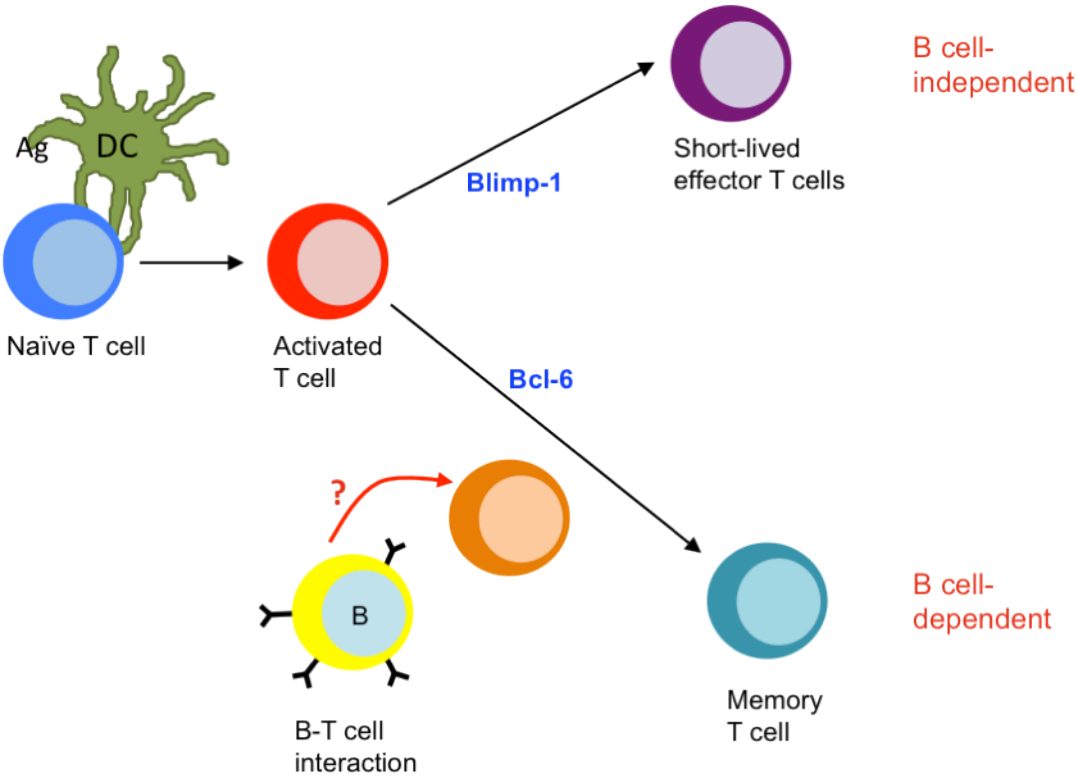

Figure 7.1: A summary model of T helper cell memory differentiation. The differentiation pathway of naïve CD4⁺ T cells into effector and memory populations remains unknown. Here, I speculate on the possible model, focussing on the involvement of B cells. While the differentiation of short-lived effector cells in a Blimp-1-dependent manner does not require B cells, the generation of memory T cells is B cell-dependent. Although it is known that memory T cell development requires a cognate B-T cell interaction, the exact signal(s) that B cells provide remains unknown (represented by the question mark).

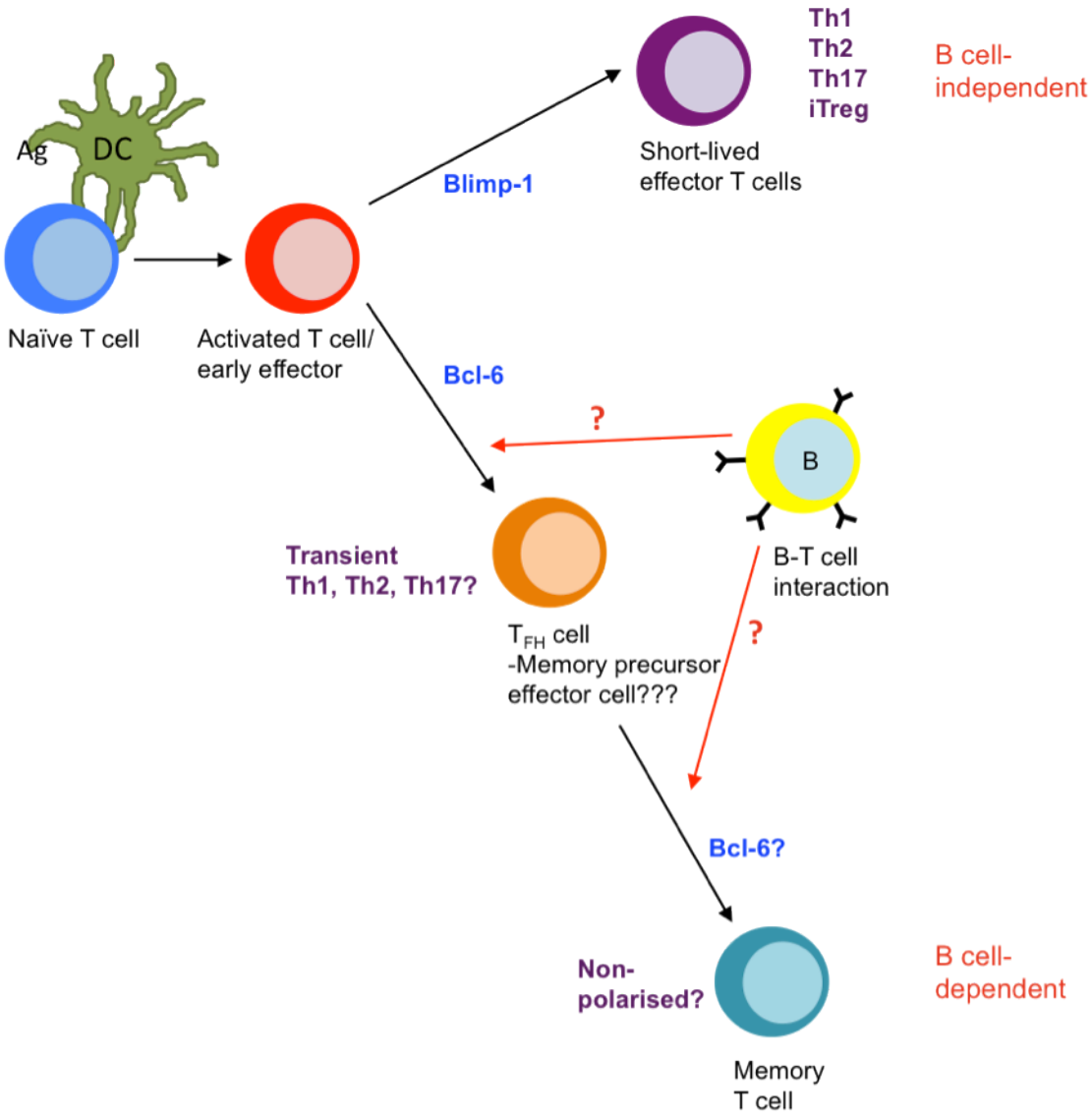

Figure 7.2: Are T follicular helper cells memory precursors? The differentiation pathway of naïve CD4⁺ T cells into effector and memory populations remains unknown. Here, I speculate on the possible model, focussing on the possibility that T_{FH} cells might be memory precursors. Antigen-activated T cells gain the CXCR5⁺ T_{FH} cell phenotype and migrate to the follicle, where they perhaps interact with B cells and receive the signal necessary for memory differentiation. However, the signal provided by B cells to promote memory T cell formation remains unknown (represented by the two red question marks).

CHAPTER 8: Appendices

Appendix 1 – Additional data

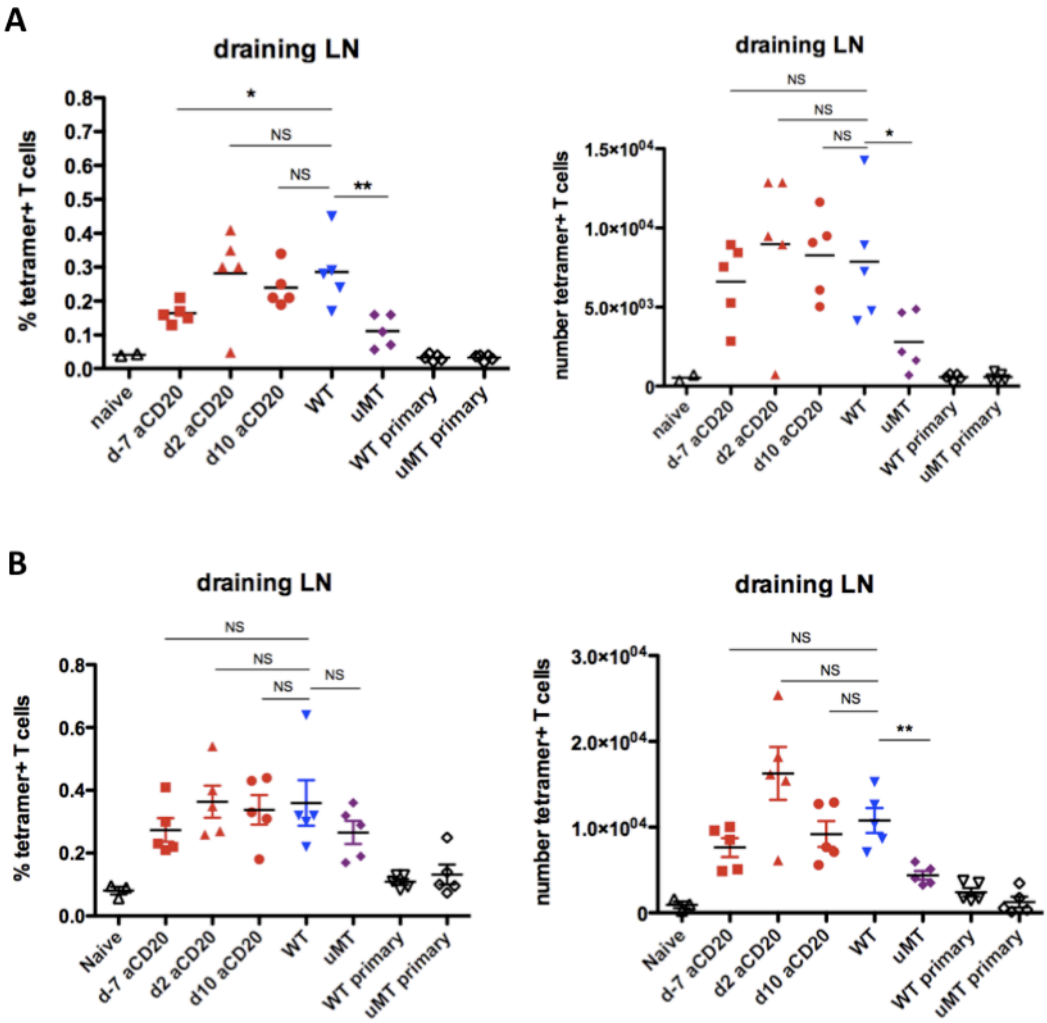

Appendix 1: Boost T cell responses following anti-CD20 treatment, from experiments 2 & 3. Mice were immunised with peptide in CFA s.c. and boosted 6 weeks later with peptide-pulsed dendritic cells. Some groups were treated with anti-CD20 on either day -7, day 2 or day 10 (red). The wild type B cell-sufficient group is in blue, with μMT mice in purple. On day 5 post-boost, draining lymph nodes were removed and the percentage (left) and absolute numbers (right) of antigen-specific T cells identified by tetramer staining. Data shown is from experiment 2 (A) and 3 (B). For experiment 1, see figure 6.5, and for pooled data analysis see figure 6.6. Statistical analysis was performed using the Student's *t*-test. NS = not significant.

Appendix 2 – Published paper

TLR-Mediated Loss of CD62L Focuses B Cell Traffic to the Spleen during *Salmonella typhimurium* Infection

Vicky L. Morrison, Tom A. Barr, Sheila Brown and David Gray

The Journal of Immunology **185:** 2737-2746

Permission for printing in this thesis has been obtained from the publisher and co-authors.

The Journal of Immunology

TLR-Mediated Loss of CD62L Focuses B Cell Traffic to the Spleen during *Salmonella typhimurium* Infection

Vicky L. Morrison, Tom A. Barr, Sheila Brown, and David Gray

B cells recognize Ags on microorganisms both with their BCRs and TLRs. This innate recognition has the potential to alter the behavior of whole populations of B cells. We show in this study that in culture and in mice, MyD88-dependent activation of B cells via TLR2 or TLR9 causes the rapid loss of expression of CD62L by metalloproteinase-dependent shedding. Adoptive transfer of in vitro CpG-activated B cells showed them to be excluded from lymph nodes and Peyer's patches, but not the spleen. In vivo, both injection of CpG and systemic infection with *Salmonella typhimurium* caused the shedding of CD62L and the consequent focusing of B cell migration to the spleen and away from lymph nodes. We propose that wholesale TLR-mediated changes to B cell migration influence the development of immunity to pathogens carrying appropriate ligands. *The Journal of Immunology*, **2010, 185: 2737–2746.**

B cells as Ag presenters and Ab producers are a major component of the adaptive immune response, however, they also have the ability to respond to pathogens in an innate fashion. They do this by recognizing structurally conserved pathogen ligands through TLRs expressed at the cell surface and in the endosomal compartment. Murine B cells are known to express TLR1–9 at the mRNA level (1), although there is differential expression in certain subsets. When stimulated through these receptors in vitro, B cells are induced to proliferate and differentiate into Ab-secreting plasma cells in a T cell-independent manner (2), whereas in vivo responses to T-dependent Ags also require TLR signaling in B cells for optimal Ab production (3, 4). TLR stimulation of B cells also induces upregulation of cell-surface MHC class II and costimulatory molecules (1), enhancing their Ag-presenting capacity, and secretion of cytokines such as IL-6, IL-10 and IFN-γ (1), allowing the regulation of helper and regulatory T cell responses (5). Therefore, the rapid innate response of B cells to pathogens via TLR stimulation has a direct impact not only on the developing adaptive B cell response, but also on the magnitude and phenotype of the Th cell response.

To study TLR-dependent B cell responses in vivo, we made use of the murine infection model of typhoid fever, *Salmonella enterica* serovar Typhimurium. Systemic infection by this intracellular Gram-negative bacterium, which resides predominantly in macrophages, results in the development of strong Th1 and Ab responses (6, 7). Early in infection, innate macrophage responses are required to control bacterial growth (8), whereas specific Th1-associated cytokines (IFN-γ, TNF-α) are also crucial (9–11). The necessity of TLR signaling for clearance of *Salmonella* infection is well characterized. C3H/HeJ mice that lack TLR4 expression and so cannot respond to LPS are highly susceptible to *Salmonella* infection (12). TLR4 is thought to be important early in infection for cytokine production and killing of bacteria, whereas TLR2 (which recognizes bacterial glycolipids and lipopeptides) plays a role later (13). The lack of the MyD88 adaptor protein during the primary immune response to an attenuated strain of *Salmonella typhimurium* results in increased bacterial load, but these mice are able to clear the infection, albeit with delayed kinetics (14, 15). These mice appear to have impaired IL-12 production and reduced Th1 responses (16) and may in fact mount a skewed Th2 response (14).

The specific role of B cells in the *S. typhimurium* infection model has also been studied (17–19). B cells appear dispensable for the primary immune response to attenuated strains of *Salmonella*, with bacterial load at the peak of infection, and the primary T cell response being equivalent in B cell-deficient and wild-type mice (17). However, protective immunity is absolutely dependent on the presence of B cells, with B cell-deficient mice showing hugely impaired IL-2 and IFN-γ production by T cells after bacterial clearance (18), suggesting an absence of T cell memory (18, 19) and, in addition, showing increased mortality during challenge (18). Transfer of immune serum did not restore protection in B cell-deficient animals, suggesting one important role of B cells in this model is the presentation of Ag to T cells for the generation of memory (18). Indeed, to transfer protection to naive mice, both immune serum and T cells are required (20).

In our recent work, we have addressed the specific role of B cell TLR stimulation in *Salmonella* infection. Using mixed bone marrow chimeras in which the B cell compartment alone is deficient in MyD88 ($MyD88^{B-/-}$) reveals that primary T cell IFN-γ production during *S. typhimurium* infection is reduced, suggesting B cells play an important role as APCs in driving the early Th1 response (4) (T. Barr, S. Brown, and D. Gray, unpublished observations). Looking at Ab production, IgG2a/c is reduced in $MyD88^{B-/-}$ mice during *S. typhimurium* infection (4), and this correlates with the impairment of T cell production of IFN-γ. Recent work, showing TLR4-mediated changes to splenic structure (21), has highlighted the potential of TLR signaling to affect cell migration. This study started with the observation that certain TLR ligands alter the expression of CD62L on B cells, and we characterize in this study how this affects their migration during infection.

School of Biological Sciences, Institute of Immunology and Infection Research, University of Edinburgh, Edinburgh, United Kingdom

Received for publication March 5, 2010. Accepted for publication June 23, 2010.

Address correspondence and reprint requests to Prof. David Gray, Institute of Immunology and Infection Research, University of Edinburgh, Ashworth Laboratories, King's Buildings, West Mains Road, Edinburgh, Midlothian EH9 3JT, U.K. E-mail address: d.gray@ed.ac.uk

The online version of this article contains supplemental material.

Abbreviations used in this paper: ADAM, a disintegrin and metalloproteinase; HEV, high endothelial venule; KO, knockout; MFI, mean fluorescence intensity; $MyD88^{B-/-}$, B cell compartment deficient in MyD88; poly I:C, polyinosinic-polycytidylic acid; TRIF, Toll/IL-1R domain-containing adaptor inducing IFN-β.

 0022-1767/10/$16.00

www.jimmunol.org/cgi/doi/10.4049/jimmunol.1000758

CD62L (L-selectin) is an adhesion molecule belonging to the C-type lectin family that binds carbohydrate ligands, such as those induced on inflamed endothelium and those constitutively expressed at high endothelial venules (HEVs) (22). More specifically, CD62L ligands include sulfated carbohydrates of glycosylation-dependent cell adhesion molecule 1 and CD34 at lymph node HEVs (23) and mucosal addressin cell adhesion molecule-1 at Peyer's patch HEVs (24). Binding of CD62L initiates tethering and rolling of cells and allows the subsequent transmigration from the bloodstream into tissues (25, 26). Blocking Abs against CD62L have been shown to inhibit lymphocyte binding to HEVs both in vitro and in vivo (27), whereas CD62L knockout (KO) mice display a 70–90% reduction in lymph node cellularity (28). Naive-lymphocytes, including B cells, are $CD62L^+$ and express varying levels of this molecule depending on the organ from which they are isolated. Upon stimulation by cognate Ag through the BCR or by phorbol esters such as PMA, CD62L is shed from the cell surface. The enzyme responsible for shedding of surface CD62L is a zinc-containing membrane-associated metalloprotease, a disintegrin and metalloproteinase (ADAM) 17 (also known as TACE), which also cleaves TNF-α (29). This cleavage of CD62L by lymphocytes occurs rapidly, with 90% of lymph node cells shedding CD62L in response to PMA within 1 h (30).

CD62L expression is important in the development of immune responses, as CD62L-deficient mice have reduced leukocyte migration to inflamed sites and impaired delayed-type hypersensitivity responses (31), as well as impaired primary T cell proliferation and cytokine production (32). Furthermore, the metalloprotease-mediated shedding of CD62L is crucial, as mice expressing a mutant form that cannot be cleaved from the cell surface exhibited impaired responses to viral infection and delayed viral clearance (33, 34). All of the work to date on CD62L has focused on T cells, and little is known about the consequence of impaired modulation of B cell CD62L.

In this study, we found that stimulation of B cells with ligands for TLR2 or TLR9 caused the rapid loss of expression of CD62L and that these cells localized to the spleen but not the lymph nodes when adoptively transferred i.v. We show that similar changes in CD62L expression occur in response to heat-killed *Salmonella* and Ag extracts. Furthermore, during *S. typhimurium* infection, B cells shed CD62L and show altered localization, increasing numbers in the spleen, with decreasing proportions in lymph nodes and Peyer's patches. This focusing of B cell migration on the spleen may be important for TLR-dependent B cell-mediated support for *Salmonella*-specific T cell responses.

Materials and Methods

Mice

C57BL/6, $MyD88^{-/-}$ (35), Toll/IL-1R domain-containing adaptor inducing IFN-β $(TRIF)^{-/-}$ (36), $TLR2^{-/-}$ (37), $TLR9^{-/-}$ (38), and $Ly5.1^+$ mice were bred and maintained in specific pathogen-free conditions at the School of Biological Sciences Animal Facility, University of Edinburgh (Edinburgh, U.K.). In all experiments, mice aged 6–10 wk were used, and all genetically modified mice were backcrossed 6–10 generations to C57BL/6. Experiments were covered by a Project License granted by the United Kingdom Home Office under the Animals (Scientific Procedures) Act of 1986. Locally, the University of Edinburgh Ethical Review Committee approved this license.

Cell isolation and B cell purification

Single-cell suspensions were prepared from spleen, lymph nodes, and Peyer's patches by manual disruption in IMDM plus 5% FCS and penicillin/streptomycin. Following RBC lysis, cells were labeled with anti-CD19 microbeads and sorted over two consecutive LS columns according to the manufacturer's instructions (Miltenyi Biotec, Bisley, U.K.). Purity was >98% (data not shown).

In vitro TLR stimulation cultures

Splenocytes or purified B cells were cultured at 4×10^6 cells/ml in complete IMDM in 24-well plates. Endotoxin-free TLR ligands (Invivogen, Autogen Bioclear U.K., Wiltshire, U.K.) were used at the following concentrations: the TLR2 ligands zymosan, peptidoglycan, and PAM_3 CSK4 were used at 10, 10, and 0.2 μg/ml, respectively; the TLR3 ligand polyinosinic-polycytidylic acid (poly I:C) was used at 25 μg/ml; LPS (TLR4) from *Escherichia coli* was used at 1 μg/ml; flagellin (TLR5) from *S. typhimurium* was used at 0.1 μg/ml; the TLR7 ligand loxoribine was used at 100 μM; and the TLR9 ligand unmethylated CpG DNA (ODN 1826, 5′-TCC ATG ACG TTC CTG ACG TT-3′) was used at 5 μg/ml. PMA and ionomycin (Sigma-Aldrich, Poole, U.K.) were used at 10 ng/ml and 1 μg/ml, respectively. Where appropriate, the metalloprotease inhibitor Ro 31-9790 (Roche Research Products, Welwyn Garden City, U.K.) was used at 50 μg/ml. For the recovery of CD62L expression, cells were harvested, washed, and plated out again at 4×10^6 cells/ml in fresh media.

In vivo CpG DNA immunization

C57BL/6 mice were immunized with 20 μg CpG DNA i.v. or mock immunized with PBS. Mice were bled pre-immunization and at various times post-immunization. Lymphocytes were isolated by separation on lymphocyte (Cedarlane Laboratories, Hornby, Ontario, Canada) and washed extensively pre-staining.

S. enterica *serovar Typhimurium infection*

The aroA-attenuated strain of *S. typhimurium* (SL3261) was used for all infections (39). Bacteria were grown as stationary-phase overnight (16 h) cultures in Luria-Bertani broth (Difco Laboratories, Surrey, U.K.). Animals were injected i.v. with 10^6 CFUs diluted in PBS. Infectious dose was determined by plating bacteria onto Luria-Bertani plates and culturing overnight at 37°C.

Preparation of S. typhimurium *Ags*

Bacterial Ags from *S. enterica* serovar Typhimurium were prepared as previously described (40). Briefly, overnight stationary-phase cultures of the SL3261 strain were heat-inactivated at 85°C for 30 min; ~2.5×10^8 CFU bacteria that had undergone heat inactivation were used for in vitro cultures. For B cell culture with live bacteria, around 2.5×10^6 CFU bacteria was used. To prepare the crude sonicate, overnight-cultured bacteria (SL3261 strain) were sonicated and debris removed by centrifugation. To make the C5 Ag, overnight culture of the C5 virulent strain of *S. typhimurium* was sonicated, alkali treated (NaOH), and neutralized in HCl. Both the crude sonicate and C5 Ag were used at 20 μg/ml.

In vivo proliferation assay

Mice were injected with 2 mg BrdU i.p. on days 2, 4, and 8 of *Salmonella* infection. The following day (days 3, 5, and 9), spleens were removed and single-cell suspensions prepared. Proliferation, as determined by BrdU incorporation, was measured by staining for BrdU using an FITC-BrdU Flow Kit (BD Biosciences, San Jose, CA) as described in the manufacturer's instructions. Briefly, cells were surface stained with anti-CD19 PE and anti-CD4 APC, washed, then resuspended in fix/perm buffer overnight. The following day, cells were washed and DNase treated for 1 h at 37°C, then stained with anti-BrdU FITC.

Cell transfers

For cultured cell transfer, purified B cells from $Ly5.1^+$ donor mice were cultured with CpG DNA as described above for 4 h or left unstimulated. Postharvesting, cells were washed extensively in PBS and 5×10^6 cells injected i.v. into recipient C57BL/6 mice. The $CD62L^{lo}$ phenotype of CpG-stimulated cells was confirmed by flow cytometry.

For $CD62L^{hi}$ blood cell transfer, blood was collected into heparin from donor mice by cardiac puncture. Lymphocytes were extracted and washed as described above. A total of 5×10^6 unsorted lymphocytes was injected i.v. into recipient uninfected or day 6 *Salmonella*-infected mice. The $CD62L^{hi}$ phenotype of donor cells was confirmed by flow cytometry.

Flow cytometry

Prestaining, cells were washed in FACS buffer (PBS with 0.05% sodium azide and 3% FCS). The following Abs were used (all from BD Biosciences unless otherwise stated): anti–CD19-PE, anti–CD4-APC, anti–CD62L-FITC (Abcam, Cambridge, U.K.), IgG2a-FITC isotype control (Abcam), anti–Ly5.1-biotin, and streptavidin-PerCP. Cells were stained for 20 min on ice and washed three times in FACS buffer. Samples were analyzed on

an FACSCalibur flow cytometer (BD Biosciences) using CellQuest software and data analyzed using FlowJo software (Tree Star, San Carlos, CA).

Statistics

The Student paired *t* test was used to calculate significance values where appropriate.

Results

Loss of CD62L expression on B cells in response to some TLR ligands

B cells are known to lose expression of CD62L following the ligation of their BCR (41). We wished to know whether activation via innate receptors, such as TLRs, altered expression of this molecule. To examine the effect of TLR stimulation of B cells on their expression of CD62L, purified B cells were cultured with a variety of TLR ligands in vitro. We found that B cells lose expression of CD62L in response to specific TLR ligands, namely PAM_3CSK4 (a TLR2 ligand), CpG DNA (TLR9 ligand), and partially shed in response to poly I:C (a TLR3 ligand). In relation to the latter (TLR3), increasing the dose of poly I:C caused a greater degree of CD62L loss (Supplemental Fig. 1), indicating the partial loss is simply a result of efficacy. Stimulation with zymosan, peptidoglycan (both TLR2 ligands), LPS, flagellin, or loxoribine (ligands for TLR4, -5, and -7, respectively) did not induce shedding (Fig. 1*A*). The highest levels of CD62L expression are found on follicular B cells (Supplemental Fig. 1) and peripheral blood B cells (similar profile to follicular B cells; data not shown); however, even the low levels seen on marginal zone B cells are significantly modulated by CpG stimulation (Supplemental Fig. 1).

Using cells from MyD88$^{-/-}$, TRIF$^{-/-}$, TLR2$^{-/-}$, and TLR9$^{-/-}$ mice, it was confirmed that loss of CD62L on B cells in response to PAM_3CSK4 is MyD88 and TLR2 dependent, its loss in response to poly I:C is TRIF dependent, and, in response to CpG DNA, is MyD88 and TLR9 dependent. All KO B cells were able to shed when stimulated with PMA/ionomycin (Fig. 1*B*) or by cross-linking their BCR (data not shown).

Loss of CD62L expression by B cells stimulated with CpG DNA is rapid and due to shedding from the surface

An analysis of CD62L expression over time after CpG stimulation revealed that B cells lost surface expression of CD62L within 2 h of culture (Fig. 2*A*). This expression was not restored within the 12 h analyzed. To establish whether B cells lose CD62L expression in vivo in response to CpG DNA, mice were injected with 20 μg CpG DNA. As can be seen in Fig. 2*B*, the percentage of B cells in the blood that express high levels of CD62L was significantly reduced at 2, 4, and 8 h postinjection. Expression levels returned to normal by 24 h postinjection.

It seems likely that the mechanism by which B cells rapidly downregulate CD62L is by shedding from the surface, as characterized previously with respect to activation by PMA (33). To demonstrate that this was the case, we used the metalloprotease

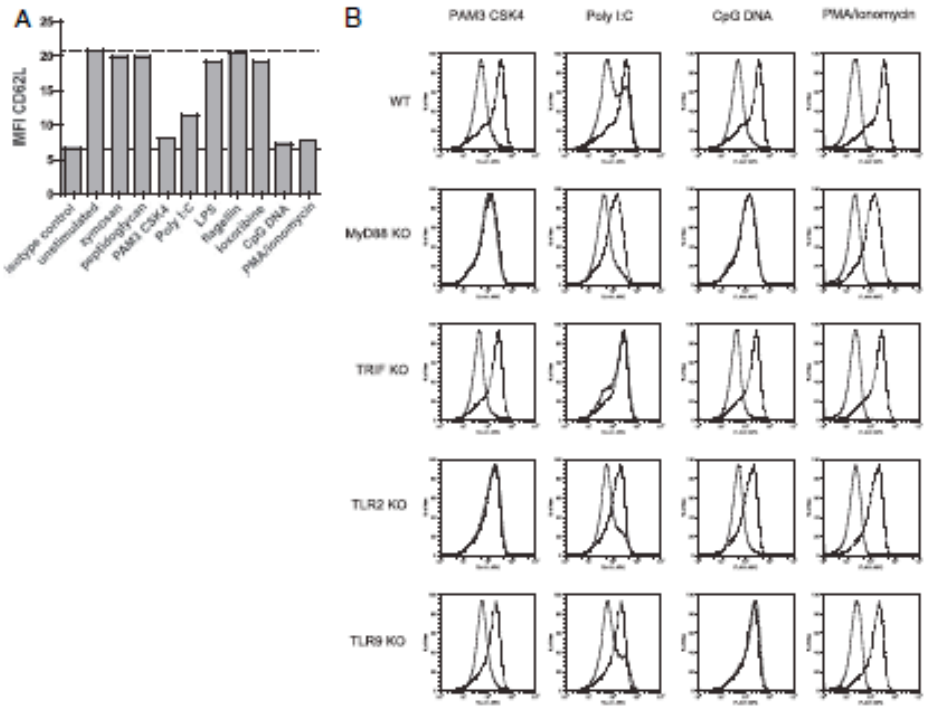

FIGURE 1. B cells rapidly shed CD62L in response to some TLR ligands. Purified splenic B cells from C57BL/6 (*A*, *B*), MyD88$^{-/-}$, TRIF$^{-/-}$, TLR2$^{-/-}$, and TLR9$^{-/-}$ mice (*B*) were cultured with a variety of TLR ligands for 4 h. B cell expression of CD62L was analyzed by flow cytometry. PMA/ionomycin is included as a positive control. In *A*, dotted line represents unstimulated, and bold line represents isotype control. In *B*, dashed line represents unstimulated, and bold line represents TLR stimulated. The data presented are from a single experiment using one spleen from each of the KO mice. Data are representative of four independent experiments.

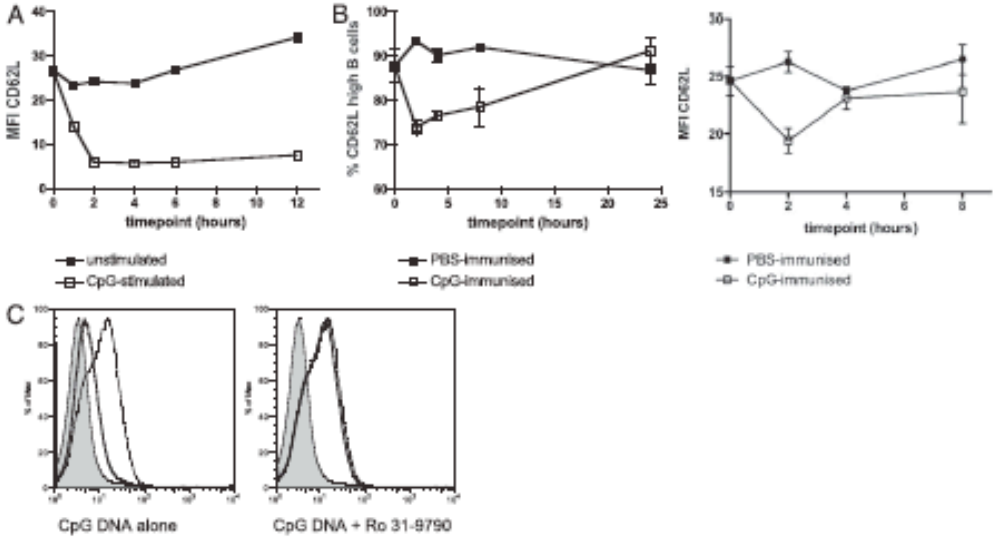

FIGURE 2. B cell shedding of CD62L in response to CpG DNA is rapid both in vitro and in vivo and is inhibited by a metalloprotease inhibitor. *A*, Purified B cells were cultured with 5 μg/ml CpG DNA for up to 12 h. *B*, C57BL/6 mice were injected with 20 μg CpG DNA and bled 2, 4, 8, and 24 h later. B cell CD62L was identified both by percentage of $CD62L^{lo}$ cells (*left panel*) and MFI (*right panel*). *C*, Purified B cells were cultured with CpG DNA for 4 h with or without the addition of 50 μg/ml metalloprotease inhibitor Ro 31-9790. The isotype control is shaded, unstimulated is a dashed line, and CpG stimulation (± Ro 31-9790) is in bold. In all cases, B cells were stained for expression of CD62L and analyzed by flow cytometry. Data in *A* and *C* are from an experiment using a single spleen and are representative of three independent experiments. In *B*, error bars display SEM with five mice per group and are representative of three experiments. MFI, mean fluorescence intensity.

inhibitor Ro 31-9790, which has previously been shown to inhibit CD62L shedding (42). Ro 31-9790 also inhibits shedding of TNF-α (43) and is, therefore, thought to target ADAM17 (TACE). When this inhibitor was included in the B cell culture with CpG DNA, the loss of CD62L from the cell surface at the 4-h time point was completely abolished (Fig. 2*C*). This confirms that the loss of surface CD62L by B cells in response to CpG DNA was due to shedding by the surface metalloprotease ADAM17 (TACE) and not any other mechanism.

CpG-stimulated B cells are excluded from lymph nodes and Peyer's patches

It is well known that CD62L is essential for leukocyte entry into the lymph nodes across the HEV (27). We predicted, therefore, that CpG-stimulated B cells that have a $CD62L^{lo}$ phenotype would show altered migration patterns in vivo. To investigate this, we transferred CpG-stimulated or unstimulated B cells, after 4 h of culture, into congenic Ly5-distinct hosts and looked the following day at their localization. The CpG-stimulated $CD62L^{lo}$ donor cells were ex-

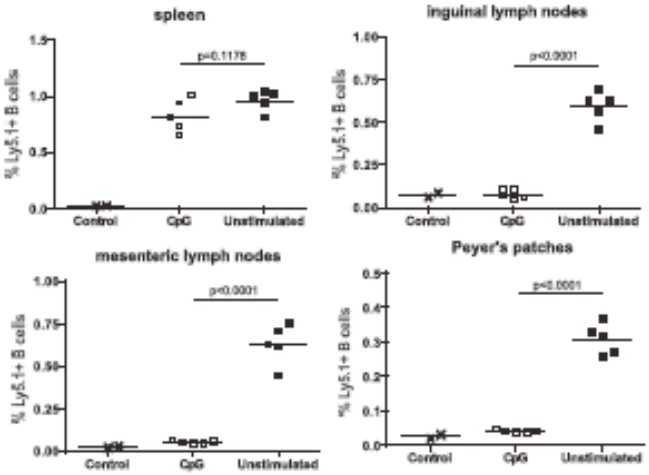

FIGURE 3. CpG-stimulated B cells are excluded from the lymph nodes and Peyer's patches. Purified $Ly5.1^+$ B cells were cultured with 5 μg/ml CpG DNA for 4 h or left unstimulated. Cells were harvested and washed, and 5 million cells were then transferred into C57BL/6 mice. The following day (~18 h post-transfer), organs were taken and donor cells identified. The control mice did not receive cell transfers, so indicate in background staining. Significance values were calculated using the Student paired *t* test.

cluded from the lymph nodes and Peyer's patches (Fig. 3) but trafficked normally to the spleen. These data indicate that TLR stimulation of B cells can impact on their migration patterns in vivo via changes in surface expression levels of CD62L.

B cells recover surface expression of CD62L ~2 to 3 d poststimulation and subsequently gain entry into lymph nodes and Peyer's patches

Having established the kinetics of CD62L shedding from the surface of B cells in response to TLR stimulation, we next analyzed the recovery of expression both in vitro and in vivo. Following culture with CpG DNA, B cells were washed extensively and either plated out again with fresh media in vitro or adoptively transferred into Ly5-distinct recipient mice. Fig. 4*A* shows that B cells recover CD62L expression after 3 d in culture, and in vivo, the re-expression happens after 2 d (Fig. 4*B*). The adoptive transfer showed that donor CpG-activated B cells were present in the lymph nodes and Peyer's patches by day 5 in numbers equivalent to unstimulated B cells. The lag of 3 d between CD62L re-expression in the spleen on day 2 and B cell migration to lymph nodes and Peyer's patches on day 5 is likely due to the normal homing patterns of B cells, in that they pause in secondary lymphoid tissues before re-entering the circulation.

B cells shed CD62L when stimulated with Ags from Salmonella

To confirm that B cells shed CD62L when encountering TLR ligands in the form of pathogenic bacteria, we stimulated B cells with Ags from the Gram-negative bacteria *S. enterica* serovar Typhimurium (hereafter referred to as *S. typhimurium*). The data presented in Fig. 5*A* reveal that B cells shed CD62L when stimulated with heat-killed bacteria, a crude sonicate of bacteria, or a semi-purified C5 Ag. However, no shedding occurred in response to live bacteria in vitro.

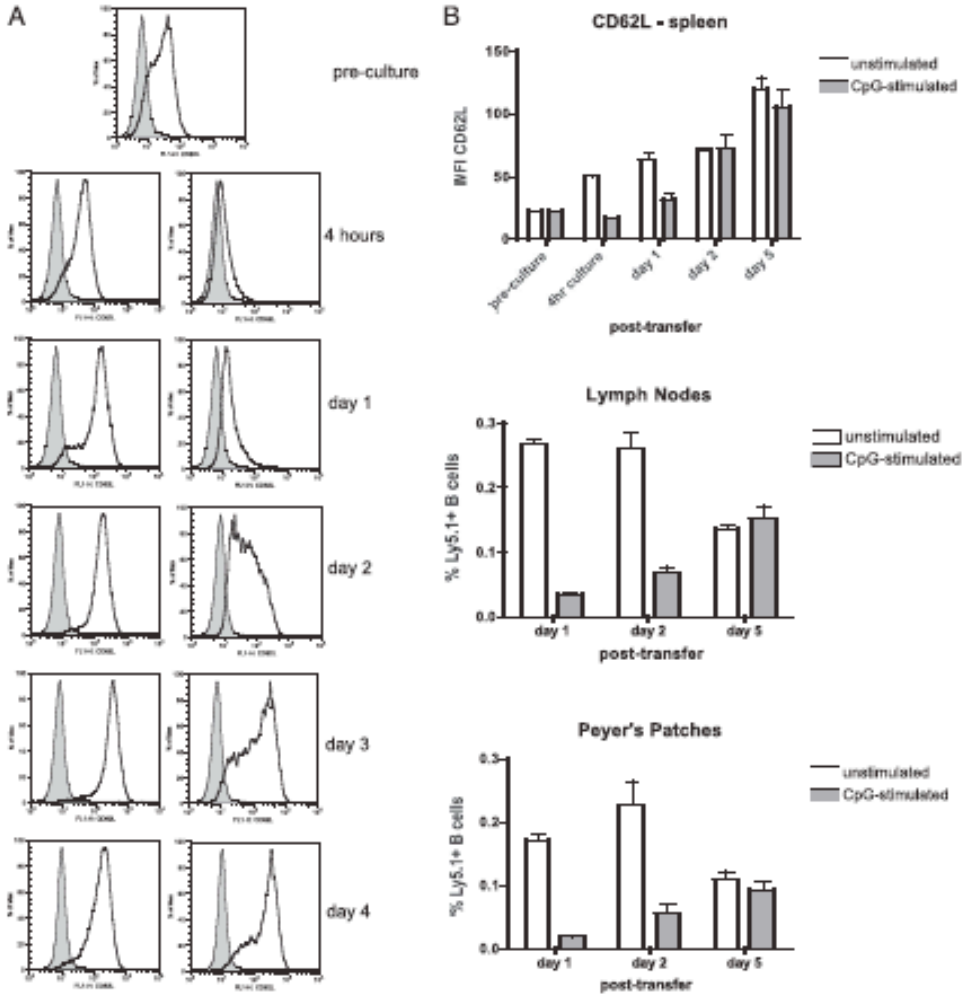

FIGURE 4. Pattern of CD62L recovery by B cells both in vitro and in vivo. B cells were stimulated with CpG DNA for 4 h in vitro. *A*, Cells were harvested, washed, and plated out again. Samples were taken up to 4 d later and analyzed for B cell expression of CD62L. *Left panels*, unstimulated; *right panels*, CpG-stimulated. *B*, After washing, 5 million cells were transferred into Ly5-distinct mice. Over the following days, organs were removed, donor cells identified, and CD62L expression levels analyzed. Error bars represent SEM with four mice per group. Data are representative of three experiments.

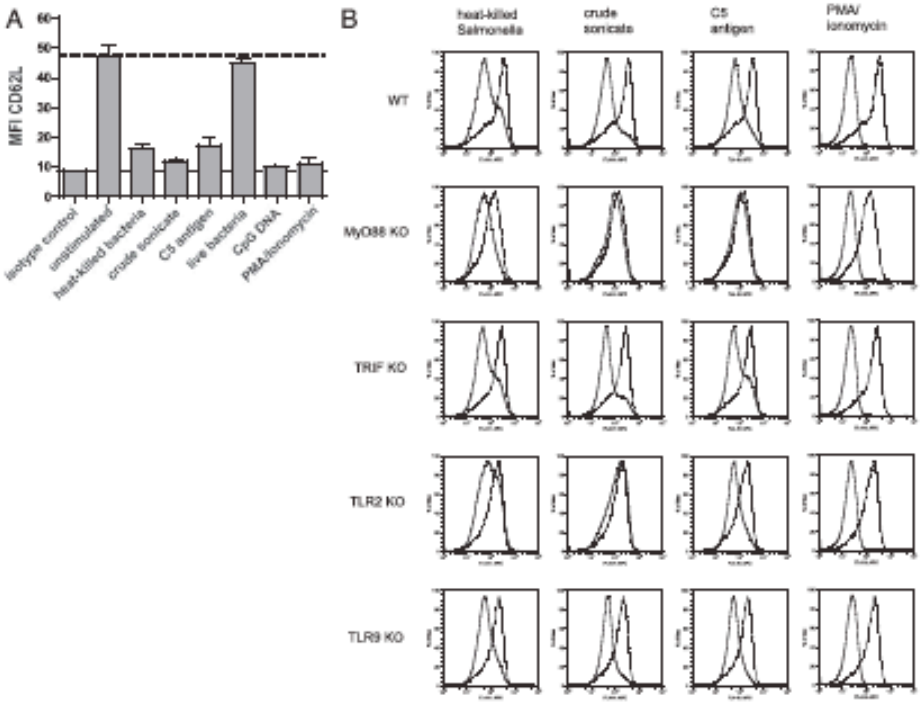

FIGURE 5. B cells rapidly shed CD62L in response to *S. typhimurium* Ags. Purified B cells from C57BL/6 (*A*, *B*), MyD88$^{-/-}$, TRIF$^{-/-}$, TLR2$^{-/-}$, and TLR9$^{-/-}$ mice (*B*) were cultured with a variety of Ags from *S. typhimurium* for 4 h. B cell expression of CD62L was analyzed by flow cytometry. In *A*, dotted line represents unstimulated, and bold line represents isotype control. Error bars indicate SEM. In *B*, dashed line represents unstimulated, and bold line shows stimulated cells.

To determine if a specific TLR and adaptor molecule is responsible for shedding induced by these bacterial Ags, KO cells were used. The data in Fig. 5*B* show that TLR2 and the adaptor molecule MyD88, rather than TLR9 or TRIF, are used to induce shedding in response to these bacterial Ag preparations.

Altered localization of B cells during S. typhimurium *infection*

The data shown so far would predict that TLR-induced changes in CD62L expression will result in altered migration of B cells during systemic infection with *S. typhimurium*. The data presented in Fig. 6*A* and 6*B* show that *S. typhimurium* infection caused profound alterations in the localization of B cells. In the lymph nodes and Peyer's patches, there was a rapid decrease in both the percentages (Fig. 6*A*) and absolute numbers (Fig. 6*B*, lymph nodes only) of B cells during the first week of infection. This was most apparent in the Peyer's patches, in which the proportion of B cells dropped from ~80% in an uninfected mouse to 20% by day 8 of infection. In the spleen, the percentage of B cells remains unchanged at day 4 and is reduced at day 8 (Fig. 6*A*), largely due to an influx of other cells (e.g., macrophages). However, looking at absolute numbers (Fig. 6*B*), there is actually a 2- to 3-fold increase in splenic B cell numbers at day 4 when compared with an uninfected mouse, and numbers remain elevated at day 8. The increase in B cell numbers in the spleen at this early stage of infection does not seem to be due to B cell proliferation, as BrdU incorporation by B cells was little above background and minimal in comparison with T cell division (Fig. 6*C*, 6*D*).

The changes in B cell populations seen in lymphoid organs (increase in spleen, reduction in lymph nodes and Peyer's patches) during *Salmonella* infection are likely due to TLR activation, as they are not so apparent in MyD88$^{-/-}$ mice (Supplemental Fig. 2).

These changes in B cell distribution within lymphoid organs are long lasting (Supplemental Fig. 3*B*). This is likely due to the chronic nature of this infection, in which bacteria were not cleared until 6–8 wk postinfection (Supplemental Fig. 3*A*). Together, the data in Fig. 6 support the notion that B cells shed CD62L in response to bacteria, are excluded from lymph nodes, and consequently enter the spleen in greater numbers, as entry to the spleen is independent of CD62L (44).

CD62L^{hi} B cells shed and migrate to the spleen, not lymph nodes, when transferred into Salmonella*-infected mice*

The data shown so far suggest that B cells shed CD62L during *S. typhimurium* infection and that this is the cause of altered migration patterns. To address this more directly, we isolated CD62L^{hi} B cells from the blood of Ly5.2$^+$ donor mice and transferred them into either *S. typhimurium*-infected or uninfected Ly5.1$^+$ recipient mice. Ly5.2$^+$ donor B cells were identified and CD62L expression analyzed after 18 h. The results displayed in Fig. 7*A* demonstrate that in uninfected mice, donor Ly5.2$^+$ B cells migrated to both the lymph nodes and spleen, whereas in infected mice, the Ly5.2$^+$ B cells were found in much greater numbers in the spleen and significantly reduced numbers in the lymph nodes. Donor cells identified in the spleens of uninfected mice have maintained their CD62L^{hi} phenotype, whereas in the spleens of infected mice, donor B cells have shed and are predominantly CD62L^{lo} (Fig. 7*C*). These data confirm that B cells shed CD62L early during *S. typhimurium* infection and that

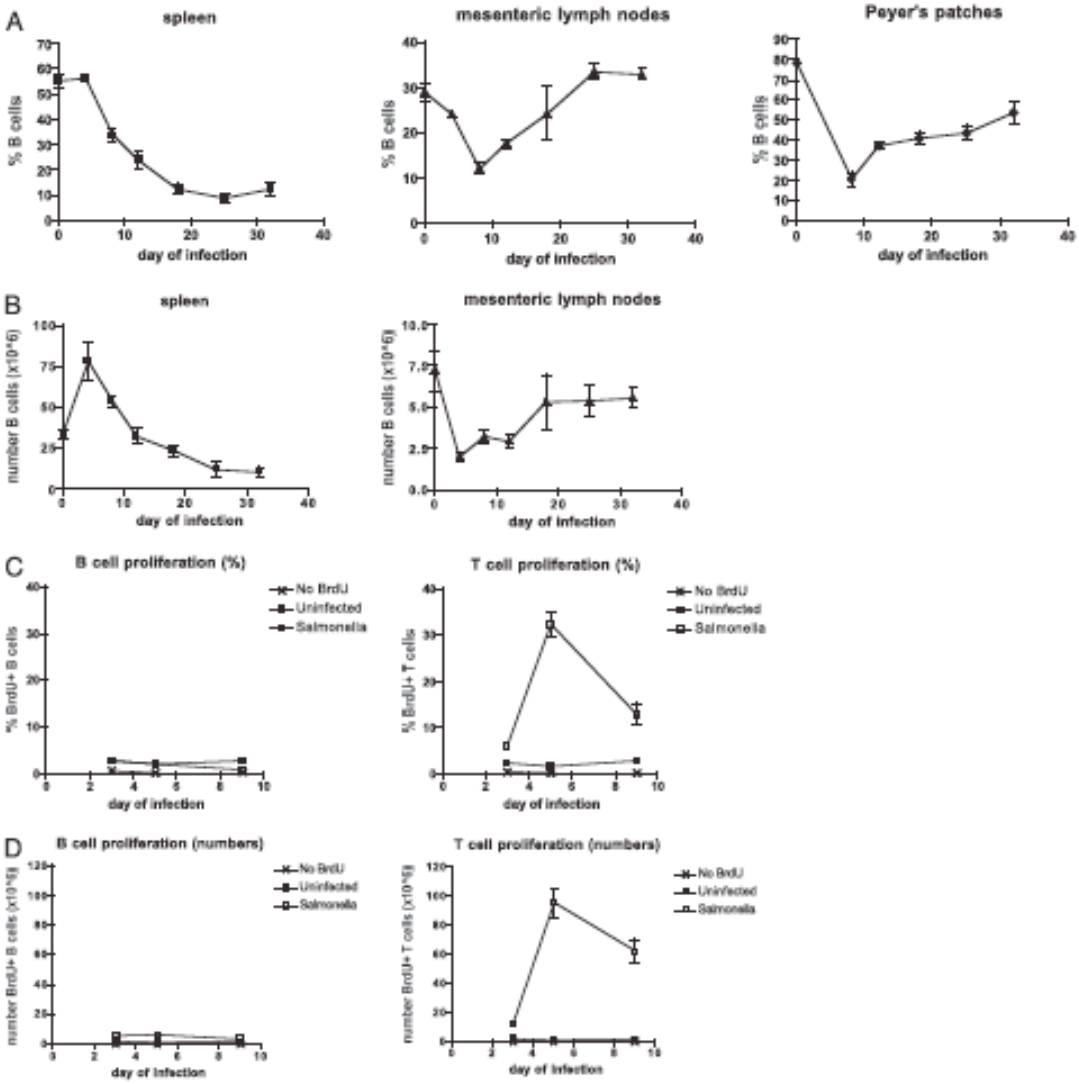

FIGURE 6. B cell localization is altered during *S. typhimurium* infection. C57BL/6 mice were infected with the attenuated SL3261 strain of *S. typhimurium*. Spleens, mesenteric lymph nodes, and Peyer's patches were taken at various times during infection and percentages (*A*) and absolute numbers (*B*) of B cells identified. Some mice were injected (at either day 2, 4, or 8) with 2 mg BrdU i.p. and splenocytes analyzed the following day for percentages (*C*) and absolute numbers (*D*) of proliferating cells. Error bars indicate SEM with four mice per group.

this is related to their enhanced entry into the spleen and relative exclusion from the lymph nodes and Peyer's patches.

Discussion

The data presented in this study indicate that stimulation of B cells through TLR2, -3, and -9 induces shedding of CD62L, which impacts on their migration patterns and results in their exclusion from lymph nodes and Peyer's patches. During *S. typhimurium* infection, this process causes B cells to accumulate in the spleen during the first week.

We found that only certain TLR ligands (PAM_3CSK4, poly I:C, and CpG-DNA) induced shedding of CD62L by B cells in vitro (Fig. 1*A*). Interestingly, PAM_3CSK4, which binds TLR2/1 heterodimers, induced shedding, whereas other TLR2 ligands, zymosan and peptidoglycan, which bind TLR2/6 heterodimers, had no such effect. Differences with the zymosan signal could be explained by its dependence on dectin 1 (45), which is not expressed by B cells (46). The reason is more likely to be due to differential expression of TLR1 and TLR6 by B cells. There is evidence to suggest that although B cells express TLR6 at the mRNA level (1, 2), they display a greater proliferative response to TLR2/1 stimulation than to TLR2/6 (2), which would support the notion of increased expression of TLR1 compared with TLR6. Therefore, although these two forms of TLR2 signal via the same pathway and so produce

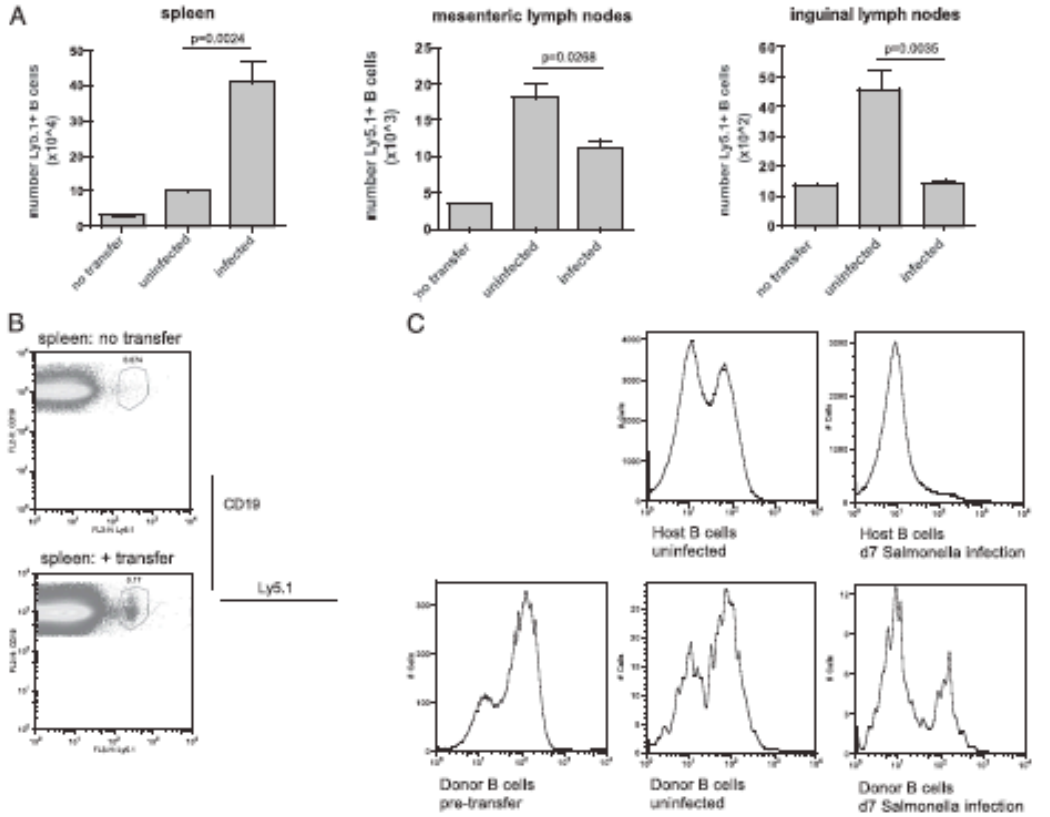

FIGURE 7. B cells shed CD62L in vivo in response to *S. typhimurium*. CD62L^{hi} cells from the blood of Ly5.1$^+$ mice were transferred into either uninfected or *Salmonella*-infected C57BL/6 mice. The following day, spleens and lymph nodes were removed from recipient mice and donor cells identified (*A*). Example staining of donor Ly5.1$^+$ cells is presented in *B*, showing gating and low-level background staining in mice receiving no donor cells. CD62L expression of splenic B cells was also analyzed (*C*). The Student paired *t* test was used to calculate significance values. Error bars indicate SEM with four mice per group. Data are representative of three independent experiments.

the same effects (47), differential expression would account for the differences seen between these stimuli.

Shedding of CD62L by B cells in response to TLR stimulation has not previously been reported. However, other groups have indicated that human neutrophils rapidly lose expression of CD62L following stimulation with TLRs in vitro (48, 49), and this method has been used to detect defects in the TLR signaling pathway (48). However, these two articles do not agree on which TLRs induce shedding. On the one hand, Von Bernuth et al. (48) suggested that shedding of CD62L by human neutrophils was stimulated by ligands for all of the TLRs expressed by granulocytes (TLR2/1, -2/6, -4, -5, -7, and -8). On the other hand, Hayashi et al. (49) only saw neutrophil shedding of CD62L in response to TLR2/1, -2/6, -4, and -7/8 but not TLR3, -5, or -9. The differences seen between these results in relation to TLR5-induced shedding may be due to different mechanisms of extracting neutrophils or the varying concentrations of flagellin used. These results also contrast our own data on mouse B cell shedding of CD62L (Fig. 1*A*), in that we do not see shedding induced by TLR4, -5, or -7. Importantly, inaddition to the shedding induced by defined TLR ligands, we also see shedding of CD62L by B cells in response to *Salmonella* Ags (Fig. 5*A*). This shedding appears to be largely MyD88 dependent, but not mediated entirely by either TLR2 or TLR9 (Fig. 5*B*). However, no shedding was observed in response to live bacteria in vitro following 4 h of culture. This is likely due to the short incubation time of this culture, in which there will be little bacterial death (B cells alone are unlikely to induce bacterial killing) and, therefore, only small amounts of accessible TLR ligand.

The TLRs that induce shedding of CD62L by B cells in response to bacteria (TLR2, -3, and -9) are not the most abundant or obvious TLR ligands to have an effect during *Salmonella* infection. Although the immune roles of LPS (TLR4) and flagellin (TLR5) in the *Salmonella* infection model have been investigated (50, 51), the TLRs highlighted in this study have received less attention. Interestingly, it has been noted that infection with *S. typhimurium* results in an increase in expression of TLR1, -2, and -9 in the infected liver (52), but the spleen was not investigated. Furthermore, incubation of hepatocytes with CpG DNA significantly inhibited the intracellular growth of *S. typhimurium* in vitro, suggesting that stimulation via TLR9 can enhance bacterial killing (53). Rumio et al. (54) also demonstrated that pretreatment with CpG-DNA for 72 h in vivo increases survival when mice are then infected with virulent *S. typhimurium*, again suggesting a role for this TLR in inducing bacterial killing. The authors propose that this increased survival is due to the responses of Paneth cells, although they did not investigate this directly. This effect may be partly due to the

TLR9-induced changes in B cell localization and activation. How B cells would be activated by bacterial DNA during infection remains to be clarified, as it seems that unless it is released as soluble material following bacterial cell death, the bacterial particles would require receptor (BCR)-mediated uptake (55, 56), and so, only *Salmonella*-specific B cells might be activated via TLR9.

The TLR-induced shedding of CD62L by B cells had a profound impact on their migration in vivo. These TLR-stimulated B cells are completely excluded from the lymph nodes and Peyer's patches and traffic only to the spleen (Fig. 3). Our data in this study suggest that, following a single stimulation with TLR ligands, B cell CD62L returns to normal levels in 2 to 3 d, and these cells are then able to traffic normally to the lymph nodes and Peyer's patches (Fig. 4). Others have shown that, in T cells, activation by anti-CD3 induces a similar short-term reduction in surface CD62L, with normal levels achieved 2 to 3 d later (57, 58). This is followed 7 d later by full activation of T cells and downregulation of surface CD62L as a result of transcriptional regulation (58). In the *Salmonella* infection model, we see that the reduction of B cell numbers in the lymph nodes and Peyer's patches is only apparent for the first 8 d of infection, and thereafter, B cell numbers in these organs begin to return to normal. In the spleen, B cell numbers are elevated on days 4 and 8, but not from day 12 onwards. This would suggest that the focusing of B cells to the spleen by TLR-induced changes in CD62L expression, as seen in *Salmonella* infection, is a short-term phenomenon.

The data presented indicate that, during *Salmonella* infection, TLR stimulation of B cells induces a short-term reduction in levels of surface CD62L, which in turn results in increased B cell trafficking to the spleen (Fig. 6). This may be a mechanism to nonspecifically attract a polyclonal population of B cells to the spleen. We propose that this will have two effects. First, it will enhance the BCR-dependent activation/selection of Ag-specific B cells in the spleen, both by exposing greater numbers of B cells to bacterial Ags but also by TLR-mediated augmentation of expression of MHC class II and costimulatory molecules (59–61). Second, the subsequent polyclonal activation by these and other TLR ligands will drive B cell cytokine production (1). This cytokine release by B cells has a significant effect on the programming of the early, primary CD4 T cell response (T. Barr, S. Brown, and D. Gray, unpublished observations). In addition, this nonspecific accumulation of B cells in the spleen may enhance the secretion of natural Ab directly to the site where the bacteria have amassed. Therefore, TLR-induced IgM production in the spleen could bind to the bacteria and contribute to the initiation of the primary response as has been reported (62, 63) and ultimately enhance bacterial killing.

Whether the TLR/CD62L-mediated changes to B cell migration enhance the initiation of the adaptive immune response to *Salmonella* or whether TLR-activated B cells may also play roles in the regulation of the inflammatory response (64–66) or changes to the lymphoid tissue structure during infection (21, 67), the global change in migration behavior upon TLR ligation seems likely to have significant consequences for the immunopathology of this infection.

Disclosures

The authors have no financial conflicts of interest.

References

1. Barr, T. A., S. Brown, G. Ryan, J. Zhao, and D. Gray. 2007. TLR-mediated stimulation of APC: Distinct cytokine responses of B cells and dendritic cells. *Eur. J. Immunol.* 37: 3040–3053.
2. Genestier, L., M. Taillardet, P. Mondiere, H. Gheit, C. Bella, and T. Defrance. 2007. TLR agonists selectively promote terminal plasma cell differentiation of B cell subsets specialized in thymus-independent responses. *J. Immunol.* 178: 7779–7786.
3. Pasare, C., and R. Medzhitov. 2005. Control of B-cell responses by Toll-like receptors. *Nature* 438: 364–368.
4. Barr, T. A., S. Brown, P. Mastroeni, and D. Gray. 2009. B cell intrinsic MyD88 signals drive IFN-gamma production from T cells and control switching to IgG2c. *J. Immunol.* 183: 1005–1012.
5. Gray, D., M. Gray, and T. Barr. 2007. Innate responses of B cells. *Eur. J. Immunol.* 37: 3304–3310.
6. Mastroeni, P., and N. Ménager. 2003. Development of acquired immunity to *Salmonella*. *J. Med. Microbiol.* 52: 453–459.
7. Kalupahana, R. S., P. Mastroeni, D. Maskell, and B. A. Blacklaws. 2005. Activation of murine dendritic cells and macrophages induced by *Salmonella enterica* serovar Typhimurium. *Immunology* 115: 462–472.
8. Mastroeni, P., S. Ugrinovic, A. Chandra, C. MacLennan, R. Dolfinger, and D. Kumaratnsine. 2008. Resistance and susceptibility to *Salmonella* infections: lessons from mice and patients with immunodeficiencies. *Rev. Med. Microbiol.* 14: 53–62.
9. Mastroeni, P., J. A. Harrison, J. H. Robinson, S. Clare, S. Khan, D. J. Maskell, G. Dougan, and C. E. Hormaeche. 1998. Interleukin-12 is required for control of the growth of attenuated aromatic-compound-dependent salmonellae in BALB/c mice: role of gamma interferon and macrophage activation. *Infect. Immun.* 66: 4767–4776.
10. Mastroeni, P., S. Clare, S. Khan, J. A. Harrison, C. E. Hormaeche, H. Okamura, M. Kurimoto, and G. Dougan. 1999. Interleukin 18 contributes to host resistance and gamma interferon production in mice infected with virulent *Salmonella typhimurium*. *Infect. Immun.* 67: 478–483.
11. Nauciel, C., and F. Espinasse-Maes. 1992. Role of gamma interferon and tumor necrosis factor alpha in resistance to Salmonella typhimurium infection. *Infect. Immun.* 60: 450–454.
12. O'Brien, A. D., D. L. Rosenstreich, I. Scher, G. H. Campbell, R. P. MacDermott, and S. B. Formal. 1980. Genetic control of susceptibility to *Salmonella typhimurium* in mice: role of the LPS gene. *J. Immunol.* 124: 20–24.
13. Weiss, D. S., B. Raupach, K. Takeda, S. Akira, and A. Zychlinsky. 2004. Toll-like receptors are temporally involved in host defense. *J. Immunol.* 172: 4463–4469.
14. Ko, H. J., J. Y. Yang, D. H. Shim, H. Yang, S.-M. Park, R. Curtiss, III, and M. N. Kweon. 2009. Innate immunity mediated by MyD88 signal is not essential for induction of lipopolysaccharide-specific B cell responses but is indispensable for protection against Salmonella enterica serovar Typhimurium infection. *J. Immunol.* 182: 2305–2312.
15. Barr, T. A., S. Brown, P. Mastroeni, and D. Gray. 2010. TLR and B cell receptor signals to B cells differentially program primary and memory Th1 responses to *Salmonella enterica*. *J. Immunol.* 185: 2783–2789.
16. Schnare, M., G. M. Barton, A. C. Holt, K. Takeda, S. Akira, and R. Medzhitov. 2001. Toll-like receptors control activation of adaptive immune responses. *Nat. Immunol.* 2: 947–950.
17. Ugrinovic, S., N. Ménager, N. Goh, and P. Mastroeni. 2003. Characterization and development of T-Cell immune responses in B-cell-deficient (Ighm-6(-/-)) mice with Salmonella enterica serovar Typhimurium infection. *Infect. Immun.* 71: 6808–6819.
18. Mastroeni, P., C. Simmons, R. Fowler, C. E. Hormaeche, and G. Dougan. 2000. Igh-6(-/-) (B-cell-deficient) mice fail to mount solid acquired resistance to oral challenge with virulent Salmonella enterica serovar typhimurium and show impaired Th1 T-cell responses to Salmonella antigens. *Infect. Immun.* 68: 46–53.
19. Mittrücker, H.-W., B. Raupach, A. Köhler, and S. H. E. Kaufmann. 2000. Cutting edge: role of B lymphocytes in protective immunity against *Salmonella typhimurium* infection. *J. Immunol.* 164: 1648–1652.
20. Mastroeni, P., B. Villarreal-Ramos, and C. E. Hormaeche. 1993. Adoptive transfer of immunity to oral challenge with virulent salmonellae in innately susceptible BALB/c mice requires both immune serum and T cells. *Infect. Immun.* 61: 3981–3984.
21. St John, A. L., and S. N. Abraham. 2009. *Salmonella* disrupts lymph node architecture by TLR4-mediated suppression of homeostatic chemokines. *Nat. Med.* 15: 1259–1265.
22. Tedder, T. F., D. A. Steeber, A. Chen, and P. Engel. 1995. The selectins: vascular adhesion molecules. *FASEB J.* 9: 866–873.
23. Berg, E. L., A. T. Mullowney, D. P. Andrew, J. E. Goldberg, and E. C. Butcher. 1992. Complexity and differential expression of carbohydrate epitopes associated with L-selectin recognition of high endothelial venules. *Am. J. Pathol.* 152: 469–477.
24. Berg, E. L., L. M. McEvoy, C. Berlin, R. F. Bargatze, and E. C. Butcher. 1993. L-selectin-mediated lymphocyte rolling on MAdCAM-1. *Nature* 366: 695–698.
25. Kansas, G. S., K. Ley, J. M. Munro, and T. F. Tedder. 1993. Regulation of leukocyte rolling and adhesion to high endothelial venules through the cytoplasmic domain of L-selectin. *J. Exp. Med.* 177: 833–838.
26. Ley, K., P. Gaehtgens, C. Fennie, M. S. Singer, L. A. Lasky, and S. D. Rosen. 1991. Lectin-like cell adhesion molecule 1 mediates leukocyte rolling in mesenteric venules *in vivo*. *Blood* 77: 2553–2555.
27. Gallatin, W. M., I. L. Weissman, and E. C. Butcher. 1983. A cell-surface molecule involved in organ-specific homing of lymphocytes. *Nature* 304: 30–34.
28. Steeber, D. A., N. E. Green, S. Sato, and T. F. Tedder. 1996. Lymphocyte migration in L-selectin-deficient mice. Altered subset migration and aging of the immune system. *J. Immunol.* 157: 1096–1106.
29. Peschon, J. J., J. L. Slack, P. Reddy, K. L. Stocking, S. W. Sunnarborg, D. C. Lee, W. E. Russell, B. J. Castner, R. S. Johnson, J. N. Fitzner, et al. 1998. An essential

role for ectodomain shedding in mammalian development. *Science* 282: 1281–1284.
30. Jung, T. M., and M. O. Dailey. 1990. Rapid modulation of homing receptors (gp90MEL-14) induced by activators of protein kinase C. Receptor shedding due to accelerated proteolytic cleavage at the cell surface. *J. Immunol.* 144: 3130–3136.
31. Tedder, T. F., D. A. Steeber, and P. Pizcueta. 1995. L-selectin-deficient mice have impaired leukocyte recruitment into inflammatory sites. *J. Exp. Med.* 181: 2259–2264.
32. Xu, J., I. S. Grewal, G. P. Geba, and R. A. Flavell. 1996. Impaired primary T cell responses in L-selectin-deficient mice. *J. Exp. Med.* 183: 589–598.
33. Venturi, G. M., L. Tu, T. Kadono, A. I. Khan, Y. Fujimoto, P. Oshel, C. B. Bock, A. S. Miller, R. M. Albrecht, P. Kubes, et al. 2003. Leukocyte migration is regulated by L-selectin endoproteolytic release. *Immunity* 19: 713–724.
34. Richards, H., M. P. Longhi, K. Wright, A. Gallimore, and A. Ager. 2008. CD62L (L-selectin) down-regulation does not affect memory T cell distribution but failure to shed compromises anti-viral immunity. *J. Immunol.* 180: 198–206.
35. Adachi, O., T. Kawai, K. Takeda, M. Matsumoto, H. Tsutsui, M. Sakagami, K. Nakanishi, and S. Akira. 1998. Targeted disruption of the MyD88 gene results in loss of IL-1- and IL-18-mediated function. *Immunity* 9: 143–150.
36. Yamamoto, M., S. Sato, H. Hemmi, K. Hoshino, T. Kaisho, H. Sanjo, O. Takeuchi, M. Sugiyama, M. Okabe, K. Takeda, and S. Akira. 2003. Role of adaptor TRIF in the MyD88-independent toll-like receptor signaling pathway. *Science* 301: 640–643.
37. Takeuchi, O., K. Hoshino, T. Kawai, H. Sanjo, H. Takada, T. Ogawa, K. Takeda, and S. Akira. 1999. Differential roles of TLR2 and TLR4 in recognition of gram-negative and gram-positive bacterial cell wall components. *Immunity* 11: 443–451.
38. Hemmi, H., O. Takeuchi, T. Kawai, T. Kaisho, S. Sato, H. Sanjo, M. Matsumoto, K. Hoshino, H. Wagner, K. Takeda, and S. Akira. 2000. A Toll-like receptor recognizes bacterial DNA. *Nature* 408: 740–745.
39. Hoiseth, S. K., and B. A. D. Stocker. 1981. Aromatic-dependent *Salmonella typhimurium* are non-virulent and effective as live vaccines. *Nature* 291: 238–239.
40. Harrison, J. A., B. Villarreal-Ramos, P. Mastroeni, R. Demarco de Hormaeche, and C. E. Hormaeche. 1997. Correlates of protection induced by live Aro- *Salmonella typhimurium* vaccines in the murine typhoid model. *Immunology* 90: 618–625.
41. Reichert, R. A., W. M. Gallatin, I. L. Weissman, and E. C. Butcher. 1983. Germinal center B cells lack homing receptors necessary for normal lymphocyte recirculation. *J. Exp. Med.* 157: 813–827.
42. Farnsworth, C., G. Prasco, and A. Ager. 2001. Transendothelial migration of lymphocytes across high endothelial venules into lymph nodes is affected by metalloproteinases. *Blood* 98: 688–695.
43. Borland, G., G. Murphy, and A. Ager. 1999. Tissue inhibitor of metalloproteinases-3 inhibits shedding of L-selectin from leukocytes. *J. Biol. Chem.* 274: 2810–2815.
44. Arbonés, M. L., D. C. Ord, K. Ley, H. Ratech, C. Maynard-Curry, G. Otten, D. J. Capon, and T. F. Tedder. 1994. Lymphocyte homing and leukocyte rolling and migration are impaired in L-selectin-deficient mice. *Immunity* 1: 247–260.
45. Brown, G. D., J. Herre, D. L. Williams, J. A. Willment, A. S. Marshall, and S. Gordon. 2003. Dectin-1 mediates the biological effects of beta-glucans. *J. Exp. Med.* 197: 1119–1124.
46. Taylor, P. R., G. D. Brown, D. M. Reid, J. A. Willment, L. Martinez-Pomares, S. Gordon, and S. Y. Wong. 2002. The beta-glucan receptor, dectin-1, is predominantly expressed on the surface of cells of the monocyte/macrophage and neutrophil lineages. *J. Immunol.* 169: 3876–3882.
47. Farhat, K., S. Riekenberg, H. Heine, J. Debarry, R. Lang, J. Mages, U. Buwitt-Beckmann, K. Röschmann, G. Jung, K.-H. Wiesmüller, and A. J. Ulmer. 2008. Heterodimerization of TLR2 with TLR1 or TLR6 expands the ligand spectrum but does not lead to differential signaling. *J. Leukoc. Biol.* 83: 692–701.
48. von Bernuth, H., C.-L. Ku, C. Rodriguez-Gallego, S. Zhang, B.-Z. Garty, L. Marodi, H. Chapel, M. Chrabieh, R. L. Miller, C. Picard, et al. 2006. A fast procedure for the detection of defects in Toll-like receptor signaling. *Pediatrics* 118: 2498–2503.
49. Hayashi, F., T. K. Means, and A. D. Luster. 2003. Toll-like receptors stimulate human neutrophil function. *Blood* 102: 2660–2669.
50. Vijay-Kumar, M., J. D. Aitken, A. Kumar, A. S. Neish, S. Uematsu, S. Akira, and A. T. Gewirtz. 2008. Toll-like receptor 5-deficient mice have dysregulated intestinal gene expression and nonspecific resistance to *Salmonella*-induced typhoid-like disease. *Infect. Immun.* 76: 1276–1281.
51. Freudenberg, M. A., T. Merlin, M. Gumenscheimer, C. Kalis, R. Landmann, and C. Galanos. 2001. Role of lipopolysaccharide susceptibility in the innate immune response to *Salmonella typhimurium* infection: LPS, a primary target for recognition of Gram-negative bacteria. *Microbes Infect.* 3: 1213–1222.
52. Totemeyer, S., P. Kaiser, D. J. Maskell, and C. E. Bryant. 2005. Sublethal infection of C57BL/6 mice with *Salmonella enterica* Serovar Typhimurium leads to an increase in levels of Toll-like receptor 1 (TLR1), TLR2, and TLR9 mRNA as well as a decrease in levels of TLR6 mRNA in infected organs. *Infect. Immun.* 73: 1873–1878.
53. Sanchez-Campillo, M., A. Chicano, A. Torío, E. Martín-Orozco, P. Gómiz, T. Hernández-Caselles, and P. García-Peñarrubia. 2004. Implication of CpG-ODN and reactive oxygen species in the inhibition of intracellular growth of *Salmonella typhimurium* in hepatocytes. *Microbes Infect.* 6: 813–820.
54. Ramiro, C., D. Bruzzo, M. Palazzo, S. Soldini, L. Sfondrini, F. Dubini, S. Ménard, and A. Balsari. 2004. Degranulation of paneth cells via toll-like receptor 9. *Am. J. Pathol.* 165: 373–381.
55. Eckl-Dorna, J., and F. D. Batista. 2009. BCR-mediated uptake of antigen linked to TLR9 ligand stimulates B-cell proliferation and antigen-specific plasma cell formation. *Blood* 113: 3969–3977.
56. Jendholm, J., M. Mörgelin, M. L. Perez Vidakovics, M. Carlsson, H. Leffler, L. O. Cardell, and K. Riesbeck. 2009. Superantigen- and TLR-dependent activation of tonsillar B cells after receptor-mediated endocytosis. *J. Immunol.* 182: 4713–4720.
57. Smalley, D. M., and K. Ley. 2005. L-selectin: mechanisms and physiological significance of ectodomain cleavage. *J. Cell. Mol. Med.* 9: 255–266.
58. Chao, C. C., R. Jensen, and M. O. Dailey. 1997. Mechanisms of L-selectin regulation by activated T cells. *J. Immunol.* 159: 1686–1694.
59. Crawford, A., M. Macleod, T. Schumacher, L. Corlett, and D. Gray. 2006. Primary T cell expansion and differentiation in vivo requires antigen presentation by B cells. *J. Immunol.* 176: 3498–3506.
60. Kurt-Jones, E. A., D. Liano, K. A. Hayglass, B. Benacerraf, M.-S. Sy, and A. K. Abbas. 1988. The role of antigen-presenting B cells in T cell priming in vivo. Studies of B cell-deficient mice. *J. Immunol.* 140: 3773–3778.
61. Liu, Q., Z. Liu, C. T. Rozo, H. A. Hamad, F. Alem, J. F. Urban, Jr., and W. C. Gause. 2007. The role of B cells in the development of CD4 effector T cells during a polarized Th2 immune response. *J. Immunol.* 179: 3821–3830.
62. Ehrenstein, M. R., T. L. O'Keefe, S. L. Davies, and M. S. Neuberger. 1998. Targeted gene disruption reveals a role for natural secretory IgM in the maturation of the primary immune response. *Proc. Natl. Acad. Sci. USA* 95: 10089–10093.
63. Boes, M., A. P. Prodeus, T. Schmidt, M. C. Carroll, and J. Chen. 1998. A critical role of natural immunoglobulin M in immediate defense against systemic bacterial infection. *J. Exp. Med.* 188: 2381–2386.
64. Hilliatsou, S., D. Gray, and S. M. Anderton. 2008. Not always the bad guys: B cells as regulators of autoimmune pathology. *Nat. Rev. Immunol.* 8: 391–397.
65. Mauri, C., and M. R. Ehrenstein. 2008. The 'short' history of regulatory B cells. *Trends Immunol.* 29: 34–40.
66. Mizoguchi, A., and A. K. Bhan. 2006. A case for regulatory B cells. *J. Immunol.* 176: 705–710.
67. Angeli, V., F. Ginhoux, J. Llodrà, L. Quemeneur, P. S. Frenette, M. Skobe, R. Jessberger, M. Merad, and G. J. Randolph. 2006. B cell-driven lymphangiogenesis in inflamed lymph nodes enhances dendritic cell mobilization. *Immunity* 24: 203–215.

CHAPTER 9: References

1. Matzinger, P. (2002). The danger model: a renewed sense of self. *Science* **296**: 301-305
2. Mebius, R. E. and G. Kraal (2005). Structure and function of the spleen. *Nature Reviews Immunology* **5**: 606-616
3. Balfanz, J. R., M. E. Nesbit, C. Jarris and W. Krivit (1976). Overwhelming sepsis following splenectomy for trauma. *Journal of Pediatrics* **88**: 458-460
4. Roozendaal, R., R. E. Mebius and G. Kraal (2008). The conduit system of the lymph node. *International Immunology* **20**: 1483-1487
5. Luther, S. A., A. Bidgol, D. C. Hargreaves, A. Schmidt, Y. Xu, J. Paniyadi, M. Matloubian and J. G. Cyster (2002). Differing activities of homeostatic chemokines CCL19, CCL21, and CXCL12 in lymphocyte and dendritic cell recruitment and lymphoid neogenesis. *The Journal of Immunology* **169**: 424-433
6. Ohl, L., G. Henning, S. Krautwald, M. Lipp, S. Hardtke, G. Bernhardt, O. Pabst and R. Forster (2003). Cooperating mechanisms of CXCR5 and CCR7 in development and organization of secondary lymphoid organs. *Journal of Experimental Medicine* **197**: 1199-1204
7. Baekkevold, E. S., T. Yamanaka, R. T. Palframan, H. S. Carlsen, F. P. Reinholt, U. H. von Andrian, P. Brandtzaeg and G. Haraldsen (2001). The CCR7 ligand elc (CCL19) is transcytosed in high endothelial venules and mediates T cell recruitment. *Journal of Experimental Medicine* **193**: 1105-1111
8. Legler, D. F., M. Loetscher, R. S. Roos, I. Clark-Lewis, M. Baggiolini and B. Moser (1998). B cell–attracting chemokine 1, a human CXC chemokine expressed in lymphoid tissues, selectively attracts B lymphocytes via BLR1/CXCR5. *Journal of Experimental Medicine* **187**: 655-660
9. Hardtke, S., L. Ohl and R. Forster (2005). Balanced expression of CXCR5 and CCR7 on follicular T helper cells determines their transient positioning to lymph node follicles and is essential for efficient B-cell help. *Blood* **106**: 1924-1931
10. Muller, G., U. E. Hopken and M. Lipp (2003). The impact of CCR7 and CXCR5 on lymphoid organ development and systemic immunity. *Immunological Reviews* **195**: 117-135
11. Breitfeld, D., L. Ohl, E. Kremmer, J. Eillwart, F. Sallusto, M. Lipp and R. Forster (2000). Follicular B helper T cells express CXC chemokine receptor 5, localize to B cell follicles, and support immunoglobulin production. *Journal of Experimental Medicine* **192**: 1545-1551
12. Ato, M., H. Nakano, T. Kakiuchi and P. M. Kaye (2004). Localization of marginal zone macrophages is regulated by C-C chemokine ligands 21/19. *The Journal of Immunology* **173**: 4815-4820
13. Kraal, G. and M. Janse (1986). Marginal metallophilic cells of the mouse spleen identified by a monoclonal antibody. *Immunology* **58**: 665-669
14. Karlsson, M. C. I., R. Guinamard, S. Bollard, M. Sankala, R. M. Steinman and J. V. Ravetch (2003). Macrophages control the retention and trafficking of B lymphocytes in the splenic marginal zone. *Journal of Experimental Medicine* **198**: 333-340
15. Nolte, M. A., R. Arens, M. Kraus, M. H. J. Van Oers, G. Kraal, R. A. W. Van Lier and R. E. Mebius (2004). B cells are crucial for both development and maintenance of the splenic marginal zone. *The Journal of Immunology* **172**: 3620-3627
16. Gatto, D., M. Bauer, S. W. Martin and M. F. Bachmann (2007). Heterogeneous antibody repertoire of marginal zone B cells specific for virus-like particles. *Microbes and Infection* **9**: 391-399

17. Oliver, A. M., F. Martin, G. L. Gartland, R. H. Carter and J. F. Kearney (2005). Marginal zone B cells exhibit unique activation, proliferative and immunoglobulin secretory responses. *European Journal of Immunology* **27**: 2366-2374
18. Martin, F. and J. F. Kearney (2002). Marginal-zone B cells. *Nature Reviews Immunology* **2**: 323-335
19. Pillai, S., A. Cariappa and S. T. Moran (2005). Marginal Zone B Cells. *Annual Reviews Immunology* **23**: 161-196
20. Lopes-Carvalho, T. and J. F. Kearney (2004). Development and selection of marginal zone B cells. *Immunological Reviews* **197**: 192-205
21. Attanavanich, K. and J. F. Kearney (2004). Marginal zone, but not follicular B cells, are potent activators of naive CD4 T cells. *The Journal of Immunology* **172**: 803-811
22. Makala, L. H. C., N. Suzuki and H. Nagasawa (2002). Peyer's patches: organized lymphoid structures for the induction of mucosal immune responses in the intestine. *Pathobiology* **70**: 55-68
23. Itano, A. A. and M. K. Jenkins (2003). Antigen presentation to naive CD4 T cells in the lymph node. *Nature Immunology* **4**: 733-739
24. Miyawaki, S., Y. Nakamura, H. Suzuka, M. Koba, Y. Shibata, R. Yasumizu and S. Ikehara (1994). A new mutation, aly, that induces a generalized lack of lymph nodes accompanied by immunodeficiency in mice. *European Journal of Immunology* **24**: 429-434
25. Banks, T. A., B. T. Rouse, P. J. Blair, V. L. Godfrey, N. A. Kuklin, D. M. Bouley, J. Thomas, S. Kanangat and M. L. Mucenski (1995). Lymphotoxin-alpha-deficient mice. Effects on secondary lymphoid organ development and humoral immune responsiveness. *The Journal of Immunology* **155**: 1685-1693
26. van Vliet, S. J., J. J. Garcia-Vallejo and Y. van Kooyk (2008). Dendritic cells and C-type lectin receptors: coupling innate to adaptive immune responses. *Immunology and Cell Biology* **86**: 580-587
27. Kapsenberg, M. L. (2003). Dendritic-cell control of pathogen-driven T-cell polarization. *Nature Reviews Immunology* **3**: 984-993
28. Iwasaki, A. and R. Medzhitov (2004). Toll-like receptor control of the adaptive immune responses. *Nature Immunology* **5**: 987-995
29. Munz, C., R. M. Steinman and S.-I. Fujii (2005). Dendritic cell maturation by innate lymphocytes: coordinated stimulation of innate and adaptive immunity. *Journal of Experimental Medicine* **202**: 203-207
30. Stoll, S., J. Delon, T. M. Brotz and R. N. Germain (2002). Dynamic imaging of T cell-dendritic cell interactions in lymph nodes. *Science* **296**: 1873-1876
31. Macian, F., S.-H. Im, J. Garcia-Cozar and A. Rao (2004). T-cell anergy. *Current Opinion in Immunology* **16**: 209-216
32. Zhou, L., M. M. W. Chong and D. R. Littman (2009). Plasticity of CD4+ T Cell Lineage Differentiation. *Immunity* **30**: 646-655
33. Min, B., M. Prout, J. Hu-Li, J. Zhu, D. Jankovic, E. S. Morgan, J. F. Urban, A. M. Dvorak, F. D. Finkelman, G. LeGros and W. E. Paul (2004). Basophils produce IL-4 and accumulate in tissues after infection with a Th2-inducing parasite. *Journal of Experimental Medicine* **200**: 507-517
34. Romagnani, S. (1992). Induction of TH1 and TH2 responses: a key role for the 'natural' immune response? *Immunology Today* **13**: 379-381
35. Anthony, R. M., L. I. Rutitzky, J. F. Urban, M. J. Stadecker and W. C. Gause (2007). Protective immune mechanisms in helminth infection. *Nature Reviews Immunology* **7**: 975-987
36. Kikly, K., L. Liu, S. Na and J. D. Sedgwick (2006). The IL-23/Th17 axis: therapeutic targets for autoimmune inflammation. **18**: 670-675
37. Zhu, J., H. Yamane and W. E. Paul (2010). Differentiation of Effector CD4 T Cell Populations. *Annual Reviews Immunology* **28**: 445-489

38. Fontenot, J. D., M. A. Gavin and A. Y. Rudensky (2003). Foxp3 programs the development and function of CD4+ CD25+ regulatory T cells. *Nature Immunology* **4**: 330-336
39. Veldhoen, M., C. Uyttenhove, J. van Snick, H. Helmby, A. Westendorf, J. Buer, B. Martin, C. Wilhelm and B. Stockinger (2008). Transforming growth factor-beta 'reprograms' the differentiation of T helper 2 cells and promotes an interleukin 9-producing subset. *Nature Immunology* **9**: 1341-1346
40. Nurieva, R. I., Y. Chung, D. Hwang, X. O. Yang, H. S. Kang, L. Ma, Y.-H. Wang, S. S. Watowich, A. M. Jetten, Q. Tian and C. Dong (2008). Generation of T follicular helper cells is mediated by interleukin-21 but independent of T helper 1, 2, or 17 cell lineages. *Immunity* **29**: 138-149
41. Nurieva, R. I., Y. Chung, G. J. Martinez, X. O. Yang, S. Tanaka, T. D. Matskevich, Y.-H. Wang and C. Dong (2009). Bcl6 Mediates the Development of T Follicular Helper Cells. *Science* **325**: 1001-1005
42. Yu, D., S. Rao, L. M. Tsai, S. K. Lee, Y. He, E. L. Sutcliffe, M. Srivastava, M. Linterman, L. Zheng, N. Simpson, J. I. Ellyard, I. A. Parish, C. S. Ma, Q.-J. Li, C. R. Parish, C. R. Mackay and C. G. Vinuesa (2009). The Transcriptional Repressor Bcl-6 Directs T Follicular Helper Cell Lineage Commitment. *Immunity* **31**: 457-468
43. Gorelik, L. and R. A. Flavell (2000). Abrogation of TGFbeta signalling in T cells leads to spontaneous T cell differentiation and autoimmune disease. *Immunity* **12**: 171-181
44. Wan, Y. Y. and R. A. Flavell (2008). TGF-beta and Regulatory T Cell in Immunity and Autoimmunity. *Journal of Clinical Immunology* **28**: 647-659
45. Yoshimura, A., Y. Wakabayashi and T. Mori (2010). Cellular and molecular basis for the regulation of inflammation by TGF-beta. *Journal of Biochemistry* **147**: 781-792
46. Kulkarni, A. B. and S. Karlsson (1997). Inflammation and TGF beta 1: lessons from the TGF beta 1 null mouse. *Research Immunology* **148**: 453-456
47. Leveen, P., J. Larsson, M. Ehinger, C. M. Cilio, M. Sundler, L. J. Sjostrand, R. Holmdahl and S. Karlsson (2002). Induced disruption of the transforming growth factor beta type II receptor gene in mice causes a lethal inflammatory disorder that is transplantable. *Blood* **100**: 560-568
48. Wieser, R., L. Attisano, J. L. Wrana and J. Massague (1993). Signaling Activity of Transforming Growth Factor beta Type II Receptors Lacking Specific Domains in the Cytoplasmic Region. *Molecular and Cellular Biology* **13**: 7239-7247
49. Huber, S., C. Schramm, H. A. Lehr, A. Mann, S. Schmitt, C. Becker, M. Protschka, P. R. Galle, M. F. Neurath and M. Blessing (2004). Cutting edge: TGF-beta signaling is required for the in vivo expansion and immunosuppressive capacity of regulatory CD4(+) CD25(+) T cells. *The Journal of Immunology* **173**: 6526-6531
50. Mamura, M., W. Lee, T. J. Sullivan, A. Felici, A. L. Sowers, J. P. Allison and J. J. Letterio (2004). CD28 disruption exacerbates inflammation in Tgf-beta 1(-/-) mice: in vivo suppression by CD4(+)CD25(+) regulatory T cells independent of autocrine TGF-beta 1. *Blood* **103**: 4594-4601
51. Li, M. O., S. Sanjabi and R. A. Flavell (2006). Transforming growth factor-beta controls development, homeostasis, and tolerance of T cells by regulatory T cell-dependent and -independent mechanisms. *Immunity* **25**: 455-471
52. Fahlen, L., S. Read, L. Gorelik, S. D. Hurst, R. L. Coffman, R. A. Flavell and F. Powrie (2005). T cells that cannot respond to TGF-beta escape control by CD4(+)CD25(+) regulatory T cells. *Journal of Experimental Medicine* **201**: 737-746
53. Veldhoen, M., R. J. Hocking, R. A. Flavell and B. Stockinger (2006). Signals mediated by transforming growth factor-beta initiate autoimmune encephalomyelitis, but chronic inflammation is needed to sustain disease. *Nature Immunology* **7**: 1151-1156

54. King, C., S. G. Tangye and C. R. Mackay (2008). T follicular helper (T-FH) cells in normal and dysregulated immune responses. *Annual Reviews Immunology* **26**: 741-766
55. Liu, Y.-J., G. D. Johnson, J. Gordon and I. C. M. MacLennan (1992). Germinal centres in T-cell-dependent antibody responses. *Immunology Today* **13**: 17-21
56. Liu, Y.-J., F. Malisan, O. de Bouteiller, C. Guret, S. Lebecque, J. Banchereau, F. C. Mills, E. E. Max and H. Martinez-Valdez (1996). Within germinal centers, isotype switching of immunoglobulin genes occurs after the onset of somatic mutation. *Immunity* **4**: 241-250
57. Good-Jacobson, K. L., C. G. Szumilas, L. Chen, A. H. Sharpe, M. M. Tomayka and M. J. Shlomchik (2010). PD-1 regulates germinal center B cell survival and the formation and affinity of long-lived plasma cells. *Nature Immunology* **11**: 535-542
58. Vogelzang, A., H. M. McGuire, D. Yu, J. Sprent, C. R. Mackay and C. King (2008). A fundamental role for interleukin-21 in the generation of T follicular helper cells. *Immunity* **29**: 127-137
59. Linterman, M., L. Beaton, D. Yu, R. R. Ramiscal, M. Srivastava, J. J. Hogan, N. K. Verma, M. J. Smyth, R. J. Rigby and C. G. Vinuesa (2010). IL-21 acts directly on B cells to regulate Bcl-6 expression and germinal center responses. *Journal of Experimental Medicine* **207**: 353-363
60. Zotos, D., J. M. Coquet, Y. Zhang, A. Light, K. D'costa, A. Kallies, L. M. Corcoran, D. I. Godfrey, K.-M. Toellner, M. J. Smyth, S. L. Nutt and D. M. Tarlinton (2010). IL-21 regulates germinal center B cell differentiation and proliferation through a B cell-intrinsic mechanism. *Journal of Experimental Medicine* **207**: 365-378
61. Murphy, E., K. Shibuya, N. Hosken, P. Openshaw, V. Maino, K. Davis, K. Murphy and A. O'Garra (1996). Reversibility of T helper 1 and 2 populations is lost after long-term stimulation. *Journal of Experimental Medicine* **183**: 901-913
62. Locksley, R. M. (2009). Nine lives: plasticity among T helper cell subsets. *Journal of Experimental Medicine* **206**: 1643-1646
63. Zhu, J. and W. E. Paul (2010). Heterogeneity and plasticity of T helper cells. *Cell Research* **20**: 4-12
64. Usui, T., J. C. Preiss, Y. Kanno, Z. J. Yao, J. H. Bream, J. J. O'Shea and W. Strober (2006). T-bet regulates Th1 responses through essential effects on GATA-3 function rather than on IFNG gene acetylation and transcription. *Journal of Experimental Medicine* **203**: 755-766
65. Zhu, J., H. Yamane, J. Cote-Sierra, L. Guo and W. E. Paul (2006). GATA-3 promotes Th2 responses through three different mechanisms: induction of Th2 cytokine production, selective growth of Th2 cells and inhibition of Th1 cell-specific factors. *Cell Research* **16**: 3-10
66. Murphy, K. M. and B. Stockinger (2010). Effector T cell plasticity: flexibility in the face of changing circumstances. *Nature Immunology* **11**: 674-680
67. Lee, Y. K., R. Mukasa, R. D. Hatton and C. T. Weaver (2009). Developmental plasticity of Th17 and Treg cells. *Current Opinion in Immunology* **21**: 274-280
68. McGeachy, M. J., K. S. Bak-Jensen, Y. Chen, C. M. Tato, W. Blumenschein, T. McClanahan and D. J. Cua (2007). TGF-β and IL-6 drive the production of IL-17 and IL-10 by T cells and restrain TH-17 cell–mediated pathology. *Nature Immunology* **8**: 1390-1397
69. Chtanova, T., S. G. Tangye, R. Newton, N. Frank, M. R. Hodge, M. S. Rolph and C. R. Mackay (2004). T follicular helper cells express a distinctive transcriptional profile, reflecting their role as non-Th1/Th2 effector cells that provide help for B cells. *The Journal of Immunology* **173**: 68-78
70. Martins, G. and K. Calame (2008). Regulation and functions of blimp-1 in T and B lymphocytes. *Annual Reviews Immunology* **26**: 133-169

71. Fazilleau, N., L. Mark, L. J. McHeyzer-Williams and M. G. McHeyzer-Williams (2009). Follicular helper T cells: lineage and location. *Immunity* **30**: 324-335
72. Crotty, S., R. L. Johnston and S. P. Schoenberger (2010). Effectors and memories: Bcl-6 and Blimp-1 in T and B lymphocyte differentiation. *Nature Immunology* **11**: 114-120
73. King, I. L. and M. Mohrs (2009). IL-4–producing CD4+ T cells in reactive lymph nodes during helminth infection are T follicular helper cells. *Journal of Experimental Medicine* **206**: 1001-1007
74. Zaretsky, A. G., J. J. Taylor, I. L. King, F. A. Marshall, M. Mohrs and E. J. Pearce (2009). T follicular helper cells differentiate from Th2 cells in response to helminth antigens. *Journal of Experimental Medicine* **206**: 991-999
75. Fillatreau, S. and D. Gray (2003). T cell accumulation in B cell follicles is regulated by dendritic cells and is independent of B cell activation. *Journal of Experimental Medicine* **197**: 195-206
76. Gray, D. (1993). Immunological memory. *Annual Reviews Immunology* **11**: 49-77
77. Kaech, S. M., E. J. Wherry and R. Ahmed (2002). Effector and memory T-cell differentiation: Implications for vaccine development. *Nature Reviews Immunology* **2**: 251-262
78. Dutton, R. W., L. M. Bradley and S. L. Swain (1998). T cell memory. *Annual Reviews Immunology* **16**: 201-223
79. Croft, M., L. M. Bradley and S. L. Swain (1994). Naive versus memory CD4 T cell response to antigen: Memory cells are less dependent on accessory cell costimulation and can respond to many antigen-presenting cell types including resting B cells. *The Journal of Immunology* **152**: 2675-2685
80. Rush, C. M., O. R. Millington, S. Hutchison, K. Bryson, J. M. Brewer and P. Garside (2009). Characterization of CD4+ T-cell–dendritic cell interactions during secondary antigen exposure in tolerance and priming. *Immunology* **128**: 463-471
81. Ahmed, R., M. J. Bevan, S. L. Reiner and D. T. Fearon (2009). The precursors of memory: models and controversies. *Nature Reviews Immunology* **9**: 662-668
82. Sallusto, F., D. Lenig, R. Forster, M. Lipp and A. Lanzavecchia (1999). Two subsets of memory T lymphocytes with distinct homing potentials and effector functions. *Nature* **401**: 709-712
83. Sallusto, F., J. Geginat and A. Lanzavecchia (2004). Central memory and effector memory T cell subsets: function, generation, and maintenance. *Annual Reviews Immunology* **22**: 745-763
84. Jameson, S. C. and D. Masopust (2009). Diversity in T cell memory: an embarrassment of riches. *Immunity* **31**: 859-871
85. Pape, K. A., E. R. Kearney, A. Khoruts, A. Mondino, R. Merica, Z.-M. Chen, E. Ingulli, J. White, J. G. Johnson and M. K. Jenkins (1997). Use of adoptive transfer of T-cell antigen-receptor-transgenic T cells for the study of T-cell activation in vivo. *Immunological Reviews* **156**: 67-78
86. Hataye, J., J. J. Moon, A. Khorurs, C. Reilly and M. K. Jenkins (2006). Naive and memory CD4+ T cell survival controlled by clonal abundance. *Science* **312**: 114-116
87. Joshi, N., W. Cui, A. Chandele, H. Lee, D. Urso, J. Hagman, L. Gapin and S. Kaech (2007). Inflammation directs memory precursor and short-lived effector CD8+ T cell fates via the graded expression of T-bet transcription factor. *Immunity* **27**: 281-295
88. Kaech, S. and E. Wherry (2007). Heterogeneity and cell-fate decisions in effector and memory CD8+ T cell differentiation during viral infection. *Immunity* **27**: 393-405
89. Rutishauser, R., G. Martins, S. Kalachikov, A. Chandele, I. Parish, E. Meffre, J. Jacob, K. Calame and S. Kaech (2009). Transcriptional Repressor Blimp-1 Promotes CD8+ T Cell Terminal Differentiation and Represses the Acquisition of Central Memory T Cell Properties. *Immunity* **31**: 296-308

90. Ichii, H., A. Sakamoto, M. Hatano, S. Okada, H. Toyama, S. Taki, M. Arima, Y. Kuroda and T. Tokuhisa (2002). Role for Bcl-6 in the generation and maintenance of memory CD8(+) T cells. *Nature Immunology* **3**: 558-563
91. Li, J., G. Huston and S. L. Swain (2003). IL-7 promotes the transition of CD4 effectors to persistent memory cells. *Journal of Experimental Medicine* **198**: 1807-1815
92. Kallies, A., E. D. Hawkins, G. T. Belz, D. Metcalf, M. Hommel, L. M. Corcoran, P. D. Hodgkin and S. L. Nutt (2006). Transcriptional repressor Blimp-1 is essential for T cell homeostasis and self-tolerance. *Nature Immunology* **7**: 466-474
93. Angelin-Duclos, C., G. Carroretti, K.-I. Lin and K. Calame (2000). Commitment of B lymphocytes to a plasma cell fate is associated with Blimp-1 expression in vivo. *The Journal of Immunology* **165**: 5462-5471
94. Lanzavecchia, A. and F. Sallusto (2000). Dynamics of T lymphocyte responses: Intermediates, effectors, and memory cells. *Science* **290**: 92-97
95. Lanzavecchia, A. and F. Sallusto (2002). Progressive differentiation and selection of the fittest in the immune response. *Nature Reviews Immunology* **2**: 982-987
96. Gramaglia, I., A. Jember, S. D. Pippig, A. D. Weinberg, N. Killeen and M. Croft (2000). The OX40 costimulatory receptor determines the development of CD4 memory by regulating primary clonal expansion. *The Journal of Immunology* **165**: 3043-3050
97. Tokoyoda, K., S. Zehentmeier, A. N. Hegazy, I. Albrecht, J. R. Grun, M. Lohning and A. Radbruch (2009). Professional Memory CD4+ T Lymphocytes Preferentially Reside and Rest in the Bone Marrow. *Immunity* **30**: 721-730
98. Peach, R. J., D. Hollenbaugh, I. Stamenkovic and A. Aruffo (1993). Identification of hyaluronic acid binding sites in the extracellular domain of CD44. *Journal of Cell Biology* **122**: 257-264
99. Voehringer, D., M. Koschella and H. Pircher (2002). Lack of proliferative capacity of human effector and memory T cells expressing killer cell lectinlike receptor G1 (KLRG1). *Blood* **100**: 3698-3702
100. Hanninen, A., I. Jaakkola, M. Salmi, O. Simell and S. Jalkanen (1997). Ly-6C regulates endothelial adhesion and homing of CD8(+) T cells by activating integrin-dependent adhesion pathways. *Proceedings of the National Academy of Sciences USA* **94**: 6898-6903
101. Walunas, T. L., D. S. Bruce, L. Dustin, D. Y. Loh and J. A. Bluestone (1995). Ly-6C is a marker of memory CD8+ T cells. *The Journal of Immunology* **155**: 1873-1883
102. Yamanouchi, S., K. Kuwahara, A. Sakata, T. Ezaki, S. Matsuoka, J.-I. Miyazaki, S. Hirose, T. Tamura, H. Nariuchi and N. Sakaguchi (1998). A T cell activation antigen, Ly6C, induced on CD4+ Th1 cells mediates an inhibitory signal for secretion of IL-2 and proliferation in peripheral immune responses. *European Journal of Immunology* **28**: 696-707
103. DeNucci, C. C., J. S. Mitchell and Y. Shimizu (2009). Integrin function in T cell homing to lymphoid and non-lymphoid sites: getting there and staying there. *Critical Reviews of Immunology* **29**: 87-109
104. Marelli-Berg, F. M., H. Fu, F. Vianello, K. Tokoyoda and A. Hamann (2010). Memory T-cell trafficking: new directions for busy commuters. *Immunology* **130**: 158-165
105. Gray, D. and P. Matzinger (1991). T cell memory is short-lived in the absence of antigen. *Journal of Experimental Medicine* **174**: 969-974
106. Gray, D., K. Siepmann, D. van Essen, J. Poudrier, M. Wykes, S. Jainandunsing, S. Bergthorsdotter and P. Dullforce (1996). B-T lymphocyte interactions in the generation and survival of memory cells. *Immunological Reviews* **150**: 45-61

107. Garcia, S., J. DiSanto and B. Stockinger (1999). Following the development of a CD4 T cell response in vivo: from activation to memory formation. *Immunity* **11**: 163-171
108. Takeda, S., H.-R. Rodewald, H. Arakawa, H. Bluethmann and T. Shimizu (1996). MHC class II molecules are not required for survival of newly generated CD4(+) T cells, but affect their long-term life span. *Immunity* **5**: 217-228
109. Kassiotis, G., S. Garcia, E. Simpson and B. Stockinger (2002). Impairment of immunological memory in the absence of MHC despite survival of memory T cells. *Nature Immunology* **3**: 244-250
110. Gray, D. (2002). A role for antigen in the maintenance of immunological memory. *Nature Reviews Immunology* **2**: 60-65
111. Surh, C. D., O. Boyman, J. F. Purton and J. Sprent (2006). Homeostasis of memory T cells. *Immunological Reviews* **211**: 154-163
112. Tan, J. T., B. Ernst, W. C. Kieper, E. LeRoy, J. Sprent and C. D. Surh (2002). Interleukin (IL)-15 and IL-7 jointly regulate homeostatic proliferation of memory phenotype CD8+ cells but are not required for memory phenotype CD4+ cells. *Journal of Experimental Medicine* **195**: 1523-1532
113. Lenz, D. C., S. K. Kurz, E. Lemmens, S. P. Schoenberger, J. Sprent, M. B. A. Oldstone and D. Homann (2004). IL-7 regulates basal homeostatic proliferation of antiviral CD4+ T cell memory. *Proceedings of the National Academy of Sciences USA* **101**: 9357-9362
114. van Leeuwen, E. M. M., J. Sprent and C. D. Surh (2009). Generation and maintenance of memory CD4+ T cells. *Current Opinion in Immunology* **21**: 167-172
115. Caserta, S. and R. Zamoyska (2007). Memories are made of this: synergy of T cell receptor and cytokine signals in CD4+ central memory cell survival. *Trends in Immunology* **28**: 245-248
116. van Essen, D., P. Dullforce and D. Gray (2000). Role of B cells in maintaining helper T-cell memory. *Philosophical Translations of the Royal Society B* **355**: 351-355
117. Martin, F. and J. F. Kearney (2001). B1 cells: similarities and differences with other B cell subsets. *Current Opinion in Immunology* **13**: 195-201
118. Lemaitre, B., E. Nicolas, L. Michaut, J.-M. Reichhart and J. A. Hoffmann (1996). The dorsoventral regulatory gene cassette spatzle/Toll/cactus controls the potent antifungal response in Drosophila adults. *Cell* **86**: 973-983
119. Rosetto, M., Y. Engstrom, C. Baldari, J. L. Telford and D. Hultmark (1995). Signals from the IL-1 receptor homolog, Toll, can activate an immune response in Drosophila hemocyte cell line. *Biochemical and Biophysical Research Communications* **209**: 111-116
120. Medzhitov, R., P. Preston-Hurlburt and C. A. Janeway (1997). A human homologue of the Drosophila Toll protein signals activation of adaptive immunity. *Nature* **388**: 394-397
121. Takeda, K., T. Kaisho and S. Akira (2003). Toll-like receptors. *Annual Reviews Immunology* **21**: 335-376
122. Kawai, T. and S. Akira (2006). TLR signaling. *Cell Death and Differentiation* **13**: 816-825
123. Zhang, G. L. and S. Ghosh (2001). Toll-like receptor-mediated NF-kappa B activation: a phylogenetically conserved paradigm in innate immunity. *Journal of Clinical Investigation* **107**: 13-19
124. Barr, T. A., S. Brown, G. Ryan, J. Zhao and D. Gray (2007). TLR-mediated stimulation of APC: Distinct cytokine responses of B cells and dendritic cells. *European Journal of Immunology* **37**: 3040-3053
125. Genestier, L., M. Taillardet, P. Mondiere, H. Gheit, C. Bella and T. Defrance (2007). TLR agonists selectively promote terminal plasma cell differentiation of B cell

subsets specialized in thymus-independent responses. *The Journal of Immunology* **178**: 7779-7786
126. Barr, T. A., S. Brown, P. Mastroeni and D. Gray (2009). B cell intrinsic MyD88 signals drive IFNg production from T cells and control switching to IgG2c. *The Journal of Immunology* **183**: 1005-1012
127. Pasare, C. and R. Medzhitov (2005). Control of B-cell responses by Toll-like receptors. *Nature* **438**: 364-368
128. Gray, D., M. Gray and T. Barr (2007). Innate responses of B cells. *European Journal of Immunology* **37**: 3304-3310
129. He, B., X. Qiao and A. Cerutti (2004). CpG DNA induces IgG class switch DNA recombination by activating human B cells through an innate pathway thaat requires TLR9 and co-operates with IL-10. *The Journal of Immunology* **173**: 4479-4491
130. Ehlers, M., H. Fukuyama, T. L. McGaha, A. Aderem and J. V. Ravetch (2006). TLR9/MyD88 signaling is required for class switching to pathogenic IgG2a and 2b autoantibodies in SLE. *Journal of Experimental Medicine* **203**: 553-561
131. Lampropoulou, V., K. Hoehlig, T. Roch, P. Neves, E. Calderón Gómez, C. H. Sweenie, Y. Hao, A. A. Freitas, U. Steinhoff, S. M. Anderton and S. Fillatreau (2008). TLR-activated B cells suppress T cell-mediated autoimmunity. *The Journal of Immunology* **180**: 4763-4773
132. Lenert, P., R. Brummel, E. H. Field and R. F. Ashman (2005). TLR-9 activation of marginal zone B cells in lupus mice regulates immunity through increased IL-10 production. *Journal of Clinical Immunology* **25**: 29-40
133. Rivera, A., C.-C. Chen, N. Ron, J. P. Dougherty and Y. Ron (2001). Role of B cells as antigen-presenting cells in vivo revisited: antigen-specific B cells are essential for T cell expansion in lymph nodes and for systemic T cell responses to low antigen concentrations. *International Immunology* **13**: 1583-1593
134. Batista, F. D. and M. S. Neuberger (1998). Affinity dependence of the B cell response to antigen: A threshold, a ceiling, and the importance of off-rate. *Immunity* **8**: 751-759
135. Rodriguez-Pinto, D. (2005). B cells as antigen-presenting cells. *Cellular Immunology* **238**: 67-75
136. Lenschow, D. J., A. I. Sperling, M. P. Cooke, G. Freeman, L. Rhee, D. C. Decker, G. Gray, L. M. Nadler, C. C. CGoodnow and J. A. Bluestone (1994). Differential Up-Regulation of the B7-1 and B7-2 Costimulatory Molecules After Ig Receptor Engagement by Antigen. *The Journal of Immunology* **153**: 1990-1997
137. Janeway, C. A., J. Ron and M. E. Katz (1987). The B cell is the initiating antigen-presenting cell in the peripheral lymph nodes. *The Journal of Immunology* **138**: 1051-1055
138. Ron, Y. and J. Sprent (1987). T cell priming in vivo: a major role for B cells in presenting antigen to T cells in lymph nodes. *The Journal of Immunology* **138**: 2848-2856
139. Ronchese, F. and B. Hausmann (1993). B lymphocytes in vivo fail to prime naive T cells but can stimulate antigen-experienced T lymphocytes. *Journal of Experimental Medicine* **177**: 679-690
140. Kitamura, D., J. Roes, R. Kuhn and K. Rajewsky (1991). A B cell-deficient mouse by targeted disruption of the membrane exon of the immunoglobulin mu chain gene. *Nature* **350**: 423-426
141. Chen, J., M. Trounstine, F. W. Alt, F. Young, C. Kurahara, J. F. Loring and D. Huszar (1993). Immunoglobulin gene rearrangement in B cell deficient mice generated by targeted deletion of the JH locus. *International Immunology* **5**: 647-656
142. Crawford, A., M. MacLeod, T. Schumacher, L. Corlett and D. Gray (2006). Primary T cell expansion and differentiation in vivo requires antigen presentation by B cells. *The Journal of Immunology* **176**: 3498-3506

143. Liu, Y., Y. wu, L. Ramarathinam, Y. Guo, D. Huszar, M. Trounstine and M. Zhao (1995). Gene-targeted B-deficient mice reveal a critical role for B cells in the CD4 T cell response. *International Immunology* **7**: 1353-1362
144. Kurt-Jones, E. A., D. Liano, K. A. Hayglass, B. Benacerraf, M.-S. Sy and A. K. Abbas (1988). The role of antigen-presenting B cella in T cell priming in vivo. *The Journal of Immunology* **140**: 3773-3778
145. Epstein, M. M., F. D. Rosa, D. Jankovic, A. Sher and P. Matzinger (1995). Successful T cell priming in B cell-deficient mice. *Journal of Experimental Medicine* **182**: 915-922
146. Topham, D. J., R. A. Tripp, A. M. Hamilton-Easton, S. R. Sarawar and P. C. Doherty (1996). Quantitative analysis of the influenza virus-specific CD4+ T cell memory in the absence of B cells and Ig. *The Journal of Immunology* **157**: 2947-2952
147. Constant, S., N. Schweitzer, J. West, P. Ranney and K. Bottomly (1995). B lymphocytes can be competent antigen-presenting cells for priming CD4+ T cells to protein antigens in vivo. *The Journal of Immunology* **155**: 3734-3741
148. Constant, S. L. (1999). B lymphocytes as antigen-presenting cells for CD4+ T cell priming in vivo. *The Journal of Immunology* **162**: 5695-5703
149. Liu, Q., Z. Liu, C. T. Rozo, H. A. Hamed, F. Alem, J. F. Urban and W. C. Gause (2007). The role of B cells in the development of CD4 effector T cells during a polarised Th2 immune response. *The Journal of Immunology* **179**: 3821-3830
150. Macaulay, A. E., R. H. DeKruyff, C. C. Goodnow and D. T. Umetsu (1997). Antigen-specific B cells preferentially induce CD4+ T cells to produce IL-4. *The Journal of Immunology* **158**: 4171-4179
151. Barr, T. A., S. Brown, P. Mastroeni and D. Gray (2010). TLR and B Cell Receptor Signals to B Cells Differentially Program Primary and Memory Th1 Responses to Salmonella enterica. *The Journal of Immunology* **185**: 2783-2789
152. Bergmann, C. C., C. Ramakrishna, M. Kornacki and S. A. Stohlman (2001). Impaired T cell immunity in B cell-deficient mice following viral central nervous system infection. *The Journal of Immunology* **167**: 1575-1583
153. Whitmire, J. K., M. S. Asano, S. M. Kaech, S. Sarkar, L. G. Hannum, M. J. Shlomchik and R. Ahmed (2009). Requirement of B Cells for Generating CD4+ T Cell Memory. *The Journal of Immunology* **182**: 1868-1876
154. Mastroeni, P., C. Simmons, R. Fowler, C. E. Hormaeche and G. Dougan (2000). Igh-6-/- (B cell-deficient) mice fail to mount solid acquired resistance to oral challenge with virulent *Salmonella enterica* serovar Typhimurium and show impaired Th1 T cell responses to *Salmonella* antigens. *Infection and Immunity* **68**: 46-53
155. Ugrinovic, S., N. Menager, N. Goh and P. Mastroeni (2003). Characterisation and development of T cell immune responses in B cell-deficient (Igh-6-/-) mice with *Salmonella enterica* serovar Typhimurium infection. *Infection and Immunity* **71**: 6808-6819
156. Linton, P.-J., J. Harbertson and L. M. Bradley (2000). A critical role for B cells in the development of memory CD4 cells. *The Journal of Immunology* **165**: 5558-5565
157. Van Essen, D., P. Dullforce, T. Brocker and D. Gray (2000). Cellular interactions involved in Th cell memory. *The Journal of Immunology* **165**: 3640-3646
158. Chan, O. T. M., L. G. Hannum, A. M. Haberman, M. P. Madaio and M. J. Shlomchik (1999). A novel mouse with B cells but lacking serum antibody reveals an antibody-independent role for B cells in murine lupus. *Journal of Experimental Medicine* **189**: 1639-1647
159. MacLennan, I. C. M., K.-M. Toellner, A. F. Cunningham, K. Serre, D. M.-Y. Sze, E. Zuniga, M. C. Cook and C. G. Vinuesa (2003). Extrafollicular antibody responses. *Immunological Reviews* **194**: 8-18

160. Paus, D., T. G. Phan, T. D. Chan, S. Gardman, A. Basten and R. Brink (2006). Antigen recognition strength regulates the choice between extrafollicular plasma cell and germinal center B cell differentiation. *Journal of Experimental Medicine* **203**: 1081-1091
161. Shapiro-Shelef, M. and K. Calame (2005). Regulation of plasma-cell development. *Nature Reviews Immunology* **5**: 230-242
162. Martin, F., A. Oliver and J. F. Kearney (2001). Marginal zone and B1 B cells unite in the early response against T-independent blood-borne particulate antigens. *Immunity* **14**: 617-629
163. Reif, K., E. H. Ekland, L. Ohl, H. Nakano, M. Lipp, R. Forster and J. G. Cyster (2002). Balanced responsiveness to chemoattractants from adjacent zones determines B-cell position. *Nature* **416**: 94-99
164. Cattoretti, G., C.-C. Chang, K. Cechova, J. Zhang, B. H. Ye, B. Falini, D. C. Louie, K. Offit, R. S. K. Chaganti and R. Dalla-Favera (1995). BCL-6 protein is expressed in germinal-center B cells. *Blood* **86**: 45-53
165. Muramatsu, M., K. Kinoshita, S. Fagarasan, S. Yamada, Y. Shinkai and T. Honjo (2000). Class Switch Recombination and Hypermutation Require Activation-Induced Cytidine Deaminase (AID), a Potential RNA Editing Enzyme. *Cell* **102**: 553-563
166. Klein, U. and R. Dalla-Favera (2008). Germinal centres: role in B-cell physiology and malignancy. *Nature Reviews Immunology* **8**: 22-33
167. Slifka, M. K., R. Anita, J. K. Whitmire and R. Ahmed (1998). Humoral immunity due to long-lived plasma cells. *Immunity* **8**: 363-372
168. Ettinger, R., S. Kuchen and P. E. Lipsky (2008). The role of IL-21 in regulating B-cell function in health and disease. *Immunological Reviews* **223**: 60-86
169. Jin, H. and T. R. Malek (2006). Redundant and unique regulation of activated mouse B lymphocytes by IL-4 and IL-21. *Journal of Leukocyte Biology* **80**: 1416-1423
170. Ozaki, K., R. Spolski, C. G. Feng, C.-F. Qi, J. Cheng, A. Sher, H. C. Morse, C. Liu, P. L. Schwartzberg and W. J. Leonard (2002). A critical role for IL-21 in regulating immunoglobulin production. *Science* **298**: 1630-1634
171. Tedder, T. F., D. A. Steeber, A. Chen and P. Engel (1995). The selectins: vascular adhesion molecules. *The FASEB Journal* **9**: 866-873
172. Smalley, D. M. and K. Ley (2005). L-selectin: mechanisms and physiological significance of ectodomain cleavage. *Journal of Cellular and Molecular Medicine* **9**: 255-266
173. Berg, E. L., A. T. Mullowney, D. P. Andrew, J. E. Goldberg and E. C. Butcher (1998). Complexity and differential expression of carbohydrate epitopes associated with L-selectin recognition of high endothelial venules. *American Journal of Pathology* **152**: 469-477
174. Berg, E. L., L. M. McEvoy, C. Berlin, R. F. Bargatze and E. C. Butcher (1993). L-selectin-mediated lymphocyte rolling on MAdCAM-1. *Nature* **366**: 695-698
175. Kansas, G. S., K. Ley, J. M. Munro and T. F. Tedder (1993). Regulation of leukocyte rolling and adhesion to high endothelial venules through the cytoplasmic domain of L-selectin. *Journal of Experimental Medicine* **177**: 833-838
176. Ley, K., P. Gaehtgens, C. Fennie, M. S. Singer, L. A. Lasky and S. D. Rosen (1991). Lectin-like cell adhesion molecule 1 mediates leukocyte rolling in mesenteric venules *in vivo*. *Blood* **77**: 2553-2555
177. Gallatin, W. M., I. L. Weissman and E. C. Butcher (1983). A cell-surface molecule involved in organ-specific homing of lymphocytes. *Nature* **304**: 30-34
178. Steeber, D. A., N. E. Green, S. Sato and T. F. Tedder (1996). Lyphocyte migration in L-selectin-deficient mice. Altered subset migration and aging of the immune system. *The Journal of Immunology* **157**: 1096-1106

179. Csencsits, K. L. and D. W. Pascual (2002). Absence of L-selectin delays mucosal B cell responses in non-intestinal effector tissues. *The Journal of Immunology* **169**: 5649-5659
180. Csencsits, K. L., N. Walters and D. W. Pascual (2001). Cutting Edge: Dichotomy of homing receptor dependence by mucosal effector B cells: αE versus L-selectin. *The Journal of Immunology* **167**: 2441-2445
181. Venturi, G. M., L. Tu, T. Kadono, A. I. Khan, Y. Fujimoto, P. Oshel, C. B. Bock, A. S. Miller, R. M. Albrecht, P. Kubes, D. A. Steeber and T. F. Tedder (2003). Leukocyte migration is regulated by L-selectin endoproteolytic release. *Immunity* **19**: 713-724
182. Kilian, K., J. Dernedde, E.-C. Mueller, I. Bahr and R. Tauber (2004). The Interaction of Protein Kinase C Isozymes α, ι, and θ with the Cytoplasmic Domain of L-selectin Is Modulated by Phosphorylation of the Receptor. *Journal of Biological Chemistry* **279**: 34472-34480
183. Kahn, J., B. Walcheck, G. I. Migaki, M. A. Jutila and T. K. Kishimoto (1998). Calmodulin regulates L-selectin adhesion molecule expression and function through a protease-dependent mechanism. *Cell* **92**: 809-818
184. Peschon, J. J., J. L. Slack, P. Reddy, K. L. Stocking, S. W. Sunnarborg, D. C. Lee, W. E. Russell, B. J. Castner, R. S. Johnson, J. N. Fitzner, R. W. Boyce, N. Nelson, C. J. Kozlosky, M. F. Wolfson, C. T. Rauch, D. P. Cerretti, R. J. Paxton, C. J. March and R. A. Black (1998). An essential role for ectodomain shedding in mammalian development. *Science* **282**: 1281-1284
185. Jung, T. M. and M. O. Dailey (1990). Rapid modulation of homing receptors (gp90 MEL-14) induced by activators of protein kinase C. *The Journal of Immunology* **144**: 3130-3136
186. Phong, M.-C., P. Gutwein, S. Kadel, K. Hexel, P. Altevogt, O. Linderkamp and B. Brenner (2003). Molecular Mechanisms of L-selectin-induced co-localization rafts and shedding. *Biochemical and Biophysical Research Communications* **300**: 563-569
187. Stoddart, J. H., R. R. Jasuja, M. A. Sikorski, U. H. von Andrian and J. W. Mier (1996). Protease-resistant L-selectin mutants. Down-modulation by cross-linking but not cellular activation. *The Journal of Immunology* **157**: 5653-5659
188. Wroblewski, M. and A. Hamann (1997). CD45-mediated signals can trigger shedding of lymphocyte L-selectin. *International Immunology* **9**: 555-562
189. Zhao, L.-c., M. Shey, M. Farnsworth and M. O. Dailey (2001). Regulation of membrane metalloproteolytic cleavage of L-selectin (CD62L) by the Epidermal Growth Factor domain. *Journal of Biological Chemistry* **276**: 30631-30640
190. Mackay, F. and J. L. Browning (2002). BAFF: A fundamental survival factor for B cells. *Nature Reviews Immunology* **2**: 465-475
191. Allman, D., R. C. Lindsley, W. DeMuth, K. Rudd, S. A. Shinton and R. R. Hardy (2001). Resolution of three nonproliferative immature splenic B cell subsets reveals multiple selection points during peripheral B cell maturation. *The Journal of Immunology* **167**: 6834-6840
192. Loder, F., B. Mutschler, R. J. Ray, C. J. Paige, P. Sideras, R. Torres, M. C. Lamers and R. Carsetti (1999). B cell development in the spleen takes place in discrete steps and is determined by the quality of B cell receptor-derived signals. *Journal of Experimental Medicine* **190**: 75-89
193. Tang, M. L. K., D. A. Steeber, X.-Q. Zhang and T. F. Tedder (1998). Intrinsic differences in L-selectin expression levels affect T and B lymphocyte subset-specific recirculation pathways. *The Journal of Immunology* **160**: 5113-5121
194. Tedder, T. F., D. A. Steeber and P. Pizcueta (1995). L-selectin-deficient mice have impaired leukocyte recruitment to inflammatory sites. *Journal of Experimental Medicine* **181**: 2259-2264

195. Xu, J., I. S. Grewal, G. P. Geba and R. A. Flavell (1996). Impaired primary T cell responses in L-selectin-deficient mice. *Journal of Experimental Medicine* **183**: 589-598
196. Richards, H., M. P. Longhi, K. Wright, A. Gallimore and A. Ager (2008). CD62L (L-selectin) down-regulation does not affect memory T cell distribution but failure to shed compromises anti-viral immunity. *The Journal of Immunology* **180**: 198-206
197. Mastroeni, P. and M. Sheppard (2004). Salmonella infections in the mouse model: host resistance factors and in vivo dynamics of bacterial spread and distribution in the tissues. *Microbes and Infection* **6**: 398-405
198. Gerold, G., A. Zychlinsky and J. de Diego (2007). What is the role of Toll-like receptors in bacterial infections? *Seminars in Immunology* **19**: 41-47
199. Hoiseth, S. K. and B. A. D. Stocker (1981). Aromatic-dependent *Salmonella typhimurium* are non-virulent and effective as live vaccines. *Nature* **291**: 238-239
200. Kalupahana, R. S., P. Mastroeni, D. Maskell and B. A. Blacklaws (2005). Activation of murine dendritic cells and macrophages induced by *Salmonella enterica* serovar Typhimurium. *Immunology* **115**: 462-472
201. Mastroeni, P. and N. Menager (2003). Development of acquired immunity to *Salmonella*. *Journal of Medical Microbiology* **52**: 453-459
202. Mastroeni, P., S. Ugrinovic, A. Chandra, C. MacLennan, R. Doffinger and D. Kumararatne (2003). Resiatance and susceptibility to *Salmonella* infections: lessons from mice and patients with immunodeficiencies. *Reviews in Medical Microbiology* **14**: 53-62
203. Mastroeni, P., S. Clare, S. Khan, J. A. Harrison, C. E. Hormaeche, H. Okamura, M. Kurimoto and G. Dougan (1999). Interleukin-18 contributes to host resistance and gamma interferon production in mice infected with virulent *Salmonella typhimurium*. *Infection and Immunity* **67**: 478-483
204. Mastroeni, P., J. A. Harrison, J. H. Robinson, S. Clare, S. Khan, D. J. Maskell, G. Dougan and C. E. Hormaeche (1998). Interleukin-12 is required for control of the growth of attenuated aromatic-compound-dependent Salmonellae in BALB/c mice: role of gamma interferon and macrophage activation. *Infection and Immunity* **66**: 4767-4776
205. Nauciel, C. and F. Espinasse-Maes (1992). Role of gamma interferon and tumour necrosis factor alpha in resistance to *Salmonella typhimurium* infection. *Infection and Immunity* **60**: 450-454
206. Cunningham, A. F., F. Gaspal, K. Serre, E. Mohr, I. R. Henderson, A. Scott-Tucker, S. M. Kenny, M. Khan, K.-M. Toellner, P. J. L. Lane and I. C. M. MacLennan (2007). Salmonella induces a switched antibody response without germinal centers that impedes the extracellular spread of infection. *The Journal of Immunology* **178**: 6200-6207
207. O'Brien, A. D., D. L. Rosenstreich, I. Scher, G. H. Campbell, R. P. MacDermott and S. B. Formal (1980). Genetic control of susceptibility to *Salmonella typhimurium* in mice: role of the LPS gene. *The Journal of Immunology* **124**: 20-24
208. Weiss, D. S., B. Raupach, K. Takeda, S. Akira and A. Zychlinsky (2004). Toll-like receptors are temporally involved in host defence. *The Journal of Immunology* **172**: 4463-4469
209. Talbot, S., S. Totemeyer, M. Yamamoto, S. Akira, K. Hughes, D. Gray, T. A. Barr, P. Mastroeni, D. J. Maskell and C. E. Bryant (2009). Toll-like receptor 4 signalling through MyD88 is essential to control Salmonella enterica serovar Typhimurium infection, but not for the initiation of bacterial clearance. *Immunology* **128**: 472-483
210. Ko, H.-J., J.-Y. Yang, D.-H. Shim, H. Yang, S.-M. Park, R. C. III and M.-N. Kweon (2009). Innate immunity mediated by MyD88 signal is not essential for induction of Lipopolysaccharide-specific B cell responses but is indispensible for protection

against *Salmonella entrica* serovar *Typhimurium* infection. *The Journal of Immunology* **182**: 2305-2312
211. Schnare, M., G. M. Barton, A. C. Holt, K. Takeda, S. Akira and R. Medzhitov (2001). Toll-like receptors control activation of adaptive immune responses. *Nature Immunology* **2**: 947-950
212. Mittrucker, H.-W., B. Raupach, A. Kohler and S. H. E. Kaufmann (2000). Cutting edge: Role of B lymphocytes in protective immunity against *Salmonella typhimurium* infection. *The Journal of Immunology* **164**: 1648-1652
213. Mastroeni, P., B. Villarreal-Ramos and C. E. Hormaeche (1993). Adoptive transfer of immunity to oral challenge with virulent Salmonellae in innately susceptible BALB/c mice requires both immune serum and T cells. *Infection and Immunity* **61**: 3981-3984
214. Schepers, K., M. Toebes, G. Sotthewes, F. A. Vyth-Dreese, T. A. M. Dellemijn, C. J. M. Melief, F. Ossendorp and T. N. M. Schumacher (2002). Differential kinetics of antigen-specific CD4+ and CD8+ T cell responses in the regression of retrovirus-induced sarcomas. *The Journal of Immunology* **169**: 3191-3199
215. MacLeod, M., M. J. Kwakkenbos, A. Crawford, S. Brown, B. Stockinger, K. Schepers, T. Schumacher and D. Gray (2006). CD4 memory T cells survive and proliferate but fail to differentiate in the absence of CD40. *Journal of Experimental Medicine* **203**: 897-906
216. Baumgarth, N., G. C. Jager, O. C. Herman, L. A. Herzenberg and L. A. Herzenberg (2000). CD4(+) T cells derived from B cell-deficient mice inhibit the establishment of peripheral B cell pools. *Proceedings of the National Academy of Sciences USA* **97**: 4766-4771
217. Macaulay, A. E., R. H. DeKruyff and D. T. Umetsu (1998). Antigen-primed T cells from B cell-deficient JHD mice fail to provide B cell help. *The Journal of Immunology* **160**: 1694-1700
218. Cerny, A., R. M. Zinkernagel and P. Groscurth (1988). Development of follicular dendritic cells in lymph nodes of B cell-depleted mice. *Cell and Tissue Research* **254**: 449-454
219. Leget, G. A. and M. S. Czuczman (1998). Use of rituximab, the new FDA-approved antibody. *Current Opinion in Oncology* **10**: 548-551
220. Uchida, J., Y. Lee, M. Hasegawa, Y. Liang, A. Bradney, J. A. Oliver, K. Bowen, D. A. Steeber, K. M. Haas, J. C. Pope and T. F. Tedder (2004). Mouse CD20 expression and function. *International Immunology* **16**: 119-129
221. Tedder, T. F. and P. Engel (1994). CD20: a regulator of cell cycle progression of B lymphocytes. *Immunology Today* **15**: 450-454
222. Cartron, G., H. Watier, J. Golay and P. Solal-Celigny (2004). From bench to bedside: ways to improve rituximab efficacy. *Blood* **104**: 2635-2642
223. Pescovitz, M. D. (2006). Rituximab, an anti-CD20 monoclonal antibody: History and mechanism of action. *American Journal of Transplantation* **6**: 859-866
224. Smith, M. R. (2003). Rituximab (monoclonal anti-CD20 antibody): mechanisms of action and resistance. *Oncogene* **22**: 7369-7368
225. Hamaguchi, Y., Y. Xiu, K. Komura, F. Nimmerjahn and T. F. Tedder (2006). Antibody isotype-specific engagement of Fc-gamma receptors regulates B lymphocyte depletion during CD20 immunotherapy. *Journal of Experimental Medicine* **203**: 743-753
226. Uchida, J., Y. Hamaguchi, J. A. Oliver, J. V. Ravetch, J. C. Pope, K. M. Haas and T. F. Tedder (2004). The innate mononuclear phagocyte network depletes B lymphocytes through Fc receptor-dependent mechanisms during anti-CD20 antibody immunotherapy. *Journal of Experimental Medicine* **199**: 1659-1669
227. McLaughlin, P., A. J. Grillo-Lopez, B. K. Link, R. Levy, M. S. Czuczman, M. E. Williams, M. R. Heyman, I. Bence-Bruckler, C. A. White, F. Cabanillas, V. Jain, A.

D. Ho, J. Lister, K. Wey, D. Shen and B. K. Dallaire (1998). Rituximab chimeric anti-CD20 monoclonal antibody therapy for relapsed indolent lymphom: half of patients respond to a four-dose treatment program. *Journal of Clinical Oncology* **16**: 2825-2833

228. Edwards, J. and G. Cambridge (2006). B-cell targeting in rheumatoid arthritis and other autoimmune diseases. *Nature Reviews Immunology* **6**: 394-403
229. Silverman, G. J. and S. Weisman (2003). Rituximab therapy and autoimmune disorders: prospects for anti-B cell therapy. *Arthritis and Rheumatism* **48**: 1484-1492
230. Stohl, W. and R. J. Looney (2006). B cell depletion therapy in systemic rheumatic diseases: different strokes for different folks? *Clinical Immunology* **121**: 1-12
231. Sfikakis, P. P., J. N. Boletis, S. Lionaki, V. Vigklis, K. G. Fragiadaki, A. Iniotaki and H. M. Moutsopoulos (2005). Remission of proliferative Lupus Nephritis following B cell depletion therapy is preceded by down-regulation of the T cell costimulatory molecule CD40 ligand. *Arthritis and Rheumatism* **52**: 501-513
232. Smith, K. G. C., R. B. Jones, S. M. Burns and D. R. W. Jayne (2006). Long-term comparison of rituximab treatment for refractory systemic Lupus Erythematosus and Vasculitis. *Arthritis and Rheumatism* **54**: 2970-2982
233. Popa, C., M. J. Leandro, G. Cambridge and J. C. W. Edwards (2007). Repeated B lymphocyte depletion with rituximab in rheumatoid arthritis over 7 years. *Rheumatology* **46**: 626-630
234. Cross, A. H., J. L. Stark, J. Lauber, M. J. Ramsbottom and J.-A. Lyons (2006). Rituximab reduces B cells and T cells in cerebrospinal fluid of multiple sclerosis patients. *Journal of Neuroimmunology* **180**: 63-70
235. Agarwal, A., C. A. Vieira, B. K. Book, R. A. Sidner, N. S. Fineberg and M. D. Pescovitz (2004). Rituximab, anti-CD20, induces in vivo cytokine release but does not impair ex vivo T cell responses. *American Journal of Transplantation* **4**: 1357-1360
236. Goldberg, S. L., A. L. Pecora, R. S. Alter, M. S. Kroll, S. D. Rowely, S. E. Waintraub, K. Imrit and R. A. Preti (2002). Unusual viral infections (progressive multifocal leukoencephalopathy and cytomegalovirus disease) after high-dose chemotherapy and autologous blood stem cell rescue and peritransplantation rituximab. *Blood* **99**: 1486-1488
237. Van der Kolk, L. E., J. W. Baars, M. H. Prins and M. H. J. Van Oers (2002). Rituximab treatment results in impaired secondary humoral immune responsiveness. *Blood* **100**: 2257-2259
238. Bearden, C. M., A. Agarwal, B. K. Book, C. A. Vieira, R. A. Sinder, H. D. Ochs, M. Young and M. D. Pescovitz (2005). Rituximab inhibits the in vivo primary and secondary antibody response to a neoantigen, bacteriophage phiX174. *American Journal of Transplantation* **5**: 50-57
239. Liossis, S.-N. C. and P. P. Sfikakis (2008). Rituximab-induced B cell depletion in autoimmune diseases: potential effects on T cells. *Clinical Immunology* **127**: 280-285
240. Ahuja, A., J. Shupe, R. Dunn, M. Kashgarian, M. R. Kehry and M. J. Shlomchik (2007). Depletion of B cells in murine lupus: efficacy and resistance. *The Journal of Immunology* **179**: 3351-3361
241. Gong, Q., Q. Ou, S. Ye, W. Lee, J. Cornelius, L. Diehl, W. Lin, Z. Hu, Y. Lu and Y. Chen (2005). Importance of cellular microenvironment and circulatory dynamics in B cell immunotherapy. *The Journal of Immunology* **174**: 817-826
242. Yu, S., R. Dunn, M. R. Kehry and H. Braley-Mullen (2008). B cell depletion inhibits spontaneous autoimmune thyroiditis in NOD.H-2h4 mice. *The Journal of Immunology* **180**: 7706-7713
243. Weber, M. S., T. Prod'homme, J. C. Patarroyo, N. Molnarif, T. Karnezis, K. Lehmann-Horn, D. M. Danilenko, J. Eastham-Anderson, A. J. Slavin, C. Linington,

C. C. A. Bernard, F. Martin and S. S. Zamvil (2010). B-cell activation influences T-cell polarization and outcome of anti-CD20 B-cell depletion in central nervous system autoimmunity. *Annals of Neurology* **68**: 369-383

244. Matsushita, T., K. Yanaba, J.-D. Bouaziz, M. Fujimoto and T. F. Tedder (2008). Regulatory B cells inhibit EAE initiation in mice while other B cells promote disease progression. *Journal of Clinical Investigation* **118**: 3420-3430
245. Di Gaetano, N., E. Cittera, R. Nota, A. Vecchi, V. Grieco, E. Scanziani, M. Botto, M. Introna and J. Golay (2003). Complement activation determines the therapeutic activity of rituximab in vivo. *The Journal of Immunology* **171**: 1581-1587
246. Adachi, O., T. Kawai, K. Takeda, M. Matsumoto, H. Tsutsi, M. Sakagami, K. Nakanishi and S. Akira (1998). Targeted disruption of the MyD88 gene results in loss of IL-1- and IL-18-mediated function. *Immunity* **9**: 143-150
247. Yamamoto, M., S. Sato, H. Hemmi, K. Hoshino, T. Kaisho, H. Sanjo, O. Takeuchi, M. Sugiyama, M. Okabe, K. Takeda and S. Akira (2003). Role of adaptor TRIF in the MyD88-independent Toll-like receptor signaling pathway. *Science* **301**: 640-643
248. Takeuchi, O., K. Hoshino, T. Kawai, H. Sanjo, H. Takada, T. Ogawa, K. Takeda and S. Akira (1999). Differential roles of TLR2 and TLR4 in recognition of Gram-negative and Gram-positive bacterial cell wall components. *Immunity* **11**: 443-451
249. Hemmi, H., O. Takeuchi, T. Kawai, T. Kaisho, S. Sato, H. Sanjo, M. Matsumoto, K. Hoshino, H. Wagner, K. Takeda and S. Akira (2000). A Toll-like receptor recognizes bacterial DNA. *Nature* **408**: 740-745
250. Mendiratta, S. K., W. D. Martin, S. Hong, A. Boesteanu, S. Joyce and L. Van Kaer (1997). CD1d1 mutant mice are deficient in natural T cells that primptly produce IL-4. *Immunity* **6**: 469-477
251. Gray, D., I. C. M. Maclennan and P. J. L. Lane (1986). Virgin B cell recruitment and the life-span of memory clones during antibody responses to 2, 4-dinitrophenyl-hemocyanin. *European Journal of Immunology* **16**: 641-648
252. Cinamon, G., M. A. Zachariah, O. M. Lam, F. W. Foss and J. G. Cyster (2008). Follicular shuttling of marginal zone B cells facilitates antigen transport. *Nature Immunology* **9**: 54-62
253. Inaba, K., M. Inaba, N. Romani, H. Aya, M. Deguchi, S. Ikehara, S. Muramatsu and R. M. Steinman (1992). Generation of large numbers of dendritic cells from mouse bone-marrow cultures supplemented with granulocyte macrophage colony-stimulating factor. *Journal of Experimental Medicine* **176**: 1693-1702
254. Harrison, J. A., B. Villarreal-Ramos, P. Mastroeni, R. D. D. Hormaeche and C. E. Hormaeche (1997). Correlates of protection induced by live Aro- *Salmonella typhimurium* vaccines in the murine typhoid model. *Immunology* **90**: 618-625
255. Oliver, A. M., F. Martin and J. F. Kearney (1999). IgMhiCD21hi lymphocytes enriched in the splenic marginal zone generate effector cells more rapidly than the bulk of follicular B cells. *The Journal of Immunology* **162**: 7198-7207
256. Reichert, R. A., W. M. Gallatin, I. L. Weissman and E. C. Butcher (1983). Germinal centre B cells lack homing receptors necessary for normal lymphocyte recirculation. *Journal of Experimental Medicine* **157**: 813-827
257. Faveeuw, C., G. Preece and A. Ager (2001). Transendothelial migration of lymphocytes across high endothelial venules into lymph nodes is affected by metalloproteinases. *Blood* **98**: 688-695
258. Borland, G., G. Murphy and A. Ager (1999). Tissue inhibitor of metalloproteinase-3 inhibits shedding os L-selectin from leukocytes. *Journal of Biological Chemistry* **274**: 2810-2815
259. Arbones, M. L., D. C. Ord, K. Ley, H. Ratech, C. Maynard-Curry, G. Otten, D. J. Capon and T. F. Tedder (1994). Lymphocyte homing and leukocyte rolling and migration are impaired in L-selectin-deficient mice. *Immunity* **1**: 247-260

260. Sengstake, S., E.-M. Boneberg and H. Illges (2006). CD21 and CD62L shedding are both inducible via P2X7Rs. *International Immunology* **18**: 1171-1178
261. Walcheck, B., J. Kahn, J. M. Fisher, B. B. Wang, R. S. Fisk, D. G. Payan, C. Feehan, R. Betageri, K. Darlak, A. F. Spatola and T. K. Kishimoto (1996). Neutrophil rolling altered by inhibition of L-selectin shedding in vitro. *Nature* **380**: 720-723
262. Korner, H., T. Winkler and J. Sedgwick (2001). Recirculating and marginal zone B cell populations can be established and maintained independently of primary and secondary follicles. *Immunology and Cell Biology* **79**: 54-61
263. Brown, G. D., J. Herre, D. L. Williams, J. A. Willment, A. S. Marshall and S. Gordon (2003). Dectin-1 mediates the biological effects of beta-glucans. *Journal of Experimental Medicine* **197**: 1119-1124
264. Taylor, P. R., G. D. Brown, D. M. Reid, J. A. Willment, L. Martinez-Pomares, S. Gordon and S. Y. Wong (2002). The beta-glucan receptor, dectin-1, is predominantly expressed on the surface of cells of the monocyte/macrophage and neutrophil lineages. *The Journal of Immunology* **169**: 3876-3882
265. Farhat, K., S. Riekenberg, H. Heine, J. Debarry, R. Lang, J. Mages, U. Buwitt-Beckmann, K. Roschmann, G. Jung, K.-H. Wiesmuller and A. J. Ulmer (2008). Heterodimerization of TLR2 with TLR1 or TLR6 expands the ligand spectrum but does not lead to differential signaling. *Journal of Leukocyte Biology* **83**: 692-701
266. von Bernuth, H., C.-L. Ku, C. Rodriguez-Gallego, S. Zhang, B.-Z. Garty, L. Maródi, H. Chapel, M. Chrabieh, R. L. Miller, C. Picard, A. Puel and J.-L. Casanova (2006). A Fast Procedure for the Detection of Defects in Toll-like Receptor Signaling. *Pediatrics* **118**: 2498-2503
267. Hayashi, F., T. K. Means and A. D. Luster (2003). Toll-like receptors stimulate human neutrophil function. *Blood* **102**: 2660-2669
268. O'Neill, L. A. J. and A. G. Bowie (2007). The family of five: TIR-domain-containing adaptors in Toll-like receptor signalling. *Nature Reviews Immunology* **7**: 353-364
269. Vijay-Kumar, M., J. D. Aitken, A. Kumar, A. S. Neish, S. Uematsu, S. Akira and A. T. Gewirtz (2008). Toll-Like Receptor 5-Deficient Mice Have Dysregulated Intestinal Gene Expression and Nonspecific Resistance to Salmonella-Induced Typhoid-Like Disease. *Infection and Immunity* **76**: 1276-1281
270. Freudenberg, M., T. Merlin, M. Gumenscheimer, C. Kalis, R. Landmann and C. Galanos (2001). Role of lipopolysaccharide susceptibility in the innate immune response to Salmonella typhimurium infection: LPS, a primary target for recognition of Gram-negative bacteria. *Microbes and Infection* **3**: 1213-1222
271. Totemeyer, S., P. Kaiser, D. J. Maskell and C. E. Bryant (2005). Sublethal Infection of C57BL/6 Mice with Salmonella enterica Serovar Typhimurium Leads to an Increase in Levels of Toll-Like Receptor 1 (TLR1), TLR2, and TLR9 mRNA as Well as a Decrease in Levels of TLR6 mRNA in Infected Organs. *Infection and Immunity* **73**: 1873-1878
272. Zanin-Zhorov, A., G. Nussbaum, S. Franitza, I. R. Cohen and O. Lider (2003). T cells respond to heat shock protein 60 via TLR2: activation of adhesion and inhibition of chemokine receptors. *The FASEB Journal* **17**: 1567-1569
273. Lembo, A., C. Kalis, C. J. Kirschning, V. Mitolo, H. Wagner, C. Galanos and M. A. Freudenberg (2003). Differential contribution of toll-like receptors 4 and 2 to the cytokine response to Salmonella enterica serovar typhimurium and Staphylococcus aureus in mice. *Infection and Immunity* **71**: 6058-6062
274. Sanchez-Campillo, M., A. Chicano, A. Torío, E. Martín-Orozco, P. Gámiz, T. Hernández-Caselles and P. García-Peñarrubia (2004). Implication of CpG-ODN and reactive oxygen species in the inhibition of intracellular growth of *Salmonella typhimurium* in hepatocytes. *Microbes and Infection* **6**: 813-820

275. Rumio, C., D. Besusso, M. Palazzo, S. Selleri, L. Sfondrini, F. Dubini, S. Menard and A. Balsari (2004). Degranulation of Paneth Cells via Toll-like receptor 9. *American Journal of Pathology* **165**: 373-381
276. Eckl-Dorna, J. and F. D. Batista (2009). BCR-mediated uptake of antigen linked to TLR9 ligand stimulates B-cell proliferation and antigen-specific plasma cell formation. *Blood* **113**: 3969-3977
277. Jendholm, J., M. Morgelin, M. L. Perez Vidakovics, M. Carlsson, H. Leffler, L. O. Cardell and K. Riesbeck (2009). Superantigen- and TLR-dependent activation of tonsillar B cells after receptor-mediated endocytosis. *The Journal of Immunology* **182**: 4713-4720
278. Cervantes-Barragán, L., C. Gil-Cruz, R. Pastelin-Palacios, K. S. Lang, A. Isibasi, B. Ludewig and C. López-Macías (2009). TLR2 and TLR4 signaling shapes specific antibody responses to Salmonella typhi antigens. *European Journal of Immunology* **39**: 126-135
279. Chao, C.-C., R. lensen and M. Dailey (1997). Mechanisms of L-selectin regulation by activated T cells. *The Journal of Immunology* **159**: 1686-1694
280. Ehrenstein, M. R., T. L. O'Keefe, S. L. Davies and M. S. Neuberger (1998). Targeted gene disruption reveals a role for natural secretory IgM in the maturation of the primary immune response. *Proceedings of the National Academy of Sciences USA* **95**: 10089-10093
281. Boes, M., A. Prodeus, T. Schmidt and M. Carroll (1998). A Critical Role of Natural Immunoglobulin M in Immediate Defense Against Systemic Bacterial Infection. *Journal of Experimental Medicine* **188**: 2381-2386
282. Fillatreau, S., D. Gray and S. M. Anderton (2008). Not always the bad guys: B cells as regulators of autoimmune pathology. *Nature Reviews Immunology* **8**: 391-397
283. Mauri, C. and M. R. Ehrenstein (2008). The 'short' history of regulatory B cells. *Trends in Immunology* **29**: 34-40
284. Mizoguchi, A. and A. K. Bhan (2006). A case for regulatory B cells. *The Journal of Immunology* **176**: 705-710
285. Angeli, V., F. Ginhoux, J. Llodra, L. Quemeneur, P. S. Frenette, M. Skobe, R. Jessberger, M. Merad and G. J. Randolph (2006). B cell-driven lymphangiogenesis in inflamed lymph nodes enhances dendritic cell mobilization. *Immunity* **24**: 203-15
286. St John, A. L. and S. N. Abraham (2009). Salmonella disrupts lymph node architecture by TLR4-mediated suppression of homeostatic chemokines. *Nature Medicine* **15**: 1259-1265
287. Hormaeche, C., P. Mastroeni, A. Arena, J. Uddin and H. Joysey (1990). T cells do not mediate the initial suppression of a Salmonella infection in the RES. *Immunology* **70**: 247-250
288. MacFarlane, A. S., M. G. Schwacha and T. K. Eisenstein (1999). In Vivo Blockage of Nitric Oxide with Aminoguanidine Inhibits Immunosuppression Induced by an Attenuated Strain of Salmonella typhimurium, Potentiates Salmonella Infection, and Inhibits Macrophage and Polymorphonuclear Leukocyte Influx into the Spleen. *Infection and Immunity* **67**: 891-898
289. Collins, F. M. (1974). Vaccines and cell-mediated immunity. *Bacteriological Reviews* **38**: 371-402
290. Aichele, P., J. Zinke, L. Grode, R. A. Schwendener, S. H. E. Kaufmann and P. Seiler (2003). Macrophages of the splenic marginal zone are essential for trapping of blood-borne particulate antigen but dispensable for induction of specific T cell responses. *The Journal of Immunology* **171**: 1148-1155
291. Han, C., J. Jin, S. Xu, H. Liu, N. Li and X. Cao (2010). Integrin CD11b negatively regulates TLR-triggered inflammatory responses by activating Syk and promoting degradation of MyD88 and TRIF via Cbl-b. *Nature Immunology* **11**: 734-742

292. Sabroe, I., E. C. Jones, L. R. Usher, M. K. B. Whyte and S. K. Dower (2002). Toll-Like Receptor (TLR)2 and TLR4 in Human Peripheral Blood Granulocytes: A Critical Role for Monocytes in Leukocyte Lipopolysaccharide Responses. *The Journal of Immunology* **168**: 4701-4710
293. Liu, Y.-J. (2001). Dendritic cell subsets and lineages, and their functions in innate and adaptive immunity. *Cell* **106**: 259-262
294. Gray, D., D. S. Kumararatne, J. Lortan, M. Khan and I. C. MacLennan (1984). Relation of intra-splenic migration of marginal zone B cells to antigen localization on follicular dendritic cells. *Immunology* **52**: 659-669
295. Rubtsov, A., C. L. Swanson, S. Troy, P. Strauch, R. Pelanda and R. M. Torres (2008). TLR agonists promote marginal zone B cell activation and facilitate T-dependent IgM responses. *The Journal of Immunology* **180**: 3882-3888
296. Malkiel, S., C. J. Kuhlow, P. Mena and J. L. Benach (2009). The Loss and Gain of Marginal Zone and Peritoneal B Cells Is Different in Response to Relapsing Fever and Lyme Disease Borrelia. *The Journal of Immunology* **182**: 498-506
297. Radwanska, M., P. Guirnalda, C. De Trez, B. Ryffel, S. Black and S. Magez (2008). Trypanosomiasis-induced B cell apoptosis results in loss of protective anti-parasite antibody responses and abolishment of vaccine-induced memory responses. *PLoS Pathogens* **4**: e1000078 (1-11)
298. Galli, G., S. Nuti, S. Tavarini, L. Galli-Stampino, C. De Lalla, G. Casorati, P. Dellabone and S. Abrignani (2003). CD1d-restricted help to B cells by human invariant natural killer T lymphocytes. *Journal of Experimental Medicine* **197**: 1051-1057
299. Galli, G., P. Pittoni, E. Tonti, C. Malzone, Y. Uematsu, M. Tortoli, D. Maione, G. Volpini, O. Finco, S. Nuti, S. Tavarini, P. Dellabone, R. Rappuoli, G. Casorati and S. Abrignani (2007). Invariant NKT cells sustain specific B cell responses and memory. *Proceedings of the National Academy of Sciences USA* **104**: 3984-3989
300. Tonti, E., G. Galli, C. Malzone, S. Abrignani, G. Casorati and P. Dellabone (2008). NKT-cell help to B lymphocytes can occur independently of cognate interaction. *Blood* **113**: 370-376
301. Campos, R. A., M. Szczepanik, A. Itakura, M. Akahira-Azuma, S. Sidobre, M. Kronenberg and P. W. Askenase (2003). Cutaneous immunization rapidly activates liver invariant Vα14 NKT cells stimulating B-1 B cells to initiate T cell recruitment for elicitation of contact sensitivity. *Journal of Experimental Medicine* **198**: 1785-1796
302. Balazs, M., F. Martin, T. Zhou and J. F. Kearney (2002). Blood dendritic cells interact with splenic marginal zone B cells to initiate T-independent immune responses. *Immunity* **17**: 341-352
303. Alugupalli, K. R., S. Akira, E. Lien and J. M. Leong (2007). MyD88- and Bruton's tyrosine kinase-mediated signals are essential for T cell-independent pathogen-specific IgM responses. *The Journal of Immunology* **178**: 3740-3749
304. Eloranta, M. L. and G. V. Alm (1999). Splenic Marginal Metallophilic Macrophages and Marginal Zone Macrophages are the Major Interferon-a/b Producers in Mice upon Intravenous Challenge with Herpes Simplex Virus. *Scandanavian Journal of Immunology* **49**: 391-394
305. Buiting, A. M. J., Z. De Rover, G. Kraal and N. Van Rooijen (1996). Humoral immune responses against particulate bacterial antigens are dependent on marginal metallophilic macrophages in the spleen. *Scandanavian Journal of Immunology* **43**: 398-405
306. Humphrey, J. H. (1985). Splenic macrophages: antigen presenting cells for T1-2 antigens. *Immunology Letters* **11**: 149-152
307. Butcher, E. C., R. V. Rouse, R. L. Coffman, C. N. Nottenburg, R. R. Hardy and I. L. Weissman (1982). Surface phenotype of Peyer's patch germinal center cells:

implications for the role of germinal centers in B cell differentiation. *The Journal of Immunology* **129**: 2698-2707

308. Holder, M., G. Grafton, I. Macdonald, M. MFinney and J. Gordon (2005). Engagement of CD20 suppresses apoptosis in germinal center B cells. *European Journal of Immunology* **25**: 3160-3164
309. Hamaguchi, Y., J. Uchida, D. W. Cain, G. M. Venturi, J. C. Poe, K. M. Haas and T. F. Tedder (2005). The peritoneal cavity provides a protective niche for B1 and conventional B lymphocytes during anti-CD20 immunotherapy in mice. *The Journal of Immunology* **174**: 4389-4399
310. Feng, N., M. C. Jaimes, N. H. Lazarus, D. Monak, C. Zhang, E. C. Butcher and H. B. Greenberg (2006). Redundant role of chemokines CCL25/TECK and CCL28/MEC in IgA+ plasmablast recruitment to the intestinal lamina propria after rotavirus infection. *The Journal of Immunology* **176**: 5749-5759
311. Vieira, P. and K. Rajewsky (1986). The bulk of endogenously produced IgG2a is eliminated from the serum of adult C57BL/6 mice with a half-life of 6–8 days. *European Journal of Immunology* **16**: 871-874
312. Davis, T. A., D. K. Czerwinski and R. Levy (1999). Therapy of B-cell lymphoma with anti-CD20 antibodies can result in the loss of CD20 antigen expression. *Clinical Cancer Research* **5**: 611-615
313. Castro-Eguiluz, D., R. Pelayo, V. Rosales-Garcia, R. Rosales-Reyes, C. Alpuche-Aranda and V. Ortiz-Navarrete (2009). B cell precursors are targets for Salmonella infection. *Microbial Pathogenesis* **47**: 52-56
314. Uppington, H., N. Menager, P. Boross, J. Wood, M. Sheppard, S. Verbeek and P. Mastroeni (2006). Effect of immune serum and role of individual Fcgamma receptors on the intracellular distribution and survival of Salmonella enterica serovar Typhimurium in murine macrophages. *Immunology* **119**: 147-158
315. Pestronk, A., J. Florence, T. Miller, R. Choksi, M. T. Al-Lozi and T. D. Levine (2003). Treatment of IgM antibody associated polyneuropathies using rituximab. *Journal of Neurology, Neurosurgery & Psychiatry* **74**: 485-489
316. Saikia, T., H. Menon and S. Advani (2001). Prolonged neutropenia following anti CD20 therapy in a patient with relapsed follicular non-Hodgkin's lymphoma and corrected with IVIG. *Annals of Oncology* **12**: 1493-1494
317. Yokohama, A., N. Tsukamoto, H. Uchiumi, H. Handa, T. Matsushima, M. Karasawa, H. Murakami and Y. Nojima (2004). Durable remission induced by rituximab-containing chemotherapy in a patient with primary refractory Burkitt's lymphoma. *Annals of Hematology* **83**: 120-123
318. Sha, Z. and R. W. Compans (2000). Induction of CD4(+) T-cell-independent immunoglobulin responses by inactivated influenza virus. *Journal of Virology* **74**: 4999-5005
319. Moulin, V., F. Andris, K. Thielemans, C. Maliszewski, J. Urbain and M. Moser (2000). B lymphocytes regulate dendritic cell (DC) function in vivo: Increased interleukin 12 production by DCs from B cell-deficient mice results in T helper cell type 1 deviation. *Journal of Experimental Medicine* **192**: 475-482
320. Zhong, X., W. Gao, N. Degauque, C. NBai, Y. Lu, J. Kenny, M. Oukka, T. B. Strom and T. L. Rothstein (2007). Reciprocal generation of Th1/Th17 and T-reg cells by B1 and B2B cells. *European Journal of Immunology* **37**: 2400-2404
321. O'Garra, A. and P. Vieira (2007). T(H)1 cells control themselves by producing interleukin-10. *Nature Reviews Immunology* **7**: 425-428
322. Moser, B., P. Schaerli and P. Loetscher (2002). CXCR5(+) T cells: follicular homing takes center stage in T-helper-cell responses. *Trends in Immunology* **23**: 250-254
323. Mallone, R. and G. T. Nepom (2004). MHC Class II Tetramers and the Pursuit of Antigen-specific T cells: Define, Deviate, Delete. *Clinical Immunology* **110**: 232-242

324. Sanjabi, S., M. M. Mosaheb and R. A. Flavell (2009). Opposing Effects of TGF-beta and IL-15 Cytokines Control the Number of Short-Lived Effector CD8(+) T Cells. *Immunity* **31**: 131-144
325. Chu, H. H., J. J. Moon, K. Takada, M. Pepper, J. A. Molitor, T. W. Schacker, K. A. Hogquist, S. C. Jameson and M. K. Jenkins (2009). Positive selection optimizes the number and function of MHCII-restricted CD4+ T cell clones in the naive polyclonal repertoire. *Proceedings of the National Academy of Sciences USA* **106**: 11241-11245
326. Morel, P. A., M. Feili-Hariri, P. T. Coates and A. W. Thomson (2003). Dendeitic cells, T cell tolerance and therapy of adverse immune reactions. *Clinical and Experimental Immunology* **133**: 1-10
327. Randolph, G. J., V. Angeli and M. A. Swartz (2005). Dendritic-cell trafficking to lymph nodes through lymphatic vessels. *Nature Reviews Immunology* **5**: 617-628
328. Chu, R. S., O. S. Targoni, A. M. Krieg, P. V. Lehmann and C. V. Harding (1997). CpG Oligodeoxynucleotides Act as Adjuvants that Switch on T Helper 1 (Th1) Immunity. *Journal of Experimental Medicine* **186**: 1623-1631
329. Baaten, B. J. G., C.-R. Li, M. F. Deiro, M. M. Lin, P. J. Linton and L. M. Bradley (2010). CD44 Regulates Survival and Memory Development in Th1 Cells. *Immunity* **32**: 104-115
330. DiLillo, D. J., Y. Hamaguchi, Y. Ueda, Y. Yang, K. Yang, J. Uchida, K. M. Haas, G. Kelsoe and T. F. Tedder (2008). Maintenance of long-lived plasma cells and serological memory despite mature and memory B cell depletion during CD20 immunotherapy in mice. *The Journal of Immunology* **180**: 361-371
331. Shah, S. and L. Qiao (2008). Resting B cells expand a CD4(+)CD25(+)Foxp3(+) Treg population via TGF-beta 3. *European Journal of Immunology* **38**: 2488-2498
332. Li, M. O. and R. A. Flavell (2008). TGF-beta: A Master of All T Cell Trades. *Cell* **134**: 392-404
333. Lin, L., A. J. Gerth and S. L. Peng (2004). CpG DNA redirects class-switching towards" Th1-like" Ig isotype production via TLR9 and MyD88. *European Journal of Immunology* **34**: 1483-1487
334. Singh, R. R., B. H. Hahn and E. E. Sercarz (1996). Neonatal peptide exposure can prime T cells and, upon subsequent immunization, induce their immune deviation: implications for antibody vs. T cell-mediated autoimmunity. *Journal of Experimental Medicine* **183**: 1613-1621
335. Shibuya, A., N. Sakamoto, Y. Shimizu, K. Shibuya, M. Osawa, T. Hiroyama, H. J. Eyre, G. R. Sutherland, Y. Endo, T. Fujita, T. Miyabayashi, S. Sakano, T. Tsuji, E. Nakayama, J. H. Phillips, L. L. Lanier and H. Nakauchi (2000). Fc alpha/mu receptor mediates endocytosis of IgM-coated microbes. *Nature Immunology* **1**: 441-446
336. Pasare, C. and R. Medzhitov (2004). Toll-like receptors: linking innate and adaptive immunity. *Microbes and Infection* **6**: 1382-1387
337. Akira, S., K. Takeda and T. Kaisho (2001). Toll-like receptors: critical proteins linking innate and acquired immunity. *Nature Immunology* **2**: 675-680
338. Hu, H., G. Huston, D. Duso, N. Lepak, E. Roman and S. L. Swain (2001). CD4+ T cell effectors can become memory cells with high efficiency and without further division. *Nature Immunology* **2**: 705-710
339. Swain, S. L. (1994). Generation and in vivo persistence of polarised Th1 and Th2 memory cells. *Immunity* **1**: 543-552
340. Harrington, L., K. Janowski, J. Oliver, A. Zajac and C. Weaver (2008). Memory CD4 T cells emerge from effector T-cell progenitors. *Nature* **452**: 356-360
341. Kallies, A., A. Xin, G. Belz and S. Nutt (2009). Blimp-1 Transcription Factor Is Required for the Differentiation of Effector CD8+ T Cells and Memory Responses. *Immunity* **31**: 283-295

342. Smith, K. M., J. M. Brewer, A. Mowat, Y. Ron and P. Garside (2004). The influence of follicular migration on T-cell differentiation. *Immunology* **111**: 248-251
343. Kondrack, R. M., J. Harbertson, J. T. Tan, M. E. McBreen, C. D. Surh and L. M. Bradley (2003). Interleukin 7 regulates the survival and generation of memory CD4 cells. *Journal of Experimental Medicine* **198**: 1797-1806